2015

A Study of the Impact of Various Geometric Factors on the Capacity of Short Range Indoor MIMO Communications Channels

Anthony Grennan
Technological University Dublin

A Study of the Impact of Various Geometric Factors on the Capacity of Short Range Indoor MIMO Communications Channels

By

Anthony Grennan MSc CEng MIET

A thesis submitted to the Dublin Institute of Technology for the degree of

Doctor of Philosophy

Supervisor: Prof. Mark Davis

School of Electrical and Electronic and Engineering

June 2015

ABSTRACT

MIMO antenna array systems have been proposed as a means of increasing the spectral efficiency of wireless systems. However, their performance is likely to be sub-optimal if typical uniform antenna array structures are arbitrarily positioned; as they depend on spatial multiplexing. This is particularly true for indoor environments in which transmission ranges are short resulting in a strong correlation of the main propagation paths, especially the line-of-sight components. This makes it difficult to achieve successful spatial multiplexing which depends on a decorrelated set of signal components. Thus, the physical propagation channel and geometry of the antenna arrays, especially the inter-element spacing, can determine how effectively spatial multiplexing can be realised. This thesis investigates MIMO communications channels involving a single transmitter and receiver operating in a simple indoor environment using a ray-tracing simulation model. The results and analysis provide system designers with an understanding of the limits of MIMO system performance in the context of both the geometric properties of the arrays and the propagation conditions. These results serve to explain the often contradictory results that appear in the wider literature on MIMO systems. Guidelines for the deployment of standard array structures in an indoor environment are provided. An original solution to optimising MIMO system performance by adjusting the geometry of uniform linear arrays is described. This is done using an iterative search method based on the Metropolis algorithm in which individual array elements are repositioned. It is demonstrated through computer simulation that capacity levels, similar to those predicted by the theory for ideal Rayleigh channels, are possible to achieve with realistic modifications to uniform linear arrays.

DECLARATION

I certify that this thesis which I now submit for examination for the award of

PhD, **is entirely my own work and has not been taken from the work of others, to save and to the extent that such work has been cited and acknowledged within the text of my work.**

This thesis was prepared according to the regulations for postgraduate study by research of the Dublin Institute of Technology and has not been submitted in whole or in part for another award in any other third level institution.

The work reported on in this thesis conforms to the principles and requirements of the DIT's guidelines for ethics in research.

DIT has permission to keep, lend or copy this thesis in whole or in part, on condition that any such use of the material of the thesis is duly acknowledged.

Signature Tony Gerrun **Date** 9 Oct 2015

ACKNOWLEDGEMENTS

Without the support and love of Catherine my wife this thesis would never have been finished. I will always be grateful for the never ending support and practical help she gave me throughout the many years and express my deep gratitude and love to her.

I would like to express special thanks to my supervisor, Professor Mark Davis, who has been extremely supportive and provided me with excellent guidance and practical help with completing this thesis and has been an inspiration to me. I also thank him for the opportunity to work in the CNRI in the FOCAS building, which is a friendly and professional location to do research, and it has been a genuine pleasure to work there. Also, thanks to Professor Hugh Byrne of the FOCAS institute for his support.

The work described in this thesis started many years ago and was driven forward by one of the nicest and most intelligent people I have ever known, Dr. Conor Downing. He made a major contribution to my research for many years. This thesis was only possible with his many inputs which are reflected here and in a number of publications. I express my sincere thanks to him. Also, I would like to thank Professor Brian Foley of TCD for his excellent support and advice and fellow researcher Dr. Pat Chambers.

I am grateful to people involved the DIT RAP (research action plan) from which I received support and all those involved in supporting staff researchers in the Institute, including Prof. Brian O' Neil, Dr. Marek Rebow and Prof. Mary McNamara and many others in the FOCAS building.

I would like to thank all the staff of the School of Electrical and Electronic Engineering, both past and present, who gave me practical and encouragement for many years and the Head of School Professor Michael Conlon. In particular I would express thanks to Professor Gerald Farrell, now the Director and Dean of the college of Engineering and the Built Environment, who was extremely supportive and a key enabler of research in DIT for many years and remains so. Also, my earlier supporter, Mr. Chris Cowley, who initially encouraged me in the direction of research. There are many others in the School who have helped me including Paula Kelly and Tom Freir who both helped with proof reading and Patricia Cuskelly and Cassilda Smith who helped with printing; a big thanks to them all. Also I thank Joe Kellegher, Niall Coakley, Tom Fallon, Betrtand Faust, Lejla Rocvanin, Ronan Murphy, Ron Gobl, Domnick Nardone, Dr. Kevin Berwick, Prof. Yulia Semenova, Dr. Padraig Mc Evoy, Ruth Coffey, Chris Bruce and many others for being supportive. Particular thanks to my friend Des Kernan for much practical help and support and Prof. Max Amman for giving me strong encouragement.

Finally, I would make special mention of my family. My late father supported me in all my endeavours and would be proud that I have completed this thesis. To my mother, Bridget, brother David, and sister Carol who have constantly encouraged me for many years; I thank them sincerely.

Abbreviations List

AOA	angle of arrival
AOD	angle of departure
AP	access point
b	bit
b/s/Hz	bits per second per Hertz
B	bandwidth
C	capacity
CDF	cumulative distribution function
CIR	channel impulse response
dB	decibel
D-MIMO	distributed multiple input multiple output
EDOF	effective degrees of freedom
GHz	gigahertz
Hz	Hertz
IEEE	Institute of Electrical and Electronics Engineers
IEMI	intentional electromagnetic interference
iid	independent and identically distributed
ISI	intersymbol interference
LOS	line-of-sight
m	metre
mm	millimetre
MIMO	multiple input multiple output
MISO	multiple input single output
NLOS	line-of-sight
OLOS	obstructed line-of-sight
PAN	personal area network
PDF	probability density function
rms	root mean square
RF	radio frequency
Rx	receiver
SNR	signal-to-noise ratio
SIMO	single input multiple output
SISO	single input single output
SVA	Saleh and Valenzuela model with Angle statistics
Tx	transmitter
ULA	uniform linear array
WLAN	wireless local area networks

TABLE OF CONTENTS

List of Tables

List of Figures

Chapter 1 Introduction

1.1 Overview

Wireless data propagation systems depend on a receiver (Rx) detecting and extracting data from signals which are corrupted by channel noise. Shannon's channel capacity theorem specifies the theoretical maximum capacity for a given signal-to-noise ratio (SNR) and signal bandwidth and from this theorem the spectral efficiency of a data transmission channel can be determined. One source of signal degradation, other than noise, is fading which may occur due to multiple copies of the same signal arriving at the Rx. This is due to various propagation mechanisms such as reflections from objects in the radio channel. This can be useful since direct paths may not be possible and reflections may be the only pathway between the transmitter (Tx) and Rx. However, if multiple pathways of varying but similar length are present, then the magnitude of the signal components will be of the same order but the phases will vary. This can lead to a summation of signal components that can lead to fluctuations, including deep fades, at the Rx. This is usually referred to as the multipath phenomenon and many wireless designs and techniques were developed to mitigate the problems associated with this phenomenon.

More recently multiple input multiple output (MIMO) antenna array based systems seek to exploit the multipath phenomenon to increase the spectral efficiency. A key aspect of these systems is the spatial multiplexing of the various data signals within the same frequency band and the same radio propagation environment. It is by successfully extracting the different data channels that the spectral efficiency is improved and this involves the implementation of complex space-time coding schemes. This requires the

multiple data signals detected at the Rx array to be decorrelated with respect to each other and both the geometry of the arrays and the physical propagation environment affects the likelihood of successfully achieving this. Thus, for example in indoor environments, the presence of line-of-sight (LOS) signal components may be desirable for good signal strength at the receiver. However, they are highly correlated when considering arrays in which the elements are close to each other, for instance with a spacing of half a wavelength (λ) or less of the carrier signal.

1.2 Problem Statement

MIMO systems operate most efficiently in transmission channels that are rich in reflections provided that these propagation paths are uncorrelated. However, the short-range indoor environment may have many correlated paths (particularly if the LOS components are considered) and the SNR at the receiver may be dominated by a limited number of such transmission paths, described as sparse multipath. Thus, the arbitrary deployment of typical regularly structured MIMO arrays, e.g. uniform linear arrays (ULAs), is likely to result in suboptimal performance compared to the values predicted for the ideal Rayleigh channel. This situation may go undetected, effectively masked in networks that employ complex protocols that may vary the transmission power, employ retransmission techniques, data aggregation and fragmentation etc.

It is possible that a MIMO system may achieve significant improvements in spectral efficiency compared to traditional single-input-single-output (SISO) systems. However the improvements realised may be far below the theoretical levels possible, depending on the size of the arrays. A 50% increase over a comparable SISO system may be

acceptable but this may be only a fraction of the gains, typically 200%-400%, for a system with multi-element arrays at both the Tx and Rx.

1.3 Objectives and Contributions

The objective of this thesis is to analyse short-range indoor MIMO systems to understand the likely performance achievable and develop strategies for system deployments to achieve optimal spectral efficiency. Specifically, this thesis investigates the performance of indoor MIMO systems with regard to the geometry of regularly structured arrays under various channel propagation conditions to determine their limitations and how best to position them. Guidelines are developed for doing this. Also, the modification of linear arrays, by adjusting the position of the individual array elements, is examined in order to determine if such an approach can result in non-regular array structures that yield improved channel performance. It is demonstrated that optimum spectral efficiency, or close to it, may be achieved using such an approach employing the Metropolis algorithm.

Although most current MIMO system deployments involve WLANs, e.g. IEEE 802.11 or Wi-Fi networks, which comprise a single access point supporting multiple clients, such systems would be extremely complex to model and analyse and unlikely to produce results that would be easy to interpret. Consequently this thesis focuses on the simplest MIMO communications channel involving a single Tx and Rx, operating in a simplified propagation environment.

A deterministic three dimensional ray-tracing simulation technique, using the method of images, was developed for this purpose. A rectangular room was modelled with

dimensions representative of those found in an open plan office or laboratory area. Ray-tracing provides both temporal and spatial data and the latter is of particular significance for investigating the geometric aspects of multi-element array structures. The precise calculation of the individual ray paths between each element at the Tx array and Rx array was performed, rather than treating each side of the channel as a point source. This method is variously referred to as a distributed source or spherical-wave model, as opposed to a plane wave model, and is the most appropriate for examining short-range MIMO systems. All LOS components, first order and second order reflections were calculated and then the spectral efficiency of the channel was determined. The model determines the impulse response of the room and from this the signal dispersion characteristics, the root mean square (rms) delay spread and excess delay, may be calculated. This was done and results are presented that compare the dispersion characteristics with capacity and explain under what conditions the two are related for MIMO systems.

The model also permits the adjustment of the individual array elements. It is demonstrated that in most cases, where capacity levels are low, it is possible to achieve significant improvement by adjusting elements at either the Tx or Rx. However, optimal capacity results if both sides are adjusted for a given pair of Tx-Rx locations. Also some array structures that provide a more general improvement at multiple locations, compared to linear structures, are described.

Main contributions and novel aspects of this thesis

- Development of a set of guidelines for system designers for the deployment of MIMO systems in a short-range indoor environment.

- Comprehensive description of the performance of uniform arrays within a short-range indoor environment based on extensive results that explain various, sometimes contradictory, results from the literature.
- Insight into the performance of MIMO systems under sparse propagation conditions.
- Explanation of the impact of channel dispersion characteristics on channel capacity.
- Investigation into the use of the Metropolis algorithm for improving channel capacity in a short-range indoor environment by adjusting the geometry of the arrays.
- Proposal of novel non-regular array structures, as a consequence of employing the Metropolis algorithm, which provide optimal spectral efficiency.

1.4 Thesis Organisation

Chapter 2 provides a background on MIMO systems theory used in the thesis and a broad review of the pertinent literature in the field. Initially concepts related to MIMO systems, such as multipath fading are discussed followed by a description of the performance of MIMO systems from an information theory perspective. The main literature review section deals with the matter in a broadly chronological manner with reference to some key topics that arise in the thesis such as array orientations, indoor systems, array element adjustments and so forth.

Chapter 3 is a detailed description of the simulation model developed and its validation. The chapter begins with a review of radio channel modelling which is followed by an overview of the specific techniques for simulating MIMO systems. This includes the

random matrix model which is used as a reference benchmark throughout the thesis for comparison with results generated by the simulation model. The chapter concludes with a summary of the main criteria associated with the ray-tracing model developed.

Chapter 4 describes the results from simulations using the deterministic model for 4x4 and 2x2 uniform arrays, primarily uniform linear arrays (ULAs); but square and cross array structures are also considered. Extensive results are presented which provide an insight into the behavior of uniformly spaced arrays encompassing some of the contradictory results in the literature. Included in the range of results is the effect of element spacing, array size and geometry, orientation of arrays, under LOS and non-LOS (NLOS) propagation conditions; the latter is sometimes referred to as obstructed LOS. The results provide an insight for system designers to understand the limits of uniform array structures and the effect of the geometric characteristics of the array and propagation conditions in an indoor environment. The chapter concludes with suggestions and guidelines for the positioning of regular arrays in a room.

Chapter 5 presents a detailed analysis of 4x4 ULAs for limited propagation conditions. Initially the LOS components in isolation (‘free space’) are considered. This is extended to first order reflections and the interaction of a limited number of propagation paths, often referred to as ‘sparse’ propagation conditions. This is followed by a comparison of the dispersion characteristics of the channel and the corresponding capacity for various scenarios. Both the excess delay and rms delay spread are considered and conclusions related to the array element spacing are presented. The chapter concludes with a

comparison of different regular array structures and suggestions for the efficient deployment of systems under sparse conditions.

Chapter 6 describes a novel approach for optimising the spectral efficiency of MIMO array structures by adjusting the individual array elements. This is done iteratively using a Monte Carlo approach based on the Metropolis algorithm. The objective was to search the spatial domain for new configurations of arrays that reduce the channel correlation and improved capacity. This was done by either adjusting the array elements at the receiver only or at both sides of the channel. The former instance is applicable in situations where multiple devices are accessing a single fixed device such as a network access point. It is demonstrated that, in most cases, significant improvement on initial capacity levels can be achieved, including cases when adaptation was only applied at one side of the channel. Also, there were some structures found, when adaptations were performed at both sides of the channel, which provided a general improvement in capacity at all locations compared to non-adjusted ULAs.

Finally chapter 7 is an overall summary of the thesis and suggestions for future work. It includes a list of the main findings and contributions of the thesis and summarises the guidelines and suggestions for MIMO system deployments. This is followed by the appendices which are organised on a chapter basis, i.e. appendix A relates to chapter 3, appendix B relates to chapter 4 etc. Appendix E contains a list of all the equations in the thesis and further details relating to the simulation model and measurement techniques. Finally a list of publications is supplied, the titles of which are also given below.

1.5 Publications arising from this Thesis

1. A. Grennan, C. Downing, B. Foley, “Capacity variation of indoor radio MIMO systems using a deterministic Model”, *Irish Signals and Systems Conference,* 2003, pp. 548-533.
2. A. Grennan, C. Downing, B. Foley, “MIMO Capacity Enhancement by adjusting Element Positions using the Metropolis Algorithm in a Deterministic Model”, *IEE Irish Signals and Systems Conference,* 2006, pp. 265-276.
3. A. Grennan, C. Downing, B. Foley, “A Geometric Interpretation of Indoor MIMO Systems using a Deterministic Model”, *European Conference on Antennas and Propagation,* Edinburgh Nov. 2007, pp. 88-93.
4. A. Grennan, C. Downing, B. Foley, “Application and analysis of MIMO systems using Metropolis algorithm”, *Loughborough Antennas and Propagation Conference (LAPC)*”, Nov. 2010, pp. 357-360.
5. A. Grennan, M. Davis, C. Downing, “Analysis of array geometries for indoor MIMO systems using a deterministic model”, *Loughborough Antennas and Propagation Conference*” Nov. 2012, pp. 337-341.
6. A. Grennan, M. Davis, C. Downing, “Near optimum array geometries for MIMO systems in a highly correlated environment”, *Loughborough Antennas and Propagation Conference (LAPC)*”, Nov. 2013, pp. 357-360.

Chapter 2 Background to MIMO Systems and Literature Review

2.1 Introduction

This chapter introduces and describes multiple input multiple output channels (MIMO) with reference to the techniques and theory pertinent to this thesis. The term MIMO is now generally understood to refer to radio communications channels that use arrays at both ends of the wireless channel with the aim of improving the spectral efficiency by using spatial multiplexing. This requires complex space-time coding schemes in the modems to implement it, however the focus of this thesis is on the impact of the antenna arrays and propagation conditions in short-range MIMO channels. Thus, array systems and other MIMO related communications techniques are initially described and then the concepts and theory associated with modern MIMO systems are introduced by reviewing the research literature in the field.

2.2 Communications Concepts related to MIMO Systems

2.2.1 Antenna array systems

In communications systems engineering MIMO is predated by some similar and related concepts, for example, beamforming [2.1]. Usually this involves an array of non-directional elements at the Tx side of the channel to direct the antenna radiation beam pattern, in effect this is a spatial filtering process. A phased array results in an electromagnetic wave front that experiences constructive or destructive interference

from the components from each of the elements of the array, thus producing the required pattern of beams and nulls within the spatial domain. The focus of radiated energy in a given direction is described as array gain.

Since the phase and amplitude of the signals at each element determine the resultant wavefront, then by varying these dynamically the beam can be steered. This may be implemented electronically, and adaptively if required, by means of digital signal processing technology to implement the adjustments associated with each element of the array. This is known as digital beamforming and can also be applied at the Rx side to detect a signal from a given direction. The beam may be focussed in a particular direction to exclude other signals of the same frequency, which may arrive from a different direction, but it can also be a means of reducing the impact of copies of the same signal, i.e. to mitigate the multipath phenomenon.

A more straight forward means of achieving the same result is to employ multiple antennas at the receiver and sometimes the transmitter, to detect or possibly generate spatially diverse versions of the same signal to overcome the problem of signal fading due to multipath propagation. Providing the separation distance is sufficient, typically greater than a wavelength, it is likely that a good signal will be detected on at least one of the antennas, in the case of Rx diversity. In such circumstances the signals are considered decorrelated and the probability that every Rx element will detect a poor quality signal is reduced, thus improving the reliability of the link. The greater the number of array antenna elements (the diversity order) the higher the probability of detecting a signal for a given SNR at the Rx. A system with one Tx element and

multiple Rx elements may be categorised as a single input multiple output (SIMO) system. There are other approaches to the beamforming/diversity methods but these are the most significant ones related to recently developed MIMO techniques, since their operation depends on the spatial aspects of the channel in a more specific manner than a standard single input single output (SISO) system.

The MIMO system initially proposed by Paulraj and Kalaith [2.2] and Foschini [2.3] is generally what is understood as the description of modern MIMO array systems and is the one considered in this thesis. In short, the earlier systems sought to mitigate the problems associated with the spatial diversity of the radio channel, e.g. multipath fading, whereas the MIMO systems considered here seek to exploit the spatial diversity. In this thesis a ray-tracing simulation model, in which precise spatial and temporal data of multipath components are calculated, is used to investigate MIMO arrays under a variety of propagation conditions.

2.2.2 Multipath fading

In most radio communications links there is more than one propagation pathway between the Tx and Rx and this leads to multiple copies of the same signal arriving at the Rx. Most commonly this is due to reflections or diffraction from surfaces/objects within the propagation environment. Clearly there is a beneficial aspect to this in systems where there is no line-of-sight (NLOS) signal, as it ensures some transmission paths connect the Tx and Rx. Diversity techniques at the Tx also attempt to take advantage of this phenomenon.

Since the paths travelled are different in length, the amplitude and phases of the multipath waves arriving at the Rx combine to produce a signal that fluctuates in time, for example, if there is relative motion between the Tx and Rx or if the propagation environment changes. This is a problem if the signal-to-noise ratio (SNR) is reduced and is called fading. Antenna diversity at the Rx is an attempt to overcome this, provided there is sufficient difference between the composite signals at the separated elements. Over time the fading is considered to be a random process (random fading) and the instantaneous gain of the channel is most commonly described by the Rayleigh distribution and hence the term 'Rayleigh channel' is often applied to such propagation environments. Modelling the Rayleigh channel has been a common approach to simulating and investigating MIMO system channels and often referred to as the 'ideal' environment as it tends to provide multiple copies of the transmitted signal between the system arrays which are decorrelated with respect to each other. In this thesis reference to the ideal channel implies a Rayleigh channel or one modelled by random matrices. Random matrix modelling is commonly used and is described later. In this thesis it is used as a benchmark for comparison with simulated results.

The term flat fading describes the most common type in which frequency components of the received signal are unchanged. This applies if the bandwidth of the signal is narrow compared to the flat fading bandwidth of the channel. If this is not the case then a frequency selective fading process may occur. If the path length differences are large then phase differences between components with small differences in frequency will exhibit frequency selective fading. Often this is characterised in the time domain in which the multiple components give rise to a spread of delays (dispersion) of the

received signal due to the arrival of the various reflections at different times. If this is viewed as a pulse representing data then the multiple echoes of successive received pulses may give rise to intersymbol interference (ISI). A similar fading process occurs in mobile radio systems due to the effect of Doppler shift. A detailed treatment of the various fading and related parameters is provided in [2.3][2.4] including definitions of dispersion metrics.

Most traditional communications systems were designed to overcome the problem of amplitude fading and minimise the signal dispersion. Techniques such as spreading a narrow band data signal over a wider range of frequencies results in a lower probability of a fade at a particular frequency. This spread spectrum method comes at the cost of increased signal bandwidth and system complexity. Alternatively fast digital signal processors allow for adaptive equalisation by inverse modelling of the propagation channel.

The modern MIMO systems described below are fundamentally different in that they seek to exploit the existence of multiple copies of the signal to carry the required information. The concept of space division multiplexing is not as intuitive to most communications engineers as frequency or time division multiplexing, as the medium is not directly operated on by the electronic systems in the manner of time or frequency division multiplexing (apart from intentionally transmitting the same signal from multiple points in order to generate signal diversity). In fact mitigating the multipath mechanism, that is in effect the spatial multiplexing system, is what traditionally concerned most communications system designers.

2.2.3 Channel coding

Many modern radio communications systems, including mobile speech and data services, employ some form of channel coding to improve the reliability of the data transmission, for instance to overcome a bit recovery error due to channel noise. The principle of channel coding is to add extra bits, which are information redundant, to the basic data word in order to generate a code word for transmission. The increased data code can be chosen to ensure that it is significantly different from the other code words used. These differences are the basis for enabling the detection of a bit error and the correction of this. For instance, a 4-bit data word may have an extra 3-bits appended to produce a 7-bit channel code word. This requires increased channel capacity to convey the extra bits and requires a wider channel bandwidth. The greater the number of extra bits (added redundancy) the more errors that can be detected and corrected. Bit interleaving can also be employed to mitigate the impact of channel burst errors which are most likely to occur on wireless channels where multipath propagation is present. Consequently if a burst error occurs, due to an instantaneous amplitude fade, then data may be recovered since it is spread over several code words which may be individually corrected. Thus channel coding, like arrays, has found application in overcoming the effect of multipath phenomenon and is treated in [2.5].

A space-time code on the other hand works better in an environment where there is significant spatial diversity provided by multipath. Space–time coding is complex and an introductory treatment is provided in [2.6]. The key aspect of these systems is the mapping of the data stream across multiple antennas at the Tx by a space-time encoding scheme after which they are effectively mixed in the multipath propagation

environment. The successful recovery of the independently launched data streams is dependent on the spatial and temporal diversity of the channel. Thus, the characteristics of the channel, including the geometric characteristics of the arrays, are significant in determining the overall capacity of the channel and it is these factors which are examined in this thesis.

2.3 MIMO Systems Overview

In this section the theory of MIMO systems and the key capacity formula used throughout this thesis are introduced with reference to the literature in the field.

2.3.1 Early background

The MIMO systems considered here are assumed to employ spatial multiplexing to achieve improvements in the spectral efficiency of the system. This is defined as the number of bits per second per Hertz (b/s/Hz) and for convenience in this thesis it is often referred to as the channel capacity. The first demonstration of such a MIMO system was by Bell labs in 1998 and was based on the theory developed and described in [2.7][2.8]. Earlier related work in the field had been published by Paulraj and Kailath [2.2] and Winters [2.9] which focussed on the capacity of the radio channel with diversity in a Rayleigh fading environment. Of significance in [2.9] was the concept of multiple antennas (arrays) with limited spacing between elements. For indoor environments Winters assumed the spacing was more than $\lambda/4$ between two antenna elements which, as stated, usually results in the fading statistics for the elements being independent. A minimum of $\lambda/2$ spacing is used in the work presented here for linear array structures at which it is assumed that there is no effect on capacity if mutual coupling occurs between array elements [52]. (Mutual coupling is not considered in this

thesis). It will be clearly demonstrated later that the element spacing significantly affects the capacity depending on a variety of criteria.

The most important work on which most subsequent research in the field was based was by Gerard Foschini and Michael Gans [2.10], and much of the mathematical framework employed in this thesis derives directly from that paper and others who have referred to it. (They acknowledged a number of colleagues with whom they had discussions, in particular P.F. Driessen). In [2.10] the authors focussed on the concept of a 'quasi-static' channel for a narrow band signal and assumed flat fading as modelled by a Rayleigh distribution.

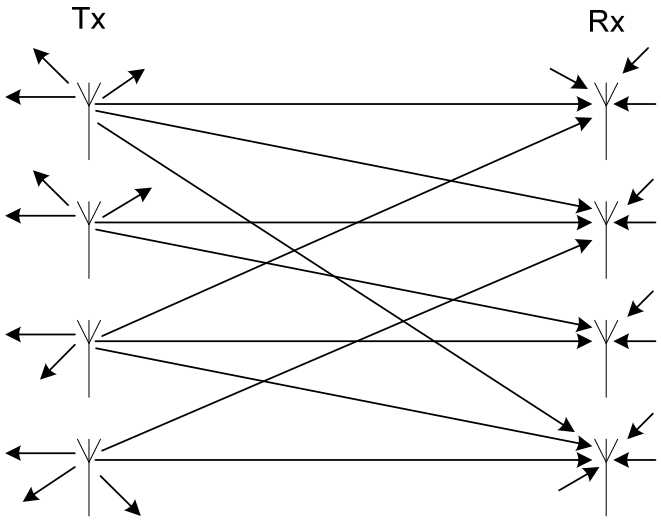

Figure 2.1 Simplified representation of a 4x4 MIMO channel showing some of the propagation paths.

Figure 2.1(a) shows a simple representation of a 4x4 MIMO system. The spatial channel linking the multiple Tx and Rx antennas is understood in terms of a matrix (rather than a vector) in which the individual entries h_{ij} represent the transmission channel transfer function (gain) from a given Tx element to a particular Rx element. This is not simply

the direct transmission LOS components, but all possible paths between the pair of array elements, and possibly no LOS components. Thus the channel matrix **H** has four entries for a 2x2 system and sixteen for a 4x4 and so forth. A general matrix description is shown in equation 2.1:

$$\mathbf{H} = \begin{bmatrix} h_{1,1} & h_{1,2} & \dots & h_{1,N} \\ h_{2,1} & \dots & \dots & h_{2.N} \\ \dots & & & \\ h_{M,1} & \dots & & h_{M,N} \end{bmatrix} \qquad (2.1)$$

where N is the number of elements at the Tx and M is the number of elements at the Rx.

2.3.2 Spectral efficiency of a MIMO system

MIMO information theory was primarily developed in [2.7] and [2.10] and was based on the general theory developed by Shannon [2.11]. For a standard 1x1 (SISO) the system capacity C may be defined as:

$$C = log_2(1 + \rho|h|^2) \qquad b/s/Hz \qquad (2.2)$$

where h is the channel gain normalised for an expected value of unity and ρ is the signal-to-noise (SNR) ratio at the Rx. Similarly, for a system with M elements at the Rx (receiver diversity), a single-input-multiple-output (SIMO) system, the capacity is defined by:

$$C = log_2\left(1 + \rho \sum_{i=1}^{M} |h_i|^2\right) \qquad b/s/Hz \quad (2.3)$$

and h_i is the gain associated with a single Rx element. The converse case with N elements at the Tx (transmitter diversity, or MISO) is given by:

$$C = log_2\left(1 + \frac{\rho}{N}\sum_{i=1}^{N}|h_i|^2\right) \qquad b/s/Hz \qquad (2.4)$$

Where dividing by N ensures that the total Tx power is equivalent to the SISO case and h_i is the gain associated with a single Tx element. In both (2.3) and (2.4) there is a logarithmic increase in the system capacity for increasing N *or* M elements. However, for an M x N system the capacity was seminally defined by Foschini [2.8][2.10] and Telatar [2.7] as:

$$C = log_2\left[det\left(I_M + \frac{\rho}{N}\,\boldsymbol{HH}^*\right)\right] \quad b/s/Hz \qquad (2.5)$$

where ***** denotes the conjugate transpose. They demonstrated that the capacity may actually grow linearly with m, which is the minimum value of either M or N. Thus for a 4x4 system the overall gain is as much as four times that of a SISO for the same level of Tx power with the channel unknown at the Tx. In [2.7] equation (2.5) was rewritten as:

$$C = \sum_{I=1}^{m} log_2\ \left(1 + \frac{\rho}{N}\lambda_i\right) \quad b/s/Hz \qquad (2.6)$$

Which effectively decomposes the matrix into m parallel sub channels whose individual gains are the eigenvalues (λ_i) of $\mathbf{HH}^*$ where:

$$\Lambda = \begin{bmatrix} \lambda_1 & 0 & \ldots & 0 \\ 0 & \lambda_2 & \ldots & 0 \\ \ldots & & & \\ 0 & \ldots & & \lambda_N \end{bmatrix} \qquad (2.7)$$

Thus the total channel capacity may be viewed as equivalent to the sum of the individual SISO channels with a gain λ_i and if the eigenvalues are all of reasonable

magnitude, good capacity is achieved. In effect the eigenvalues reflect the channels 'goodness', particularly in relation to spatial multiplexing, and for a poor channel configuration there tends to be only one significant eigenvalue indicating that the system is effectively reduced to a SISO channel. In this thesis the simulation model determines the channel capacity by calculating the eigenvalues and using equation (2.5) to determine the channel capacity assuming a SNR of 20 dB, which is a widely used value throughout the literature, e.g. [16][29][35] and Foschini and Gans used 21 dB in [10].

2.3.3 Effective degrees of freedom of a MIMO channel

In [2.12] the effect of correlation between array systems was investigated under the assumption of a narrow band Rayleigh fading environment for fixed position Tx and Rx. They used a 'one ring' model [2.13] to deterministically generate multipath rays and determined the capacity as the sum of the individual sub channels as described above. From the model they determined that increasing the correlation between the rays arriving at the different antennas reduced the capacity, as it effectively reduced the number of sub channels. They found that the correlation depended on the antenna spacing, arrangement and the angular spread of the rays at the Rx, factors also considered in this thesis. They defined the number of effective sub channels that contribute to capacity as the 'effective degrees of freedom' (EDOF), a term that is occasionally used in the literature. In [2.14] the EDOF and capacity was explicitly calculated for various indoor and outdoor scenarios using a ray tracing tool called WISE [2.15]. They generated cumulative distribution functions (CDFs) that for a given room location clearly showed increasing capacity as the element spacing was increased from

λ/2 to 3 λ at both the Tx and Rx and found a similar result for an outdoor environment they modelled. The EDOF is defined as:

$$EDOF = \frac{1}{\lambda_{max}} \sum_{i=1}^{m} \lambda_i \qquad (2.8)$$

where λ_i is the eigenvalues referred to above in (2.6) and λ_{max} is the maximum eigenvalue determined in (2.6). In [2.16] a comparison of various array techniques was conducted and the concept of parallel channels was introduced. It was determined that for large numbers of antennas that the eigenvalues are bounded by:

$$\left(\sqrt{N} - \sqrt{M}\right)^2 < \lambda_i < \left(\sqrt{N} + \sqrt{M}\right)^2 \qquad (2.9)$$

where N and M are the number of array elements at the Tx and Rx respectively. Any perturbation of the Tx or Rx location can change the channel matrix and consequently the eigenvalues. This matter was studied in [2.17] in which they considered the problem from the perspective of choosing eigenvalues to maximise the capacity expression. They solved this maximisation problem and concluded that providing the SNR is large enough then the creation of m parallel channels of equal strength is the optimal solution. With low SNR they concluded that beamforming with the array, effectively creating a single channel, is the best solution. The relative position of the Tx and Rx to each other and the perturbation of individual array elements at a given location are considered in this thesis and some results pertaining to their impact on the channel eigenvalues are presented including those in [2.18].

2.4 Review of MIMO Systems

This section reviews some of the literature on research work in MIMO systems related to this thesis and is done in a broadly chronological manner with subsections that discuss key issues for this thesis. There is some reference to simulation and modelling

of MIMO systems, however, further details of those areas and of radio modelling in general are discussed in the next chapter.

2.4.1 Impact of signal-to-noise level

The impact of SNR levels was considered for indoor channels in [2.19] based on channel sounding measurements they made at 5.2 GHz, which is also the assumed frequency of the signal carrier used in the simulation model in this thesis (although some simulations also assumed a carrier frequency of 2.4 GHz). They used a large rectangular laboratory for their measurement campaign with eight element dipole/monopole arrays spaced at 0.4 λ and 0.5 λ apart. The significant aspect of their findings was that variations in the capacity levels they achieved were primarily due to the SNR at the Rx, due to the presence or absence of LOS components. They found that the increased signal power due to the LOS components gave better capacity despite the increased correlation of the channel matrix **H** compared to the non-LOS (NLOS) case. Normalisation of the determined channel matrix (from measurements or simulations) is common in the literature but the effect of SNR changes due to obstruction of some signal components, particularly the LOS, is not always considered and over short ranges this may be significant. Normalisation is used in this thesis and is discussed in [2.20] and in the next chapter. Also, some results are presented later that take into account the effect of removing the LOS component; some of which were originally presented in [2.21]. Another interesting result from the same research group [2.22] considered the variation in the performance of the same MIMO system, under NLOS conditions at a fixed location, with regard to time (temporal variation). Their results showed that the variation of a MIMO channel was slower than that of the individual channels between

the Tx and the Rx elements. This result was related to the diversity and reduced correlation that existed between the channels under NLOS conditions.

A similar channel sounding technique and MIMO system was used in [2.23] which examined the impact of receive direction and position for both normalised power and taking path loss into account. The direction pointed at by the Rx was the direction perpendicular to the axis of the array, the intention being to model a realistic system, e.g. antennas positioned on the back of a laptop computer. They found similar results to [2.19] when taking path-loss into account. This was due to the propagation path factors, e.g. if a dominant quasi-LOS component was present due to an open door, then the power from that general direction ensured that the capacity at that angle of reception was the best of the three angles tested. However when they normalised for path loss, then all three directions tested had similar levels of capacity. Without the LOS components it is possible that some reflections from a particular direction may be strong and have an effect on capacity due simply to a greater power delivery, increasing the SNR.

2.4.2 Array orientations

Broadside arrays were simulated using a ray-tracing tool in [2.24] to investigate the effects of correlated fading due to the finite separation between antenna elements for various size arrays. The results demonstrated ‘scaling’ of capacity as the array size increased, also that both the element spacing and array orientations impacted on the capacity by affecting the correlation between the signals from the elements at the Tx to Rx. The larger the spacing of elements, e.g. 5 λ, the better (i.e. the lower the correlations) compared to $\lambda/2$ but also the broadside orientation of Tx and Rx was better

than in-line orientation. This result is also examined and confirmed in this thesis where it is demonstrated that the benefits of wider spacing are not always present and depend on a variety of factors such as orientation, array structure, relative position to walls and the characteristics of the propagation environment. Thus the arbitrary positioning of Tx and Rx arrays, without consideration of these factors, is likely to result in suboptimal system performance.

A number of the results in [2.24] refer to channels with feedback to the transmitter and apply a power allocation algorithm to the individual elements to optimise throughput. If the data channel associated with a given element is good, then more power is applied, if it is poor then less power is applied. This is called 'waterfilling' and increases the overall system complexity. It has not been considered in the work presented here which assumes equal power at Tx elements and no knowledge of the channel.

2.4.3 Indoor systems

An analysis of an indoor open plan office (6 m x 10 m) using a simulation technique partly based on random matrices, to model fading components, and deterministic calculation of the LOS components, was done in [2.25]. They were particularly concerned with the geometric characteristics of the channel such as element separation and both the location and the orientation of the Rx. They investigated parallel (broadside) and perpendicular 4x4 arrays as considered in this thesis and were discussed in [2.18] and [2.21]. They assumed a carrier frequency of 5 GHz which is used in wireless local area networks (WLAN) systems such as those defined by IEEE 802.11 standards. They found that increasing antenna separation increased the capacity for pure LOS channels (free space) and 4 λ spacing achieved high capacity gain throughout the

room for parallel arrays. Moreover, they stated that a large spacing was successful for pure LOS channels and 'much more significant than power allocation schemes'. They also noted that rotating the array axis of the Rx affected the capacity, an observation that is discussed in more detail in this thesis, and their graphs indicate an approximate difference of 15% between the two arrays with the parallel arrangement found to be higher. They superimposed fading components with random matrices (Rayleigh distribution) on the LOS deterministic calculations. Their results showed that if the power level of the fading components (the reflections) was relatively strong, perhaps equal to LOS components, then the dependence on element separation distance was negligible assuming a minimum of $\lambda/2$ element spacing. They concluded that variation of the fading components, or the position/orientation of the arrays, can ensure large capacity and these factors are also investigated in this thesis.

2.4.4 Deterministic simulations

A ray-tracing simulation approach was used in [2.26] to investigate antenna spacing in an empty room with the reflectivity of the walls specified to model good reflection surfaces, e.g. ferroconcrete, thus providing strong reflection components. Different array structures were modelled, the main one being a four element square Tx array and linear Rx array. The results presented indicate that for antenna element spacing above 0.5 λ there was little variation for the various configurations and scenarios (with or without LOS components) and capacity was more or less independent of element spacing. They also determined similar levels of capacity from data extracted from echo sounding measurements in the room. It would appear that (similar to [2.25]) the strength of the reflections relative to the LOS components helped them arrive at this conclusion, although they did not explicitly state this. Earlier in the paper they did express concern

that the strong reflectivity of the walls may affect their desired goal to investigate the antenna element spacing. Notwithstanding this point, they demonstrated the benefits of highly reflective surfaces which enhance the relative power of the 'pseudo-random' reflections and therefore more closely approximate ideal conditions. The simulation model in this thesis permits the variation of the reflection coefficient of the various surfaces, or some of the surfaces only or a section of a surface. It is demonstrated in this thesis that enhancing the relative power in the reflections, compared to the LOS components, significantly improves propagation conditions for MIMO systems.

Some of the same authors in [2.26] extended their work in [2.27] to confirm the possibility of good performance with closely spaced antennas. They suggested that the performance was affected by a mutual coupling of antenna elements which affects the radiation pattern of the array. They calculated the capacity for different spacings based on data obtained from echo sounding measurements and appear to have shown that it is possible at small spacing to realise a good capacity indoors, but they obtained weaker results for outdoor measurements. The suggestion in [2.27] was that this was due to the power delivery of the reflections which was affected by the radiation pattern. However, it is possible that the reflections were stronger due to other reasons, such as the reflectivity of the walls, and it is not clear what the impact of the relative positions of the Tx and Rx was, or if the radiation pattern was affecting the strength of the reflections in a given direction. In this thesis it has been assumed that no mutual coupling is present and an element spacing of $\lambda/2$ is the minimum considered for uniform arrays.

A ray-tracing simulation was used by Burr [2.28] to evaluate MIMO capacity based on the 'method of images', which is the technique used in this thesis. This is a two-dimensional scheme which he argued was sufficient for most scenarios. (However, this is not sufficient if three dimensional variations to array structures are considered, as in chapter 6 of this thesis). A key aspect of this method is that both the signal strengths and angles of departure and arrival of the rays, from Tx or to Rx, are determined, since the cross correlation of the components of the matrix channel are affected by these factors. A number of scenarios were modelled in [2.28], including a corridor with both perfect and imperfect reflecting surfaces and a rectangular room, all in two-dimensions. In the first instance, using a reflection order of 100, he found that the deterministically calculated capacity generated 'random-like' fluctuations similar to those associated with independently fading Rayleigh models such as those used in [2.10]. For this case he provided two notable results, firstly that only for small array sizes, 4x4 uniform linear arrays (ULAs) the capacity was close to the ideal but did not scale upwards for larger arrays, e.g. 16x16 ULAs. Also he states (though does not provide the results) that capacity does not increase with element spacing. It is a similar scenario and result to that in [2.26]. This suggests that deterministically calculated reflections of strong power relative to LOS components result in a channel matrix which is 'pseudo random' in terms of many of the individual entries, and this models independent Rayleigh fading quite well. This may be unrealistic and does not permit the effect of the arrays geometric properties to be properly assessed or take into account the issue of path loss. With imperfect reflectors they found increased capacity with increased element spacing but 'only beyond' a certain distance. They explained this as being due to the angle of incidence of the reflections which appears to have resulted in narrow angles of arrival

and departure between the Tx and Rx for the corridor scenario, over short array separation distances.

A significant drawback of the modelling approach used in [2.28], and first suggested by Jiang and Ingram in [2.29], is the treatment of the Tx and Rx arrays as point sources; resulting in the angles of arrival and departure as being the same for all elements at the Tx and Rx. In [2.29] the precise inter-element paths were calculated (and called the distributed source model) and this approach is used here and described in the next chapter. Since this method is capable of determining precise path differences then, even for LOS only channels (free space), there is a greater diversity between the calculated entries of the channel matrix or as they described it, 'the richness'. Over short ranges this is significant if the LOS is dominant, but also for cases where reflections may be limited but of reasonably good signal strength (sometimes referred to as sparse multipath). The same approach is used in the ray-tracing simulation in this thesis. For the free space model in [2.29] they determined a minimum Tx to Rx separation threshold distance, below which the point source model did not accurately provide good channel estimates. They indicated a clear improvement in capacity as inter-element spacing increased for 4x4 ULAs and suggested 1 λ as a minimum for indoor wireless local area networks (WLANs). They also estimated the capacity for broadside arrays with reflections from the model and compared this to measured capacity from 'virtual arrays' in a dedicated radio laboratory facility. Their virtual array measurements used a single element at both Tx and Rx and the arrays were simulated from repeated measurements while repositioning the antennas. This method assumes equal power at each Tx location and is the method used in simulation form here. For their measured

and modelled capacity the results were similar and showed a notable variation in capacity with element spacing. It is noted that using a virtual array for measurements does not allow for the possibility of mutual coupling, so it is possible that the small spacing examined (λ/4) is questionable. Another interesting aspect of the results, not commented on, was the fact that the CDF for λ/2 spacing was marginally better than the λ spacing and a similar result was found in this thesis. This was also the case in [2.30] in which they examined the effect of interference from another MIMO channel.

2.4.5 Adjustment of arrays

Two of the same authors [2.31] examined the effect of repositioning/adapting the locations of the antenna elements in a similar manner to that used here and in [2.32],[2.33]. They extracted data from virtual array measurements which were made with a small virtual element spacing of 0.1 λ, thus allowing them to simulate ULAs with both equal and unequal spacing along the axis of the array. For a given test location with no direct LOS components, they varied the spacing at one side of the channel (Rx) and demonstrated large capacity fluctuations. It is notable that while some were suggesting limited benefit to a wider spacing, particularly in NLOS conditions, this paper reported capacities from 28.6 b/s/Hz to 38.3 b/s/Hz at the same average SNR of 30dB with different element spacing at the Rx array. A more extreme range of 22.6 to 41 b/s/Hz was realised when both Tx and Rx arrays were adjusted. The overall array width was 6 λ, equivalent to 2 λ spacing for fixed equal spacing elements and they only adjusted the two inner elements. For the maximum values achieved (either scenario) those two elements were separated from each other by more than 2 λ but never closer than λ/2 to the outer elements of the arrays. From the limited numeric values supplied the array elements appear to almost become two separate 2x2 array structures, however

they did not comment on this aspect. It is interesting to note that results presented later in this thesis and in [2.21] indicate that 2x2 systems are often effective at providing good capacity. They also used the same virtual measurements to clearly confirm capacity scaling for arrays from 2x2 array pairs to larger 6x6 systems. They tabulated the calculated eigenvalues for maximum and minimum cases and confirmed that a single dominant value was present for poor capacity cases while four similar magnitude values (or channels) existed when maximum capacity was achieved; which is also demonstrated in this thesis.

Using a simulation they adaptively repositioned each element using a steepest descent algorithm. The method they used seems to have been similar to that in [2.29] although not explicitly described. They presented a number of results comparing simulated and measured data for a number of fixed array geometry combinations for different element spacing. There was good correspondence between the two, emphasising the suitability of the ray-tracing approach for matching virtual array measurements. The search for better element locations was done in an iterative manner with incremental moves of 0.001 λ of each element in a 4x4 array with 2 λ spacing. Over short ranges of a few metres with LOS present and NLOS they improved the capacity on the initial values by approximately 20% in less than 10 iterations requiring very small element shifts. The results presented highlight the importance of the geometric properties of the array, particularly over short ranges, and provided they are modelled in the manner of [2.29] then simulation is a good approach to investigating array geometries.

Another paper which attempted some form of adaptation to improve capacity was by Fernandez et al [2.34] in which the radiation pattern was adapted. However, the paper does not give any details regarding the conditions, such as element spacing and Tx-Rx separation distance. Furthermore, they specify 2x1 and 2x2 systems with one of the elements replaced by an array, which is adjusted in order to modify the beam pattern. Thus it is difficult to compare the results presented when the overall array geometry used is not clear. They indicated that one of their approaches was to minimise channel correlation by adjusting the radiation pattern using the least mean squares algorithm, but again it is not clear how this was done.

Indoor systems were evaluated using a two-ring scatter model for Tx and Rx by Tang and Mohan in [2.35] and they confirmed that capacity can increase with wider element spacing but also that the relative orientation of the arrays was significant; which has also been investigated in this thesis. They presented results that showed that broadside arrangements of ULAs provided better results than an in-line arrangement of the Tx and Rx and that over short ranges the reduction in capacity, due to reduced SNR levels, can be a significant factor. Similar results appeared in [2.36] in which a ray-tracing technique was used in a room containing a desk and table. Although they did not specifically comment on orientations of arrays, they considered a fixed Tx 4-element ULA (aceess point) in a corner of a square room, and a four element ULA mobile terminal moved along the length of the opposite wall. The orientations were perpendicular to each other and, at the location when they were directly opposite, the capacity significantly reduced despite the SNR being above average due to the proximity of their positions. They also presented an interesting result concerning what

they described as a ‘macro’ MIMO system. In this case the four elements of the access point were distributed to each corner of the room. This gave much higher levels of capacity than the ULA, but the suggestion of a doubling of theoretical capacity is questionable. (It may be due to them not applying any form of normalisation for different conditions, again it is not clear whether this is the case). Notwithstanding this, the suggestions that wide spacing of elements at one side of the channel is likely to produce improvements in capacity do correspond to some of the results presented in chapter 6 of this thesis.

2.4.6 Distributed MIMO systems

In other papers the concept of widely distributed antennas is termed distributed-MIMO (D-MIMO). For example in [2.37] they considered distributing the Tx array elements along the inside roof of an aircraft cabin spaced 2.9 m apart. The Rx was a ULA with 0.5 λ element spacing moved along the cabin aisle on a food trolley type conveyance. The results presented (based on channel sounding measurements) did not exceed anything that would be expected by an indoor MIMO environment of similar dimensions, for instance the 4x4 system yielded an average capacity of approximately 16 b/s/Hz for an average SNR of 20 dB, compared to an ideal of approximately 22 b/s/Hz. (This was a similar to the level of performance in [2.28] for a corridor structure). They did achieve capacity scaling with more antennas and certainly compared to a SISO system it did provide system gain. They considered what the optimum positions were for locating the Rx antennas and made suggestions that indicate the affect of wide angles of arrival/departure of the LOS components to the individual Tx elements. As a result the middle of the cabin with Tx elements at either side gave rise to the lowest correlation among Tx elements. Also, they concluded that if the Tx and Rx were close,

in the region of a metre, then larger SNR had a notable impact and a better eigenvalue distribution. If a 2x2 system is considered as an example then this is probably as a direct result of the wide spacing between the adjacent Tx elements and the consequent beneficial affect this has on LOS components is discussed later in this thesis. A question regarding distributed MIMO methods is the practicality of the wide separation of the array elements. An obvious point is that significant antenna feed wiring defeats the purpose of wireless in small spaces. If it is assumed that the wide distribution only applies to the Tx side then it may be reasonable to do this, but it is not clear that it would be beneficial compared to other geometric characteristics, such as orientation of arrays. That could explain the optimum Tx location in [2.37], and such an approach could be implemented without excessive antenna feed wiring that distributed systems may require.

In [2.38] a distributed and a conventional system were compared using ray-tracing and channel sounding and they found that the distributed approach yielded better results; similar to ideal Rayleigh conditions. An interesting aspect of the data presented was that the simulated and modelled results were the same for the conventional system (and increased for wider spacing), but ray-tracing produced slightly lower results for the distributed approach. Another paper [2.39] dealing with an outdoor environment found improved performance for a distributed access point due to the increased diversity. A notable and simple conclusion that they stated was that distributed antennas were more likely to find a LOS transmission path to the Rx, when some may be obstructed, simply because of the diverse locations of the elements. As a consequence the SNR at the Tx would be improved, on average.

2.4.7 Normalisation of MIMO channel matrix

An experimental MIMO measurement platform for narrowband channels was described by Wallace and Jensen [2.20] using various linear arrays transmitting coded modulated data streams and from which the channel matrix **H** was estimated. They applied a normalisation to the estimated channel matrix in order to remove the effect of receiver power fluctuations due to different Tx and Rx locations and varying multipath components. The same technique is applied here and is described in chapter 3. This approach is what the term 'normalisation' usually refers to in the literature and in this thesis. (Sometimes the term arises to describe 'dividing by N antennas', as in equation (2.5), which is done to constrain the total transmitted MIMO system power to be equal to that of a SISO system, to permit a valid comparison, but this is not the meaning in this thesis).

In [2.20] they did provide some examples that demonstrate that if path loss is significant, resulting in lower SNR, then regardless of the multipath richness there is a significant drop in capacity. These results were for indoor environments where transmission was between different rooms across corridors. However, assuming the Tx is fixed and Rx is moved to different locations in another room, then SNR changes are minimal. The multipath diversity and the geometric characteristics of the arrays are more significant for determining variations in capacity and this is also demonstrated by the results in this thesis. In this regard they examined the number of antennas and showed an 'excellent agreement' between measured and ideal 2x2 arrays of 2.25 λ element separation and similar results were in [2.21]. They stated that 'packing in' more antennas (up to ten) resulted in a significant drop in capacity per antenna due to higher

correlation between adjacent elements. From their results it appears that arrays larger than 4x4 would have limited benefit for indoor environments if practical matters such as system complexity and array geometry are considered, as described in [2.20]. They also considered antenna polarisation and directivity (not considered here) but the results were not particularly conclusive and would appear to be of less significance than the issue of element spacing, array orientation or size. Clearly in an indoor scenario the exploitation of multipath may be best served by omnidirectional antennas particularly if there is no dominant signal component from a specific direction.

2.4.8 Ricean channels

Tang and Mohan [2.40] claimed the first experimental validation of indoor LOS Ricean channels using a classroom for their measurements. They did impulse response measurements using four element virtual arrays implementing a circular structure for the Tx and a rectangular array for the Rx, with element spacing of 0.5 λ. They made measurements with the LOS component and obstructed LOS (OLOS or NLOS here) using an absorber panel which provided good short range blocking, but less effective as the Tx-Rx separation distance increased. The channel transfer matrix derived was normalised for a 20 dB SNR at each location using the same technique as in [2.20] for both conditions (LOS and OLOS). However, they also used the normalisation constants calculated for the LOS conditions to calculate the OLOS normalised channel matrices. This takes into account the path loss due to the removal of the LOS components and avoids an exaggerated capacity calculation for this condition. (The same technique is used in this thesis and some similar array structures were examined in [2.21]). At separation distances of 3 m and 5 m there was a notably lower capacity than ranges of about 10 m (3.5 b/s/Hz lower, according to their tables) with the LOS component.

Although not discussed in detail this is unsurprising for the array structures used and element spacing, since the LOS paths were likely to have been closely correlated. (In another paper [2.41], the same authors considered the effect of the strongest signal component and concluded that the LOS was detrimental due to the increased spatial correlation that results). At a further distance when the LOS was less dominant, the capacity was approximately 19 b/s/Hz compared to an ideal value of 22 b/s/Hz, which is a realistic value, for the conditions and was similar for different distances when the LOS was blocked. Of note in their results were the differences in performance over relatively short distances. They considered the relationship between capacity and root mean squared (rms) delay spread [2.3]. However apart from tabulating and noting a relationship there was little detail provided. This is also investigated in this thesis and the relationship is explained. Results presented earlier in [2.42] and [2.18] also noted the relationship between the capacity and rms delay spread which may partly explain the variation in capacity under obstructed LOS conditions.

Antenna spacing effects [2.43] and the evaluation of capacity for different antenna array structures [2.44] for indoor systems were considered by the same authors using a ray-tracing simulation model for large arrays of 6x6 and 8x8 dimensions. In [2.43] they considered ULAs with element spacing ranging from 0.1 λ to 5 λ for a separation distance of approximately 25 m under LOS and NLOS conditions. For both scenarios the small spacing was weaker although better in the NLOS case for which the 1 λ and 5 λ spacing were similar to Rayleigh channels. Only the 5 λ spacing achieved the same level with the LOS present. The same results (LOS) were compared in [2.44] with two other array structures, rectangular (effectively two parallel ULAs) and circular, with the

8 elements arranged with spacing of 0.5 λ or 5 λ. For the rectangular and circular arrays the results were similar but notably weaker than the ULAs. This is unsurprising in the context of the results for increasing element spacing in [2.43]. This is because both the rectangular and circular arrays have much less space between many of the elements if the various inter-element spacings are considered and not simply between adjacent elements, a factor which was not commented on in the paper. Overall there were likely to be many channel matrix entries which were similar (i.e. more correlated) particularly for the smaller 0.5 λ spacing and those results were shown to be approximately 50% of the ideal Rayleigh case (based on random matrices normalised to the same average SNR).

In [2.45] a free space scenario (LOS components only) was investigated by Sarris and Nix, to determine the minimum array element separation distance necessary for maximum MIMO capacity. Their analysis was primarily for 2x2 systems and they determined and plotted the required element spacing as a function of Tx–Rx separation distance for various frequencies, including 5 GHz. They considered short ranges and demonstrated a requirement for wider spacing as the separation distance increased. Thus, for example, at ranges of 8 m a separation of approximately 0.5 m was required for both sides of a 2x2 system. They also calculated that higher order systems would require less extreme spacing of elements thus making them feasible. The most significant aspect of the results was the confirmation of the usefulness of wide element spacing for free-space or scenarios with a dominant LOS component; also considered in this thesis. Achieving such high levels of capacity despite using only the LOS paths is shown to be completely dependent on the geometric characteristic as described in

[2.18]. Another paper from the same research centre [2.46], dealing with on-body LOS MIMO systems for personal area networks (PANs), confirmed that operating under such conditions over short ranges could result in good capacity despite the high correlation of the channel matrix.

In [2.47] the same authors examined the 2x2 system for capacity changes for various adjustments. They determined a configuration for maximum capacity and then displaced the Rx by several metres from its original location. They found the capacity was relatively insensitive to changes of up to 2 m from the optimal location. When they adjusted the relative orientation of the arrays from the optimal angle the capacity collapsed; which is similar to other results in the literature and here. They also introduced to their model some multipath (stochastically) and presented results showing the clear capacity improvement for their indoor systems as the ratio of LOS power to that of the multipath (Ricean K factor) increased. For comparison they showed the corresponding capacity decrease in a system when the Tx-Rx separation distances were much larger as explained in [2.18]. They modelled data for free-space, which compared favourably with calculations derived from measurements (channel sounding) done in an anechoic chamber. Similarly they modelled an indoor environment and made measurements in a room and found that there was far less sensitivity to the relative orientation of the Tx and Rx due to the presence of multipath. In a separate measurement in a home environment [2.48] they reported similar results for their optimal spaced arrays, but also concluded that the performance was the same as standard spaced arrays (one wavelength between elements) in NLOS conditions. Overall the various papers from these authors confirm the significance of geometric

characteristics of the arrays, orientations and Tx-Rx separation distance, particularly for indoor environments.

The affect of antenna location was also analysed by a numerical hybrid modelling method (method of moments and finite difference time domain) for 2x2 systems in [2.49]. The Tx was located at a limited number of positions (four) at one side of the room and the Rx was moved throughout a wider area on the far side of the room. A number of pillars provided obstructions in order to model the NLOS case, no pillars implied LOS present. For these two scenarios they found notable differences for the ensemble of Rx locations modelled depending on the Tx location. For the Tx near the centre point of the wall the best performance was found and this degraded for positions closer to the edge; the weakest was for the corner location. This may be explained by the same geometric characteristics discussed later in this thesis such as the angular spread of paths from the Tx elements to those at the Rx. This is, on average, better for the centre point location and poor for the corners. Also they took path loss into account (without normalisation) and this may have resulted in lower power at the Rx positions when the Tx was in the corner. Similarly they had notably lower capacity for the NLOS case due to paths being blocked by the pillars when no normalisation was applied. When they did apply normalisation to remove the effect of path loss for different Tx-Rx positions, they found roughly similar results for the LOS case. However, for the NLOS case the capacity was independent of Tx locations. This confirms the impact of the LOS component when it is dominant factor, conditions in which the geometric properties of the arrays are significant as in [2.45].

In [2.50] the impact of sparse multipath components on the LOS channel were examined using channel sounding measurements on an 8x8 indoor MIMO system and in simulations. The term ‘sparse’ is used in the sense that the LOS components, or some reflections, are likely to be dominant as far as the power at the Rx is concerned compared to typical ‘scattered’ multipath components (relatively low power reflections) and is similar to the scenarios of [2.45-48] and [2.51]. They considered the relative orientation of the arrays, broadside or perpendicular, and introduced reflections by using two metal boards either behind the arrays or between the arrays (at the sides of the channel between the Tx and Rx though not contacting the arrays). They found, as others have and in this thesis, the significance of the geometric antenna arrangement and the notable reduction in capacity for the LOS case when the arrays were rotated from broadside to perpendicular arrangements. Also, they found that when the reflections were present that the perpendicular arrangement was not as poor but of little benefit when the LOS components dominated, compared to the broadside case. In effect they determined that there were really two distinct channel propagation mechanisms that impact on the performance of the systems, the LOS components, which dominates if the spacing and geometry are suitable, but also the more varied set of paths, reflections and LOS, which give rise to a more Rayleigh like environment that is less dependent on the geometric characteristics of the overall channel environment. Similar results were presented in [2.18] [2.21] [2.51] and overall it is clear that the propagation conditions of the channel are the main determinant of achievable spectral efficiency and this can vary significantly for an indoor environment over short ranges and results presented in this thesis support that finding.

2.5 Conclusions

A range of papers relevant to the work in this thesis have been discussed. Many of them deal, in broad terms, with geometric aspects of MIMO channels and how this impacts on system performance. A goal of this thesis is to investigate such characteristics, particularly the geometry and position of arrays, and a number of the results described in the literature have been confirmed. Included were some papers in which work was done in order to improve MIMO system performance by adjusting the individual array elements. This is also investigated in this thesis and is described in chapter 6.

Some of the results described in this chapter concerning array geometries, for instance element spacing, appear contradictory with regard to conclusions. However, in the chapters that follow results derived from a reliable simulation model in which the outcomes are precisely calculated (deterministic), encompass these varying conclusions and explain them. This is done by taking into account a number of geometric and propagation factors and extensive simulation modelling. The details of the simulation model are described in the next chapter.

2.6 References

[2.1] T. Haynes, *A Primer on Digital Beamforming*, Spectrum Signal Processing, http://www.spectrumsignal.com, March 26, 1998. (last accessed 25th May 2015).

[2.2] A.J. Paulraj and T. Kailath, "Increasing capacity in wireless broadcast systems using distributed transmission/directional reception", Patent 5 345 599, 1994.

[2.3] T. S. Rappaport, *Wireless Communications*, Prentice Hall, 1996.

[2.4] K. Pahlavan and A.H. Levesque, *Wireless Information Networks*, J. Wiley and Sons, 1995.

[2.5] A. Bateman, *Digital Communication*, Prentice Hall, 1999.

[2.6] D. Gesbert, M. Shafi, D. Shiu, P. Smith, A. Naguib, "From Theory to Practice: An Overview of MIMO Space-Time Coded Wireless System", *IEEE Journal on Selected Areas in Communications*, Vol: 21 , No. 3, April 2003, pp. 281-302.

[2.7] E. Teletar, "Capacity of Multiantenna Gaussian Channels", *AT&T Bell Laboratories, Tech. Memo.*, June 1995.

[2.8] G. J. Foschini (1996). "Layered Space-Time Architecture for Wireless Communication in a Fading Environment When Using Multi-Element Antennas", *Bell Laboratories Technical Journal*, Autumn, 1996, pp. 41-59.

[2.9] J.H. Winters, "On the capacity of radio communications systems with diversity in a Rayleigh fading environment", *IEEE Journal on Selected Areas in Communications*, Vol: 5, June 1997, pp. 871-878.

[2.10] G. J. Foschini and M. J. Gans, "On limits of wireless communications in a fading environment when using multiple antennas", *Wireless Personal Communications,* Vol. 6, March 1998, pp. 311–335.

[2.11] C.E. Shannon, "A mathematical theory of communications: Parts 1 and 2", *Bell Systems Technical Journal,* Vol. 27, 1948.

[2.12] D. Shiu, G. J. Foschini, M. J. Gans, J.M.Kahn, "Fading correlation and its effect on the capacity of multielement antenna systems", *IEEE Transactions on Communications*, Vol. 48, Issue 3, 2000, pp. 502-513.

[2.13] W. C. Jakes, *Microwave Mobile Communications*. New York: Wiley,1974, pp. 60–65.

[2.14] C.N. Chuah, G.J. Foschini, R. Valenzuela, D. Chizik, J.M. Kahn, “Capacity growth of multi-element arrays in indoor and outdoor wireless channels”, *IEEE Wireless Communications and Networking Conference*, 2000, pp. 1340-1344.

[2.15] S.J. Fortune, D.M. Gay, B.W. Kernighan, O. Landron, R. Valenzuela, M.H. Wright, “WISE design of indoor wireless systems: practical computation and optimisation*”, IEEE Computational Science & Engineering*, Vol. 2, issue, 1995, pp. 58-68.

[2.16] J.B. Andersen, “Array gain and capacity for known random channels with multiple element arrays at both ends”, *IEEE Journal on Selected Areas in Communications*, Vol. 18 Nr. 11, Nov. 2000, pp. 2172-2178.

[2.17] N. Chiurtu, B.Rimoldi,”Varying the antenna location to optimise the capacity of multi-antenn Gaussian channels”, *IEEE Conference on Acoustics, Speech and Signal Processing*, Vol. 5, 2000, pp. 3121-3123.

[2.18] A. Grennan, C. Downing, B. Foley, “A Geometric Interpretation of Indoor MIMO Systems using a Deterministic Model”, *European Conference on Antennas and Propagation,* Edinburgh Nov. 2007, pp. 88-93.

[2.19] D.P. McNamara, M. Beach, P.N. Fletcher, P. Karlsson, “Capacity variation of indoor multiple-input-multiple-output channels*”, Electronics Letters*, Vol. 36, Issue 24, Nov. 2000, pp. 2037-2038.

[2.20] J.W. Wallace, M.A. Jensen, A.L. Swindlehurst, B.D. Jeffs, ”Experimental characterization of the MIMO wireless channel: data acquisition and analysis”, *IEEE Transactions on Wireless Communications,* Vol. 2, issue 2, March, 2003, pp. 335-343.

[2.21] A.Grennan, M. Davis, C. Downing, “Analysis of array geometries for indoor MIMO systems using a deterministic model”, *Loughborough Antennas and Propagation Conference*, Nov. 2012, pp. 337-341.

[2.22] D.P. McNamara, M. Beach, P.N. Fletcher, P. Karlsson, “Temporal variation of multiple-input-multiple-output (MIMO) channels in indoor environments”, *IEEE International Conference on Antennas and Propagation*, Vol.2, April 2001, pp 578-582.

[2.23] M.Herdin, H. Ozcelik, H. Hofstetter and E. Bonek, “Variation of measured indoor MIMO capacity with receive direction and position”, *Electronics Letter*s, Volume: 38, Issue: 21 , Oct. 2002, pp. 1238-1285.

[2.24] C.N. Chuah, N.C. David, J.M. Kahn, R.A. Valenzuela, “Capacity scaling in MIMO wireless systems under correlated fading”, *IEEE Transactions on Information Theory*, Vol. 48 Nr. 3, March 2002, pp. 637-649.

[2.25] A.A. Hutter, F. Platbrood, J. Ayadi, “Analysis of MIMO capacity gains for indoor propagation channels with LOS component”, *IEEE 13th International Symposium on Personal, Indoor and Mobile Radio Communications (PIMRC)*, Vol. 3, 2002, pp. 1337-1341.

[2.26] V. Pohl, V. Jungnickel, T. Haustein, C. von Helmolt, “Antenna Spacing in MIMO Indoor Channels*”,IEEE Vehicular Technology Conference*, Spring 2002, pp. 749-753.

[2.27] V. Jungnickel, V. Pohl C. von Helmolt, “Capacity of MIMO systems with closely spaced antennas*”, IEEE Communications Letters*, Vol. 7 No. 8 Aug. 2003, pp. 361-363.

[2.28] A. Burr, “Evaluation of capacity of indoor wireless MIMO channel using ray-tracing”, *International Zurich Seminar on Broadband Communication*, 2002, pp. 281-286.

[2.29] J.S. Jiang, M.A. Ingram,"Distributed source model for short-range MIMO", *IEEE 58th Vehicular Technology Conference 2003*,Vol.1, Autumn 2003, pp. 357-362.

[2.30] J.S. Jiang, M.F. Demirkol, M.A. Ingram, "Measured capacities at 5.8GHz of indoor MIMO systems with MIMO interference", *IEEE 58th Vehicular Technology Conference 2003*,Vol.1, Autumn 2003, pp. 388-393.

[2.31] J-S. Jiang, M.A. Ingram, "Enhancing Measured MIMO Capacity by Adapting the Locations of the Antenna Elements*", IEEE Personal, Indoor, and Mobile Radio Communications,* Vol.3, 2002, pp. 1027-1031.

[2.32] A. Grennan, C. Downing, B. Foley, "Application and analysis of MIMO systems using Metropolis algorithm", *Loughborough Antennas and Propagation Conference (LAPC)*, Nov. 2010, pp. 357-360.

[2.33] A. Grennan, M. Davis, C. Downing, "Near optimum array geometries for MIMO systems in a highly correlated environment", *Loughborough Antennas and Propagation Conference (LAPC)*", Nov. 2013 pp 357-360.

[2.34] O. Fernandez, M. Domingo, R.P. Torres, "Simple adaptive system to improve channel capacity", *29th U.R.S.I. General Assembly*, Oct. 2005.

[2.35] Z. Tang, A.S. Mohan, "Evaluation of the performance of indoor MIMO systems", *IEEE 6 International Symposium on Antennas, Propagation and EM Theory*, , 2003, pp. 535-555.

[2.36] F. Tila, P.R. Shepherd, S.R. Pennock, "Theoretic capacity evaluation of indoor micro and macro-MIMO systems at 5GHz using site specific ray-tracing", *Electronics Letter*s, Volume: 39, Issue: 5, Mar. 2003, pp. 471-472.

[2.37] Z. Li, F. Luan, Y. Zhang, L. Xiao, L. Huang, S. Zhou, hidong, X. Xu, J Wang, "Capacity and spatial correlation measurements for wideband distributed MIMO channel in aircraft cabin environment", *IEEE Wireless Communications and Networking Conference (WCNC)*, 2012, pp. 1175-1179.

[2.38] R. Iernon-Fernandez, J. Molina-Garcia-Pardo, L. Juan-llacer, "Comparison between measurements and simulations of conventional and distributed MIMO system", *IEEE Antennas and Wireless Propagation Letters,* Vol. 7, 2008, pp. 546-549.

[2.39] M. Alatossava, A. Taparugssanagorn, V-M. Holappa, J. Ylitalo, "Measurement based capacity of distributed MIMO antenna system in urban microcellular environment at 5.25 GHz", *IEEE Vehicular Technology Conference, 2008*. VTC, Spring, 2008, pp. 430-434.

[2.40] A. Z. Tang, A.S. Mohan, "Experimental Investigation of Indoor MIMO Ricean Channel", *IEEE Antennas and Wireless Propagation Letter*, Vol.4, 2005, pp. 55-58.

[2.41] A. Z. Tang, A.S. Mohan, "Effect of the strongest multipath component on indoor MIMO performance", *IEEE Antennas and Propagation Society International Symposium, 2005*, Vol. 2B, 2005, pp. 727-730.

[2.42] A. Grennan, C. Downing, B. Foley, "Capacity variation of indoor radio MIMO systems using a deterministic Model", *Irish Sigs. and Systems Conf.*, 2003, pp. 548-553

[2.43] L. Jiangang, L. Yinghua, Y. Wang, Z. Hongtao, C. Yuan Han, "Antenna spacing effect on indoor MIMO channel capacity", *Asia-Pacific Microwave Conference (APMC)*, 2005.

[2.44] L. Jiangang, L. Ying-hua, H Peng-fei, L. Peng, "Evaluation of capacity of indoor MIMO channel with different antenna arrays", *IEEE International Symposium on Microwave, Antenna, Propagation and EMC Technologie*s, Vol. 1, 2005, pp. 204-207.

[2.45] I. Sarris, A.R. Nix, "Maximum MIMO capacity in line-of-sight", *IEEE Int. Conference Communications and Signal Processing*, Dec. 2005, pp.1236-1240.

[2.46]D. Neirynck, C. Williams, A. Nix, M. Beach, "Personal area networks with line-of-sight MIMO operation", *IEEE Vehicular Technology Conference (63rd)*, Spring, 2006, pp. 2859-2862.

[2.47] I. Sarris, A.R. Nix, "Design and performance assessment of High capacity MIMO architectures in the presence of a line-of-sight component", *IEEE Transactions on Vehicular Technology*, Vol. 56. issue 4, 2007, pp2194-2202.

[2.48] I. Sarris, A.R. Nix, "Capacity Evaluation of LoS-optimised and standard MIMO antenna arrays at 5.2 GHz", *IEEE Spring, 2007 Vehicular Technology Conference (VTC),* 2007, pp. 554-558.

[2.49] X. P. Yang, Q. Chen, K. Sawaya, " Effect of antenna locations on indoor MIMO System", *IEEE Antenna and Wireless Propagation Letters*, Vol. 6, 2007, pp. 165-167.

[2.50] A. Knopp, R.T. Sshwarz, C.A. Hofmann, M. Chouayakh, B. Lanki, "Measurement on the impact of sparse multipath components on the LOS MIMO channel capacity", *International Symposium on Wireless Communication Systems, ,* 2007, pp. 55-60.

[2.51] A.M. Sayeed, V. Raghavan, " Maximizing MIMO Capacity in Sparse Multipath with Reconfigurable Antenna Arrays", *Selected Topics in Signal Processing, IEEE Journal*, Vol. 1, Issue 1, 2007, pp. 156-166.

[2.52] M.A. Jensen, J.W. Wallace, A Review of Antennas and Propagation for MIMO Wireless Communications", *IEEE Transactions on Antennas and Propagation*, Vol. 52, Nr.11, 1992, pp. 2810-2824.

Chapter 3 Review of Propagation Modelling and Simulation Model Description

3.1 Introduction

Because MIMO systems exploit the space-time characteristics of a communications link, the radio propagation channel is critical in determining the system performance. This chapter examines radio channel modelling and in particular deterministic techniques for MIMO systems. A review of related propagation modelling is initially presented, followed by a description of the simulation model developed for this thesis; this is based on a three dimensional method of image ray-tracing technique. The various characteristics of the base model are described and the validation by comparison with measured and other data is presented. The model, in which the precise path lengths and phases are calculated, was extended to determine the capacity of MIMO systems. Results generated by the MIMO model are comparable with those based on random matrices and other similar deterministic approaches in the literature.

3.2 Radio Channel Modelling

3.2.1 Signal coverage

The most basic approach to modelling received signal strength is to assume an unobstructed line-of-sight (LOS) path between the Tx and Rx, the so called 'free space' model. The Friis free space equation (3.1) demonstrates that the received power, $P_{r,}$ is a function of the square of the separation distance between the Tx and the Rx (LOS),

$$\frac{P_r}{P_t} = G_t G_r \left(\frac{\lambda}{4\pi R}\right)^2 \qquad (3.1)$$

where G_t and G_r are the antenna gains at the Tx and the Rx respectively, λ is the wavelength, R is the separation distance between the antennas and P_t is the transmitted power. This basic model is often extended to incorporate a ground reflection wave using an optical imaging method and is a basic ray tracing method. The 2-ray model provides a good approximation of Rx power levels for outdoor radio systems and is treated in [3.1]. Most modelling of radio channels has been concerned with predicting large scale coverage and the key factor they attempt to establish is path loss between Tx and Rx, i.e. power coverage as a function of distance/location. There are a number of path loss models based on empirical studies from which analytical models have been developed for both outdoor and indoor environments. For example, sets of data curves for median signal attenuation were developed by extensive measurement in an urban area by Okumura [3.2]. These curves give the mean attenuation as a function of distance and frequency and are used to 'plug in' values to his modelling equation; correction factor data is also available for different types of terrain.

3.2.2 Indoor propagation modelling

Indoor propagation models have also been concerned with power coverage, for instance between several rooms in a building; although network access points are now often widely distributed. The indoor environment is considered more complex due to the wide variety of partition materials and obstacles which vary. Researchers have attempted to define path loss taking into account different scenarios such as multi-storey office blocks. For instance Seidel [3.3] developed an attenuation factor model which was implemented by selecting inputs for the modelling equation from tables based on measurements from different types of buildings, number of floors and distance from the transmitter.

Saleh and Valenzuela [3.4] developed a statistical model from measurements in an indoor office/laboratory environment to predict discrete multipath characteristics. Their objective was to estimate the channel dispersion characteristics such as the root mean squared (rms) delay spread (discussed later). Their measurements indicated that the indoor environment was quasi-static apart from the movement of people. They observed that there was a temporal clustering of received rays whose amplitudes they modelled as independent Rayleigh random variables. Furthermore, they found that the impulse response was independent of antenna polarization as far as reflections were concerned. The model produced results that were a good fit to their measurements and were applicable to other buildings. However, it only dealt with time-of-arrival characteristics, and not the angle of arrival of the rays. This spatial characteristic was modelled by Spencer et al. [3.5] as an extension of the model proposed in [3.4] in order to consider systems with multiple antennas; for which the spatial characteristics are important. They found a clustering of angles was also present, although not necessarily the same rays as the temporal clusters found, the later supporting the findings in [3.4]. They also concluded from their results, obtained in two buildings, that the model could be used as a generalised representation for other buildings.

In [3.6] (German et al. and some of those involved in [3.4] and [3.5]) advanced the work by making a comparison between channel sounding and the statistical model results of [3.5] when using data from a deterministic channel modelling tool *WISE* [3.7]. The WISE tool is a sophisticated package that, in part, uses a three-dimensional (3-D) ray-tracing technique to model building propagation scenarios. Ray-tracing, discussed in greater detail below, provides both temporal and spatial information regarding the

impulse response of the environment. In [3.6] they estimated process parameters (from the ray-tracing simulation) for the statistical model in [3.5] and found a close comparison with those from measured data. They concluded that the WISE tool could provide a reliable alternative to expensive field measurements. In [3.6] they also presented some results for synthesised MIMO arrays based on the ray-tracing data and found that as the SNR increased the capacity increased linearly with increasing array size.

The availability of inexpensive computing systems makes site specific modelling realisable and at the most advanced level this permits architectural data inputs for a building. However, a model of such precision, regarding the physical characteristics of the building, is mostly concerned with predicting power coverage throughout the structure. Notwithstanding the importance of that factor for all radio communications systems, it is the characteristics of the signal components and geometric properties of the arrays which are critical in determining the performance of MIMO channels and are the primary concern in this thesis. Realistically it is not possible over large distances (across multiple rooms or floors) to accurately model small geometric effects. This scenario reduces to a non-LOS (NLOS) situation where the primary performance criterion is power delivery provided it is across an uncorrelated number of propagation paths. The complexity of these paths can be modelled in a less sophisticated simulation without reducing the accuracy of the results as far as MIMO systems are concerned. In fact, the use of normalisation to remove the effect of path loss is the most common approach employed to study MIMO systems under different geometric and propagation conditions. Furthermore the physical environment is affected by the introduction and

movement of objects and people, which is unpredictable and likely to alter results generated by precision modelling. For the work carried out in this thesis a model providing realistic spatial and temporal data was required to investigate the geometric aspects of arrays, usually under normalised SNR conditions. It was not intended to develop a simulation tool to determine power coverage or one which generated benign conditions for MIMO channels as in the case of random matrix models described below. The intention was to generate realistic simulation data that permitted various propagation conditions and array geometries to be accurately investigated.

3.3 Simulating MIMO Systems

3.3.1 MIMO channel estimation

Many of the studies detailing MIMO systems modelling compare their results with either some form of physical experimental measurement of the communication channel or estimations based on computer generated random matrix models. The purpose of these is to characterise the channel matrix **H,** including the effects of the radio propagation channel and hardware, to provide estimates of channel capacity achievable for particular propagation scenarios.

The experimental measurements divide into two categories which are broadly described as ‘true’ or ‘virtual’ techniques. In the former, actual arrays are used and one such scheme was described for an indoor environment by Wallace et al. [3.8]; which used as many as ten elements at the Tx and Rx. They made narrowband measurements centred at 2.45 GHz, in which multiple uniquely coded signals were transmitted from separate antennas. At the Rx each signal from the antennas was down converted, filtered,

sampled (for analogue-to-digital conversion) and stored for post processing in which a channel estimation was made; a complex and costly approach.

A simpler approach was described by McNamara et al. in [3.9]. They used a switched array method in which each element was excited in sequence but fast enough to assume the channel was stationary for the data recording period. A similar technique was used by Jiang and Ingram [3.10] in which a single pair of antennas were used and repositioned to different locations to represent the array elements, a so called virtual array. This is a relatively slow method and requires that the channel remains constant over the period of measurement.

3.3.2 Random matrix model

In [3.11] (Foschini and Gans) a narrowband channel assumption was made to analyse the capacity limits of antenna arrays. On the basis that there are multiple paths between the Tx and the Rx then, as the channel varies, the received signal undergoes fading. Since the channel gain and phase response is constant over a bandwidth greater than that of the transmitted signal, this is known as a flat (or amplitude) fading channel. In a statistical sense the amplitude variation of such a signal can be represented by a Ricean probability density function (PDF) which reduces to a Rayleigh distribution in the absence of dominant (typically LOS) components. In [3.11] the communications channel between each individual array element at the Tx and Rx was treated as an independent Rayleigh channel. Thus, the random matrix model took into account the number of array elements at the Tx and Rx but not other physical aspects of real channels. There was an assumption that the array elements were spaced apart by at least $\lambda/2$ when according to [3.12] these Rayleigh channels can be considered uncorrelated,

i.e. no LOS components and rich in multipath reflections; in effect ideal conditions for realising the benefits of MIMO systems.

If there are two random variables with Gaussian distributions represented along two quadrature axis of any orthogonal coordinate system the envelope is Rayleigh distributed and the phase is uniformly distributed. This Rayleigh function, with independent identically distributed (iid) variables with zero mean and unit variance, was used in [3.11] as the entries of the channel matrix **H**. These random element matrices were shown in [3.11] to be capable of producing cumulative distribution functions (CDFs) that represent high capacity channels when many matrices are generated by computer simulation. Some examples of these are presented later in this chapter and compared with deterministically derived CDFs (e.g. Figure 3.9).

$$H_{ij} = Normal\left(0, 1/\sqrt{2}\right) + \sqrt{-1}\cdot Normal\left(0, 1/\sqrt{2}\right) \qquad (3.2)$$

Each matrix realisation represents a static channel the period of which is assumed long enough for a short data transmission without the channel changing. In [3.13] there was some early work presented that found a reasonable level of matching between indoor measurements (made in a similar method to [3.15]) and predictions derived from random matrices. In particular they examined the eigenvalue distribution. However, the same author in [3.14] suggested such an approach was more limited for predicting measured channels even when more sophisticated methods were involved that attempted to take the scattering environment into account. Generally, the basic random matrix model is considered to provide results that overestimate the capacity compared to most real indoor scenarios. However, it does provide a benchmark for comparing measured or simulated results and is widely employed for that purpose. It is used in this thesis and

the term ‘ideal’ and ‘random’ is variously used to refer to data generated by random matrices whose entries are defined by equation 3.2.

3.3.3 Statistical modelling

The statistical modelling developed in [3.5] and [3.6] based on the work by Saleh and Valenzuela [3.4] was further explored in [3.15] for narrow-band indoor MIMO systems. This is referred to as the *SVA* model (Saleh and Valenzuela model with Angle statistics). They extracted parameters for the model from the high resolution measurements in [3.5], particularly those concerning the angle of arrival of signal paths. (They assumed that for an indoor environment the angle of departure was approximately the same). By running Monte Carlo simulations of the SVA model they produced probability density function plots of capacity (and magnitude and phase data) and compared these with measured data and found good correlation between them. They concluded that their model was producing realistic results because it partially took into account the physical characteristics of the channel.

Another approach, which also took into account some physical characteristics mixed with elements of a statistical approach, was used in [3.16] to investigate the fading correlation of MIMO systems by extending the ‘ring’ model first introduced by Jakes [3.12]. In this approach the Tx and Rx are centred on a ring which has reflective points located on it; sometimes only one ring is used at the Rx. Thus, using a deterministic ray-tracing approach, paths may be calculated from the scatterers on the ring to the Tx (or Rx) and between scatterers at each end of the channel if two rings are used. The connections between the Tx and the Rx may be randomly chosen and the distribution of reflection points on the ring(s) may be chosen to represent the statistical characteristics

of a given environment. For instance, closely spaced clusters on a ring may be used to represent an indoor environment.

Molisch [3.17] extended this approach for incorporating scatterers both near and far from the Tx and Rx. He also proposed the inclusion of other parameters affecting propagation including diffraction and waveguide effects mainly based on geometric calculations. Overall he proposed 11 factors for calculation of the overall channel response and provided a list of typical parameters, some based on statistical data sets and similar to the data used in earlier models, in order to define a generic model.

3.3.4 Deterministic modelling

The main advantage of statistical and related models is that they provide an efficient way of predicting the general performance of MIMO systems and can accommodate a range of physical characteristics for a given environment. They provide estimates of channel capacity analogous to how earlier propagation loss models provided information for power requirements for transmission from point to point. However, they are not appropriate for analysing specific array configurations and the impact of other geometric aspects of the environment. The most suitable approach, and the one used in this thesis, is geometric ray-tracing. This permits analysis of precise Tx and Rx array locations and can be used to investigate if arbitrary positioning of the arrays results in suboptimal performance or otherwise.

The earliest significant work that applied ray tracing to MIMO system was done by Driessen and Foschini [3.18] in which they examined mobile radio cellular systems. They used a method of images technique. Amongst the geometries they considered was

that of a simple street canyon with parallel reflectors of width 25 metres, which is similar to the basic room structure considered here. They demonstrated that if sufficient images (and thus reflections) are used then significant capacity may be calculated from such a model; comparable with a Rayleigh channel. In particular they noted that increased angular spread of rays is related to increased capacity and that the received signal envelopes became more Rayleigh-like as more images were added. When they added LOS components (creating a Ricean channel) they noted that the capacity decreased for closely spaced array elements (less than a wavelength) at the Tx and Rx.

In [3.19] a two-dimensional ray-tracing model was proposed by Burr as a ‘particularly useful technique’ for simulating indoor MIMO systems. It was noted that the significance of such a model was that it provided both the magnitude of multipath components and the angle of departure (AOD) and angle of arrival (AOA) of these components (i.e. the angular spread). It was argued that a two-dimensional model was adequate for most indoor scenarios where most reflections are either vertical or horizontal and uniform linear arrays were used. Results were presented which showed that the capacity exhibited a random like variation although generated by a deterministic model. This was attributed to the dependence of the channel matrix on the relative phase of the multipath components which add both in-phase and out-of-phase ‘in a complex and essentially unpredictable manner’. He concluded that capacity does not increase indefinitely with array size for indoor systems. Thus, for analysis of the geometric variations in array structures smaller arrays are sufficient and most likely to provide optimal capacity if the geometry is adjusted and is the approach taken in this thesis.

A similar approach was taken by Inanoglu et al [3.20] in which a two dimensional model based on vertical dipoles was used to examine capacity and how it is affected by the dielectric constant of the reflection walls. They found that changing the reflective material (from drywall to concrete) had a minor effect on the calculated capacity. They also suggest that the differences in measured capacity (derived from a channel sounding techniques) compared closely with theoretical capacity but not as closely with predictions from their model. They concluded that this was due to insufficient reflection paths and suggested that increasing these would improve the predictions. A similar approach was used in [3.21] which also suggested that oversimplification, e.g. using insufficient reflections, can lead to an underestimation of capacity compared to channel matrices whose entries are complex Gaussian representing a Rayleigh fading channel. However, it is questionable if this is realistic since more sparse conditions are often present indoors; also higher order reflections (above second order) are relatively weak indoors compared to LOS and lower order reflections [3.25]. In fact, using very high order reflections and no LOS components is essentially the same as using random matrices as suggested in [3.19].

It was also demonstrated by [3.22][3.23] that for short range geometry the approach taken in [3.19-21] underestimated capacity because of the lack of precision in calculating the various paths between the Tx and Rx elements. In [3.19] for example there was an assumption that the Tx and Rx are point sources and as a consequence the angle of departure/arrival (AOD/AOA) of rays travelling between the Tx and the Rx is the same regardless of the individual array elements. (This is described as a point-source or plane wave model). In [3.22-23] the precise path lengths between each pair of Tx and

Rx elements were calculated, which they named the distributed source model, (the name spherical-wave model is used in [3.23]). In this thesis the same method was used as it is the most suitable for detailed analysis of different array geometries over short ranges. This approach ensures that phase differences are established between a given set of rays from the various elements of the Tx to Rx, e.g. first-order reflections from a particular wall. In the point-source case only the phase differences between the reflections (group) from one wall and another are determined. In [3.23] the LOS only case was considered and they concluded that increased element spacing at the Tx and Rx improves performance significantly. This conclusion was possible due to the precise calculations of the model and they also demonstrated, by comparison with physical measurements, that the error between the distributed and point-source models was greater for increased element spacing in general, but particularly when the LOS component was present.

A significant aspect of the results presented in [3.23] was the impact of antenna spacing. They noted the positive effect of increasing it at both ends of the link. This characteristic is considered in detail here using the same modelling approach. Similarly other geometric aspects, such as the relative orientation of the Tx and and Rx arrays are considered and were treated in [3.24], which more generally considered the ‘deficiencies of common MIMO channel models with regard to indoor line-of-sight channels’. They concluded that there was no model that treated all possible variables but stated the necessity of using a spherical wave model, and not the plane-wave model, for indoor LOS MIMO channels, as adopted in this thesis.

3.4 The Simulation Model

3.4.1 Overview

Much of the work presented in this thesis is concerned with identifying factors that limit and influence short-range indoor MIMO channel performance and methods that attempt to overcome these limitations. Thus the use of a ray-tracing technique as described here is appropriate for the environment since it provides both the temporal and spatial data required as suggested in [3.22-23]. The indoor environment is largely time static and unless a precise geometric knowledge of the environment and the position of the Tx and Rx is known, then generally these characteristics are variables and unknown; certainly as far as the person installing an indoor system is concerned. Thus, a highly refined modelling of the geometric aspects of the channel are unlikely to be replicated in reality and even if they could be then any small change in some aspect, such as the orientation or position of the Rx, is sufficient to alter the values calculated by the model. Furthermore, it has been shown in [3.25] that for such an environment the received signal power is primarily determined by the LOS component if present. Otherwise the first and second order reflections are the only significant components as far as the SNR is concerned. In the context of indoor MIMO systems this is important to note since over short ranges, and particularly if some LOS components are present, then the true system capacity for a given SNR at the Rx is often dependent on a limited number of rays; so called sparse conditions. That is to say the contribution from higher order reflections to received signal strength is minimal compared to LOS and strong first order reflections, which are likely in many modern building structures.

Thus a simplified environment and technique provides an accurate means for testing the MIMO system configurations and is less likely to overestimate performance. In order to establish the validity of proposals for deploying MIMO systems it is better to avoid unduly favourable and arguably unrealistic scenarios. Ray-tracing, despite being a wholly deterministic approach suitable for examining the effect of geometric characteristics, generates results which are random-like in their characteristics as described in [3.19], thus providing realistically complex data sets when repeated computer simulations are executed. Also, the method used here may be executed in reasonable simulation time and thus permit extensive Monte Carlo testing of different scenarios, e.g. to generate 3000 realisations of a 4x4 MIMO channel requires approximately 30 minutes (on a laptop with a 2.4GHz processor and 3.4 GB of RAM).

3.4.2 Indoor propagation model

The characterisation of a wideband indoor channel is performed in the time domain by determining the channel impulse response (CIR). If an impulse is transmitted the receiver will detect multiple copies due, for instance, to reflections from walls. Practical measurement techniques using an ‘echo sounding’ method are possible and a simplified version is reasonable for simulation purposes and ray-tracing achieves this. Although diffraction and scattering, due to obstructions in the channel, gives rise to multipath signals; the model only takes into account reflections from walls, ceiling and floor in an empty rectangular room. Such reflections are dominant indoors, unless the LOS is present in which case it normally dominates. In [3.25] results are presented that show that the fluctuation in received signal power is minimal for reflections higher than second order. However, the model enables the simulation of a wide variation of conditions by varying the number of signal components and reflection strength. Figure

3.1 shows the plan and elevation of the room with dimensions used for the simulations in the following chapters.

Extending the model beyond second order reflections is likely to produce overestimated results, particularly when normalisation to remove path loss effects is employed. Normalisation, described below, is performed in order to compare different channel realisations. It effectively removes the path loss due to different Tx-Rx locations and it is often appropriate to do this when the channel itself is so complex and variable.

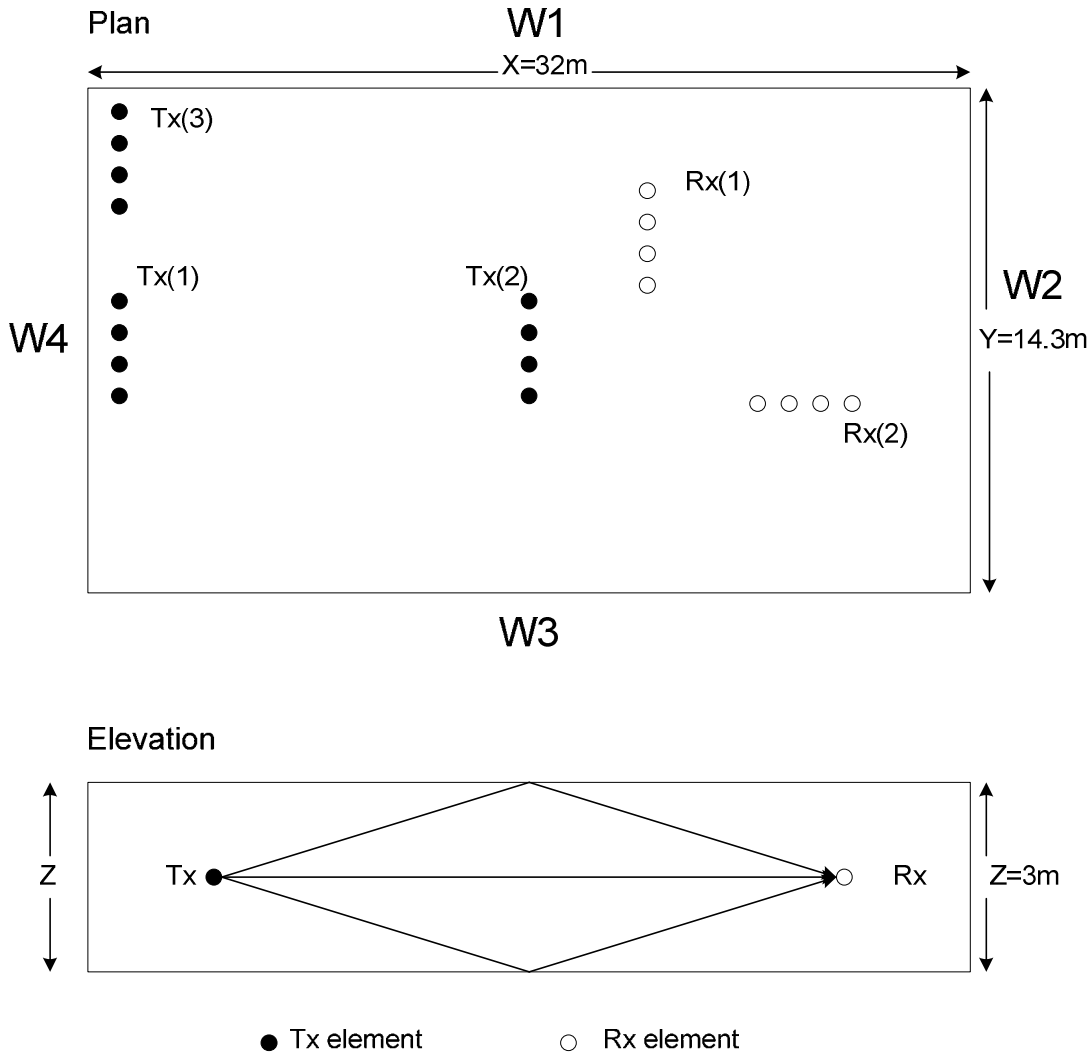

Figure 3.1 Plan and elevation of room with dimensions and representative array positions.

Intuitively it is clear that the higher the order of reflections the more ‘random like’ the fluctuations in the received power envelop at the Rx throughout the room. This may provide a benign environment for MIMO systems if considered in isolation, but is unlikely in an indoor environment unless large distances are involved with many obstructions. In such a case the level of Tx power required to achieve an arbitrary level of signal-to-noise at the Rx would have to be increased significantly compared to the same case with LOS or strong lower order reflections. The spectral efficiency of a communications system is dependent on the SNR at the Rx and to depend on weak higher-order reflections or other similar scattered signals would require increased transmission power, which partly undermines the benefit of deploying MIMO systems. In fact, the multipath nature of indoors is often far less rich than the ideal Rayleigh environment desirable for MIMO systems. Thus, limiting the model to first and second order reflections is sufficient when considering the geometric characteristic of the system and ensures reasonable computer simulation time.

3.4.3 Single-input-single-output ray-tracing model

Initially a single Tx–Rx pair (SISO system) was used to determine the channel impulse response. The method of images [3.1][3.19] based on the principles of geometric optics was used as the basis of a program to determine the various ray paths between the Tx and Rx. (A diagram describing this technique is given in appendix E, Figure E.1). When a traced ray meets a wall some of the energy is absorbed and some of the energy is reflected. This depends on the material in the wall and the angle of incidence of the reflected wave (θ). The model determines the reflection coefficient (Γ) for each surface using the relative permittivity (ε_r) of the wall material and the angle of incidence (θ). A relative permittivity of ε_r =5.0 was used, which corresponds to a typical value for

concrete materials and was used in [3.5] [3.10]. Also, it is assumed that the reflecting surface is smooth. The simulation model treated the antennas as vertically polarized and this determined which of the equations (3.3) or (3.4) was used to calculate Γ.

$$\Gamma_{||} = \frac{-\varepsilon_r \sin\theta + \sqrt{(\varepsilon_r - \cos^2\theta)}}{\varepsilon_r \sin\theta + \sqrt{(\varepsilon_r - \cos^2\theta)}} \qquad (3.3)$$

$$\Gamma_{\perp} = \frac{\sin\theta - \sqrt{(\varepsilon_r - \cos^2\theta)}}{\sin\theta + \sqrt{(\varepsilon_r - \cos^2\theta)}} \qquad (3.4)$$

These are simplified equations which are derived in [3.1] in which plots of the magnitude of reflection coefficients are given. (The plots were used for comparison to calculated values in the simulation used in this thesis). For equation (3.3) the electric field of the transmitted wave is parallel to the plane of incidence, i.e., the plane containing the incident and reflected wave, and for equation (3.4) the electric field is perpendicular to the plane of incidence. Thus, for vertical polarization (3.3) is used for the ceiling and floor (E-field normal to the reflecting surface [2.25]) and 3.4 is used for the walls. (The angle θ, the angle of incidence, is between the path of the ray and the reflecting surface and an example is shown in appendix E figure E.1).

The radiation pattern for a half wave dipole antenna was incorporated into the simulation. This required the calculation of the angle $\theta_{Tx/Rx}$ of the path of the ray relative to the vertical axis of the antenna, at both the Tx and the Rx, as described in equation (3.5). Figure 3.2 shows a typical graphical representation of the simulation output for a SISO.

$$Magnitude\ of\ Signal\ \propto \frac{cos(\frac{\pi}{2}cos\theta_{tx})}{sin\theta_{tx}} \times \frac{cos(\frac{\pi}{2}cos\theta_{rx})}{sin\theta_{rx}} \qquad (3.5)$$

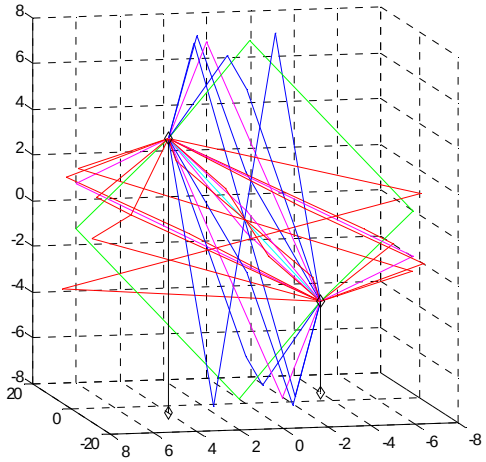

Figure 3.2 Example of ray-tracing model plot for a SISO system.

3.4.4 Validation of SISO model

The SISO system was validated by comparison with measurements done in a physical model room enclosure as shown in Figure 3.3. This was done to simplify the identification of transmission paths. The enclosure was constructed from highly reflective material mounted on boards inside a laboratory and the simulation parameters were set to match this. A vector microwave network analyzer was used to determine the impulse response in the time domain. From this response the power of the LOS signal and various reflections were identified and compared to the predicted values from the simulation model, (which permits the removal of any particular reflections or LOS component thus making it easier to identify and match particular transmission paths). Both sets of data were similar.

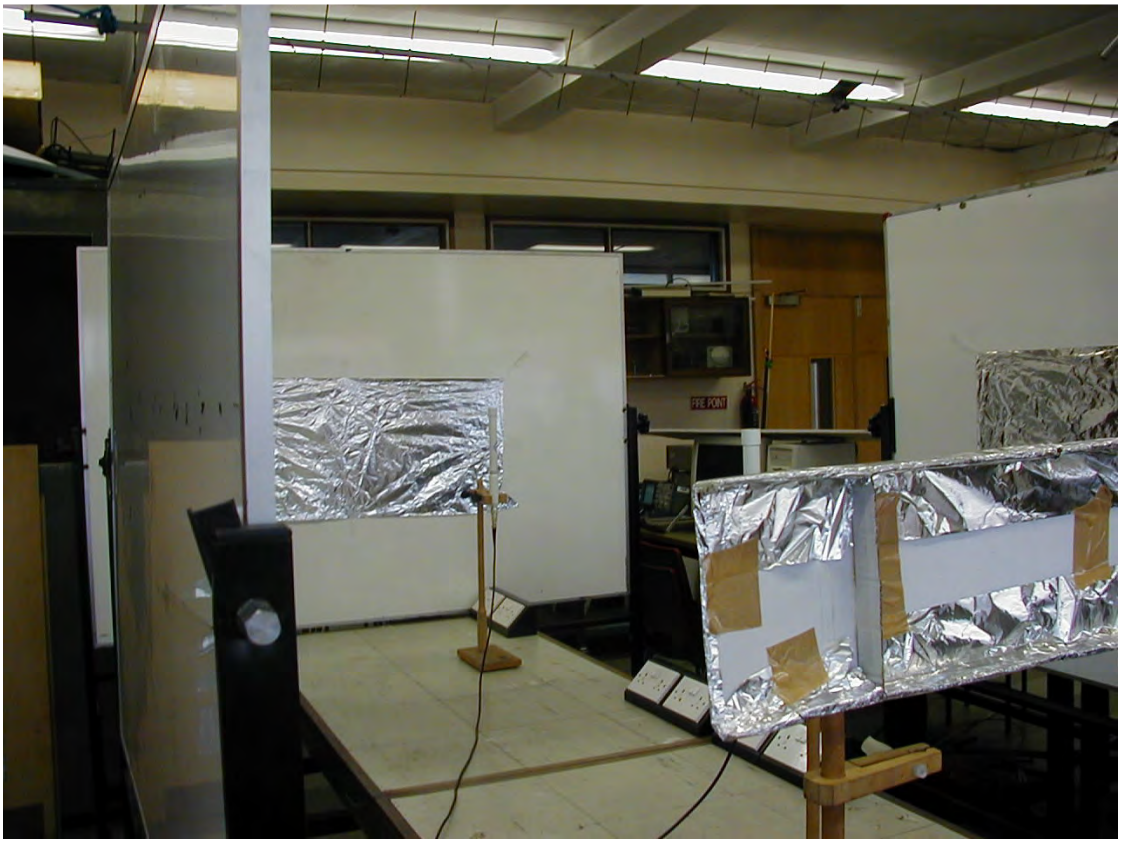

Figure 3.3 Model room used for simplified measurement and comparisons with the simulation model.

Although, a direct RF (radio frequency) pulse sounding technique, as described in [3.1], is a possible means of measuring the channel dispersion a more common and readily implemented technique is frequency domain channel sounding from which time domain data is recovered; the latter was done. This requires a network analyzer with a swept frequency oscillator, an S-parameter test set and inverse discrete Fourier transform processor. All of this is integrated into the Hewlett Packard 8753b and 85047a used and the methodology and theory is described in [3.1] [3.25] and appendix E. An example of the equivalent data downloaded for offline processing is shown in Figure 3.4. Ideally the peaks should correspond to individual transmission paths, i.e. the reflections. A pair of wideband antennas was used with a span of 1 GHz and centre frequency of 2.45

GHz. The antennas were vertically polarized and radiated omnidirectionally in the plane perpendicular to the polarization, i.e. the X-Y plane in the simulation room. This was confirmed by observation and that no significant reflective components from the ceiling or floor (top of bench) were present compared to the reflections from the aluminium-covered surfaces. Thus, only the X-Y reflections generated by the simulation were required for this purpose.

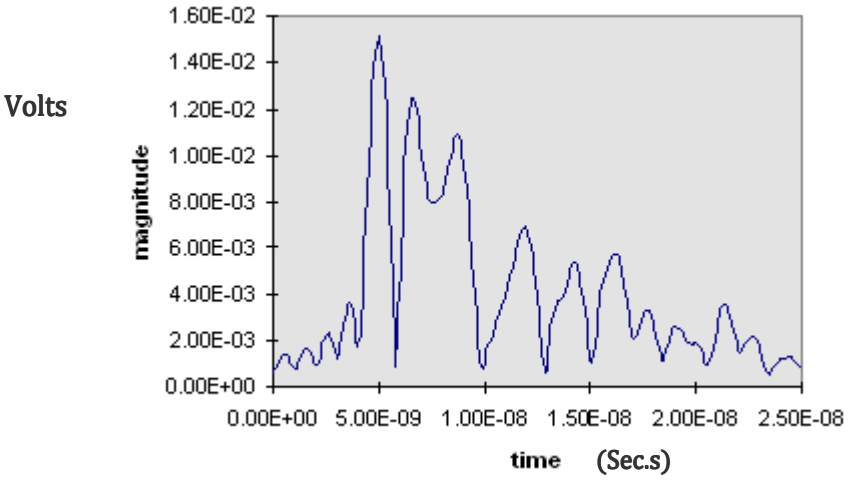

Figure 3.4 Example of time domain response obtained from network analyzer.

In order to establish a clear correspondence between the simulated and measured results a step by step approach that involved a limited number of reflections was used, using one reflection plane, i.e. one wall, then a second and so forth. Thus, in the first set of measured data with only one wall, the LOS component was present with a single first order reflection. Figure 3.5 shows the network analyzer output, green curve, and the corresponding data (the blue 'spikes') from the simulation program. The simulated magnitudes were arbitrary but the important aspect was their relative values and correspondence in the time domain to those from the network analyzer, as normalisation is applied in the MIMO simulation.

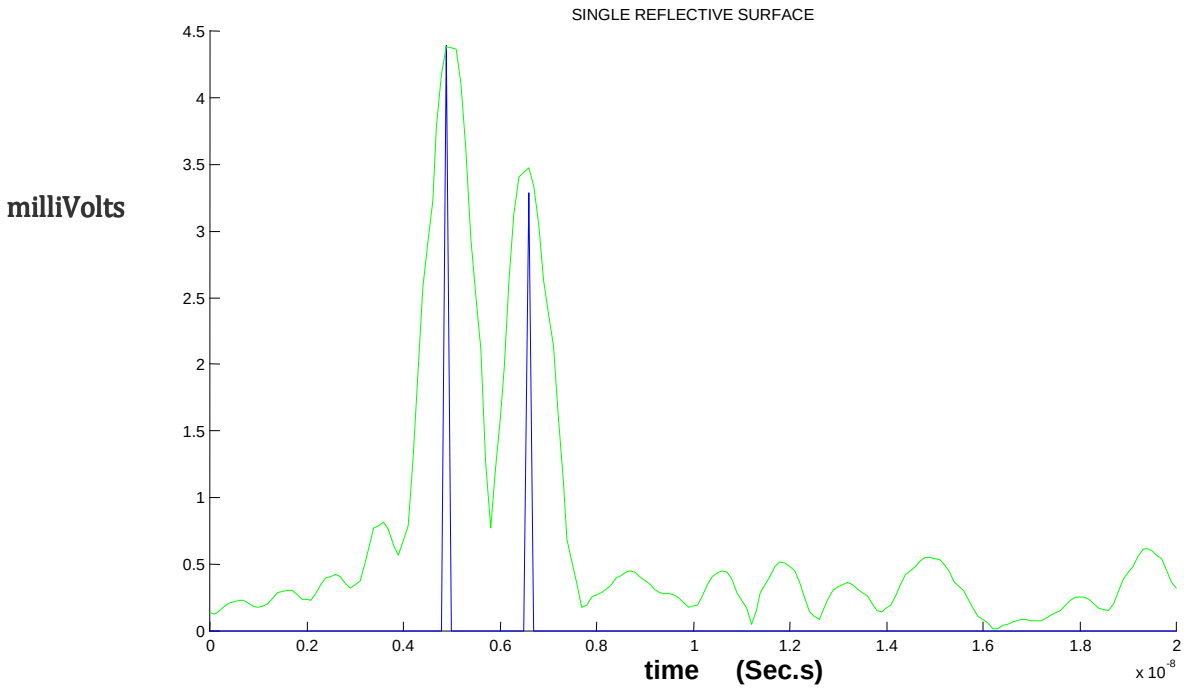

Figure 3.5 Simplified measured and simulation outputs for comparison, showing LOS component and single first order reflection. (The blue spikes are the simulated calculation of the LOS and reflection).

A reasonable path length difference was necessary in order to distinguish between different ‘pulses’ in the time domain output from the network A good match existed between both the relative magnitude and time instants of the simulated and measured data in the first case (direct and a single first order reflection) as shown in the figure 3.5. Then the second wall was introduced adding two more reflections, a first order from the extra wall and a second order from both walls. In this case there was also a strong correlation between the measured and simulated signals as shown in Figure A.1 appendix A. However, it was clear that the network analyzer was unable to distinguish between the two first order reflections that had similar path lengths. Introducing additional walls gave rise to more reflections but also more instances of resolution

problems. It was always the case that the simulated results closely corresponded in relative magnitude and time delays to those measured, notwithstanding the resolution issue.

3.4.5 Mean excess delay and rms delay spread

To compare radio channels (or more precisely the communication systems operating in them) parameters which quantify the multipath dispersion were used, notably the mean excess delay and the rms delay spread [3.1]. The mean excess delay is the average power weighted path delay relative to the shortest path, typically the LOS if present. The mean excess delay ($\bar{\tau}$) is the first moment of the power delay profile [3.1] and is defined as,

$$\bar{\tau} = \frac{\sum_k p(\tau_k)\tau_k}{\sum_k p(\tau_k)} \qquad (3.6)$$

Where τ_k is the time of the k^{th} propagation component (which is a maximum of 25 if second order reflections are considered) measured relative to the first arriving signal component (usually the LOS, k=1) and p is the associated power. The rms delay spread (σ_τ) is the square root of the second central moment of the power delay profile [3.1] and is defined to be,

$$\sigma_\tau = \sqrt{\overline{\tau^2} - (\bar{\tau})^2} \qquad (3.7)$$

where

$$\overline{\tau^2} = \frac{\sum_k p(\tau_k){\tau_k}^2}{\sum_k p(\tau_k)} \qquad (3.8)$$

If the delay spread is excessive, then in the case of a digital transmission, this will lead to intersymbol interference if the symbol period $T_s < \sigma_\tau$. Thus, the calculation of σ_τ is often used as a benchmark for comparing different receiver systems. Using the model room with four walls and taking the 12 most significant reflections (earliest arriving)

and the corresponding simulated data; the rms delay spread was calculated at 2.23 ns (model room) and 2.37 ns (simulation). Figure A.2 in appendix A shows the variation in rms delay spread (smoothed data points) with regard to distance for both the simulated and analyzer results. The LOS distance was changed for each measurement by approximately 100 mm, from 1 m to 2 m. The graph demonstrates a clear correspondence between the simulated measurements and those derived from the model room. In any real environment the actual rms delay spread exhibits wide fluctuations from one location to another as reported by Bultitude et al. [3.26]. There was a strong correspondence between the results in [3.26] generated by their simulation, which also used a similar ray-tracing model to determine delay spreads, and those generated by the simulation here; as shown by Figure A.3 in appendix A. Thus the SISO simulation data generated was an accurate representation of the impulse response of a simple indoor environment.

3.4.6 MIMO simulation model

In order to simulate a MIMO system the basic SISO model was used but with each element located in different positions to represent array elements. Thus, for a system with 4-element transmit and receive arrays (4x4), 16 iterations of the core SISO model were executed. The minimum element spacing used was λ/2 at which it was assumed that mutual coupling could be ignored. The impulse response data calculated by the model was used to compute an M x N complex matrix **H**.

$$\mathbf{H} = \begin{bmatrix} h_{1,1} & h_{1,2} & \dots & h_{1,N} \\ h_{2,1} & \dots & \dots & h_{2.N} \\ \dots & & & \\ h_{M,1} & \dots & & h_{M,N} \end{bmatrix} \qquad (3.9)$$

Each element H_{ij} of this matrix represents the complex transmission coefficient from the j^{th} antenna array element at the transmitter to the i^{th} element at the receiver array taking into account all k paths determined, thus

$$H_{ij} = \sum_k a_k e^{j(2\pi d_k)/\lambda} \qquad (3.10)$$

where a_k is the amplitude of the k^{th} component, d_k is the corresponding path distance and λ is the wavelength of the carrier. In order to analyse the channel for a fixed average signal-to-noise (SNR) ratio independent of distance, the matrix was normalised using the method described in [3.15] such that on average the power transfer between a single transmit and single receive antenna was unity. This method uses the Frobenius norm and is widely applied including in [3.27]. A normalisation constant A is calculated and the normalised channel matrix **H** used for determining the capacity was,

$$\mathbf{H} = A\mathbf{H'} \qquad (3.11)$$

where $\mathbf{H}'$ is the original matrix and A, is determined for an **M** x **N** matrix as

$$A = \left(\frac{1}{MN} \sum_{m=1}^{M} \sum_{n=1}^{N} |H_{mn}|^2 \right) \qquad (3.12)$$

The gain for the array is determined by calculating the eigenvalues, λ_i of **HH*** (see section 2.3.2).

$$\mathbf{\Lambda} = \begin{bmatrix} \lambda_1 & 0 & \dots & 0 \\ 0 & \lambda_2 & \dots & 0 \\ \dots & & & \\ 0 & \dots & & \lambda_N \end{bmatrix} \qquad (3.13)$$

The eigenvalues correspond to the channel transfer coefficients of the individual 'parallel sub channels' and the overall channel efficiency (in bits/sec/Hz) is given by

$$C = \sum_{i=1}^{m} \log_2 \left(1 + \frac{\rho}{N} \lambda_i\right) \quad \text{b/s/Hz} \qquad (3.14)$$

where N is the total number of elements at the transmitter and is divided into ρ (the signal-to-noise ratio) to maintain the total power at the same level as for the single transmitter/receiver case. This corresponds to dividing the transmit power equally at the transmitter elements and is the simplest method since it does not require a knowledge of the channel at the transmitter to implement.

3.4.7 Accuracy of MIMO model

A room size was chosen to represent a large open-plan area, for instance a laboratory as shown in Figure 3.1. Some simulations were run in which both the transmitter and receiver were randomly repositioned. The purpose of this was to generate and compare a highly randomised set of data with results predicted by random matrices**.** Although, it was not expected that the deterministically generated CDFs would be as good as the ideal case, it was necessary to determine if under different conditions the results would be appropriate and not generate significantly different or overestimated capacity data. The arrays simulated were 2x2 or 4x4 ULAs oriented broadside as shown Figure 3.1, Tx(1) and Rx(1) for example. The power level was normalised for a SNR of 20 dB at the Rx. Figure 3.6 shows CDF curves for arrays with λ/2 and 2 λ element spacing; the wave length was 0.0576 m based on a carrier frequency of 5.2 GHz. The LOS case (including all first and second order reflections), second order reflections only and the ideal Rayleigh case are shown; the latter is derived from matrices with entries using equation (3.2).

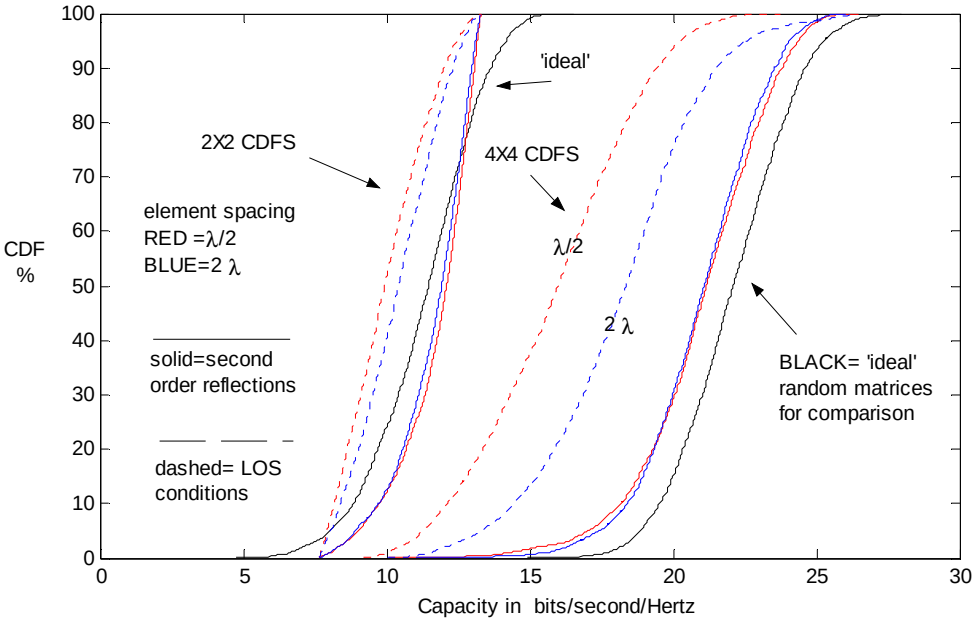

Figure 3.6 Cumulative distribution functions (CDFs) for LOS conditions (with reflections) and for second-order reflections only.

NOTE: These curves were generated from several thousand (3000) realisations of the MIMO channel for the various scenarios presented. The percentage value on the left indicates the probability of capacity being below the corresponding capacity on the horizontal axis for any particular curve, and is the same as the techniques used in [10] which examines similar problems to this thesis. In some of the literature the complementary CDFs (CCDFs) are drawn e.g. [19] or only the maximum capacity end of the curve known as the 'CCDF tails' [11]. In the later case the diagrams are emphasising the probability of the capacity being above a certain threshold level. The number of realisations (3000) used in this thesis ensures a smooth curve for easy comparison with CDFs (or CCDFs) elsewhere, e.g. [11] and requires a simulation period of approximately 30 minutes.

Second order reflections provide the most diverse set of paths in terms of angles of departure (AOD) from the Tx and angles of arrival (AOA) as suggested in [3.19]. Thus unsurprisingly, they provide CDFs that approximate those of random matrices for the 4x4 case, although with slightly lower capacities overall. This is realistic in a simple

room of similar dimensions to that shown in Figure 3.1 and demonstrates that the model is unlikely to generate overestimated results with regard to capacity level. (Although some results are presented later in the thesis, for 4x4 systems, which are almost identical to random arrays or slightly better). Similarly with the LOS and first order reflections present, the less diverse and more correlated paths, there was a notable drop in capacity. The 2x2 cases were similar although the relatively simple structure did not exceed 13.3 b/s/Hz but the mean and median values with second-order reflections only, were comparable to random matrices.

In [3.22] the discrepancy between a point source model and distributed model was discussed. The latter was deemed more accurate for short range geometries and the model used here is equivalent. For 4x4 broadside arrays they demonstrated a good correspondence between simulated data results using the latter technique and those based on measured data using a channel sounding technique. The model used in this thesis produced similar CDFs for the same array sizes, orientation and element spacing. Of note was the fact that the CDFs for 0.5 λ spacing were slightly better than those of 1 λ, also the relative capacity increase from 0.5 λ to 2 λ to 3 λ were similar. This pattern also occurred in the simulated data sets generated by the model used here (another paper by the same authors [3.23] also showed a good general correspondence with the results presented here). A key aspect of the distributed (or spherical wave) model is the ability to differentiate between similar rays, particularly the LOS components. In some of the literature this was only applied to the LOS components, but in this thesis every significant reflection is precisely calculated. This is important as some first order

reflections may be similar in strength to a LOS component, particularly if a strong reflective surface is present.

In general, investigations based on channel sounding measurements gave broadly similar results to simulated measurements using ray-tracing and often this was done by the same researchers. For both measured and simulated data the calculation was usually done with the application of normalisation, as described, to compare results at different locations while ignoring path loss.

In [3.27] a channel sounding technique was used to determine data sets for a class room (approximately half the size of the room of Figure 3.1). The estimated capacity values were broadly similar for the Tx to Rx separation distance as those generated by the simulation model here. A notable aspect of that paper was the attempt to take into account the true effect of obstructing the LOS component. This second normalisation scheme uses the normalisation constant determined for a LOS case to normalise the channel matrix for the equivalent case without the LOS component (obstructed). Thus,

$$\mathbf{H} = A_{LOS}\, \mathbf{H'}_{NLOS} \qquad (3.15)$$

Some of the results presented in Table 4.3 (chapter 4) and [3.28] were found using this approach. The results were consistent with those presented in [3.27] and largely reflect characteristics of the MIMO system performance related to Tx-Rx separation distance. Thus, for example, at close ranges the LOS may dominate and when obstructed there was a large drop in capacity, while at longer ranges there was little change.

3.5 Review of Model Characteristics

3.5.1 Model validation summary

1. The SISO model was validated against experimental measurements and generated comparable results. Also, it was used to generate dispersion characteristics and compared favourably with a similar dispersion simulation model in the literature. The SISO model is the basis of the MIMO model.

2. The MIMO simulation model generated channel matrices based on the SISO calculations. It produced CDFs, based on thousands of iterations (in which the locations of the Rx and possibly Tx was changed for each simulation) that were easily compared with those generated by large numbers of random matrices. In this regard the model did not generate exaggerated results for uniform linear arrays and exhibited reduced spectral efficiency in comparison.

3. When random positioning of both the Tx and Rx was simulated, the CDFs produced were comparable to those generated by random matrices. In some instances, for NLOS second order reflections only, the CDFs were approximately the same if small adjustments were made to the arrays (see chapter 6).

4. The MIMO simulation generated CDFs which were comparable with results in the literature for similar scenarios. For instance for uniform arrays, both simulated and measurement based analysis, for the two most common propagation scenarios considered, LOS and NLOS conditions (also see chapter 4).

5. Variation in linear array structures, e.g. element spacing and relative orientation of arrays generated results that were predictable (e.g. reduced channel correlation when the element spacing was increased for LOS conditions) and comparable with other results in the literature (also see chapter 4 and 5).

6. Variation in propagation conditions, e.g. free space only or enhancement of reflections relative to LOS components (i.e. more Rayleigh like) also produced comparable results to others in the literature that were predictable based on theory.

3.5.2 Summary of main functions of simulation model

1. Calculation of impulse response that may be used for determining dispersion metrics such as rms delay spread (σ_τ) and excess delay ($\bar{\tau}$).

2. Accurate modelling of each propagation path between Tx and Rx, not just the LOS components, which is necessary for short-range scenarios. The LOS, first and second order reflections are determined.

3. Three-dimensional calculation allows for accurate determination of the effect of varying geometric characteristics such as relative positioning of arrays and element spacing which may be varied.

4. The three dimensional model and precise determination of paths allows for the adjustment of the individual elements (in 3-dimensions) thus permitting accurate assessment of the effects of changing the geometry of the arrays (see chapter 6).

5. It is flexible and adaptable in regard to propagation conditions. It may be adjusted for investigation into LOS, NLOS and various sparse (limited number of propagation paths) scenarios. Also, enhancing reflections by changing reflection coefficient of surfaces is possible, and this can result in Rayleigh type channels and other interesting configurations of the propagation environment.

6. The propagation conditions are realistically modelled as they depend on the signal components primarily responsible for SNR at the Rx; the LOS, first and second order components only. The SNR affects the achievable capacity level and is not significantly

dependent on higher order reflections. This conservative modelling approach avoids creating benign conditions that lead to high performance results.

7. Normalisation is used to remove the effect of path loss in order to compare different Tx –Rx locations in the room under varying conditions. However, the impact of using normalisation, e.g. removal of LOS components may be compensated for in the model.

8. Relatively fast simulation time allows for extensive results to be generated which can easily be compared with results from large numbers of random matrices or other results in the literature.

The flow charts in Figure 3.7 are a simplified description of the structure of the simulation code, which was written in Matlab [29]. A summary of the simulator operation is provided in appendix E.

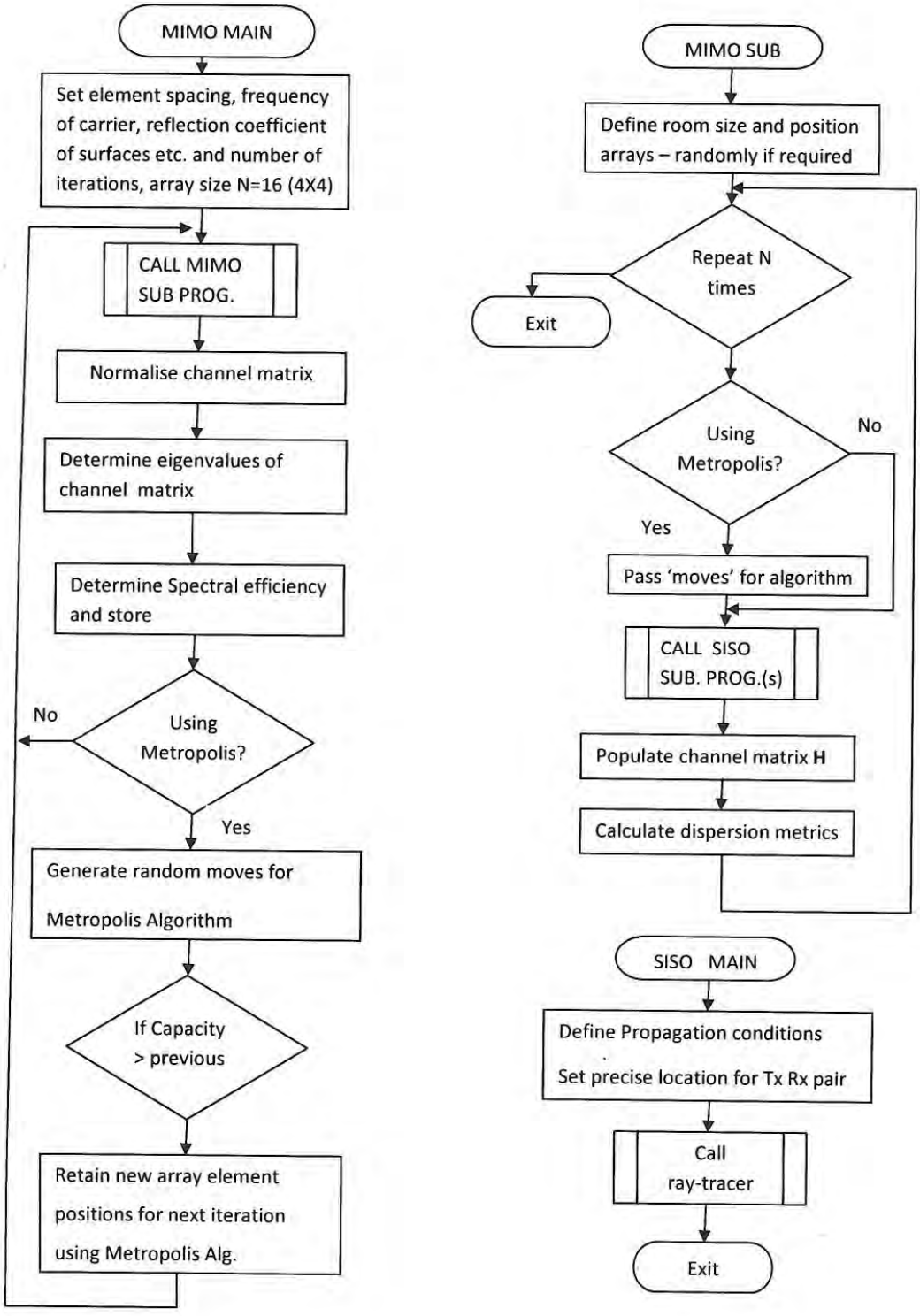

Figure 3.7 Flowchart summarising the main actions of the MIMO simulation code.

3.5.3 Limitations of model

1. Does not account for large scale variations in the physical environment, e.g. specific objects located in particular parts of the room, and the modelling scenario is a simple box structure. More complex structures or scenarios could give rise to results that are more difficult to interpret.

2. Details regarding the generation/modulation of the MIMO signals are not considered. The modelling scenario is only concerned with the interaction of the array structures, signal propagation conditions and the physical environment. This may be viewed as idealised in comparison to real systems but is a reasonable approach and consistent with the majority of research work in the field dealing with the same characteristics.

3. It is not an information theoretic approach and the capacity is indirectly calculated from the simulated impulse response using the Shannon capacity theorem; ignoring the various assumptions made in the formulation of that theorem. This may result in overestimates of the actual spectral capacity of real systems. The analysis seeks to establish the relative performance of MIMO systems for various geometric and propagation conditions and does not attempt to determine absolute real system values. However, the values derived are comparable with similar studies in the field.

4. Variations in antenna element types are not considered. Omni-directional antennas are the ideal option for MIMO systems for a wide reception of varying reflections, but may give rise to results which are overly optimistic compared to those that may occur with real antennas. This thesis simulated the radiation pattern of vertically polarised ideal half-wave dipoles only.

3.5 Summary

This chapter provided a review of radio channel modelling in general followed by an overview of the specific techniques for simulating MIMO systems. This included the random matrix model which is used as a reference benchmark throughout the thesis for comparison with results generated by the simulation model. Statistical and deterministic models were also reviewed. This was followed by a detailed description of the simulation model developed and its validation.

In that regard the objective was not to produce a simulation model that precisely replicated a given indoor scenario, but one which generated realistic data sets that would be clearly affected by geometric changes in the channel environment, for instance adjusting the dimensions, orientation or element positions of the arrays. Over short-ranges a spherical-wave ray tracing model is the best choice for taking into account spatial and temporal data that impact on MIMO channels. The simulation model developed is a tractable model capable of providing accurate results which are comparable to those found elsewhere in the literature.

3.7 References

[3.1] T. S. Rappaport, *Wireless Communications*, Prentice Hall, 1996.

[3.2] T. Okumura, E. Ohmori, K. Fukuda, “Field Strength and its variability in VHF and UHF Land Mobile Service”, *Review Electrical Communication Laboratory*, Vol. 16, Nr. 9-10, 1968 pp. 825-873.

[3.3] S.Y. Seidel, T.S. Rappaport, “914MHz path loss prediction models for indoor wireless communications in multifloored buildings”, *IEEE transactions on Antennas and Propagation*, Vol. 40, Nr.2, 1992, pp. 207-217.

[3.4] A.A.M, Saleh, R.A. Valenzuela, “A statistical model for indoor multipath propagation”, *IEEE Journal on Selected Areas in Communications,* Vol. 5, issue 2, 1997, pp. 128-137.

[3.5] Q.H. Spencer, B.D. Jeffs, M.A. Jensen, A.L. Swindlehurst, “Modeling the statistical time and angle of arrival characteristics of an indoor multipath channel”, *IEEE Journal on Selected Areas in Communications,* Vol. 18, issue 3, 2000, pp. 347-360.

[3.6] G. German, Q.H. Spencer, A.L. Swindlehurst, R.A. Valenzuela, “Wireless indoor channel modelling: statistical agreement of ray-tracing simulations and channel sounding measurements”, *Int. Conf. on Acoustics, Speech and Signal Processing (ICASSP ’01),* Vol. 4, 2001, pp. 2501-2504.

[3.7] S.J. Fortune, D.M. Gay, B.W. Kernighan, O. Landron, R. Valenzuela, M.H. Wright, “WISE design of indoor wireless systems: practical computation and optimisation*”, IEEE Computational Science & Engineering*, Vol. 2, issue 1, 1995, pp. 58-68.

[3.8] J.W. Wallace, M.A. Jensen, A.L. Swindlehurst, B.D. Jeffs, “Experimental characterization of the MIMO wireless channel: data acquisition and analysis”, *IEEE Transactions on Wireless Communications,* Vol. 2, Issue 2, March, 2003 pp. 335-343.

[3.9] D.P. McNamara, M. Beach, P.N. Fletcher, P. Karlsson, “Capacity variation of indoor multiple-input-multiple-output channels”, *Electronics Letters*, Vol. 36, Issue 24, Nov. 2000, pp. 2037-2038.

[3.10] J-S. Jiang, M.A. Ingram, “Enhancing Measured MIMO Capacity by Adapting the Locations of the Antenna Elements*” IEEE Personal, Indoor, and Mobile Radio Communications,* Vol.3, (2002), pp. 1027-1031.

[3.11] G. J. Foschini and M.. J. Gans,. “On limits of wireless communications in a fading environment when using multiple antennas”, *Wireless Personal Communications,* Vol. 6. March 1998, pp. 311–335.

[3.12] W. C. Jakes, *Microwave Mobile Communications*. New York: Wiley1974, pp. 60–65.

[3.13] R.R. Muller, H. Hofstetter, “Confirmation of random matrix model for antenna array channel by indoor measurements”, *IEEE Int. Symposium on Antennas and Propagation*, Vol.1, 2001 pp. 472-475.

[3.14] R.R. Muller, “On the Accuracy of modelling the antenna array channel with random matrices”, *IEEE International Symposium on Antennas and Propagation*, Vol.1, 2001 pp. 472-475.

[3.15] J.W. Wallace, M.A. Jensen, “Modelling the indoor MIMO wireless channel”, *IEEE Transactions on Antennas and Propagation,* Vol. 50, issue 5, March, pp. 591-599 2002.

[3.16] D. Shiu, G. J. Foschini, M. J. Gans, J.M.Kahn, “Fading correlation and its effect on the capacity of multielement antenna systems”, *IEEE Transactions on Communications*, Vol. 48, Issue 3, 2000 pp. 502-513.

[3.17] A.F. Molisch, “A generic model for MIMO wireless propagation channels in macro- and microcells”, *IEEE Transactions on Signal Processing,* Vol. 52, issue 1, 2004, pp. 61-71.

[3.18] P.F. Driessen, G.F. Foschini, “On the capacity formula for multiple input-multiple output wireless channels: a geometric interpretation”, *IEEE Transactions on Communications*, Vol. 47, Issue 2, 1999, pp. 173-176.

[3.19] A. Burr, “Evaluation of capacity of indoor wireless MIMO channel using ray-tracing”, *International Zurich Seminar on Broadband Communication*, 2002 pp. 281-286.

[3.20] H. Inanoglu, M. Menon, P. Monsen, S. Howard, “Ray based modeling of indoor channels for capacity evaluation”, *13th IEEE Int. Symposium on Personal, Indoor And Mobile Radio Communications*, Vol. 2, 2002, pp. 906-910.

[3.21] M. Elnaggar, S. Safavi-Naeini, S.K. Chaudhuri, “Effect of oversimplifying the simulated indoor propagation on the deterministic MIMO capacity”, *Canadian Conf. on electrical and Computer Engineering*, Vol. 1, 2004, pp. 221-224.

[3.22] J.S. Jiang, M.A. Ingram, “Distributed source model for short-range MIMO”, *IEEE 58th Vehicular Technology Conference*, 2003,Vol.1, Autumn 2003, pp. 357-362.

[3.23] J.S. Jiang, M.A. Ingram, “Spherical-wave model for short-range MIMO”, *IEEE Transactions on Communications*, Vol. 53, Issue 9, 2005 pp. 1534-1541.

[3.24] C.A. Hofmann, A. Knopp, D. Ogermann, R.T. Schwarz, B. Lanki, “Deficiencies of common MIMO channel models with regard to indoor line-of-sight channels”, *IEEE 19th Int. Symposium on Personal, Indoor and Mobile Radio Communications (PIMRC 2008)*, pp. 1-6.

[3.25] K. Pahlavan and A.H. Levesque, *Wireless Information Networks*, J. Wiley and Sons, 1995.

[3.26] R.J.C. Bultitude, P. Melancon, H. Zaghoul, G. Morrison, M. Prokki, “The Performance of Indoor Radio Channel Multipath Characteristic on Transmit/Receive Ranges”, *IEEE Journal on Selected Areas in Communications*, SAC. 11, No.7, 1993, pp. 979-990.

[3.27] A. Z. Tang, A.S. Mohan, “Experimental Investigation of Indoor MIMO Ricean Channel”, *IEEE Antennas and Wireless Propagation Letter*, Vol.4, 2005, pp. 55-58.

[3.28] A. Grennan, M. Davis, C, Downing, “Analysis of array geometries for indoor MIMO systems using a deterministic model”, *Loughborough Antennas and Propagation Conference*, Nov. 2012, pp. 337-341.

[3.29] Matlab, *The Mathworks Inc.*, Version 6, Release 12, Sept. 2000.

Chapter 4 Simulation Results for Regular Arrays

4.1 Introduction

This chapter provides an extensive set of data results and comment derived from the simulation model described in the previous chapter. A variety of simulation results for line-of sight (LOS) and non-LOS (NLOS) conditions for an indoor environment are presented; representing the most common propagation conditions investigated in the literature. The main focus is on 4x4 uniform linear dipole arrays and some 2x2 channels with consideration of element spacing, array orientation and some alternative 4x4 array configurations. The results are comparable with those in [4.1 - 4.8] (and other work referred to in chapter 2 and 3) which considered similar scenarios. A selection of the results was originally presented in [4.9] and [4.10].

The objective of this chapter is to demonstrate the wide variation in system performance that may occur in an indoor environment due to the geometry of the arrays, their position in the room and the propagation conditions. From the results it is clear that an arbitrary positioning of MIMO arrays in such an environment is likely to result in suboptimal system performance. The chapter concludes with some guidelines for positioning the system arrays based on the results and some commentary on related material in the literature. Some results are also presented in appendix B.

4.2 Simulation Methodology

The dimensions of the room simulated are shown in chapter 3 (Figure 3.1). A series of simulations were performed with the Tx array at a particular position and the Rx randomly positioned throughout the room at 3000 locations. The initial results presented are based on arrays with four vertically polarised dipole elements at both ends of the channel that were positioned with their axis broadside as shown, for example, by Tx(1) and Rx(1) in Figure 3.1. Some alternative orientations were simulated, for example with the Rx array axis perpendicular to the Tx array axis, e.g. Tx(1) and Rx(2) in Figure 3.1, and some 2x2 arrays. Also, a square array (the 4 elements located at corners of a square) and a cross pattern array (the 4 elements located at 4 points of a cross) were examined in the same manner. In all cases the power level was normalised for a SNR of 20 dB using the normalisation method [4.11] described earlier. Normally the transmitter was located at either the left end wall centre or in the centre of the room as shown on Figure 3.1, Tx(1) and Tx(2), and the Rx was randomly positioned 3000 times; this was performed for various element spacings, for example, $\lambda/2$, λ, 2 λ, and 4 λ. All LOS, first and second order reflections were calculated to determine the capacity.

From inspection of the CDFs of the 3000 trials, it was noted that for the majority of trials the extremes of either good or bad performance, for most scenarios, were above the 80% and below the 20% levels on these curves. By plotting the location of the sample Rx location points, above or below these thresholds, regions of probable strong and weak capacity can be identified for the particular Tx position within the room. A number of these are presented below or in the appendices and referred to as location

plots, e.g. Figure 4.2. Although the simulations presented were done in three dimensions the significance of the results that follow are clear when viewed in two dimensions, in terms of the plan of the room. Also the mean and median values for most CDF curves were approximately the same with a typical deviation in capacity from the mean in the region of +/- 15%.

4.3 Simulation Results

4.3.1 All reflections and LOS with Tx in centre of room

An important characteristic of array systems is the element spacing and this has been widely discussed including, for example, in [4.3][4.4][4.6][4.9][4.12][4.13]. Increased spacing of elements is a simple and often effective method of reducing the correlation coefficients of the channel matrix **H** (as defined at the end of the chapter in NOTE 1), particularly when a limited number of dominant transmission paths are present. This results in an improved system performance and is later analysed for the LOS paths only (free space) in chapter 5 and other sparse conditions. The drawback of this approach is the excessive element spacing that results, which is problematic when the number of array elements increases causing the overall array span to become wide, possibly many multiples of the wavelength involved. Also, under certain NLOS conditions the benefits are less clear and this was commented on in [4.12]. However, they generated a rich set of reflections for their simulation and by doing so approximated Rayleigh conditions; thus their results are not surprising in that context, i.e. there is little benefit to spacing greater than $\lambda/2$. Some of the results presented here support their conclusion with regard to similar conditions and this is discussed later. This section investigates the effect of

varying the element spacing at different array locations in a room under LOS and NLOS conditions; the latter meaning the LOS are not determined in the simulation.

The CDFs in Figure 4.1 show the performance for five different element spacing with the Tx centred in the room at Tx(2) as shown in Figure 3.1. The Rx was randomly positioned and the axes of both arrays were always broadside. For comparison the ideal Rayleigh case, based on random matrices, is also shown which has a mean of approximately 22 b/s/Hz for a SNR of 20 dB (and the equivalent SISO maximum is approximately 6.65 b/s/Hz). The mean performance for the 5 cases simulated, λ/2, λ, 2 λ, 3 λ, and 4 λ, was approximately 16, 16, 17.2, 18.7 and 20.3 b/s/Hz respectively.

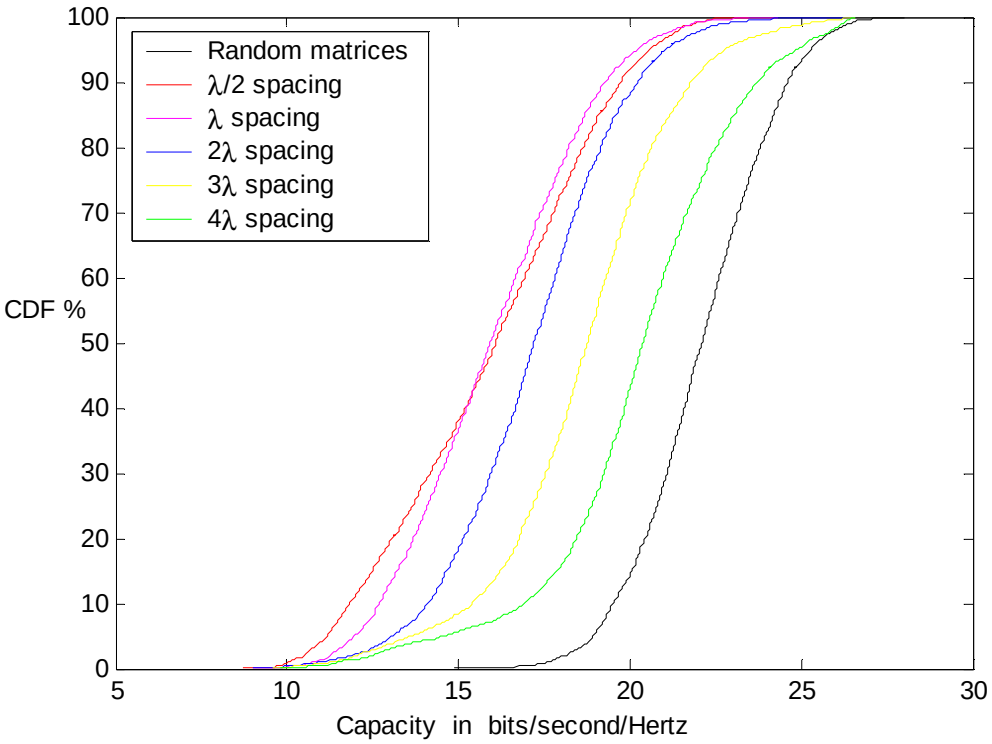

Figure 4.1 CDFs for various element spacing of 4x4 broadside arrays with Tx located at centre of room and Rx randomly positioned 3000 times.

The increased spacing generally improved the performance and the shape of the CDF curves became more similar to the ideal case for the wider 3 λ and 4 λ spacing. The shape of CDF curve tends to be more similar to that of the ideal case as the distribution of good capacity locations is widely spread throughout the room; indicative of reduced channel correlation for many realisations of the channel matrices. At λ/2 and λ spacing there was little difference between the CDF curves, the 2 λ case was only marginally better at values above the 60% level and overall the λ/2 spacing was almost as good. However, below the lower 40% level the 2 λ spacing did not deteriorate as much as the other two. In order to investigate the reasons for these results the location of the weak and strong performance positions were plotted. Figure 4.2 shows the maximum capacity positions (identified as higher than the 80% threshold on corresponding CDFs) in red, and minimum capacity locations (identified as lower than the 20% threshold on corresponding CDFs) in green, for the four cases in which the element spacing doubles from λ/2 to 4 λ.

It was evident that there was no significant capacity improvement in the region of the transmitter for the smaller element spacing of λ/2 or λ. This was due to the poor contribution from the LOS components and is explained by the narrow angular spread (angles of arrival and departure) between these components travelling from the Tx to Rx. This has been noted for the LOS only case in [4.3] and further analysed in chapter 5. Clearly this is a highly limiting factor for short range MIMO channels considering it is often the case that the LOS components are dominant and reflections may be comparatively weak. Over short ranges the LOS component is the main factor in

determining the received power and only small fluctuations occur, due to reflections, over distances of up to 5 m, as demonstrated in [4.14].

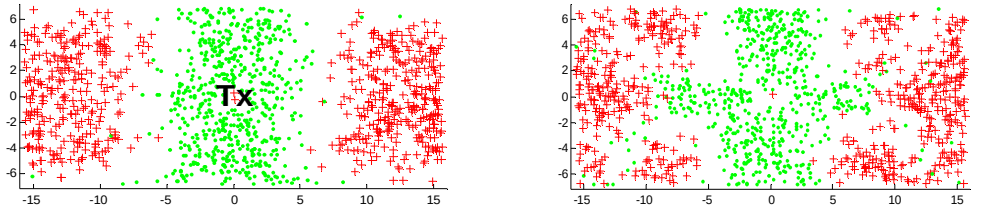

λ/2 element spacing

λ element spacing

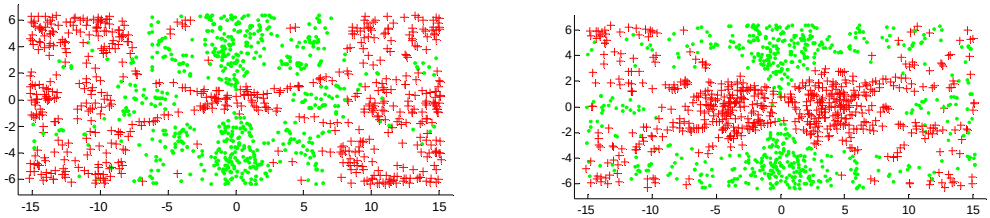

2 λ element spacing

4 λ element spacing

Figure 4.2 Location of maximum and minimum 20% of capacity with Tx at centre of room, Tx(2) on Figure 3.1. The red crosses indicate maximum; green dots indicate the minimum locations.

As the element spacing increases most of the improvement is due to the increased angular spread of LOS paths in the region close to and in front of the Tx. However, as the position of the Rx changes the angle and the capacity reduces, such that when the axes of the two arrays are in-line with each other, the capacity collapses to a minimum, due to the dominance of the LOS components over the short distance involved. In LOS

dominated or sparse multipath conditions, over short ranges, the element spacing and relative orientation of arrays are the key factors determining capacity. However, this is really a particular case; when Tx-Rx separation distances increases to several meters it is not that significant, especially if path loss is taken into account; as some results presented here will demonstrate.

4.3.2 Tx at left side of room towards centre of wall

To further establish the impact of distance, the transmitter was positioned at one side of the room as indicated by Tx(1) on Figure 3.1. Since there was symmetry in the results with the Tx in the central position, a wider variation was observed. However, it should be noted that the central position may often be an optimum location to position the Tx for overall coverage since it reduces path loss for the LOS components; which are the key components affecting the SNR level at the Rx. Figure B.1 in appendix B shows the CDF for 3 different Tx positions, in Figure 3.1 they are Tx(1), Tx(2), and Tx(3), with the Rx positions randomly varied and an array element spacing of 2 λ. The corner position was marginally weaker than the others because of the larger area over which the relative position of the Tx and Rx is close to an angle of 90 degrees, i.e. the top left hand corner to lower left hand corner region. For this reason the location of the Tx in a corner position of a room should be avoided. Thus, the remaining results focus on the case of the Tx fixed at the centre left end wall; Tx(1) unless otherwise stated. For position Tx(1) and normalised power levels at the receiver, the mean performance for λ/2, λ, 2 λ, 3 λ and 4 λ element spacing is approximately 17.2, 17.0, 17.5, 19 and 20 b/s/Hz respectively. Overall, these results were not significantly different from the centre room location. Figure 4.3(a) shows a location plot of the maximum and minimum

20% of capacity for two cases; element spacing λ/2 and 2 λ broadside arrays.

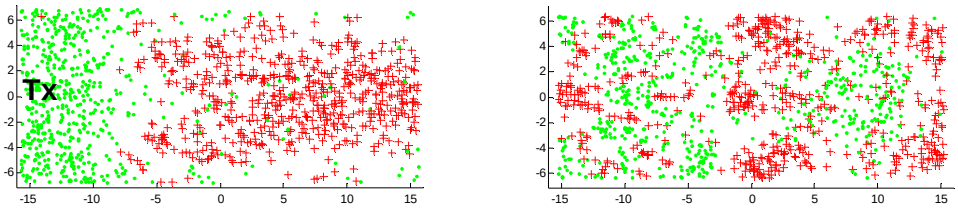

a) λ/2 elements spacing 2 λ elements spacing

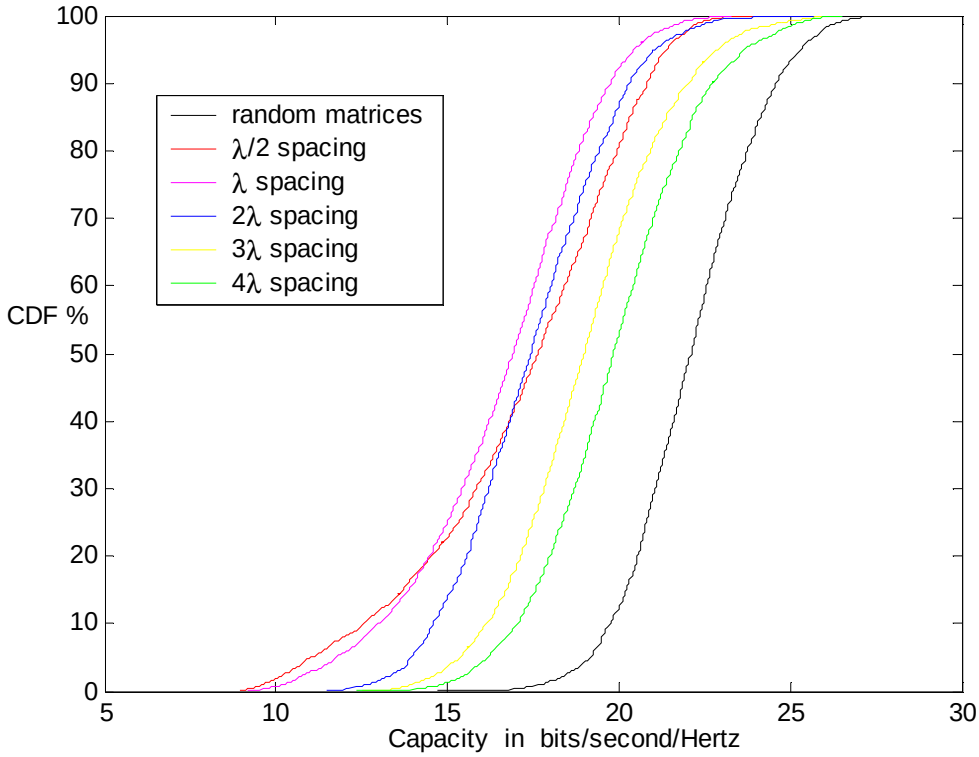

(b) CDFs Tx centre end position in room.

Figure 4.3 Tx at centre left end of room, Tx(1), simulation results. a) Indicates locations of maximum 20% (red) and minimum 20% (green) for λ/2 and 2 λ element spacing, broadside arrays, and b) is the CDF plots.

Figure 4.3(b) shows the CDF for the four cases. The overall performance throughout the room for normalised power levels was not much different for λ/2 to 2 λ element spacing and only 3 λ and 4 λ spacing are noticeably improved. However, there were some distinct variations in the locations most likely to provide weak or strong capacity and clearly to achieve levels of capacity comparable to random matrices is a challenge.

4.3.3 Various broadside array element spacings under different conditions

As expected for λ/2 spacing there was no significant contribution from LOS components in the region near the Tx, whereas there was in the case of 2λ spacing. From comparing the plots in Figure 4.3, there appeared to be two distinct regions present. The first has an approximate range of 10 m from the Tx along the central axis of the room. In this short range region, roughly one third of the room area, the LOS rays were the most significant components affecting capacity levels. Beyond this range other reflections dominated. This was verified by comparing the capacity in both regions for both the LOS case and when it was absent (NLOS), but taking into account the effect of removing those components by using the same normalisation factor [4.2]. In both cases, at distances greater than about 10 m, the capacity was reduced by approximately the same amount 1.5 b/s/Hz; representing a reduction of less than 10%. This suggests that LOS components do not contribute much, relative to the other reflection paths at longer ranges (e.g. 10 m) in the room.

This observation was also confirmed for a carrier frequency of 2.4 GHz. For the lower frequency (longer wavelength) there was increased element spacing for a given configuration (spacing specified in wavelengths). As a consequence there was some

slightly different pattern of strong locations, particularly at short ranges for wide element spacing, since the actual separation between elements was greater. The two regions, for broadside ULA array orientations, are dependent on the dimensions of the room and scale accordingly. This is approximately 30% of the area of the room near the Tx, and the remaining 70%, of a comparable rectangular room shape. For other shapes of rectangular dimensions, for instance a square or corridor structure, there are some variations in the distances which are dependent on the width (Y-dimension) relative to the length (X-dimension). This is due to the impact of reflections from the side walls relative to the LOS components and if the width is smaller the reflection path lengths are also smaller. Based on the Tx(1) position, it was observed that the range beyond which the interaction of the various multipath components is generally dominant, rather than the LOS components, is a distance equivalent to approximately 60% of the width of the room. For corridor structures (narrow room) at short ranges the the reflections from the side walls are shorter and the SNR is less dominated by the LOS components. This results in better capacity for a λ/2 element spacing in short ranges and is similar to the results in the next chapter that will deal with sparse conditions.

From Figure 4.3(a) it was observed that few high capacity values were present at less than 10 m for the λ/2 case and the mean value was only 14.3 b/s/Hz. Also, a relatively small reduction of approximately 2 b/s/Hz occurred when the LOS components were removed and accounted for, since they contributed little due to the narrow angular spread, despite being the dominant signal components over short ranges. For the 2 λ element spacing the mean capacity, with the LOS present, was similar either side of the

10 m range. However, within the 10 m range this was reduced by 4 b/s/Hz when the LOS was removed since the LOS components were much more significant contributors to the total capacity due to the wider spacing of the array elements. In [4.1] there is a suggestion that obstructing the LOS components could improve capacity since they are the most correlated group of rays. However, this does not take into account the impact on actual SNR, which affects system capacity, and over short ranges if wide element spacing is possible then blocking the LOS components is not advisable.

Although the average values from the simulations presented do not tell the whole story in terms of identifying specific good or weak capacity locations, they do provide sufficient data to explain the overall impact of different element spacing. For the various element array spacings considered here ($\lambda/2$ to 4 λ) there was a significant increase in capacity (45%) over short ranges of approximately 10 m or less, in the room considered, as the element spacing increased. However, at longer ranges the mean values changed from a minimum to maximum of less than 10% and the smallest spacing of $\lambda/2$ was slightly better than both the wider λ and 2 λ cases. When the LOS was removed and taking this into account, there was a small change of 5% beyond 10 m; indicating no significant benefits for the different element spacing considered. Tables 4.1 (a) and (b) list the mean results for various scenarios described. Thus within an indoor environment it is clear that various results may be observed that relate to a combination of factors including element spacing and Tx-Rx separation distance.

	Mean All paths	Mean with Γ=1	Rx Dist. >10 m	Rx Dist. >10 m Γ=1	Rx Dist. <10m	Rx Dist. <10m Γ=1	NLOS (Acc.) All paths	NLOS (Acc) Dist. >10 m	NLOS (Acc) Dist. <10m	NLOS (Std) All paths	NLOS (Std) Dist. >10m	NLOS (Std) Dist. <10m
λ/2	17.2	19.2	18.6	20.4	14.3	16.9	15.6	17.3	12.1	18.7	19.6	16.6
λ	16.6	19.1	17.5	20.2	15.0	17.1	14.8	16.1	12.1	18.0	18.6	17.1
2λ	17.5	19.7	17.6	19.9	17.1	19.3	15.4	16.4	13.1	18.7	18.8	19.0
3λ	19.0	20.5	19.0	20.3	19.0	20.7	16.1	17.2	13.9	19.9	19.7	20.2
4λ	19.9	20.8	19.5	20.5	20.7	21.6	16.2	17.2	14.2	20.5	20.1	21.3

a) Centre end wall (W4) Tx(1) position.

	Mean All paths	Mean with Γ=1	Rx Dist. >10 m	Rx Dist. >10m Γ=1	Rx Dist. <5m	Rx Dist. <10m Γ=1	NLOS (Acc) All paths	NLOS (Acc) Dist. >10m	NLOS (Acc) Dist. <10m	NLOS (Std) All paths	NLOS (Std) Dist. >10m	NLOS (Std) Dist. <10m
λ/2	16.0	19.0	18.3	20.3	14.6	18.4	12.5	16.3	10.4	20.2	20.6	19.9
2λ	17.2	20.2	18.4	20.8	16.5	20.0	11.9	15.7	9.9	20.1	20.3	20.0
4λ	20.3	21.8	20.5	21.4	20.3	22.0	12.4	16.5	10.2	21.2	21.2	21.3

b) Centre of room Tx(2) position.

Table 4.1 Mean capacity in bits/Sec./Hz for various conditions. (Acc) means removal of LOS component accounted for. (Std) means standard normalisation applied, not accounting for LOS.

The results presented assume the reflections were from surfaces with relative permittivity of $\varepsilon_r = 5$ (see equations 3.3 and 3.4). The power in the reflections, relative to the LOS paths, can be enhanced if a highly reflective material covers the reflecting surfaces. To simulate this scenario a reflection coefficient $\Gamma = 1$ was used in some trials. This can be viewed as an approximation for instances when some reflections are stronger and possibly some LOS components are blocked; which is possible in a real room. The results showed a general improvement in capacity throughout the room; of

approximately 10% (see Table 4.1). The effect for the six different arrays considered, was to reduce the influence of the LOS components such that the improvement for the increased spacing was notably less. It was still improved, by approximately 28% rather than 45%, at ranges less than 10 m, when comparing the 4 λ to λ/2 spacing cases. However, at longer ranges the improvement was less than 5%. This is confirmation of the reduced influence of the LOS components at longer ranges and in cases with stronger reflections; when the benefits from increased element spacing are minimal. This is similar to the scenario in [4.12] where they suggested there was little benefit from wider spacing. However, over short ranges with LOS components or near walls from which strong reflections occur; wider element spacing may be beneficial. In a real environment the situation of some blocked LOS components and some strong reflections due to metal structures is plausible. The deterministic simulation model used here was capable of providing such varied data encompassing the diverse results in the literature, for example [4.3], [4.6] and [4.12], concerning the effect of increased element spacing. A limited amount of simulations or measurements in a complex MIMO environment is likely to lead to results that cannot be readily applied more generally.

4.3.4 LOS component blocked

When the LOS was completely blocked and its removal taken into account (see equation 3.15), there was a general reduction in capacity (using $\varepsilon_{\mathbf{r}} = 5$ for reflecting surfaces). This was more pronounced over short ranges for wider element spacing, e.g, 6.5 b/s/Hz for the 4 λ case, compared to only 2.2 b/s/Hz for the λ/2 array. At longer Tx-Rx ranges the differences were less significant and the reduction was always less than 2 b/s/Hz. Thus, for different array element spacing the impact of highly correlated paths,

such as the LOS components, which have relatively low path loss associated with them, means that care must be taken in comparing normalised power level data sets in order to correctly interpret any given set of results. It has been demonstrated [4.14] that the average received power versus distance in a large room is overwhelmingly determined by the LOS component and that second (and higher) order reflections cause fluctuations around the average. Most of the pronounced fluctuations in received power over short distances are primarily due to first order reflections. This must be borne in mind when considering cases of normalised power at the Rx when the LOS components or first order reflections are omitted, giving rise to less correlated channel matrices. This tends to result in higher levels of capacity, but in reality would require a higher transmission power level to achieve the same SNR ratios without the stronger signal components being present.

Notwithstanding this point, it is still worthwhile to determine the performance under normalised power conditions for NLOS cases. Apart from the real possibility of obstructions being present to the LOS components, the complexity of the received signal power envelope over short distances is such that normalisation reduces the concerns about the capacity being affected by this characteristic rather than primarily the spatio-temporal characteristics of the channel; and that the higher order reflections have a limited impact on the SNR.

For the NLOS $\lambda/2$ and $2\ \lambda$ cases, using normalisation (and ignoring the effect of removing the LOS components) a similar pattern of results to those of Figure 4.2 were

found. This was because the first-order reflection from the left-end wall, close to the Tx, acts similarly to the LOS but is less dominant relative to the other components This results in a higher average capacity in the near 10 m range (16.6 b/s/Hz) as the other reflections have a greater impact than when the LOS component is present. However, in the area beyond 10 m, there was no significant difference in the results for arrays with different spacing.

Overall regardless of the measurement considered, the λ/2 element spacing was less effective over short ranges of 10 m compared to the wider element spacing of 2 λ. However, the former was slightly better on average, in each scenario at longer ranges that cover two thirds of the room. There was a significant improvement for the largest (4 λ) spacing over short ranges with LOS present, but in most other scenarios the benefit was limited. Also, the blocking of some LOS components is more likely as element spacing and array dimensions increase, thus reducing the SNR at the Rx and the capacity. Furthermore, the fluctuation of capacity over short distances, as shown in Figure 4.3(a) 2 λ spacing for instance, complicates the matter. Thus overall the benefits of increased element spacing are not that obvious as suggested by [4.12] in contrast to others for example [4.3][4.6][4.7][4.15] dealing with strong components such as the LOS. Results presented later clarify the benefit for enhancing capacity for the case of LOS only components (or similar) and this is significant for short range indoor environments in order to take advantage of the path loss advantage and thus minimise transmission power requirements.

Comparing the results when the transmitter is close to the wall, Table 4.1(a), with the centre room location, Table 1(b), there are some differences which are easily explained. Most obvious is the fact that a larger proportion of the room, about two thirds, are within the short range of approximately 10 m from the Tx position (centre room) and the furthest distance is approximately 15 m (half of the other case). Consequently slightly lower overall mean values were present for the $\lambda/2$ case and slightly higher for 4 λ when the LOS was present with standard power normalisation. Also, removing the LOS and taking this into account has a greater impact over the short ranges. These particular values are further affected by the lack of any relatively strong first-order reflections since the Tx is not close to any particular wall. Thus, in the NLOS case, using standard normalisation, there is little difference in any of the results for different spacing and is similar to the longer range case for Table 4.1(a). In fact the short range scenario for Table 4.1(b) is when many of the reflections will travel the same distance as the long range case for Table 4.1(a) and the results are similar. This confirms the minimal benefit of wider spacing in many NLOS scenarios; however, it also highlights the same result from Table 4.1(a) in which there is a more pronounced effect due to the impact of reflections from the wall near the Tx. Thus, the position of the Tx relative to reflecting surfaces affects measurements determining the effect of element spacing. Also, if a surface has a high reflection coefficient the first order reflections are similar to LOS components. These results confirm the significant variation that may occur in an indoor environment over relatively short distances due to the propagation conditions of the channel. Further analysis of more sparse propagation path conditions is considered in the next chapter and also the related dispersion characteristics of the channel.

4.4 Variation of Array Orientations

4.4.1 Description of array configurations

Another factor that affects measurements is the relative orientation of the arrays and this was investigated in [4.16] and [4.17]. Figure 4.4 shows three different orientations for the receiver relative to the Tx, apart from broadside considered thus far. In the first Figure 4.4(a), the Rx is rotated 90 degrees so that the plane of the axes of the Tx and Rx arrays are always perpendicular to each other and is referred to as the perpendicular case. For Figure 4.4(b) both the Tx and Rx are rotated 90 degrees and referred to as in-line. Finally, a combination of both was examined where the rotation of the Rx was adjusted for each location such that a line taken from the Rx to Tx always forms a right-angle with the axis of the Rx (in the XY plane only). This last one is referred to as 'adjusted' and effectively avoids an end-to-end orientation of the arrays and seeks to maximise the angular spread as far as the direct LOS paths are concerned. Note that if the LOS components only are considered, then increasing the element spacing tends to increase the angular spread between array elements from the Tx to the Rx. Thus, capacity is enhanced for broadside arrangement positions of the Tx and the Rx when they are directly opposite at short range in LOS conditions and is discussed further in chapter 5.

4.4.2 Perpendicular case

If one (or both) arrays were rotated from the broadside positions then the angular spread of LOS components was reduced in the region directly in front of the Tx and this affected the capacity. This can be clearly observed from the results obtained for 2 λ and

4 λ spacing, as shown in Figure 4.2, as the position of the Rx moves around the centrally located Tx.

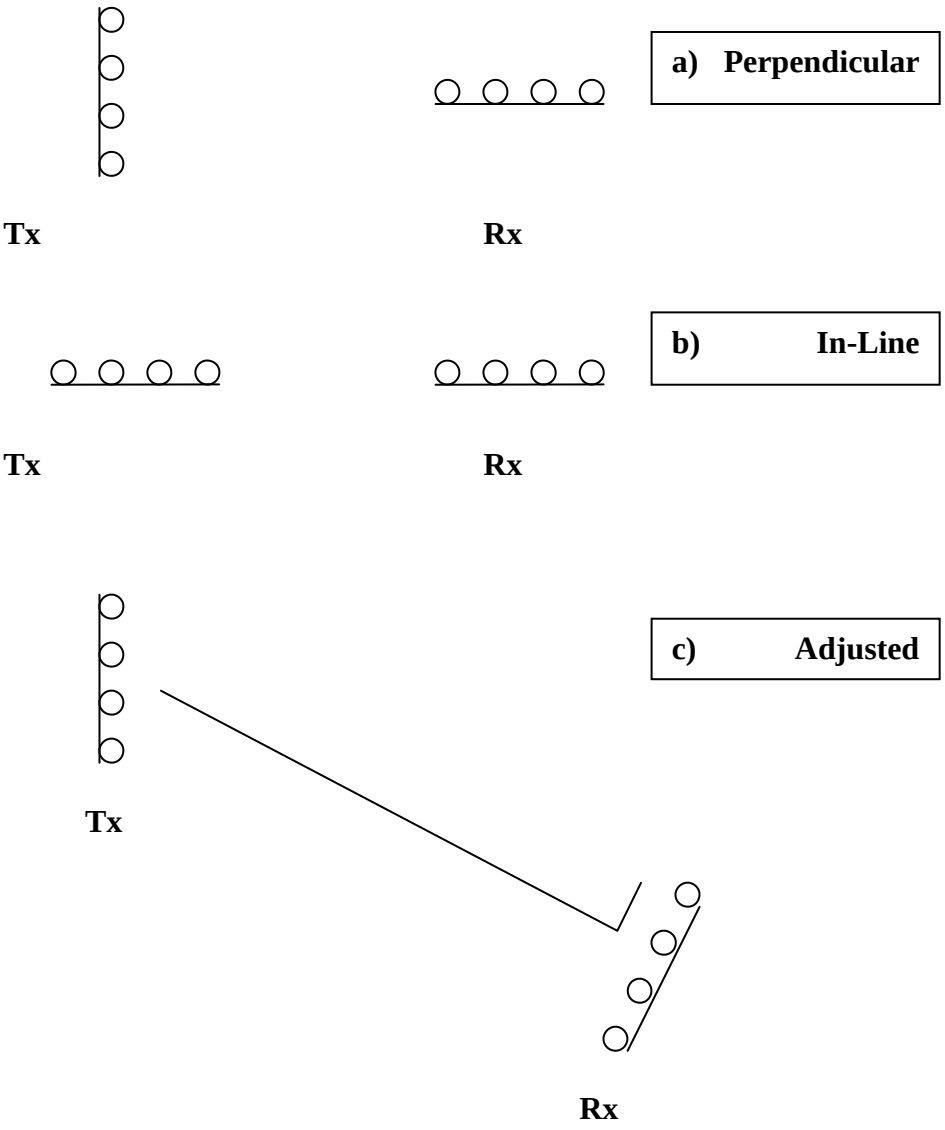

Figure 4.4 Different array orientations.

However, for the λ/2 spacing in the perpendicular case the net effect over short ranges, up to approximately 10 m, was to improve the overall contribution from LOS components. Conversely by blocking the LOS components, and taking this into account, the reduction in capacity in this region (approximately 4 b/s/Hz) was twice as much as

for the broadside case as indicated in Table 4.2. This is clear from the result in Figure 4.5 which shows the location of the weak and strong areas. This was not a reversal of the broadside case as the mean capacity beyond a range of 10 m was approximately the same; it was simply that the perpendicular arrangement was better overall for the narrow element spacing. The small element spacing was such that the rotation of the Rx affected the similar pairs of transmission paths in such a way as to increase the angular spread. This is similar to the effect discussed in chapter 5 and in [4.3][4.9] and [4.15]. The main effect of rotating the Rx was to provide improved capacity near the Tx (particularly with the LOS present) and consequently the overall performance was better.

The perpendicular rotation of the Rx also provides for an increase in the angular spreading of the reflection paths from the W1 and W3 walls (as indicated on Figure 3.1) which are parallel to the axis of the Rx array. As a result, the pattern of good locations was more widely spread around the central axis of the room. The NLOS case, shown in Figure 4.5(b), demonstrates the effect more clearly. However, as the Tx to Rx separation distance increases, for instance along the centre line of the room, the angular spread of reflections between the Tx and Rx from W1 and W3 decreases. This reduced the capacity towards the far end of the room, furthest away from the Tx. The higher capacity locations were also near the Tx towards the central line where the strongest reflection, from W4, has the greatest impact in the left side of the room.

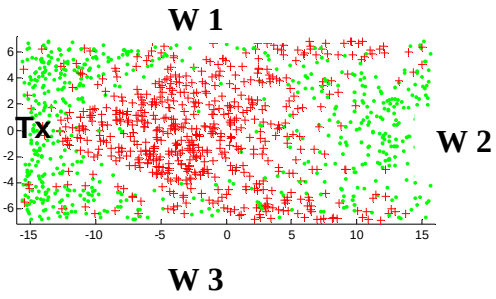

a) LOS λ/2 spacing

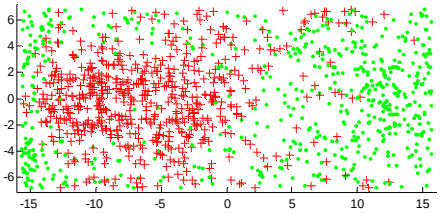

b) NLOS case λ/2 spacing

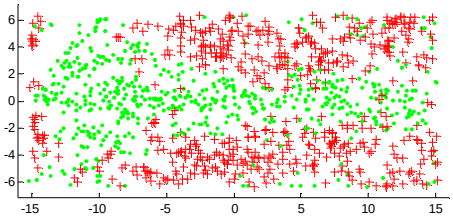

c) LOS 2 λ spacing

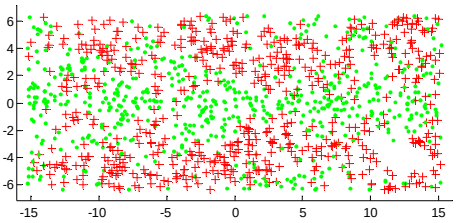

d) NLOS case 2 λ spacing

Figure 4.5 Location of maximum and minimum 20% of capacity with Tx centre left end of room Tx(1) for perpendicular array orientations. Red crosses indicate maximum, green dots minimum.

Another factor is the time separation between paths from, for example, a single element at the Tx to an adjacent pair of elements at the Rx. (This is explored in more detail in chapter 5 when the dispersion characteristics are considered). The path lengths of some reflections such as those from W1 and W3 undergo an increased difference in lengths when the Rx is rotated by 90 degrees. Consequently there is increased time dispersion between such reflections arriving at the Rx and this reduces the correlation between these components. It is shown later that an increased dispersion of reflections,

particularly for narrow element spacing tends to reduce the overall channel correlation and improve capacity. In the case of LOS components this is minimal over short ranges and is primarily due to reflections which, due to the longer paths involved, can undergo greater dispersion. Consequently this factor is more significant for the NLOS case when the first order reflections are dominant.

At a wider element spacing of 2 λ, the overall capacity was also greater than for the broadside case, by about 12%. However, the weakest region was now along the central axis of the room due to the reduced angular spread of LOS components particularly in the region close to the Tx, apart from the corners. Outside of this region the LOS contribution was still significant as the reduction in capacity was greater overall when it was removed and taken into account, as compared with the broadside case, particularly over the short ranges close to W1 and W2. At longer ranges, nearer to the walls W1 and W3, good regions were found due to the reflections experiencing greater angular spread and dispersion as indicated in the NLOS case shown in Figure 4.5(d). In both LOS and NLOS cases the central (directly in front of the Tx) section of the room is shown as the weakest region. For the perpendicular case when the reflections were enhanced (relative to the LOS) by changing the reflection coefficient of walls, the overall capacity increased slightly and the pattern of strong and weak locations was almost the same as the NLOS case.

For a spacing of 4 λ there was a further slight improvement in capacity. As would be expected the LOS case was similar to the 2 λ case and there was a wider area in the

corners of the room (Tx end) where there was good performance for both LOS and NLOS. Table 4.2 summarises the results for the various configurations of the perpendicular orientation of the arrays and the CDF of Figure B.2 in appendix B shows the overall performance for the LOS and NLOS cases based on 3000 trial locations for each curve. Enhancing the reflections for the perpendicular case improved capacity by only a small degree, approximately 6%, and did not significantly change the location of strong and weak regions.

	Mean All paths	Mean with Γ=1	Rx Dist. >10 m	Rx Dist. >10 m Γ=1	Rx Dist. <10 m	Rx Dist. <10 m Γ=1	NLOS (Acc.) All paths	NLOS (Acc) Dist. >10 m	NLOS (Ac) Dist. <10 m	NLOS (Std) All paths	NLOS (Std) Dist. >10 m	NLOS (Std) Dist. <10 m
λ/2	18.1	19.2	18.3	19.1	17.8	19.4	15.5	16.3	13.9	18.8	18.5	19.3
2λ	19.7	21.0	20.1	21.1	19.0	20.9	17.1	18.2	14.6	20.7	20.7	20.6
4λ	20.4	21.4	20.5	21.3	20.3	21.6	17.4	18.6	15.1	21.2	21.07	21.47

Table 4.2 Perpendicular orientation results summary. (Acc) means removal of LOS component accounted for, and (Std) means standard normalisation applied; i.e. not accounting for LOS path loss.

4.4.2 In-line case

In this case the angular spread of the LOS components (see section 5.2.2 also) was significantly reduced for much of the room and this resulted in reduced capacity compared to both the broadside and perpendicular arrangements for the λ/2 case, (it was 12.9 b/s/Hz overall, compared to 17.2 and 18.1 respectively). Over short ranges the drop in capacity due to removing the LOS component was only 1 b/s/Hz, indicating its limited contribution despite being the strongest components. In the regions near the Tx towards the corner area of the room, the configuration is equivalent to the broadside

arrangement and as such there was a reasonable level of performance for the various element spacings.

For both 2 λ and 4 λ spacings there was only a slight reduction in the overall performance level compared to the other configurations for the LOS cases, indicating the usefulness of a wider spacing for this orientation of arrays. However, of more significance in this regard was the NLOS case which was slightly better than the broadside case and took advantage of the increased angular spread and dispersion associated with reflections from W1 and W3 (see Figure 3.1). Figure 4.6 illustrates this point where the strong regions were primarily beyond 10 m and either side of the central axis of the room. Thus there are two factors, namely orientation of arrays and particular location of Tx and Rx, that can lead to differing conclusions about the benefits of increased array width under NLOS conditions. Enhancing the reflections for this case gave an improvement of approximately 12%, emphasising the greater influence of the reflections, relative to the LOS components. In effect as far as reflections from W1 and W3 are concerned, the arrays can be viewed as broadside. Thus, for array positioning in NLOS conditions, wider element spacing can result in improved capacity if the orientation of the Rx is broadside to a surface with a high reflection coefficient. It is possible that surfaces which produce strong reflections may be present, or introduced, and this would increase the likelihood of achieving this. The CDFs for the in-line case are shown in Figure B.3 appendix B.

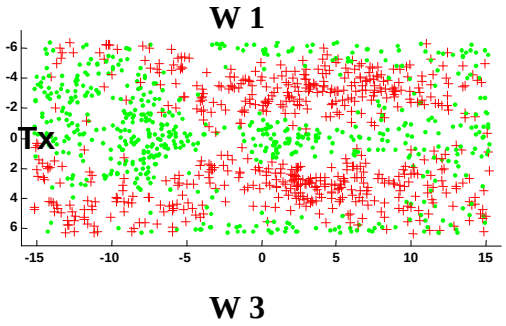

Fig 4.6 In-line orientation 2 λ element spacing broadside NLOS case.

4.4.2 Adjusted case

For the adjusted Rx array case there was a similar pattern to the broadside trials but overall the performance was slightly weaker for both LOS and NLOS cases. For 2 λ and 4 λ spacings there was a clustering of good performance towards the region in front of the Tx which was similar to the broadside case. Overall there were no significant differences in the patterns of weak and strong locations. The CDFs in Figure B.4 appendix B illustrate the benefit of wider element spacing for the NLOS case for this approach. In general small adjustments of the entire array do not yield much difference in overall performance compared to the broadside case. However, it is also clear that larger rotations, or simply relocations, can have a significant effect on performance and must be considered before positioning the arrays in a MIMO system.

4.5 Different Array Configurations

4.5.1 Description of array configurations

The other main array structures considered were 2x2 systems and variations on 4x4 systems, i.e. square 4x4 arrays and a cross configuration 4x4 as shown below in Figure

4.7. These are effectively pairs of 2x2 arranged parallel or perpendicular or may be considered as circular arrays, i.e. the elements are at various points on a circumference of a circle whose dimensions are dependent on the element separation distance.

Figure 4.7 Square and cross array pattern in XY dimension of room.

4.5.2 Two element arrays

The 2x2 simulations could not achieve the highest levels of capacity possible using random matrices and generated data sets with values ranging from approximately 8 to 13 b/s/Hz. About 15% of random matrix samples were above this level with the top 5% exceeding 14b/s/Hz. This may appear to reduce the attractiveness of 2x2 systems; however the mean values achieved by these smaller arrays were relatively good compared to the corresponding 4x4 cases when compared to the mean values for ideal Rayleigh channels. Figure 4.8 shows a selection of the CDFs for the case of randomly repositioning both the Tx and the Rx for both the broadside arrays and perpendicular 2x2 arrays. The accompanying table lists the mean values and it is notable that the perpendicular configurations is generally weaker and in the case of second order only reflections the results for $\lambda/2$ and 2λ element spacing are similar.

There was little difference between the weak and strong regions for 2x2 and 4x4 systems when the Tx was fixed, for instance, at the left centre end as in most of the preceding results. As an example Figure B.5 in appendix B shows the distributions for

the λ/2 case all paths broadside (a) and perpendicular (b) configurations. As in the case of the 4x4 systems over short ranges there was a low capacity due to the strong correlation of LOS components. Also, since the angular spread was much reduced at longer ranges the performance of the perpendicular arrangement falls away after about 20 m.

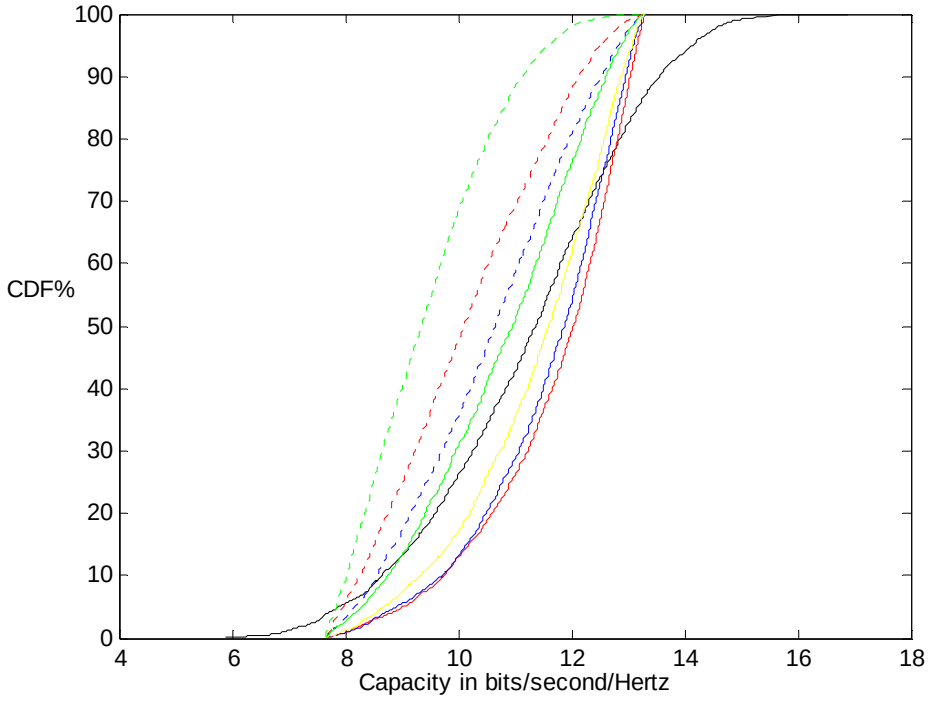

2x2 Array	λ/2 spacing LOS All paths	λ/2 spacing Second Ord.	2λ spacing LOS All paths	2λ spacing Second Ord.
Broadside	10.2 (red)	11.7 (red)	10.6 (blue)	11.6 (blue)
Perpendic.	9.5 (green)	10.8 (green)	10.4 (yellow)	11.3 (yellow)

Figure 4.8 CDFs for 2x2 arrays broadside (solid) and perpendicular (dashed) and table showing mean values and legend. Second Ord. refers to reflections.

4.5.3 Square and cross arrays

The square and cross array structures did not yield any improvement compared to the standard broadside arrangement. The results presented in Table 4.3 are for the case of both the Tx and Rx being a square or cross array structure which were broadside to each other as shown in Figure 4.7 (with both being either square or cross). The results were generally a little better when the Tx remained as a ULA and only the Rx was modified; by about 1 b/s/Hz. or less and is summarised in Table B.1 appendix B. For an inter-element spacing of λ/2, for both cases, the capacity was notably less than for ULAs. Under NLOS conditions with a wider spacing of 2 λ they performed, on average, the same as the broadside case.

The square array behaved similarly to the perpendicular arrangement of 2x2 arrays (see figure 4.4) in that, similar to Figure B.5(a) in appendix B, the best performance was within a region that was neither too close or far from the Tx. This was consistent as the pair of square arrays could be viewed as two sets of 2x2 in perpendicular configuration. Figure B.6(a) in appendix B shows the regions of minimum and maximum capacity for the λ/2 square array with all paths. The capacity within the good region shown, close to the centre of the room, was almost 20 b/s/Hz, compared to the overall average of less than 17 b/s/Hz. The cross array structure example shown in Figure B.6(b) in appendix B was for an element spacing of 2 λ. This had a similar performance to the λ/2 broadside case in that the region near the Tx was weak but there was a good spread of strong locations beyond 10 m. In effect the cross array, particularly concerning LOS paths over short ranges, appears to approximate a 3 element linear array with a slightly wider span

than the 4 element λ/2 broadside case (which has a total width of 1.5 λ, compared to 2 λ). Unsurprisingly the mean capacity values for both cases were similar at 17.2 and 16.8 b/s/Hz (cross array). Selections of CDFs are shown for comparison in Figure 4.9 and the mean values are listed in the accompanying table.

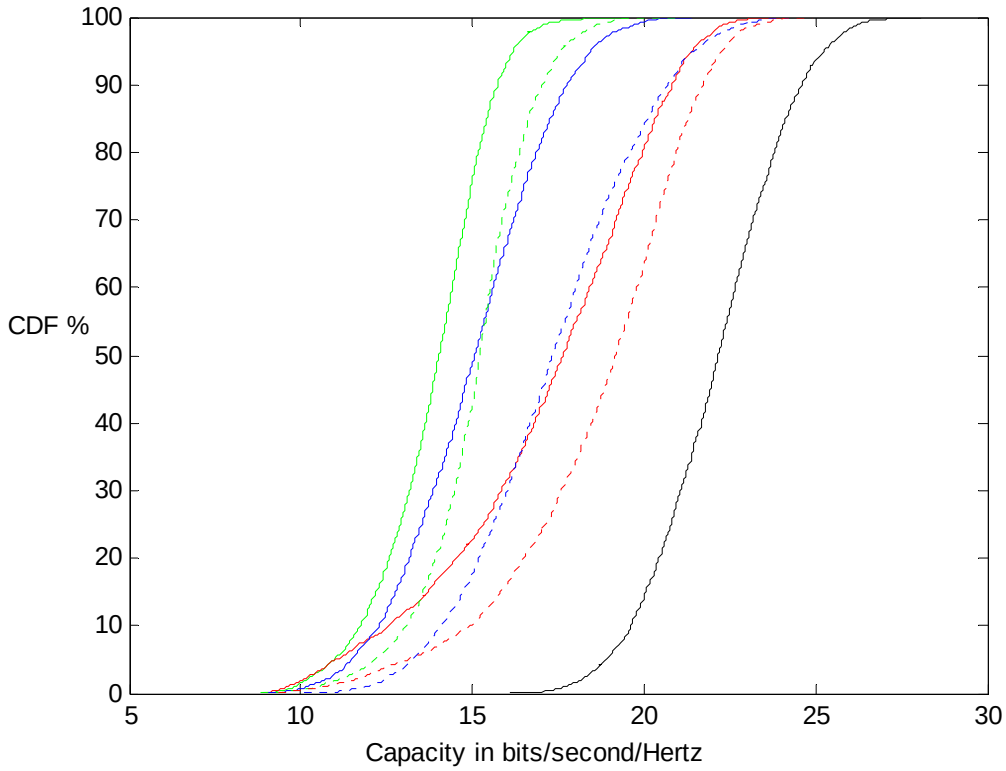

4x4 arrays	Square λ/2 (green)	Cross λ/2 (blue)	Broad λ/2 ULAs (red)	Square 2λ (not shown)	Cross 2λ (not shown)	Broad 2λ ULAs (not shown)
All Paths (solid)	13.9	15.0	17.2	17.0	16.8	17.5
NLOS (dashed)	15.1	17.4	18.7	18.4	18.4	18.7

Figure 4.9 CDFs for square, cross and ULAs (all broadside arrays) with table showing mean values and legend. The black curve represents the Rayleigh distribution.

The main reason for avoiding array structures different from ULAs is that overall the inter element spacing, not just of adjacent elements, is reduced. Thus, for example, the spacing between the outer elements in a linear array is large compared to the widest spacing in a circular array with the same spacing between adjacent elements. The consequence is an overall increase in the channel correlation and lower capacity, particularly when LOS dominated conditions are present. In [4.18] they also found that linear arrays performed better than rectangular or circular structures although at relatively wide spacing (5 λ). They used a similar room dimension as here but only considered a single location for the Tx and randomly positioned the Rx in the room, for LOS conditions, and gave no explanation of why this occurred. The square and cross array do provided a more compact structure which may have some advantage for certain system deployments where space is limited. Also, the cross array may be a reasonable choice under strong reflection conditions as discussed below.

4.5.4 Comparison of various array structures at Tx-Rx ranges >10 m in room

As much of the performance was significantly different at short ranges compared to longer ranges, further than 10 m (within the room structure and dimensions considered) and possibly as little as 5 m, a number of the configurations were compared in this regard. Table 4.3 lists the mean capacities for the various array configurations, with the Tx located as shown in Figure 3.1 at Tx(1) position, and a separation distance greater than 10 m. The table includes an estimate of the true effect (on capacity) of removing the LOS component [4.9] since the SNR is reduced; for which there was a general reduction of over 2 bits/sec/Hz in the mean values for 4x4 systems, corresponding to more than 12% of typical capacity. It was estimated that a 20 db SNR at the Rx for LOS

conditions would in fact require approximately 21.4 dB SNR to compensate for the removal of the LOS components beyond 10 m, thus requiring a higher transmission power. At shorter ranges this was more exaggerated and taking advantage of the LOS components with wider element spacing is the best option. Also included, is the result for when $\boldsymbol{\Gamma} = 1$ (a perfect reflecting surface) which enhanced the power in the reflections relative to the LOS components. This is equivalent to raising the SNR levels but without raising the transmission power, a not insignificant issue because a stronger more diverse Rayleigh like set of reflections tends to result in higher capacity. Some trials, with a limited surface area acting as a perfect reflector, did not appreciably affect the results; hence large areas on as many surfaces as possible are required to have a high reflectivity. If for example only a single first order reflection is enhanced then, in effect, it becomes similar to another highly correlated component similar to the LOS and with limited benefit. (Higher order reflections not considered here, could be notably stronger if multiple surfaces are good reflectors; resulting in benign conditions for MIMO systems). The table also includes some results for cases where the Tx (ULAs only) has a wider element spacing than the Rx, which is fixed at $\lambda/2$, which is a realistic option for deployments of fixed position network access points.

4.6 Conclusions

In [4.1] and [4.2] the authors suggested that obstructing LOS paths could improve capacity since at the same SNR a higher capacity was achieved. However, this does not consider the fact that by doing so the actual SNR would be reduced and this negatively impacts on capacity. Also, they employed circular and rectangular arrays (similar to [4.18]) which exaggerate the channel correlation under LOS conditions.

At a range of nearly 10 m for λ/2 element spacing they found little difference in capacity for either LOS or NLOS conditions and this is because the LOS does not contribute much at that distance due to the low angular spread of ray paths; they did not note the significance of different distances regardless of employing normalisation for path loss. They indicated a better performance at a shorter range of 5 m through obstructing the LOS; however the impact of reduced SNR was not taken into account (2-3 b/s/Hz). In general it is not a good idea to block or absorb the LOS components, if present, and it is better to consider the array geometry and positioning. Also in [4.5], they concluded that the benefits of increased SNR due to the LOS outweigh the negative effect of increased correlation.

In [4.3] and [4.4] the authors demonstrated the clear benefits to wider spacing, particularly with LOS present, based on the distributive model simulation and virtual array measurements. However, the Tx-Rx separation distance was only 2.6 m and is too limited a range to be applicable in many indoor scenarios and, as Table 4.3 shows, at ranges from 10 m (and less sometimes) the benefits of wider spacing are more questionable. Similarly the benefits of wide element spacing, discussed in the next chapter and [4.5],[4.6],[4.7] and [4.8], are generally to be found only over short ranges, certainly less than 10 m for the arrays considered, with dominant LOS components.

4x4 Arrays	LOS	Γ=1	NLOS(Acc).	NLOS(Std.)
Broad. λ/2	18.6	20.4	17.3	19.7
2λ	17.6	19.9	16.3	18.6
2λ(Tx) –to λ/2 (Rx)	19.7	20.7	18.0	20.5
4λ	19.5	20.5	17.5	20.1
4λ(Tx) –to λ/2 (Rx)	19.9	20.8	18.0	20.5
Perpnd. λ/2	18.3	19.1	16.3	18.5
2λ	20.1	21.1	18.2	20.7
4λ	20.5	21.3	18.6	21.1
Square λ/2	14.1	15.7	13.2	14.9
2λ	17.6	19.7	16.2	18.7
4λ	18.1	19.8	16.3	19.3
Cross λ/2	15.4	17.8	15.4	16.9
2λ	17.6	20.1	16.3	18.9
4λ	17.4	19.0	15.9	18.4
2x2 Arrays				
Broad. λ/2	11.1	11.6	10.3	11.6
2λ	10.6	11.1	9.7	11.0
4λ	10.6	11.2	9.9	11.3
Perp. λ	9.3	9.9	8.4	9.5
2λ	10.8	11.3	9.8	11.2
4λ	10.9	11.3	9.7	11.2

Table 4.3 Mean capacities (in b/s/Hz) achieved at ranges beyond 10 m in the room for 4x4 and 2x2 systems under various configurations and element spacing. (Acc) means removal of LOS component accounted for. (Std) means standard normalisation applied, not accounting for LOS.

In such cases the SNR is not primarily dependent on weaker reflections, which provide Rayleigh type conditions, and verifies that good capacity is not solely dependent on that ideal scenario. Again the question arises as to the practicality of these geometries for more general use and the applicability to the positioning of more typical indoor array systems.

The question of distance was discussed in [4.11] where it was recognized that the complexity of the propagation environment increases with increasing distance, providing a more benign scenario for MIMO systems. But the true effect of paths loss is not always considered when using normalisation, which means care must be taken in determining the actual spectral efficiency. In this regard the results in [4.12] and [4.13], which indicate there is little benefit to increased element spacing, depended on the creation of a reflection rich environment which, when normalised for a given SNR, is likely to generate high capacity. The question that arises is whether the SNR when spread across many reflections is realistic when in reality higher order reflections are weak. They found capacity levels of approximately 90% of the Rayleigh case and some of the results in Table 4.3 confirm this for ranges of 10 m and more.

The indoor modeling in this thesis and the extensive range of scenarios simulated has confirmed some of the various conclusions in the literature regarding the geometric aspects of arrays and the propagation environment indoors. There is further insight provided in the next chapter, concerning more sparse propagation conditions and the rms delay spread of the channel, but for the more general cases of either LOS or NLOS,

channels (the conditions most commonly studied in the literature), there are a number of conclusions regarding the deployment of arrays that can be considered realistic and likely to ensure good performance and avoid potential pitfalls. Overall there are two broad categories that can be considered, namely short ranges of less than approximately 10 m and longer than 10 m (in the room geometry considered); assuming the Tx is located at one end of the room (Tx(1) position) and corner positions are avoided as mentioned earlier.

1. Short ranges

Overall it appears that uniform linear arrays (ULAs) are the most likely to yield good capacity in a highly correlated environment. The variations considered, square and cross patterns, tended to reduce the overall spacing between different pairs of elements for whatever element spacing was considered. Consequently over short ranges, particularly with LOS components present, they are not a good choice. However, it is easy to envisage systems employing MIMO technology with arrays which are similarly structured due simply to the physical space available on a product; for instance the corners of a box structure. Certainly over distances of less than 10 m, in the room considered, it would be difficult to operate anywhere near optimal levels of performance unless the propagation environment was guaranteed to be Rayleigh like. This would, at the very least, require obstructing the LOS components which is inefficient if path loss is taken into account.

The orientation of the Tx and Rx arrays relative to each other is probably the easiest factor to influence if a fixed linear array structure is being deployed. For example for a

small element spacing the contribution from LOS components is limited in the broadside arrangement at short ranges for an element spacing of λ/2. The relative orientation of the Tx and Rx arrays are highly significant in determining the regions of strong and weak capacity and, for that case, the overall capacity is improved by the perpendicular orientation over short range (14.3 b/s/Hz to 17.8 b/s/Hz). The perpendicular arrangement improves the contribution to capacity from the reflections and this is evident if the NLOS cases are compared. The broadside arrangement, under normalised power, is 16.6 b/s/Hz and this rises to 19.3 b/s/Hz for the perpendicular case. Clearly a large drop in capacity occurs if the absence of the LOS components is accounted for, as the SNR over short ranges significantly depends on them. Alternatively if the reflections can be enhanced, relative to the LOS components, the capacity is 19.6 b/s/Hz. In reality, if the reflections are enhanced the SNR increases and as a consequence higher capacity is achievable (some examples are given below in Table 4.4). It may not be possible to cover every surface with highly reflective material but enough to ensure the capacity achieved would be greater than 20 b/s/Hz and close to that achievable in a Rayleigh environment.

Thus, the recommendation for fixed uniformly configured small spaced arrays over short ranges is to arrange them perpendicularly and enhance reflections from as many reflecting surfaces as possible. Alternatively if a wide spacing of elements is possible, say greater than 10 λ, then broadside arrangements are likely to be optimal due the reduced correlation of the LOS components.

It may be possible that at least one side of the channel could be deployed with wider element spacing (2 λ or 4 λ) for ULAs while maintaining the other side at λ/2, which is often the optimal as indicated by the results in the next chapter. In such scenarios the location of the fixed access point could be a central room location to reduce transmission range, but care would need to be taken to avoid in-line orientations of the Tx and the Rx and the corners of the room are not a good location for the Tx.

2. Longer ranges (>10m within room considered)

Although there are clear benefits to increased element spacing over short ranges it makes little difference at ranges greater than 10 m, unless wide spacing of elements is used, and λ/2 appears to be a reasonable spacing for the broadside case. However, if one side can be made wider without causing difficulties, this should be done. Maintaining a directly facing broadside orientation between the Tx and Rx is advisable. Enhancement of reflections from surfaces using some form of metallic coating may yield benefits, although RF shielding of a room would not be acceptable; but protection from IEMI (intentional electromagnetic interference) may be plausible for security reasons in the future. It also has the benefit of enhancing the strength of higher order reflections compared to the LOS components which tends to reduce the cross correlations in the channel matrix when a small element spacing is involved. This is effectively modifying the propagation channel characteristics to become more similar to a Rayleigh environment and also increases the SNR level at the Rx. Table 4.4 below indicates the typical improvement that can be achieved for various scenarios with this approach for 4x4 broadside linear arrays with an element spacing of λ/2 and 2 λ. The normalisation applied is the reverse of that used to account for the removal of LOS components, i.e.

the normalisation factor determined for all paths under standard conditions is used when the improved reflection surface is introduced. When all surfaces have a reflection Γ= 1, the capacity improvement is greater than 50%. More realistically a single surface would ensure, at ranges greater than 10 m for λ/2 spacing, capacities of at least 90% of those predicted for a Rayleigh channel. Under similar conditions the cross array structure performs well providing the spacing is 2 λ. This structure takes advantage of reflections from W1 and W3 as two of the elements are effectively broadside to those surfaces. The NLOS environment is similar, and may be the only possibility, but does require a higher SNR to achieve the same level of capacity if the absence of the LOS components is taken into account. However, improved reflective surfaces could also offset this factor.

	λ/2 (mean)	λ/2 Dist. >10 m	2λ (mean)	2λ Dist. >10 m
Standard case	17.2	18.6	17.5	17.6
4 walls Γ=1	26.9	28.8	27.6	28.8
W1 Γ=1	20.9	22.7	21.2	21.5
W2 Γ=1	20.1	21.4	20.7	21.2
W4 Γ=1	19.7	21.1	19.9	19.9
Ceiling Γ=1	19.1	20.6	19.6	19.4
Ceil. + W2 Γ=1	20.5	21.8	21.5	21.8
Ceil.Floor Γ=1	19.7	21.0	20.2	19.8
W1 + W2 Γ=1	22.4	24.0	22.8	23.5
W1 + W3 Γ=1	23.6	25.9	24.3	25.0

Table 4.4 Mean capacities (in b/s/Hz) achieved overall and at ranges beyond 10 m in the room for 4x4 broadside ULAs for varying number of highly reflective surfaces (Γ=1) as per Figure 3.1, normalised for increased SNR due enhanced reflections. The Rayleigh channel mean is approximately 22 b/s/Hz.

Smaller 2x2 systems provide good mean capacity (often close to ideal) regardless of propagation conditions. They are potentially a good solution for indoor environments noting the reduced complexity associated with such systems, albeit at much lower levels of spectral efficiency than 4x4 systems. Most results in Table 4.3 demonstrate mean capacities similar to those achieved using random matrices.

NOTE 1:

In this thesis the degree of channel correlation is determined from a matrix of correlation coefficients formed from the channel matrix **H**, using the Matlab function CORRCOEF(X) [19]. The mean of the off-diagonal entries is an indication of the overall level of correlation between the entries in the original channel matrix **H**. These mean correlation values are used in various figures in the thesis, e.g. Figure 5.3.

NOTE 2:

A selection of location plots for maximum and minimum capacity regions, similar to Figure 4.5, for various array configurations and propagations conditions is included at the end of appendix B in Figure B.7(a to r). These demonstrate the wide variation that occurs due to geometric variations of the arrays etc.

4.7 References

[4.1] A. Z. Tang, A.S. Mohan, "Experimental Investigation of Indoor MIMO Ricean Channel", *IEEE Antennas and Wireless Propagation Letter*, Vol.4, 2005, pp. 55-58.

[4.2] A. Z. Tang, A.S. Mohan, "Effect of the strongest multipath component on indoor MIMO performance", *IEEE Antennas and Propagation Society International Symposium, 2005*, Vol 2B, 2005, pp. 727-730.

[4.3] J.S. Jiang, M.A. Ingram,"Distributed source model for short-range MIMO", *IEEE 58th Vehicular Technology Conference 2003*,Vol.1, Autumn 2003, pp. 357-362.

[4.4] J.S. Jiang, M.F. Demirkol, M.A. Ingram, "Measured capacities at 5.8 GHz of indoor MIMO systems with MIMO interference", *IEEE 58th* Vehicular Technology Conference 2003,Vol. 1, Autumn 2003, pp. 388-393.

[4.5] D.P. McNamara, M. Beach, P.N. Fletcher, P. Karlsson, "Capacity variation of indoor multiple-input-multiple-output channels", *Electronics Letters*, Vol. 36, Issue 24, Nov. 2000, pp. 2037-2038.

[4.6] I. Sarris, A.R. Nix, "Maximum MIMO capacity in line-of-sight", *IEEE Int. Conference Commumications and Signal Processing*, Dec. 2005, pp. 1236-1240.

[4.7] D. Neirynck, C. Williams, A. Nix, M. Beach, "Personal area networks with line-of-sight MIMO operation", *IEEE Vehicular Technology Conference(63rd*, Spring, 2006*)*, pp. 2859-2862.

[4.8] I. Sarris, A.R. Nix, "Design and performance assessment of High capacity MIMO architectures in the presence of a line-of-sight component", IEEE Transactions on Vehicular Technology, Vol. 56. issue 4, 2007, pp. 2194-2202

[4.9] A. Grennan, C. Downing, B. Foley, "A Geometric Interpretation of Indoor MIMO Systems using a Deterministic Model", *European Conference on Antennas and Propagation,* Edinburgh Nov. 2007, pp. 88-93.

[4.10] A.Grennan, M. Davis, C. Downing, "Analysis of array geometries for indoor MIMO systems using a deterministic model", *Loughborough Antennas and Propagation Conference*, Nov. 2012, pp. 337-341.

[4.11] J.W. Wallace, M.A. Jensen, A.L. Swindlehurst, B.D. Jeffs, “Experimental characterization of the MIMO wireless channel: data acquisition and analysis” , *IEEE Transactions on Wireless Communications,* Vol. 2, issue 2, March, 2003 pp. 335-343.

[4.12] V. Pohl, V. Jungnickel, T. Haustein, C. von Helmolt, “Antenna Spacing in MIMO Indoor Channels*” IEEE Vehicular Technology Conf.*, Spring 2002, pp. 749-753.

[4.13] V. Jungnickel, V. Pohl C. von Helmolt, “Capacity of MIMO systems with closely spaced antennas*”, IEEE Communications Letters,* Vol. 7 No. 8 Aug. 2003, pp. 361-363.

[4.14] K Pahlavan and A.H. Levesque, *Wireless Information Networks*, J. Wiley and Sons, 1995.

[4.15] A. Burr, “Evaluation of capacity of indoor wireless MIMO channel using ray-tracing”, *International Zurich Seminar on Broadband Communication*, 2002 pp. 281-286.

[4.16] M.Herdin, H. Ozcelik, H. Hofstetter and E. Bonek, “Variation of measured indoor MIMO capacity with receive direction and position”, *Electronics Letter*s, Volume: 38 , Issue: 21, Oct. 2002, pp. 1238-1285.

[4.17] R. Iernon-Fernandez, J. Molina-Garcia-Pardo, L. Juan-llacer, “Comparison between measurements and simulations of conventional and distributed MIMO system”, *IEEE Antennas and Wireless Propagation Letters*, Vol. 7, 2008, pp. 546-549.

[4.18] L. Jiangang, L. Ying-hua, H Peng-fei, L. Peng, “Evaluation of capacity of indoor MIMO channel with different antenna arrays”, *IEEE International Symposium on Microwave, Antenna, Propagation and EMC Technologie*s, Vol. 1, 2005, pp. 204-207.

[4.19] Matlab, *The Mathworks Inc.*, Version 6, Release 12, Sept. 2000.

Chapter 5 Sparse Conditions and Dispersion Analysis

5.1 Introduction

This chapter presents an analysis of propagation scenarios with a limited number of propagation rays between the Tx and the Rx, i.e. sparse conditions. This includes the LOS only or 'free space' case. In short-range scenarios it is possible that the propagation environment is equivalent to this, if the reflections are weak, as the SNR is dominated by those rays, which are sixteen in total if a 4x4 MIMO system is considered. The distributed source model used here permits precise calculation of each path and is necessary for accurate determination of the capacity in such circumstances. A similar analysis of individual first-order reflections and combinations of the LOS components and limited reflections is also presented.

The second part of the chapter deals with the dispersion characteristics of the channel, the excess delay and rms delay spread. The relationship between these characteristics and the spectral efficiency is investigated. New results are presented that explain why smaller spacing, for instance $\lambda/2$, can perform at near optimal levels in certain regions of the room and are a good choice for many applications. Although this has been suggested by others, i.e. the suitability of small spacing, the dispersion characteristics have not been considered in detail as part of the explanation.

5.2 LOS Only (Free Space) Analysis

5.2.1 Effect of element spacing

LOS components are important over short ranges as they provide the most efficient means for power delivery between the Tx and Rx. However, they are also the most correlated group of transmission signals. Thus, the impact they have on the channel matrix **H** is significant for determining the system performance, including when reflections are present. There is the possibility of situations in which the LOS components are so dominant that the system reduces to LOS only as far as meaningful signal power delivery is concerned, with other components effectively below the noise floor or a limited number of strong reflections, i.e. sparse multipath. Considering the LOS components in isolation produced a simpler pattern of good and bad performance locations as shown in Figure 5.1 with the Tx centred in the room, 4x4 broadside arrays (2 λ spacing), the SNR normalised to 20 dB and a carrier frequency of 5.2 GHz.

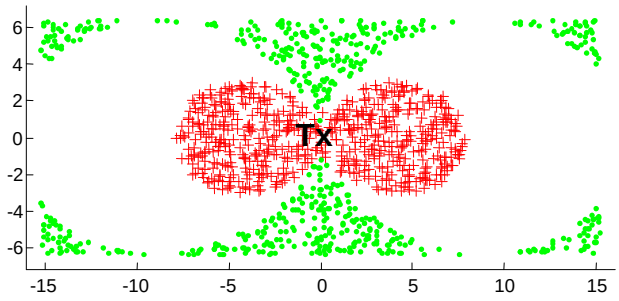

Figure 5.1 Location of maximum and minimum 20% of capacity with the Tx at centre of room for LOS components only (free space) broadside arrays. The SNR is normalised to 20 dB at each location. Red crosses indicate maximum, Green dots minimum.

The pattern shown is approximately the same for various element spacings with the maximum 20% of results close to the Tx. Power normalisation was applied to all locations and it was the geometric factors that changed. The capacity values varied with different element spacings as shown in the CDFs of Figure 5.2. There was little benefit for narrow spacing (λ/2) with a limited set of paths, 16 LOS components in total, but the widest spacing considered (4 λ) delivered worthwhile values for slightly more than 80% of locations (nearly all the non-green areas shown in Figure 5.1). Thus, if a system can use a wide element spacing, a capacity range of 16-22 b/s/Hz may be achieved without requiring reflections; in some cases it may be possible to implement wide spacing, e.g. 8 λ, at one side of the channel only to improve efficiency.

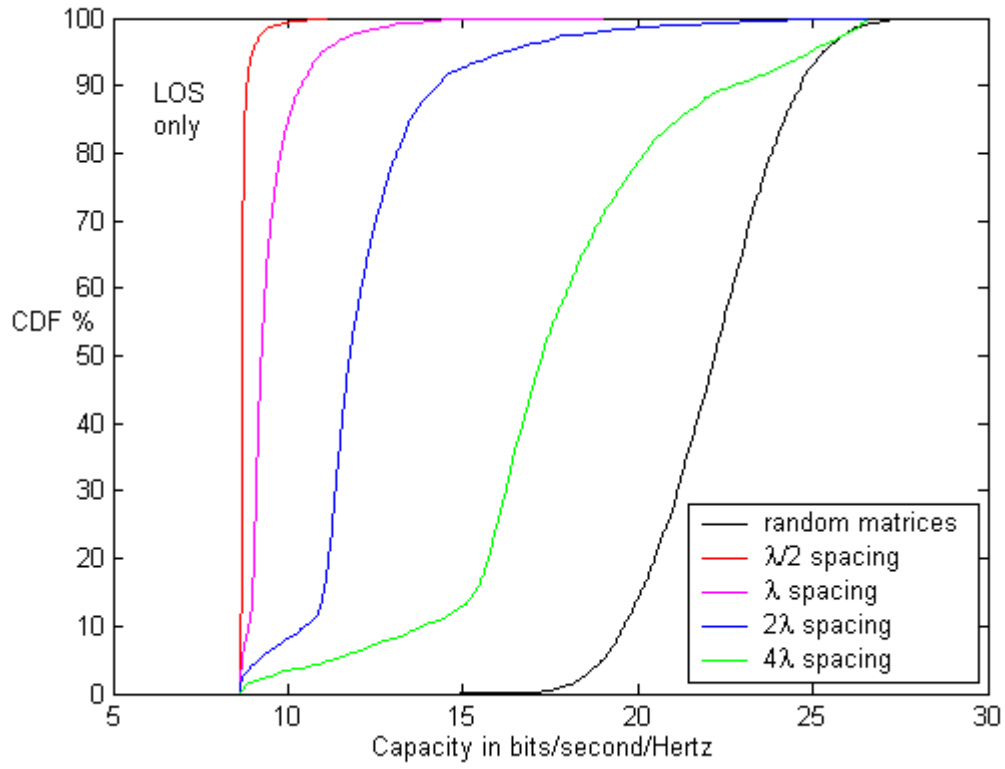

Figure 5.2 CDFs for LOS only case for various element spacings with the Tx positioned in centre of room as per Figure 3.1 at Tx(2).

Table 5.1 lists results for different element spacings of broadside ULAs with the Tx at the left side of the room; Tx(1) in Figure 3.1. The table includes examples for a wider element spacing at the Tx side of the channel, up to 8 λ, possibly representing a network access point. The LOS only case has been discussed in [5.1] which described this as the 'green field channel' and derived guidelines for determining when such a channel is decorrelated (or orthogonal) based on simple geometric propagation parameters. Their work was referred to by others [5.2] [5.3] who also considered strong LOS propagation cases. In order to observe this in simulation, it is necessary to calculate the precise path distances between each element of the Tx array and the Rx arrays in the manner suggested in [5.4] using a distributed source model as referred to in [5.2][5.3] and [5.5].

LOS ONLY	mean	Dist.>10 m
λ/2(Tx and Rx)	8.7	8.7
λ(Tx) - λ/2(Rx)	12.4	12.2
2λ(Tx) - λ/2(Rx)	13.2	13.1
4λ(Tx) - λ/2(Rx)	13.6	13.3
8λ(Tx) - λ/2(Rx)	14.3	14.0
λ (Tx and Rx)	9.2	8.9
2λ(Tx) - λ(Rx)	13.6	13.5
4λ(Tx) - λ(Rx)	14.5	14.2
8λ(Tx) - λ(Rx)	16.0	15.4
2λ (Tx and Rx)	11.2	10.7
4λ(Tx) - 2λ(Rx)	15.9	15.4
8λ(Tx) - 2λ(Rx)	17.9	17.2
4λ (Tx and Rx)	15.8	15.5
8λ(Tx) - 4λ(Rx)	20.5	20.5
8λ(Tx and Rx)	23.4	23.8

Table 5.1 Calculated average capacities for various element spacings at the Tx and Rx for free space conditions (LOS only), including at a distance greater than 10 m in the room considered. The Tx is at Tx(1) position as shown in Figure 3.1 and the arrays are broadside ULAs.

5.2.2 Mean of channel correlation matrix

The increased element spacing decorrelates the channel matrix and at wide spacing this results in maximum capacity. A correlation matrix, derived from the channel transfer matrix **H**, provides a good indication of the relationship between element spacing and capacity. This is a matrix of correlation coefficients formed from **H**, and from now is referred to as the channel correlation matrix (see NOTE 1 on page 122). A similar approach was used in [5.5] which examined personal area networks (PANs) in relation to LOS MIMO. To illustrate this, the mean of the entries in the matrix (channel correlation) elements are plotted as a moving average in Figure 5.3 for the CDFs shown in Figure 5.2.

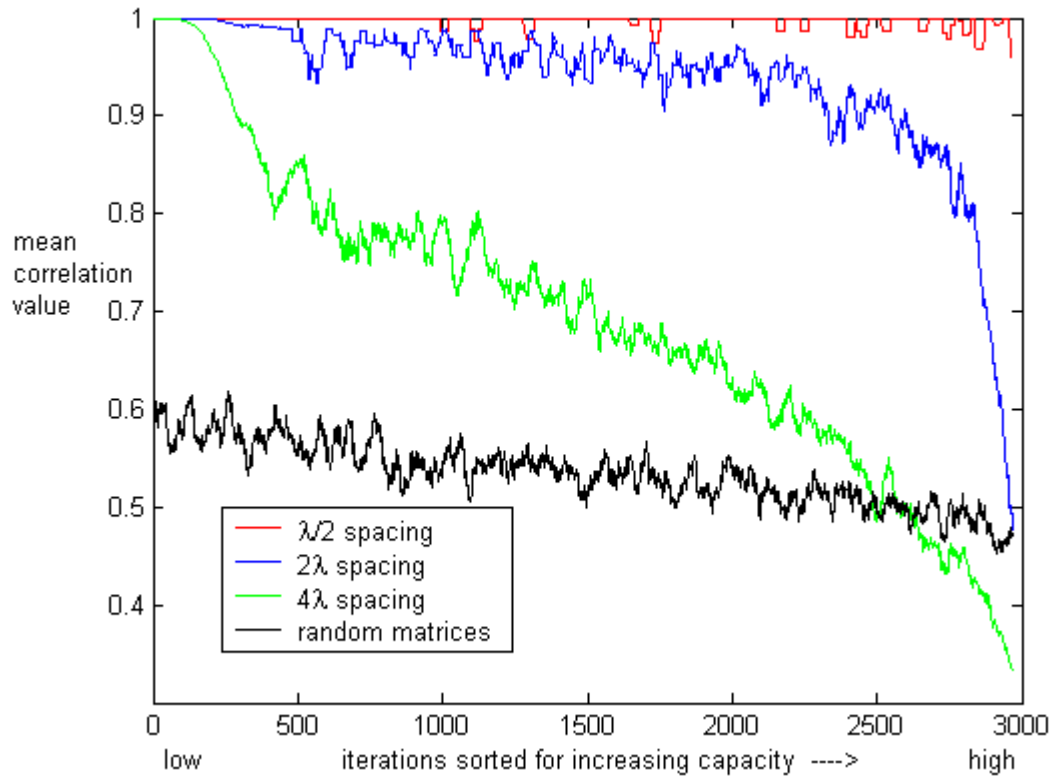

Figure 5.3 Trend of mean values of channel correlation matrices versus increasing capacity for LOS only case and random matrices case for comparison. A 25 point moving average was employed to simplify the plot.

In Figure 5.3 for λ/2 spacing (red curve) the mean correlation value remained almost entirely at the value 1 or close to it, indicating the highly correlated nature of the channel, resulting in low capacity. The 4 λ case reduced to less than 0.7 for half the values and below 0.5 for the peak values, which is typical for channels of good capacity as suggested by the black curve derived from random matrices.

From inspection of the results in Figure 5.1 (for broadside arrays) it is clear that even with power level normalisation at the receiver there is an inverse relationship between the separation distance, from transmitter to receiver, and the channel efficiency. Also, the relative positioning of the Tx and Rx affects the performance. Although the measurements were in three dimensions there was no difference in comparison to just two dimensions when considering the capacity levels throughout the room, i.e. with a fixed height for both the Tx and Rx, and this simplifies the explanation.

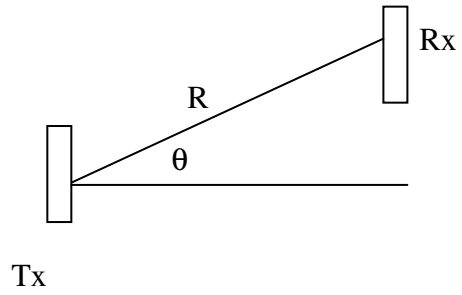

Figure 5.4: Relative positioning of Tx and Rx as defined by the angle θ, which is angle between the line perpendicular to the Tx array and the path connecting the Tx and the Rx. (R is the distance from the Tx to the Rx).

Referring to Figure 5.4, the angle θ is formed between the line perpendicular to the array and the line marked R. When the Tx and Rx are directly opposite (θ = 0) and close, then the capacity peaks for the particular element spacing.

As the angle rotates towards 90° degrees, at a given separation distance R, the capacity collapses and are weakest at 90°. This can be explained in terms of the spatial separation of any pair of paths from an element at the Tx to a pair of elements at the Rx. This is effectively the angle of arrival/departure of a transmission path component from one element to a pair at the other end of the channel; or the angular spread as it is referred to here and is demonstrated in Figure 5.5.

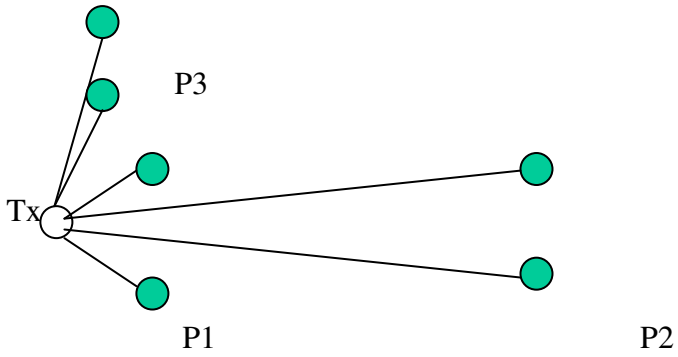

Figure 5.5 Pairs of Rx elements in 3 locations relative to a single Tx element showing the spatial separation of paths, or angular spread, between the Tx and Rx .

In Figure 5.5 the unfilled dot represents an element at the Tx. Each pair of filled dots (P1, P2 and P3) is a pair of elements at the receiver and the same spacing is assumed in each case. The spatial separation between the paths from the Tx to Rx are maximised at close range and decreases with increasing separation distance. Similarly as the position of the receiver rotates to an angle of 90° (in-line Tx and Rx axes), the angular spread reduces and capacity collapses. The spatial separation of paths is directly affected by the element spacing and this accounts for the dramatic improvements when the element spacing becomes large. As either the range or the angle describing the relative orientation between the Tx and Rx increases, the capacity is reduced at a similar rate.

Thus for a given Tx-Rx location pair the element spacing is the primary determinant of capacity and is approximately defined by the relationship;

$$C \propto \cos\theta \times \frac{d}{R} \qquad (5.1)$$

Where C is capacity, d is the element separation and R is the Tx to Rx range as shown Figure 5.4 which also shows the angle θ which is formed between the line perpendicular to the array and line marked R. Clearly the orientation of the arrays relative to each other affects this relationship and is why the broadside array structure is often optimal. In [5.1] they derived the relationship between Tx-Rx range, element spacing and the number of elements at the receiver for decorrelating the closest pair of paths from an element at the Tx to the Rx, when they were broadside and directly opposite as;

$$\frac{d_t d_r}{R} \geq \frac{\lambda}{M} \qquad (5.2)$$

where d_t and d_r are the element spacing at the Tx and Rx respectively, R is the separation distance, λ the wavelength of the carrier and M is the number of elements at the Rx. Assuming that a capacity level at a maximum range for R is required to be approximately the same as the peak values (not mean) obtained under Rayleigh conditions (as generated by random matrices), then for a 4x4 system this should approximate to 26 b/s/Hz; assuming normalisation at 20 dB. At 2 λ and 4 λ element spacing the range up to which this capacity could be achieved was calculated from equation (5.2) as approximately 0.92 and 3.7 metres respectively. Examination of the results for both cases at these distances confirmed this to be the case. Furthermore, in regions at an angle of 45° (similar to Figure 5.4) there was a reduction that followed the cosine of the angle (0.707); capacity reduced from approximately 26 b/s/Hz to approximately 18 b/s/Hz in agreement with equation (5.1). At a smaller element spacing

the reduction in capacity was more severe and equation (5.2) was not followed. In [5.1] and [5.2] the element spacing considered was several wavelengths and was similar to some of the arrangements treated in chapter 6. For instance, an element spacing of 8 λ for a 4x4 system and 5.2 GHz carrier frequency would result in near peak capacity at distances of up to 15 metres in LOS dominated conditions. However, the arrays would require a total span of 1.4 m and at that stage they are becoming closer in dimensions to a distributed system such as that discussed in [5.6] and are arguably impractical.

5.2.3 Eigenvalue distribution

By checking the distribution of eigenvalues it was clear that in highly correlated conditions a single large value dominates. For good performance the distribution becomes evenly spread as described in [5.7]. Figure 5.6 shows the standard deviation of the eigenvalues for the LOS only cases (of Figure 5.2) and confirms this theory with a marked difference for the wider element spacing. There was virtually no spread across the 3000 values for λ/2 spacing with a single eigenvalue dominating.

5.3 Reflections Analysis

5.3.1 Reflections from a single and multiple walls

Compared to a LOS component any single reflection path set, for instance all first order reflections from a particular wall, do not contribute much to capacity if considered in isolation. This is in part because the path lengths involved are relatively long and consequently the angular spread is narrow. Also, there is the power loss at the reflection point (depending on the reflection coefficients, which may vary) and for higher order reflections these factors are exaggerated. However, first order reflection groups may still have a noticeable impact individually in the regions close to the reflection wall if

the element spacing is wide; particularly if the transmitter to wall range is short with a metallic type reflective surface.

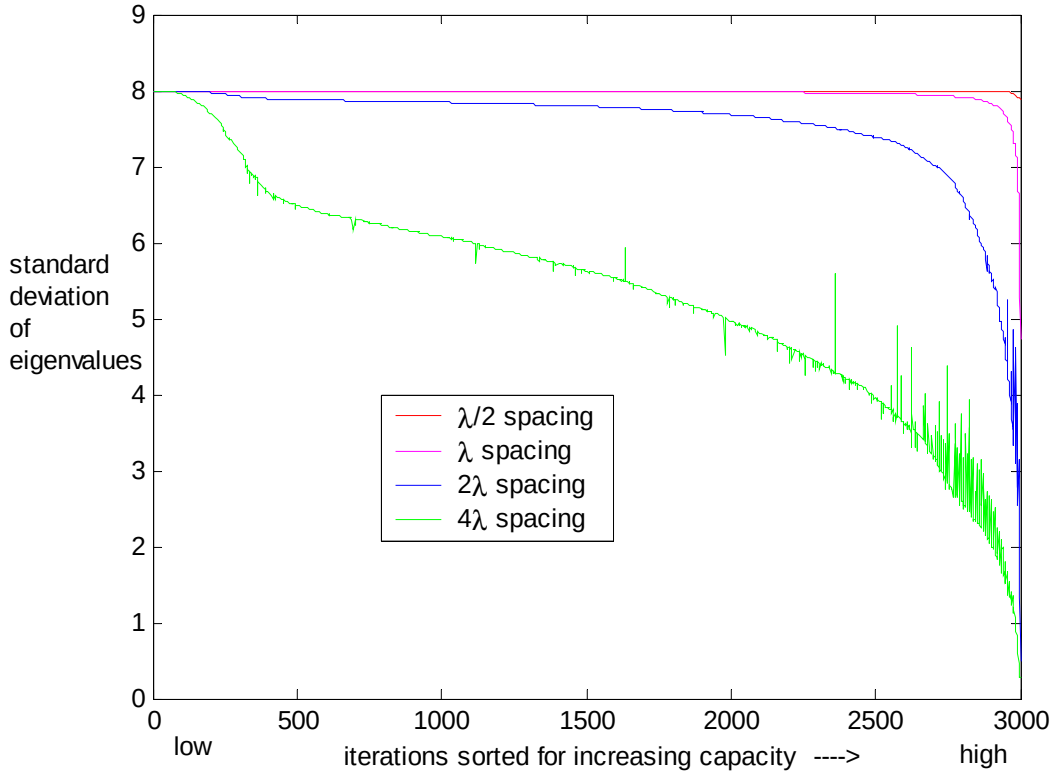

Figure 5.6 Standard deviation of eigenvalues for LOS only case.

Figure 5.7(a) shows the maximum and minimum regions for first order reflections from a single wall (W1 on Figure 3.1) with the Tx in the centre of room for 4 λ element spacing. The maximum value in the green region is less than 9 b/s/Hz while in the red region it varies from 12.5 to 14.5 b/s/Hz. Any individual reflection pattern may be visualised by considering the LOS pattern (e.g. Figure 5.1) but not until after the ray has reflected from the wall. Hence the circular pattern associated with the good regions as shown in Figure 5.7(b) for the reflections from the same wall when the Tx is at the left end centre. Figure 5.7(c) shows a more varied pattern for all first order reflections (four walls) for the regions of weak and strong performance. Some of these are due to the

angular spreading of reflection paths and this was most pronounced in the corners where the reflections from the adjoining walls were relatively strong. Different element spacing affects the patterns and overall there was a better performance as it increased. This explains why some NLOS results are impacted by increased element spacing, at least when first order (or any strong) reflections are present and the Rx is near a reflecting surface. Also the orientation of the Rx array will have an impact, for instance if the array is broadside to the reflecting surface as noted in chapter 4 for the perpendicular orientation.

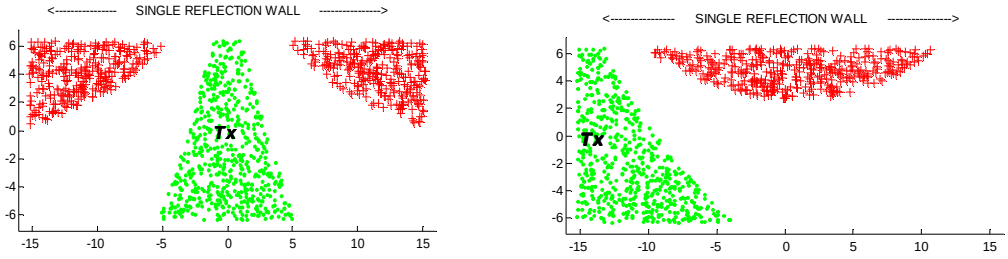

(a) Single wall

(b) Single wall

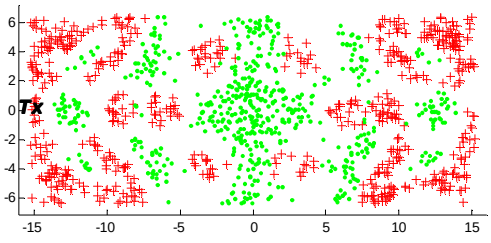

(c) Four walls first order reflections only

Figure 5.7 Maximum and minimum location patterns associated with first order reflections from limited surfaces (Tx identifies locations).

If only second order reflections are present the effect is not noticeable. As indicated in the previous chapter the result is a wider distribution of weak and strong locations and a similar overall level of performance regardless of element spacing or orientation of arrays. Although the second-order reflections generated less correlated channels, the absence of the LOS components or first order reflections may be unlikely and not desirable due to the reduced SNR at the Rx. The mean capacity may decrease by more than 30% if adjustments are made for removing the LOS and first order components in the room considered.

5.3.2 Mean of channel correlation matrix

Figure C.1 in appendix C shows a moving average of the mean of the channel correlation matrix for first order wall reflections only (red) and second order reflections only (green) sorted according to increasing capacity for 4 element arrays with 4 λ spacing. There is a clear correspondence between the levels of correlation shown (roughly 0.6 and 0.7 on average) and the mean calculated capacity (18.4 and 21.8 b/s/Hz). The difference between the two is approximately 15% overall. The second-order reflection set exhibits more Rayleigh type characteristics and tends to generate higher capacity under normalised power and a level of correlation closer to that of random matrices as shown in Figure 5.3.

To extend the analysis a limited number of reflection paths, with the LOS, were examined. Figure 5.8 shows the strong location regions for the case of reflections from wall (W1) and the LOS components for 2 λ array element spacing. To emphasise the effect from the reflections, the wall was given a reflection coefficient of Γ=1. (Overall there was little difference between the capacity in this case compared to simulating a

block wall, 14.3 b/s/Hz compared to 13.7 b/s/Hz, and similar locations of strong performance existed). The mean value of the locations, highlighted in Figure 5.8, was approximately 18 b/s/Hz. The capacity was good (approximately 80% of the mean for Rayleigh conditions) considering the limited number of transmission paths present which included the strongly correlated LOS components. In [5.8] it was noted that in reality such sparse multipath MIMO channels are common, particularly in relation to LOS indoor channels.

The good regions, identified in Figure 5.8 primarily relate to the interaction of the two sets of transmission paths rather than solely due to one, the LOS. The effect of introducing a reflection path is not obvious in certain regions but the increased diversity accounts for the unusual varying pattern of strong capacity. Thus, in front of the transmitter (except for close proximity) marked 'M' on the diagram, the capacity was weaker than in adjacent positions either side (above or below on the diagram marked 'U' and 'L'). This was despite the LOS only case being better on its own in the same location. The reduced dominance of the LOS components allows extra capacity to be delivered by the presence of the reflections, which have a limited impact on their own, but provide sufficient diversity to increase capacity. This effect is most evident by the sizeable increase in the smallest eigenvalue at these locations. A plot of the Rx locations (Figure C.2 and Table C.1 in appendix C), for when the smallest eigenvalue is large, demonstrates the correlation with the pattern of the strong capacity locations. A similar situation arises in a corridor when some reflections, at short range distances, are similar in length to the LOS components.

A notable aspect of the two side lobes is that the mean values calculated from the channel correlation matrices are not in the minimum 20%. Figure C.3 in appendix C shows a plot of these values and there is a clear correspondence with much of the high capacity regions of Figure 5.8, but not for the side lobes or sections of the other good regions. This suggests that at least some high capacity locations are not dependent on Rayleigh-like conditions and that enhanced performance with predominantly LOS components (or a single strong reflection group) is possible with a limited number of weaker reflections.

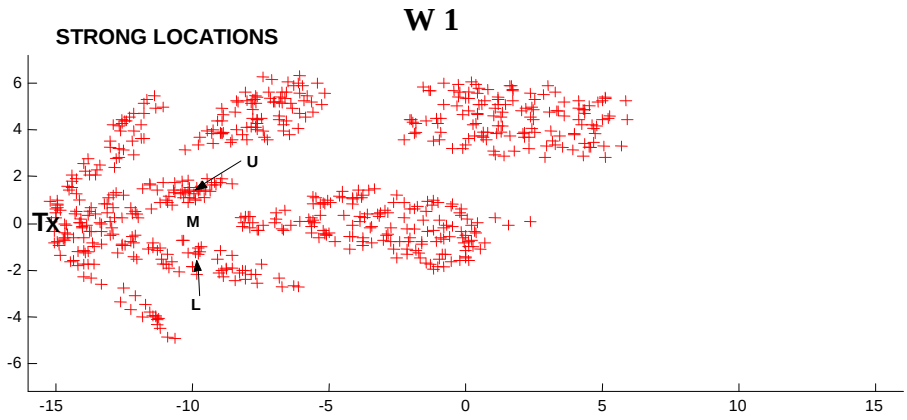

Figure 5.8 Maximum (20%) capacity locations with LOS and reflections from one wall (W1 see Figure 3.1).

5.4 Dispersion Analysis

5.4.1 rms delay spread and mean excess delay analysis

A standard method for quantifying the effect of multipath radio channels is the time delay spread measurement of the multipath components [5.9][5.10]. These metrics have been defined in chapter 3 by equations (3.6) and (3.7) page 68. In this section the relationship between the dispersion quantities and channel capacity is examined. Intuitively it can be understood that a small time spread in the reflections may be an indication of increased correlation between some rays. For instance, for Rx locations along the centre line of the room broadside to the Tx, reflections from opposite walls have similar path lengths. Conversely, for increased dispersion it may be possible to reduce correlation and improve capacity. In [5.9] it was found that variations in capacity were related to fluctuations in delay spread. There was no detailed analysis done but they noted that in cases when LOS was obstructed, both the rms delay spread and capacity increased.

In many regions of the room there is a dominant signal component, i.e. the LOS, or an interaction of components; typically the LOS and a reflection from a wall. These factors mostly determine good system performance in regions close to the Tx and the reflecting surfaces. However in other locations, particularly towards the centre of the room, when the Tx is at an end wall and the element spacing is small, these factors are not present. The rms delay spread and mean excess delay provide a measure of the time gap between multipath components, i.e. the dispersion. Although the absolute power level of the signal components is not considered, the relative power across components of the signal set is taken into account. Thus, they are appropriate measures for comparison with

channel capacity measures that employ power normalisation in which the SNR is maintained constant for different locations.

A point to note about traditional time dispersion measurements is that they are normally a measure between two point sources at the Tx and Rx. Thus, in the case of MIMO systems, they describe the dispersion between reflections from different walls, but not the dispersion between reflections from the same wall to different array elements. This second factor is only significant when the element spacing is large. Thus, the relationship between time dispersion measures and MIMO channel capacity is most useful when examining closely spaced arrays, for instance $\lambda/2$. Figure 5.9(a) shows the minimum and maximum rms delay spread region for that case when the Tx is positioned towards the left end of the room and all paths were present. Figure 5.9(b) shows the corresponding mean excess delay regions and (c) shows the corresponding capacity for a 4x4 broadside MIMO system ($\lambda/2$ spacing) with all paths present.

As stated previously there was a low capacity observed over short ranges under these conditions and both the rms delay spread and mean excess delay spread were also low in this region. The central regions, covered by a combination of the higher 20% of values from both measures, also overlap much of the region in which strong capacity was present. The maximum mean excess delay points have a better correspondence with the peak capacity region compared to the rms delay spread. However, between the 5 m and 10 m markers the high capacity region encompasses much of the same region as the maximum rms delay spread.

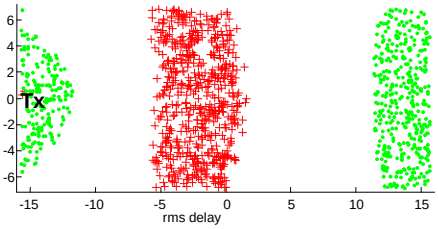

a)

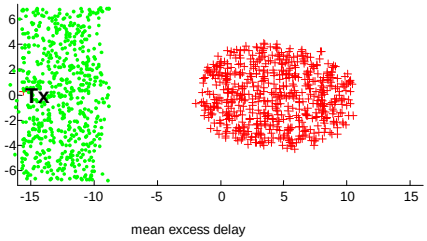

b)

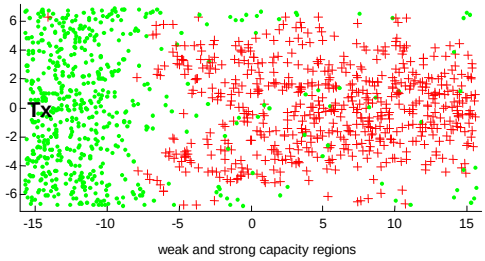

c)

Figure 5.9 Temporal characteristics compared with capacity. a) rms delay b) mean excess delay, c) capacity, for a 4x4 MIMO system with all paths present (λ/2 spacing).

5.4.2 Analysis along straight line in the centre of the room

An alternative approach is to compare the dispersion against the capacity fluctuations along a straight line from one end of the room to the other (broadside arrays). This method is useful since it minimises the impact of first-order reflections when they are relatively strong; such as close to walls when angular spreading of that particular reflection set may dominate. Also, for an element spacing of λ/2, there is a limited contribution from the LOS components if present; and in the more central regions of the

room there is a greater dependence on the overall set of reflection paths without any one group dominating. Similar measurements were made in [5.11].

Since the dispersion, as quantified by the rms delay spread is usually measured relative to the LOS and therefore does not quantify it, a comparison with the capacity for NLOS cases is more accurate to determine if correlations are present. The results presented below use the standard normalisation for the NLOS case and do not adjust for removal of the LOS component, which is appropriate in this case. Figure 5.10(a) shows the excess delay curve and the rms delay curve and Figure 5.10(b) shows the corresponding capacity for the NLOS case (the LOS capacity is shown in Figure C.4 appendix C).

In both capacity cases the overall shape was similar to the shape of the excess delay curve and a correlation factor for the NLOS and excess delay was above 0.9. However, this was not present at wider element spacing. This was because the wider element spacing cases improved angular spreading of paths and this factor, rather than signal dispersion, dominated the system performance. Overall the fluctuations in capacity were greater in most cases compared to the $\lambda/2$ case.

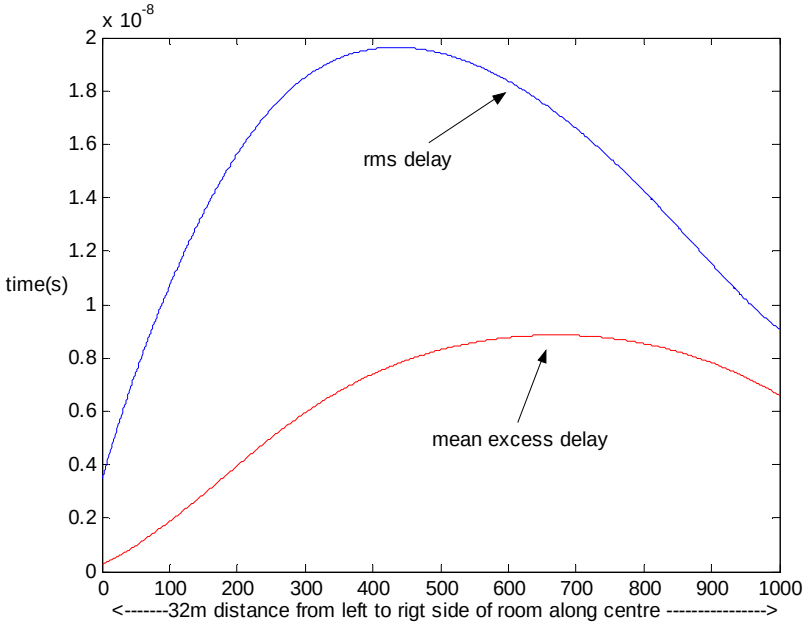

Figure 5.10 Temporal characteristics compared with capacity: (a) is the rms delay spread and excess delay curves and (b) is the capacity in the NLOS case for a 4x4 broadside MIMO system (λ/2 spacing element) with the Rx moving along centre axis of room from left to right.

The λ/2 NLOS case appears to be optimal for correlation with mean excess delay. For example at λ element spacing, NLOS, the correlation was 0.85. (The capacity for this case is shown in Figure C.5 appendix C). At approximately the point when the excess delay peaks and the Rx approaches the far wall there was a notable change in the capacity with large fluctuations. This was present in many cases including λ/2 spacing, LOS and NLOS, and there was a change in the general trend of increasing capacity. However, for most cases of NLOS up to 2 λ element spacing there was a general trend of increasing capacity that approximated the excess delay curve until it peaked. No single factor provides an explanation of the channel capacity in a multipath environment and the fluctuations over short spans were due to the complex interaction of multiple propagation paths between multiple array elements.

Thus to gauge the overall correlation between the capacity, rms delay spread and mean excess delay the first 700 points (as shown in Figure 5.10 for instance) were directly compared for λ/2 and λ element spacing. The resulting correlation values are shown in Table 5.2(a) for various scenarios; all paths and NLOS, first order reflections only, second order only and both the later cases with LOS components. For each case the dispersion is measured relative to the LOS and compared with the corresponding capacity. The NLOS and excess delay have a strong correlation that is greater than 0.9 for all reflections and first order reflections only, while the second order cases, although reasonable, were distinctly weaker. Also the correlation with the rms delay spread was less. To check the trend over the total length of the room, the capacity curve was smoothed using a 25 point moving average to remove the excessive fluctuations after iteration 700. Again high values of correlation with the excess delay were present and

are shown in Table 5.2(b), but this time the rms delay spread shows significantly lower correlations.

	LOS (ALL)	NLOS	FIRST ORDER	FIRST + LOS	SECOND ORDER	SECOND +LOS	OVERALL MEANS
λ/2 Xdel.	0.83	0.90	0.85	0.93	0.80	0.85	0.86
λ/2 rms	0.56	0.72	0.64	0.81	0.60	0.80	0.69
λ Xdel	0.84	0.92	0.96	0.96	0.83	0.78	0.88
λ rms	0.76	0.79	0.83	0.90	0.71	0.87	0.81

(a)

	LOS (ALL)	NLOS	FIRST ORDER	FIRST - +LOS	SECOND ORDER	SECOND +LOS	OVERALL MEANS
λ/2 Xdel	0.88	0.92	0.76	0.93	0.93	0.94	0.89
λ/2 rms	0.40	0.40	0.67	0.64	0.48	0.58	0.53
λ Xdel	0.82	0.96	0.91	0.96	0.92	0.78	0.89
λ rms	0.28	0.51	0.40	0.63	0.50	0.85	0.53

(b)

Table 5.2 Correlation between various scenarios of capacity calculation and temporal measures along the central axis of the room; Xdel refers to the mean excess delay and rms to the rms delay spread. In (a) this is done over the first 700 steps before large capacity fluctuations occurred. In (b) the capacity curves were smoothed to reduce this effect over the 1000 steps.

For narrow spacing the dispersion across paths, as quantified by the mean excess delay, was a good indicator of capacity since the overall spread of paths was not that different from a SISO system. For instance, consider the first order reflections from a particular surface. For narrow element spacing all paths from the Tx to the Rx are closely spaced and the time spread between them is minimal. However, the time gap between this group of paths and a similar group, reflecting from another surface, is more significant.

This is particularly the case at locations identified by the higher values of mean excess delay. When the element spacing increases, the time spread across a group of reflections from a given surface increases. However, this results in the time difference between groups of reflections from different surfaces reducing and potentially overlapping, thus making it difficult to clearly distinguish the different transmission paths and appears to increase the overall correlation of the channel matrix **H**. This issue has not been clearly identified in the literature.

The same issue arises when only second order reflections are considered, compared to first order only. These have longer path lengths and consequently the time spread of a given group tends to be greater than first order reflections; thus the time spread between groups tends to reduce. The result is lower correlation with capacity as indicated by the second order cases listed in Table 5.1. Some first order reflections, from W1 and W2, are widely dispersed with respect to each other and the LOS components and the results, in Table 5.1, indicate a strong correlation with capacity and dispersion for the case of LOS and first order reflections only.

For different room structures and dimensions the overall characteristics were similar but more exaggerated. Thus for a corridor structure the rms delay spread (and excess delay) was notably lower. This was significant towards the far end of the corridor and explains the low capacity in that section of the structure. Conversely there is higher overall rms delay for a square room and results in a wider distribution of good capacity, though overall the capacity was not much different to the rectangular structure considered, under normalised SNR levels. However, assuming a corridor structure to be relatively

long, then this factor combined with the effect of reduced actual SNR suggests that locating a Tx at one end would be likely to result in suboptimal performance if the Rx was towards the far end of the corridor.

5.4.3Mean excess delay and channel correlation

In order to compare the mean excess delay with channel correlation, the mean of the correlation matrix of the channel matrix **H** was determined for 1000 instances of the channel along the central axis of the room. As in the case of capacity measurements there were fluctuations over short distances for the NLOS λ/2 element spacing cases as shown in Figure C.6 appendix C. For visual comparison with the excess delay curve of Figure 5.10(a), the value of the mean of the channel correlation matrix is plotted. The correlation of this curve with the excess delay curve was approximately 0.89 and this increased to 0.94 using a 25 point moving average to compare the trend. It was noticeable that over short Tx-Rx separation distances, for all element spacings, that some relatively low channel correlation values were observed. However, these were not related to the time dispersion of paths, which was low in this region, and did not result in a significant level of capacity for λ/2 and λ element spacing.

For λ element spacing the mean channel correlation reduced significantly at longer distances when large fluctuations in capacity were present, an example is shown in Figure C.5 appendix C. Until this point the mean correlation trend did correlate reasonably well (0.92) with mean excess delay. (Over the first 600 iteration steps, as the Rx moves away from the Tx, it is approximately 0.8). At the wider spacing of 2 λ and 4 λ there was similar fluctuations and only the smaller spacing of λ/2 did not fluctuate significantly near the far wall and had a better capacity in that region. For the NLOS

case the mean capacities along the straight line at a range of greater than 10 m, were 22.1, 20.2, 19.7 and 20.6 b/s/Hz for element spacing λ/2, λ, 2 λ and 4 λ respectively. In all three cases of different element spacing there were relatively low levels of channel correlation and high levels of capacity in the region of the peak excess delay.

Since first-order only cases have more distinct groupings of reflection paths compared to second order ones, it is worth considering the cases of limited reflections, e.g. first order only from only two or three walls (for all regions of the room). This permits the possibility of maximum time dispersion between reflection groups from a given surface and those from another, allowing a clearer examination of the impact of dispersion on capacity. Figure C.7 (a) appendix C shows the maximum and minimum excess delay regions when reflections from W1 and W2 (adjacent walls) were determined and the Tx is located close to the left end centre of room as marked. Figure C.7(b) appendix C shows the corresponding capacity for λ/2 element spacing (NLOS conditions) and Figure C.7(c) shows the corresponding mean channel correlation values. For direct comparison the lower correlation values are shown in red. A clear overlap of the maximum regions for excess delay, capacity and minimum channel correlation is evident. Conversely, the lower capacity regions are distinctly different. These results confirm the relationship between signal dispersion and reduced channel correlation if small element spacing is involved.

An even more distinct overlap was present for the opposite side walls W1 and W3, as shown in Figure 5.11. This is unsurprising since the regions are close to the central axis

of the room and as such confirm the previous result for increased separation distance in the centre of the room when angular spread from reflections is less significant.

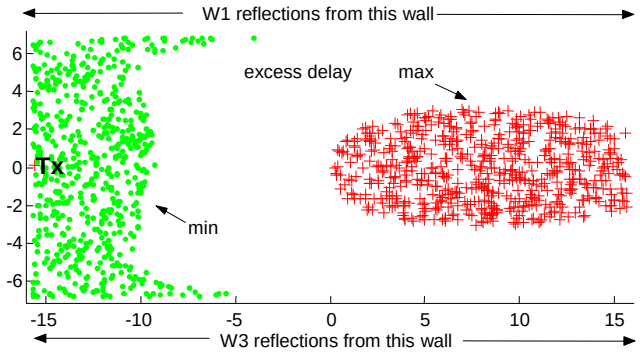

(a) Excess delay

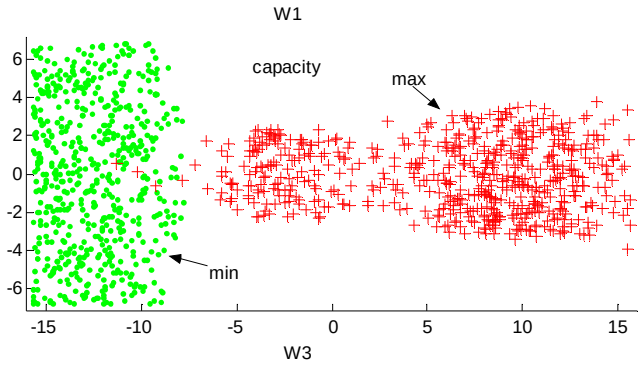

(b) Capacity

Figure 5.11 (continues on next page)

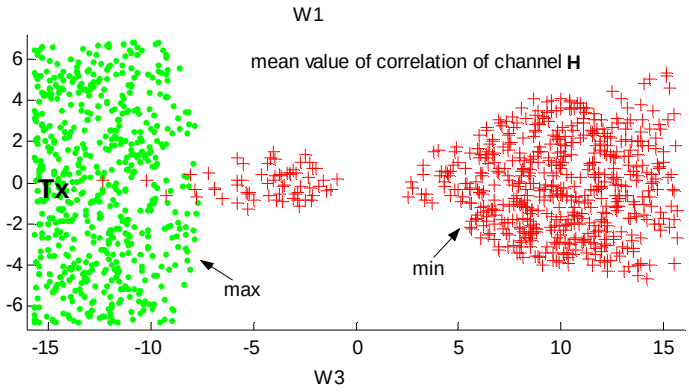

(c) mean value of correlation of channel **H**

Figure 5.11 Comparison of (maximum) 20% excess delay region (a) with maximum capacity (red) (b) and minimum 20% mean value of correlation of channel **H** (red) in (c). The corresponding 'weakest' 20% regions are green. First order reflections from W1 and W3 as indicated. Tx at Tx(1) position as marked on Figure 3.1.

5.5 2x2 Arrays

Other array configurations and smaller 2x2 structures did not provide any different or more useful information. However, as noted in the previous chapter, 2x2 systems did generally provide mean capacity levels closer to that predicted by random matrices. Figure 5.12 shows CDFs for 2x2 and 4x4 arrays at ranges beyond 10 m from the Tx, approximately 66% of the room area, in order to compare different element spacing beyond short ranges (where the LOS can dominate).

In Figure 5.12, with the LOS present, for the 2x2 system there was an interesting result which was that the smaller element spacing λ/2 was slightly better than both 2 λ and 4 λ

spacing; although all are similar. For 4x4 systems the CDFs were more distinct and λ/2 was also better than 2 λ. A similar result was present in [5.4] for two different simulation methods and physical measurement data but was not explained. This was directly related to the channel being less correlated due to the excess delay as discussed above. In both sets of CDFs the wider element spacing, 6 λ and 8 λ, affected the capacity due to the impact of angular spread of LOS paths.

In Figure C.8 appendix C the second order reflections case is shown. For this case the element spacing did not affect angular spreading as the path lengths were too long. In the case of 8 λ spacing the strong and weak locations showed widespread distribution throughout the room, suggesting a Rayleigh characteristic and the CDF is similar to that from random matrices. In this case the wide element spacing contributed to reducing the channel correlation albeit in an environment (second-order reflections) which is already diverse and behaves more like a distributed system [5.6] and those described in the next chapter and [5.12], which deals with the repositioning of individual array elements.

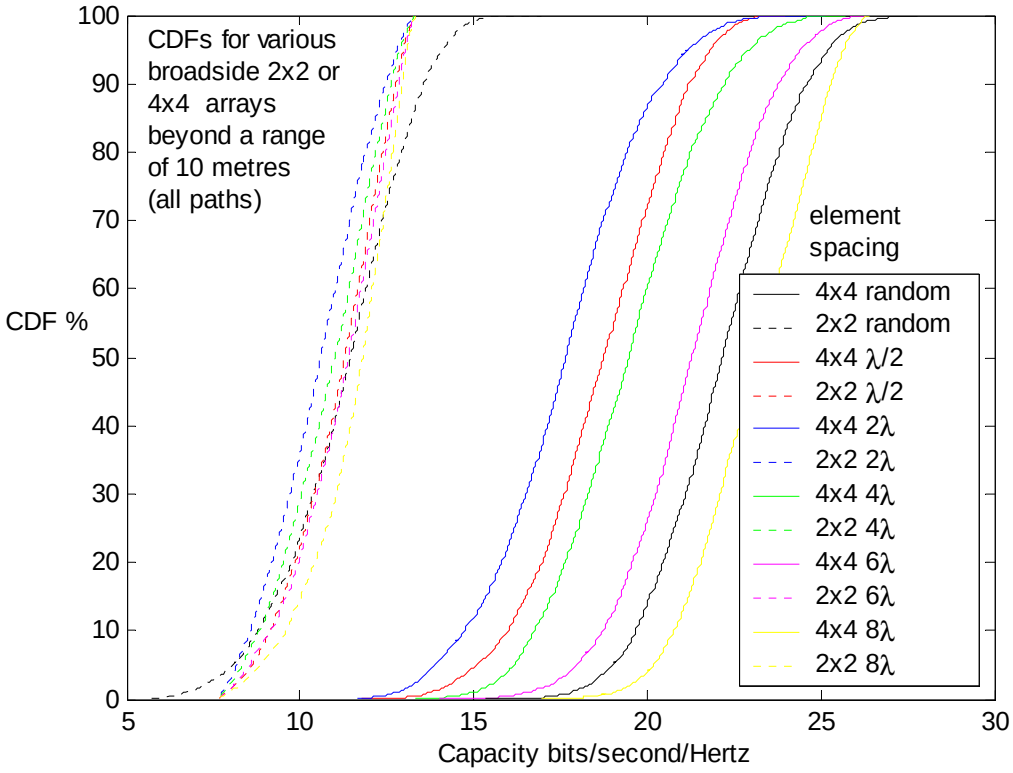

Figure 5.12 CDFs for uniform linear arrays with minimum Tx–Rx distance of 10 m in LOS conditions (all paths present).

For the 2x2 system results shown in Figure C.8 appendix C the λ/2 spacing was the best result and with only two elements closely approximating a point source, the effect of the dispersion of reflections was emphasised, particularly since only second order ones were present. From the above it can be concluded that smaller arrays with relatively limited variation in spacing in reflection rich environments, do not exhibit much variation in capacity. This confirms the results presented in [5.13] and [5.14] which indicated little benefit from increased element spacing beyond λ/2 and the results in [5.15]. However, it was also the case that larger arrays and wide spacing of elements particularly in LOS or sparse multipath environments do have a major impact and it is too simplistic, even for reflection rich channels, to not consider the geometric characteristics of the arrays.

5.6 Conclusions

There are various physical conditions that affect the performance of MIMO systems as demonstrated by the results of chapter 4 and the analysis in this chapter. It has been shown that apparently contradictory results regarding the impact of element spacing and some other geometric properties, such as relative orientation of arrays, can be explained by one or more of the following mechanisms that may exist, within the same simulation model, under different conditions.

1 Angular spread of paths, particularly LOS and first order reflections.

2 Interaction of limited number of transmission paths in a sparse environment.

3 Dispersion of transmission paths for small element spacing in central regions of the room (not near a reflecting surface).

4 Diversity of reflections, particularly if enhanced relative to LOS components, by strongly reflective surfaces.

Some authors have suggested, as discussed in the previous chapter, that there are benefits of wide elements spacing while others have suggested the opposite under certain conditions. The detailed results provided here demonstrate that both scenarios can arise and can be explained if both spatial and temporal characteristics are considered, in the context of the geometric characteristics of the arrays and propagation conditions.

The element spacing can have a major impact on system performance for short-range LOS only channels and those dominated by a limited number of strong paths, rather than the ideal Rayleigh channel. In particular, it also affects the first order reflections

and explains the varied pattern of good and bad locations at the same SNR in the room under sparse propagation conditions.

Conversely, at large distances with many reflections there is little benefit for wide spacing and in fact smaller spacing (λ/2) is often marginally better due to larger dispersion between the various reflection groups. At wide element spacing, approximating a distributed system, there is some small benefit for indoor environments but such arrays may not be practical, at least not at both ends of the channel. The wide spacing of individual elements and adjustments at one side of channel only are considered in the next chapter.

If only the LOS components are considered, then wide spacing of broadside linear array elements is always the best solution. Clearly for indoor environments that scenario is unlikely except as an approximation for short range conditions, typically 2 to 3 metres. Table 5.1 indicates that if spacing of ULAs at both ends of the channel can be wide (8 λ) then good near optimal spectral efficiency can be achieved throughout most of the room.

In the more general case of some LOS components and reflections, the recommendations from the previous chapter are broadly applicable; particularly the enhancement of some reflections if possible. This would result in more Rayleigh type propagation conditions and enhance the SNR and smaller element spacing would significantly benefit in such sparse environments. However, for a given SNR the levels of spectral efficiency achievable for small element spacing (λ/2 -2 λ) with limited number of paths is limited to a mean of 60-70% percent of the Rayleigh channel. This is

a significant improvement compared to the LOS only case and if small element spacing is unavoidable, under LOS dominated conditions, then the introduction of some stronger reflections should be considered. The situation is summarised in Table 5.3 below which shows results normalised for the impact of increased SNR due to enhanced reflections from some surfaces in the room (similar to Table 4.4). This emphasises the more general conclusion that the propagation conditions are the main determinant of spectral efficiency as far as typical array structures such as ULAs are concerned.

Element Spacing →	λ/2	λ/2 Dist. >10 m	2λ	2λ Dist. >10 m
LOS only	8.7	8.7	11.2	10.7
LOS W1	13.0	13.8	13.6	13.5
LOS W1(r)	14.7	15.4	15.0	14.9
LOS W1 W2	13.3	14.0	14.1	14.1
LOS W1(r) W2	15.0	15.6	15.5	15.5
LOS W1(r) W2(r)	15.8	16.2	16.6	16.7
LOS W1 W2 CL.	13.2	13.9	14.1	14.0
LOS W1(r) W2(r) CL(r)	16.1	16.4	17.4	16.9

Table 5.3 Summary of capacity performance (spectral efficiency in bits/second/Hertz) for various sparse propagation conditions for 4x4 ULAs with broadside arrangements. The 'r' in brackets beside a wall number indicates that the reflection coefficient has been modified to Γ=1.

From a deployment perspective the most significant factor derived from analysing dispersion characteristics is that those factors correlate strongly with spectral efficiency for arrays with smaller element spacing. (The dispersion between reflections from one wall and another tends to be greater than for widely separated array elements and this factor tends to reduce the channel correlation). This is most effective in central regions of the room, when angular spread from reflections is less significant. This position should be considered for positioning the Rx when λ/2 spacing is used. Conversely, if wide element spacing is available then positions close to a strong reflecting surface is preferable and overall the results in this chapter confirm that the arbitrary positioning of

arrays without consideration of propagation conditions or array geometry is unlikely to result in optimal spectral efficiency.

5.7 References

[5.1] D. Gesbert, H. Bolcskei, D.A. Gore, A.J Paulraj, " Outdoor MIMO wireless channels: models and performance predictions", *IEEE Transactions on Wireless Communications,* Vol. 50, issue 12, December, 2002, pp. 1926-1934.

[5.2] I. Sarris, A.R. Nix, "Maximum MIMO capacity in line-of-sight", *IEEE Int. Conference Commumications and Signal Processing*, Dec. 2005, pp.1236-1240.

[5.3] I. Sarris, A.R. Nix, "Design and performance assessment of High capacity MIMO architectures in the presence of a line-of-sight component", *IEEE Transactions on Vehicular Technology*, Vol. 56. issue 4, 2007, pp. 2194-2202.

[5.4] J.S. Jiang, M.A. Ingram, "Distributed source model for short-range MIMO", *IEEE 58th Vehicular Technology Conference 2003*,Vol.1, Autumn 2003, pp 357-362.

[5.5] D. Neirynck, C. Williams, A. Nix, M. Beach, "Personal area networks with line-of-sight MIMO operation", *IEEE Vehicular Technology Conference (63rd* Spring, 2006*)*, pp. 2859-2862.

[5.6] Z. Li, F. Luan; Y. Zhang, L. Xiao, L. Huang, S. Zhou, hidong; X. Xu; J. Wang, "Capacity and spatial correlation measurements for wideband distributed MIMO channel in aircraft cabin environment", *IEEE Wireless Communications and Networking Conference (WCNC*, 2012*)*, pp. 1175-1179.

[5.7] A. Grennan, C. Downing, B. Foley, "A Geometric Interpretation of Indoor MIMO Systems using a Deterministic Model", *European Conference on Antennas and Propagation,* Edinburgh Nov. 2007, pp. 88-93.

[5.8] A.M. Sayeed, V Raghavan, "Maximising MIMO Capacity in Sparse Multipath with Reconfigurable Antenna Arrays", *IEEE Journal of Selected Topics in Signal Processing*, Vol. 1 Issue 1, pp. 156-166, 2007.

[5.9] T. S. Rappaport, *Wireless Communications*, Prentice Hall, 1996

[5.10] R.J.C. Bultitude, P. Melancon, H. Zaghoul, G. Morrison, M. Prokki, "The Performance of Indoor Radio Channel Multipath Characteristic on Transmit/Receive Ranges", *IEEE Journal on Selected Areas in Communications*, SAC. 11, No.7, 1993, pp. 979-990.

[5.11] A. Z. Tang, A.S. Mohan, "Experimental Investigation of Indoor MIMO Ricean Channel", IEEE Antennas and Wireless Propagation Letter, Vol.4, 2005, pp. 55-58.

[5.12] A. Grennan, C. Downing, B. Foley "Application and analysis of MIMO systems using Metropolis algorithm", *Loughborough Antennas and Propagation Conference (LAPC),* Nov. 2010, pp. 357-360.

[5.13] V. Pohl, V. Jungnickel, T. Haustein, C. von Helmolt, "Antenna Spacing in MIMO Indoor Channels*", IEEE Vehicular Technology Conference*, Spring 2002, pp. 749-753 .

[5.14] A.A. Hutter, F. Platbrood, J. Ayadi, "Antenna Spacing in MIMO Indoor Channels Analysis of MIMO capacity gains for indoor propagation channels with LOS component", *IEEE 13th International Symposium on Personal, Indoor and Mobile Radio Communications (PIMRC)*, Vol. 3, 2002, pp. 1337-1341.

[5.15] A. Burr, "Evaluation of capacity of indoor wireless MIMO channel using ray-tracing", *International Zurich Seminar on Broadband Communication*, 2002, pp. 281-286.

Chapter 6 Array Element Adaptation using Metropolis Algorithm

6.1 Introduction

The condition of the propagation channel is the factor that most influences the performance of MIMO systems. The conclusions for system deployment in the previous chapters recognise this, particularly for longer Tx-Rx ranges. However, the suggestion to enhance reflections may not always be feasible. An alternative approach is to reconfigure the arrays in an attempt to reduce the correlation of the channel. From the previous chapters it has been demonstrated that uniform linear arrays are the most likely to result in optimal performance. Thus the focus of this chapter is on the adjustment of the relative position of the individual elements of ULAs in order to improve the spectral efficiency. This was done by using a random walk technique, based on the Metropolis algorithm. Original results are presented and explained, for various propagation conditions, that demonstrate how near optimal spectral efficiency may be achieved.

6.2 Background

6.2.1 Related work

In the previous chapters results were presented that demonstrated that for many instances of channel realisations, and for a given pair of Tx and Rx locations, it was difficult to achieve a high capacity compared to those predicted for ideal Rayleigh channels in [6.1]. The alternative approach presented here for improving spectral efficiency was first described in [6.2] and was further developed in [6.3]. In those papers it was demonstrated that significant improvement in spectral efficiency could be achieved by using the Metropolis algorithm [6.12] to adjust the elements of the arrays at

a given pair of Tx and Rx locations. In [6.3] it was demonstrated that capacity improvement of over 50% could be achieved with small adjustments of the individual elements of ULAs, compared to initial values, using the Metropolis algorithm. Better performance was achieved when elements at both the Tx and the Rx were adjusted in three dimensions; but it was also possible to achieve a good improvement by limiting the adjustment to a single dimension. In [6.4] results based on modified array structures found using the Metropolis algorithm were presented; it was shown that some configurations provided a general improvement in system performance compared to the non-adjusted case, for most channel realisations.

Other studies, involving repositioning/adapting of the antenna element positions, were described in [6.5], (see section 2.4.5). Also [6.6] used an adaptation approach but the technique and results were unclear. Similar work to [6.5] was described in [6.7] under the heading of reconfigurable arrays. They proposed modifying the spacing between elements in large linear arrays to affect the radiation beam pattern in order to enhance capacity in sparse multipath environments. They provided a theoretical framework for adapting the element spacing based on their numerical modelling of the MIMO channel. However, they did not provide examples of arrays or related dimensions and no subsequent results based on linear arrays as described are given. Another paper dealing with reconfigurable arrays was [6.8] in which they employed a large grid of array elements from which some were selected to implement 2x2 or 4x4 arrays. They used the Saleh-Valenzuela model with angle statistics (SVA) [6.9] to estimate capacities and found significant improvements compared to their non-reconfigured array

measurements. They concluded that their approach ‘may enable aggressive spectral reuse’, i.e. improve the spectral efficiency of the channel.

In section 2.4.6 distributed MIMO systems [6.10] [6.11] were introduced; and if a wide separation of elements occurs during an adaptive repositioning of elements then the resultant array can be viewed as being similar. However, a general aim of the work presented here is to avoid excessive element displacements; since long antenna feeds in short range environments are not desirable; although at one side of the channel it may be acceptable.

6.2.2 Metropolis algorithm

The Metropolis algorithm was developed for simulating physical (chemical) systems and is named after Nick Metropolis [6.12]. It is discussed in [6.13] where it is described as the ‘most successful and influential’ algorithm that comes under the heading of Monte Carlo Methods (MCMs) and uses randomly generated ‘moves’, as described below to find an improved state. If the new state is an improvement, then it is kept, otherwise it is rejected and another attempt is made. The size of the move may be scaled, which can affect the rate of convergence to a final state. Smaller moves are more likely to result in testing a greater number of states and thus possibly optimising the search, but at the expense of more trials. The normal distribution was used to determine each move; although this is an arbitrary choice as the important aspect is the acceptance/rejection of the most recent trial results. The application here is particularly appropriate since the moves are directly based on randomly repositioning the antenna array elements and calculating the new capacity.

$$\boldsymbol{Element\ displacement} = \pm \boldsymbol{n} \times \boldsymbol{step} \times \boldsymbol{\lambda} \qquad (6.1)$$

where n is a random value with normal distribution between 0 and 1, *step* is a scaler between 0 and 1 and λ is the wavelength of the carrier. The sign is randomly determined with a 50% probability of being plus or minus. This is done for each element being adjusted and then the channel capacity is calculated. In summary,

If (new capacity > previous capacity)

Accept new array element locations

Else

Reject and repeat using previous array element locations

The step factor used was typically 0.1 and resulted in the individual element adjustments being in the approximate range of $\pm$ λ/4 of a wavelength. Some trials were also done in which a minimum floor was applied (i.e. 5 mm) to determine the practicality of the method by avoiding unduly small increments. This was done independently for each array element at either the Rx only or both the Tx and Rx. Typically 1000 iterations were done per trial although less than half that was usually required to achieve a final peak capacity for a given scenario.

6.2.3 Simulation methodology

It was not feasible to consider the optimisation at every possible pair of Tx and Rx locations in the room. It was expected that each pair of locations was likely to generate a different optimised set of adjustments and trials confirmed this. Thus, locations were arbitrarily chosen for a given system configuration (e.g. 2 λ element spacing 4x4 system under LOS conditions) but which corresponded to a low-level of capacity as previously determined; for instance from some of the results presented in chapter 4.

The same room dimensions were used as in Figure 3.1 of chapter 3 and Figure 6.1 below which shows different Rx locations with the precise location for the centre point of the array is in the legend; the Tx location is Tx(1). The main adjustments done were either for a single dimension, referred to as X, Y or Z dimension as indicated on Figure 3.1, or for all three simultaneously, i.e. 3-D. The Tx array elements were sometimes fixed and adjustments only done at the Rx, in other cases both the Tx and the Rx elements were adjusted.

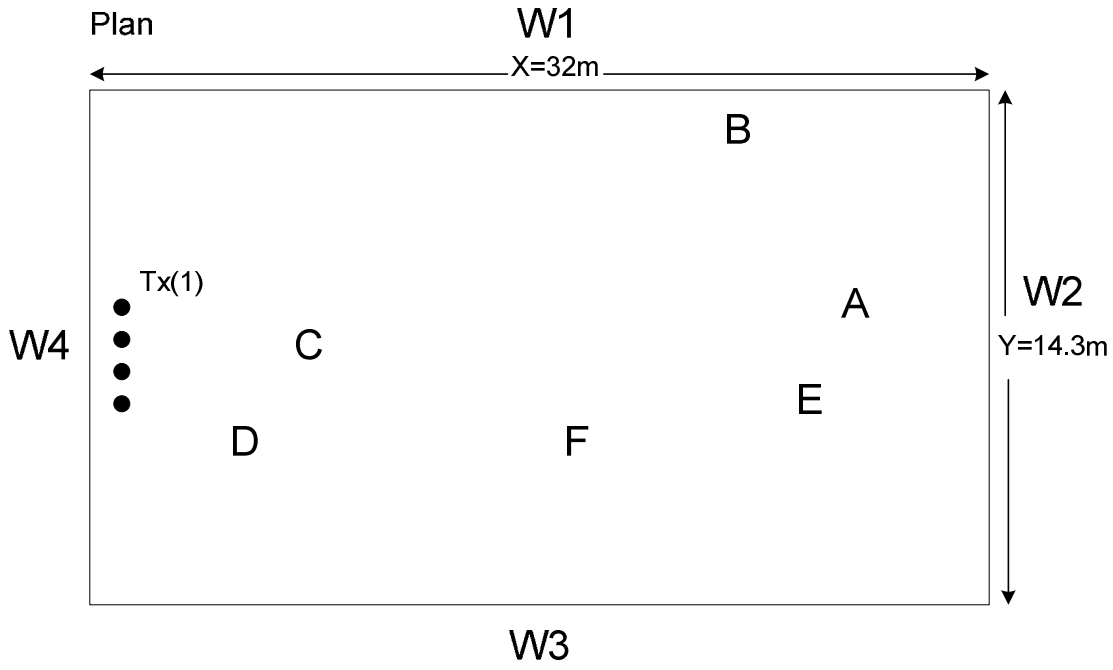

Legend

LOCATION	X	Y	Z
A	13.9	0.47	0.32
B	2.7	6.7	-0.426
C	-11	0.0	-0.167
D	-12	-4	-0.167
E	12.9	-3.1	0.26
F	0.524	-3.6	0.45

Figure 6.1 Various Rx locations used for simulations in this chapter. The plan of the room is shown (X and Y dimensions) with the centre of the room being (X, Y, Z) = (0, 0, 0).

6.3 Simulation Results for 4x4 Arrays

6.3.1 Adaptation of single dimension at Rx side of channel only

The first position chosen was for a 4x4 system at Tx(1) position and the Rx at A, broadside to each other. The initial element spacing was 2 λ. The SNR at the Rx was normalised at 20 dB, under LOS conditions, and the capacity was 16.4 b/s/Hz. As the arrays were broadside the first adjustments attempted were restricted to the axes of the array in the Y-dimension. This resulted in an improvement of approximately 25% as indicated in Figure 6.2, which shows a typical trial (the green curve) which peaks at about 20.5 b/s/Hz. This was a maximum upper limit, approximately, for all cases of single dimension adjustments. The figure shows the successive peaks achieved and not the instantaneous changes for each trial. The capacity levels correspond to the best position achieved at that iteration point (when a new position resulted in higher capacity) until the next improvement. Most of the increases in capacity took about 10-12 improvements requiring about 50 iterations. The mean value of the element displacements was less than λ/2 with maximum shifts between 0.75 λ and λ. Overall the span of the array (6 λ) did not significantly alter as can be seen in the examples shown in Figure 6.3. In general for wider arrays of 2 λ or more, it was always possible to achieve the best improvement without exceeding the arrays initial span.

For the X-dimension only shifts, a similar sequence of iterations occurred, however the element displacements were notably smaller (see Figure 6.4). The maximum never exceeded λ/2 and the mean values were in the region of λ/5 for the various trials. For the vertical Z-dimension only adjustments, the displacements averaged greater than 2 λ and maximums were close to 3 λ (see Figure 6.4). Also, the number of iterations and the

small capacity improvements to the peak achieved were different from the other cases as illustrated by the smooth blue curve on Figure 6.2. Typically, about 100 small iteration steps that improved capacity were required, whereas for the X-plane only case about 10 iteration steps occurred. The capacity value at successive iterations including those not yielding improvement is almost the same as the curve in Figure 6.2; in the other cases, notable variations occurred.

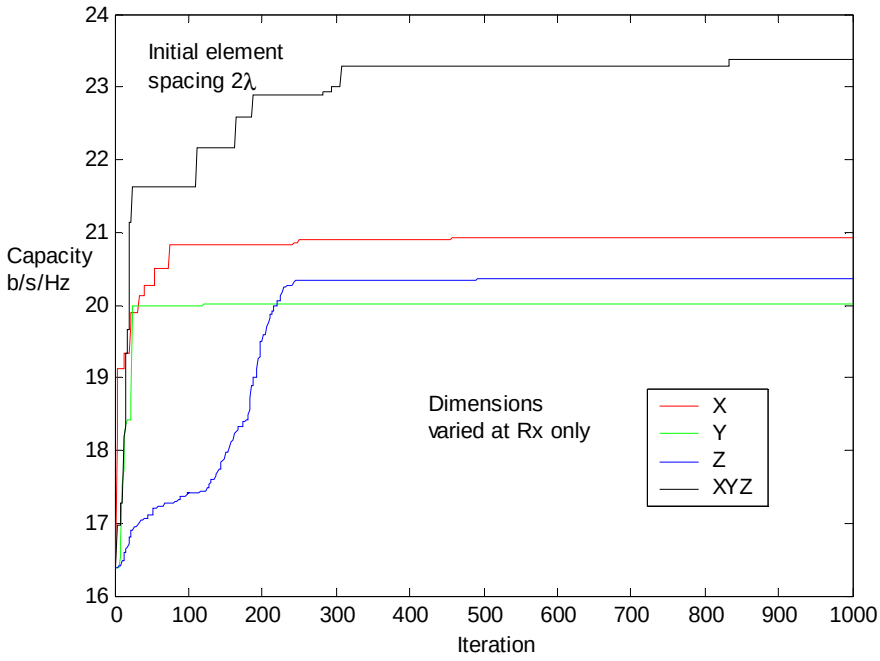

Figure 6.2 Capacity improvement steps when only the Rx was varied at position A.

Figure 6.3 Examples of adjusted arrays at the Rx showing Y-dimension shifts only. The crosses mark the original position and star the final positions.

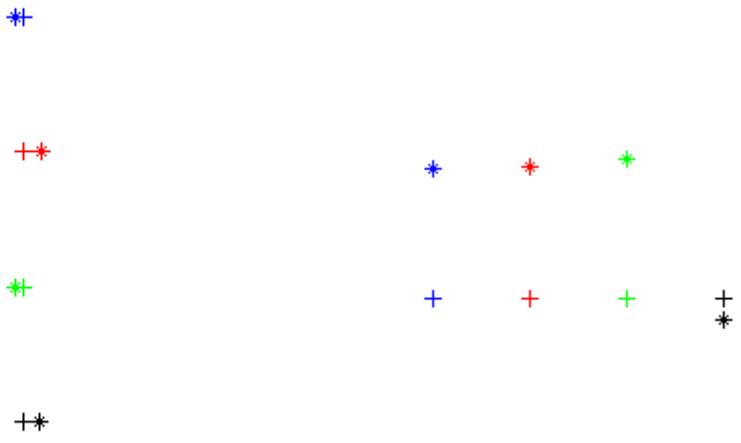

X-dimension only Z-dimension only

Figure 6.4 Examples of element displacements for Rx side adjustments only. The crosses mark the original position and star the final positions.

6.3.2 Adaptation in three dimensions (3D) at the Rx

Permitting 3-dimensional shifts (XYZ dimensions simultaneously adjusted) resulted in improved capacity compared to any single dimension, in most trials. Each individual array element was adjusted independently and each random move determined was for a single dimension with the final position of the array element resulting after three moves (X, Y, and Z). Although there was more variation in the results in terms of final capacity and the magnitude of the element displacements in any given plane, the minimum level achieved was approximately 22 b/s/Hz (35% improvement). More than half the trials resulted in a final capacity in excess of 24 b/s/Hz representing improvements in the range of 50% on the initial value, an example of which is shown on Figure 6.2. The capacity levels achieved were often in excess of the mean predicted for ideal Rayleigh channels which is approximately 22 b/s/Hz for 20dB SNR. The magnitude of the positional shifts for these trials (those improved by about 50%), compared to the single adjustment cases, was slightly bigger X-shifts (in the region of $\lambda/4$ average), similar for Y-shifts and much smaller for Z-shifts. The mean excess delay spread was similar to the larger fluctuations of the X-dimension only case. Overall there were large variations in capacity and mean excess delay for the initial 100-200 iterations, when most improvement occurred, but followed a broadly similar trend.

Using a larger step size of 0.5 the search algorithm did not yield better results (in most cases slightly poorer) but required less iterations and the average size of the element displacements was larger. The main advantage of larger steps was a faster convergence to higher values but not the best achievable outcome; thus most of the results presented are at the smaller step of 0.1 unless stated otherwise. Limiting the element repositioning

to any combination of two dimensions, e.g. X and Z, did not achieve any significant improvement over a single dimension. Typically the improvement was approximately 0.5 - 1.5 b/s/Hz. However, there was generally a smaller displacement of the elements in any given direction compared to the single dimension case. This was most pronounced for the Z-dimension in the X-Z case (reduced to between $\lambda/4$ to $\lambda/2$). In effect there was a trade-off between capacity improvement and the degrees of freedom permitted in adjusting the position of the elements. Adjusting in a sequential manner, a single dimension followed by another dimension, did not improve the capacity above that achieved in a single dimension. Also, some simulations were conducted in which the minimum move from the existing position was controlled to be not less than 5 mm to determine if adjustments could be practically implemented. In all such trials the rate of improvement and the final capacity achieved were approximately the same as before. This was done for single dimensions, three dimensions and for adaptation at both sides of the channel as described below. Thus it is a feasible proposition to make adjustments and if one side of the channel was fixed, for instance a network access point, the other side may be adjusted in cases when the spectral efficiency is poor.

6.3.3 Adaptation at both sides of channel

An alternative approach is to adjust a single dimension at both ends of the channel. The main drawback of this approach, apart from the double location adjustment is the uniqueness of each solution. In other words, one optimised Tx-Rx pair will not be optimised for a second Rx location, assuming a fixed Tx position. In Figure 6.5 the improvement steps for the double adjustments are shown and indicate a clear benefit for both the X and Y-dimensions compared to the single-ended adjustment. Better results were obtained for the Z-dimension only case in most trials, close to the levels achieved

adjusting all three dimensions. As before, the array elements were displaced by a larger degree and an example at both the Tx and the Rx is shown in Figure 6.6. The pattern of displacements varied for different trials but generally at least one element displaced at both sides of the channel by a relatively large distance (e.g. 20-25 cm) and one element by a small amount (3-6 cm).

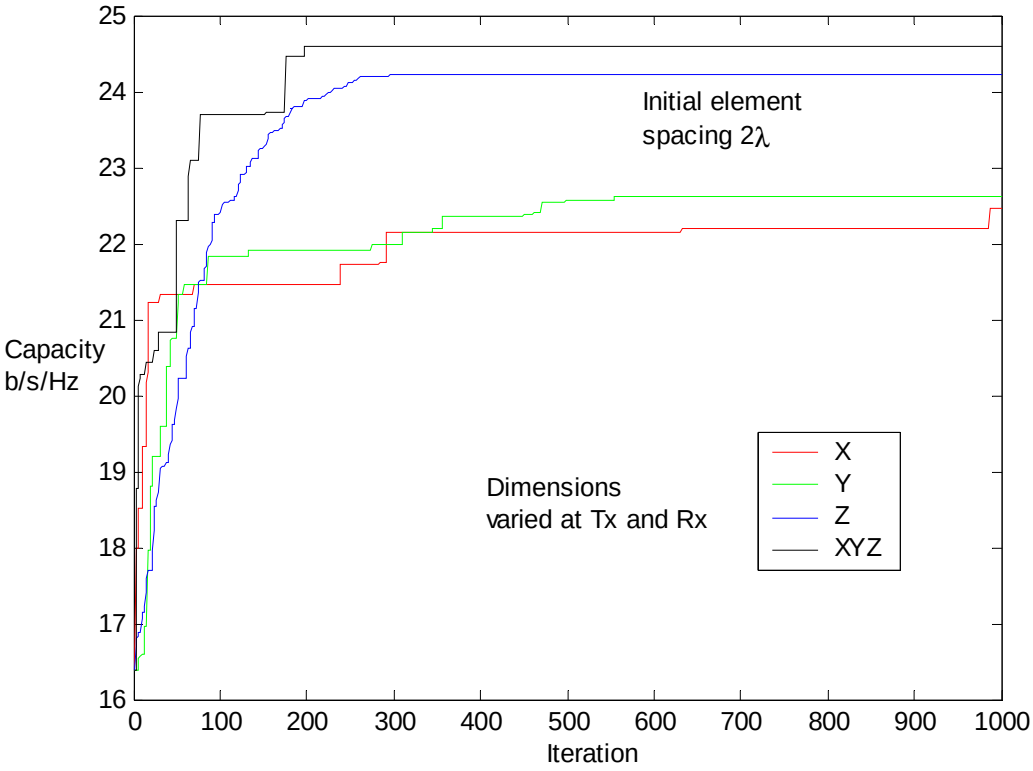

Figure 6.5 Improvements in capacity levels when both the Tx and the Rx were adjusted at position A.

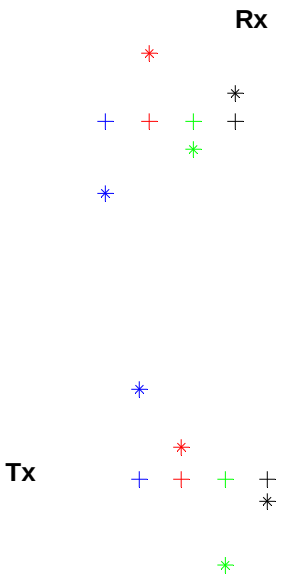

Figure 6.6 Example of Z-dimension only adjustments at the Tx and Rx using an average determined configuration. The initial element spacing (between a pair of crosses, the initial position marker) is 2 λ, approximately 12 cm. The maximum displacement shown is approximately 24 cm and the minimum is 6 cm.

6.3.4 Validation tests for reconfigured arrays

The expectation was for a given reconfigured array performance to be specific to a given pair of Tx – Rx locations. Thus a number of simulations were performed to verify this or determine if a more general improvement could be achieved. This was done using the same method as in chapter 4; a fixed Tx position and randomly repositioned Rx (3000 trials) using the Metropolis search determined array configurations for the optimal capacities achieved. In most cases there was little difference from the non-adjusted case as shown in Figure 6.7, which shows a selection of these results. (In fact X and Y only adjustments, which are not shown, were slightly poorer than the non-adjusted case). The only result that was notably improved was for the Z-adjustment at

both the Tx and the Rx, which had a mean value of close to 21 b/s/Hz, which compares favourably with the ideal Rayleigh case of approximately 22 b/s/Hz.

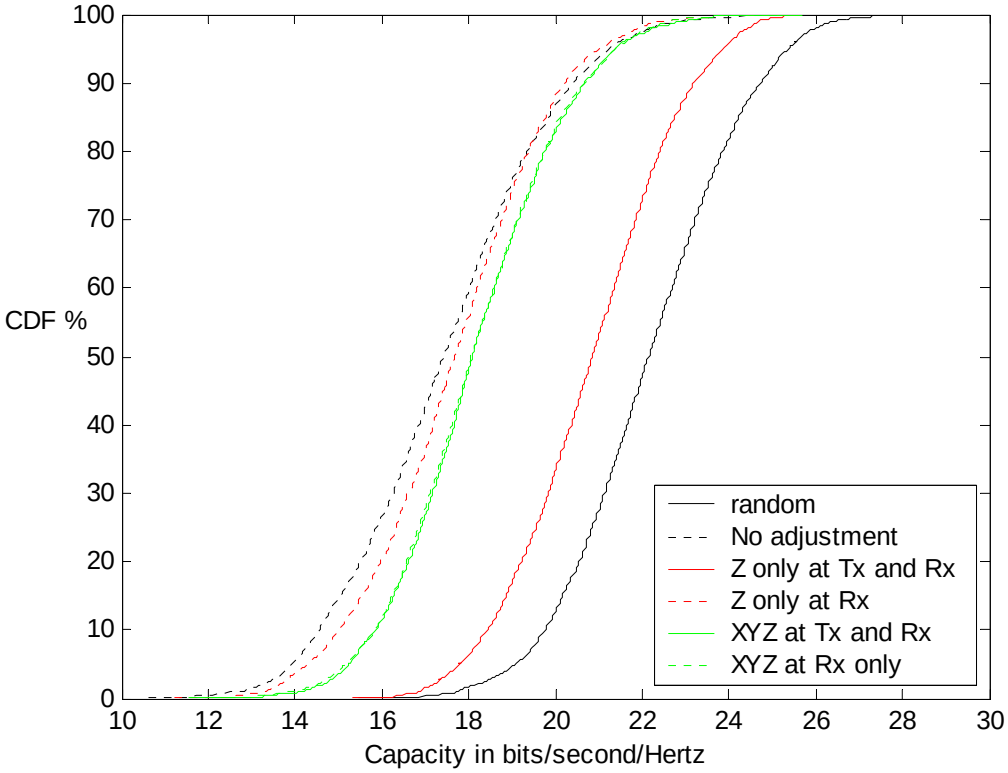

Figure 6.7 CDFs of capacity throughout the room for different reconfigured arrays with only the Z-dimension adjusted or all 3 dimensions adjusted (XYZ).

In order to determine if there was any significance in the particular configuration at the Tx and Rx, when Z only adjustments were made, a number of arbitrary values were used, with similar magnitudes of displacements. The CDFs derived are shown in Figure 6.8. Although the determined case (red curve) is best, it is only by a relatively small margin with a median difference in the region of 0.5 b/s/Hz. Also, a slightly better result was obtained using the determined value at the Tx but an arbitrary value at the Rx (red dashed curve).

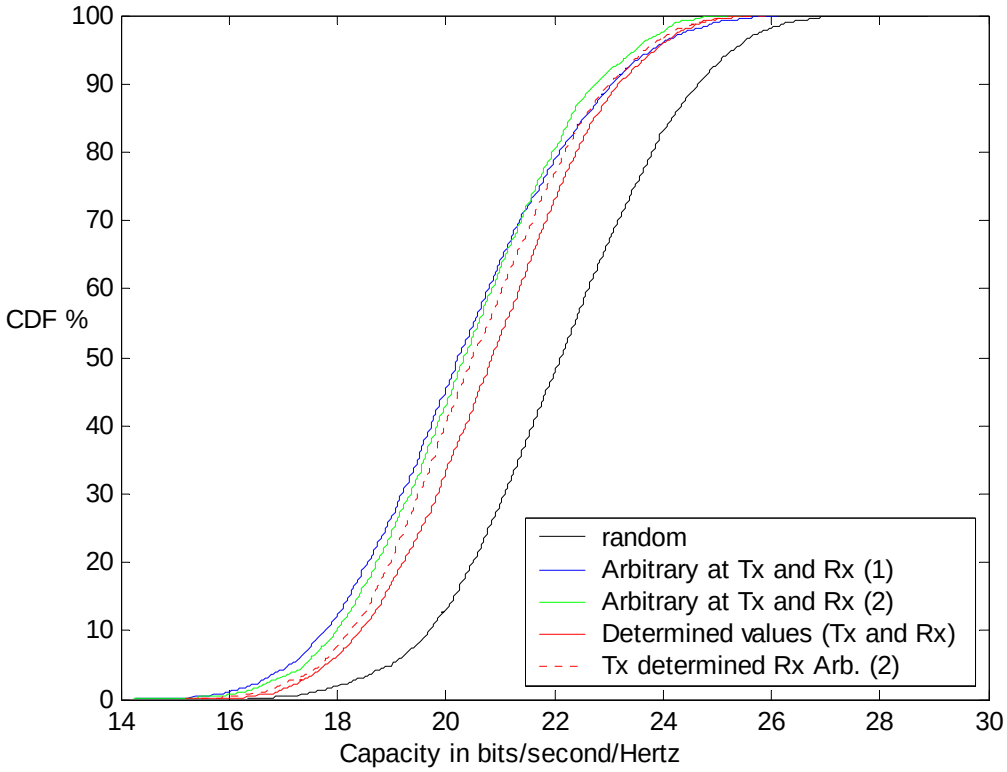

Figure 6.8 CDFs of capacity throughout the room for different configurations obtained from Metropolis searches for Z-dimension adjustments compared with some arbitrary adjustments in Z-dimension. The Tx was at location Tx(1).

Further investigations using the Metropolis searches yielded several cases where the capacity, at location A, converged to approximately the same final value. This was the maximum achievable. Furthermore, there were similar element displacements along the Z-axis. Of particular note was the fact that the final orientation of the shifts, up or down, was the same for the individual elements at both the Tx and the Rx for the different trials that gave the best results. This suggested that an optimal configuration would most likely be similar and thus an average configuration was determined, using a selection of the results. This average configuration was then used in a number of simulations to investigate the system performance under different conditions. (The maximum displacement of this configuration was approximately 24 cm and the minimum was 6

cm as shown in Figure 6.6). Figure 6.9 shows the CDFs for the average configuration for LOS (all paths), NLOS and second order reflections only. For comparison the non-adjusted cases are shown (dashed lines) for the corresponding conditions with the SNR normalised at 20 dB at the Rx.

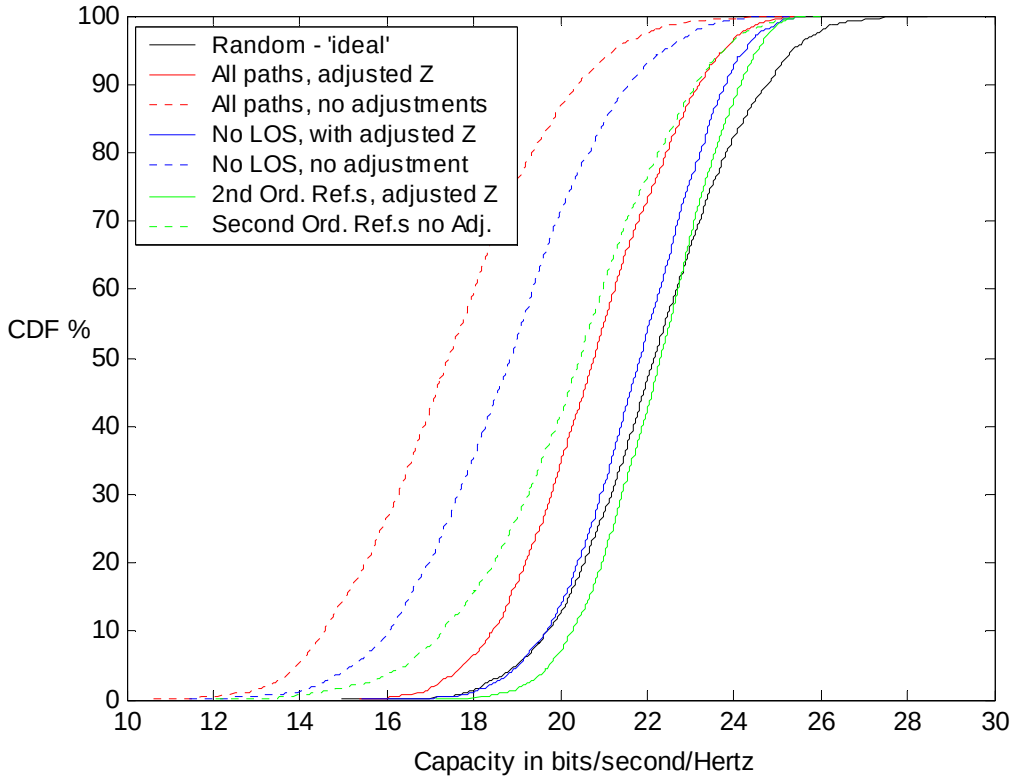

Figure 6.9 CDFs of capacity throughout the room, using average configurations obtained from Metropolis searches for Z-dimension adjustments under different conditions (LOS/all paths, NLOS and second-order reflections only). The non-adjusted case is shown for comparison.

In all cases there was an improvement in the mean capacities obtained and for the most uncorrelated set of reflections, second order only, this was approximately the same as for the ideal Rayleigh case. Although a comparison of the performance should be treated cautiously, since for the second order only cases the capacity was reasonably good without adjustment. The condition with LOS present resulted in the best

improvement (+19%). However for system deployments the benefits of the Z axis adjustments were obtained for all propagation conditions. They are the most likely way of increasing the spatial diversity of the channel for various Tx and Rx location pairs regardless of the conditions and without major repositioning of the antenna elements and has the advantage of being in a single dimension only.

Noting the benefits of wider spacing for decorrelating LOS components, simulations were done in which one element at the Tx was repositioned by a more significant distance. In this case one of the outer elements at the Tx, which was not displaced by a large distance initially, was moved to a new position. The original displacement magnitude was 0.057 m and this was scaled by a factor of ten to 0.57 m. This resulted in a slightly improved overall performance. Similarly one of the elements at the Rx was adjusted (Tx remaining at original values) and this yielded a better result. However, the mean was improved by only 0.5 b/s/Hz compared to the original displaced set. Other simulations in which the Rx was not adjusted, or only 1 element was adjusted at both ends (by the larger displacement), were also investigated. None of these variations yielded any improvements compared to the original displaced Tx-Rx pair found by the Metropolis search. In chapter 4 results were presented for the 2 λ broadside element spacing in which both the Tx and Rx were randomly positioned throughout the room for second order reflections only. This result compared favourably with those of random matrices. Using the same approach but with the modified arrays in the Z-dimension the results were better. Although the magnitude of the improvement was small and the CDF curve was slightly different, the achievement of any improvement in a deterministic model under such conditions is notable.

Figure D.1 appendix D shows the distribution of strong and weak locations throughout the room, in the manner used in chapter 4 for the average adjusted Tx and Rx displacements (with the Tx at the Tx(1) position). There was an overall improvement in capacity throughout the room compared to the non-adjusted case. In particular there was a high capacity close to walls W1 and W2. This corresponds (approximately) to the region in which the angular spread of the first order reflections from the walls is a maximum. The average capacity with the average adjustments in a region of a few square metres close to the wall (W1) was 22 b/s/Hz and without adjusted arrays it was 19 b/s/Hz. There was also a higher average capacity level, 22.5 b/s/Hz, in the region near the Tx due to the LOS components (although this is always a good region particularly for wider element spacing). In both of these regions the average capacity approximated that of the ideal case and thus it is reasonable to assume optimal levels of mean capacity were achieved.

At short ranges the increased spacing of elements gives rise to large angular spreading of rays which can result in improved capacity as noted previously. Thus, to determine if the adjusted arrays were effective at longer ranges when the angular spread of LOS components is minimal, results are shown in Table 6.1 for distances beyond 10 m from the Tx. This covers a region of approximately two thirds of the room, the right hand side of Figure 6.1. Mean capacity values of 22 b/s/Hz (corresponding to levels achieved using random matrices) were achieved for most cases using the average adjustments and, as found in earlier results, the smaller spacing (in Y-dimension) of $\lambda/2$ was slightly better overall. (This includes results for scaled versions of 0.5 or 2 times the original average displacement values).

Element spacing	Std. LOS	Std. NLOS	Std 2^{nd}	Z avg LOS	Z avg NLOS	Zx2 LOS	Zx2 NLOS	Z/2 LOS	Z/2 NLOS	Zx2 2^{nd}	Z/2 2^{nd}
$\lambda/2$	18.7	19.8	21.2	22.5	22.4	22.0	22.2	21.1	22.4	22.4	22.2
2λ	17.6	18.8	20.4	21.3	22.1	21.8	22.1	20.3	21.3	22.2	21.9

Table 6.1 Mean capacity for distances beyond 10 m from the Tx for various 'average' Z-adjustments and scaled versions of them. Std (standard) means not adjusted and 2^{nd} means second order reflections only.

To confirm the general application of the Z-plane adjustments, the Tx was repositioned to other locations relative to Tx(1). The X and Y distances from the original Tx(1) location are shown in Table 6.2. There was little variation in the capacity achieved and this was not the case for other configurations which were only optimal for the location that the adjustments were done.

Element spacing	1	2	3	4	5	6	8	9	10	12	11	12
Position Relative To Tx(1) >>	LOS at Tx(1)	NLOS at Tx(1)	2^{nd} at Tx(1)	LOS X+5 Y-3	NLOS X+5 Y-3	2^{nd} X+5 Y-3	LOS X+10 Y-3	NLOS X+10 Y-3	2^{nd} X+10 Y-3	LOS X+20 Y-6	NLOS X+20 Y-6	2^{nd} X+20 Y-6
$\lambda/2$	20.9	21.8	22.2	20.7	21.8	22.0	19.9	21.7	21.8	19.7	21.3	21.8
λ	20.8	21.8	22.2	20.7	21.8	21.9	20.1	21.7	22	20.1	21.4	21.9
2λ	20.8	21.8	22.2	20.8	21.8	21.9	20.1	21.8	21.7	20.3	21.4	21.7

Table 6.2 Mean capacity at distances beyond 10 m from the Tx(1) position for average Z-adjustments for various Tx locations identified relative to Tx(1) position in X and Y coordinates.

6.4 Simulation Results for 2x2 Arrays

6.4.1 Adaptation for various scenarios for 2x2 channels

Fig 6.10 shows the CDFs associated with 2x2 systems for various conditions. Unlike the corresponding 4x4 case there was a much smaller difference between ideal and deterministically simulated results with the Tx fixed at location A. Regardless of the conditions there was generally a good overall performance, although a lower limiting

maximum was present; close to 90% of the maximum level achieved in the ideal case of (13.3 b/s/Hz). This also applied to the case of randomly repositioned Tx and Rx pairs, as shown by the dashed lines, including the second order only case, although there was little difference between the three results. The mean for this case was approximately 11.9 b/s/Hz, while for the fixed Tx equivalent it was 11.42 b/s/Hz and the ideal random case was actually lower at 11.23 b/s/Hz. (the LOS cases were 11.6 and 10.4 respectively).

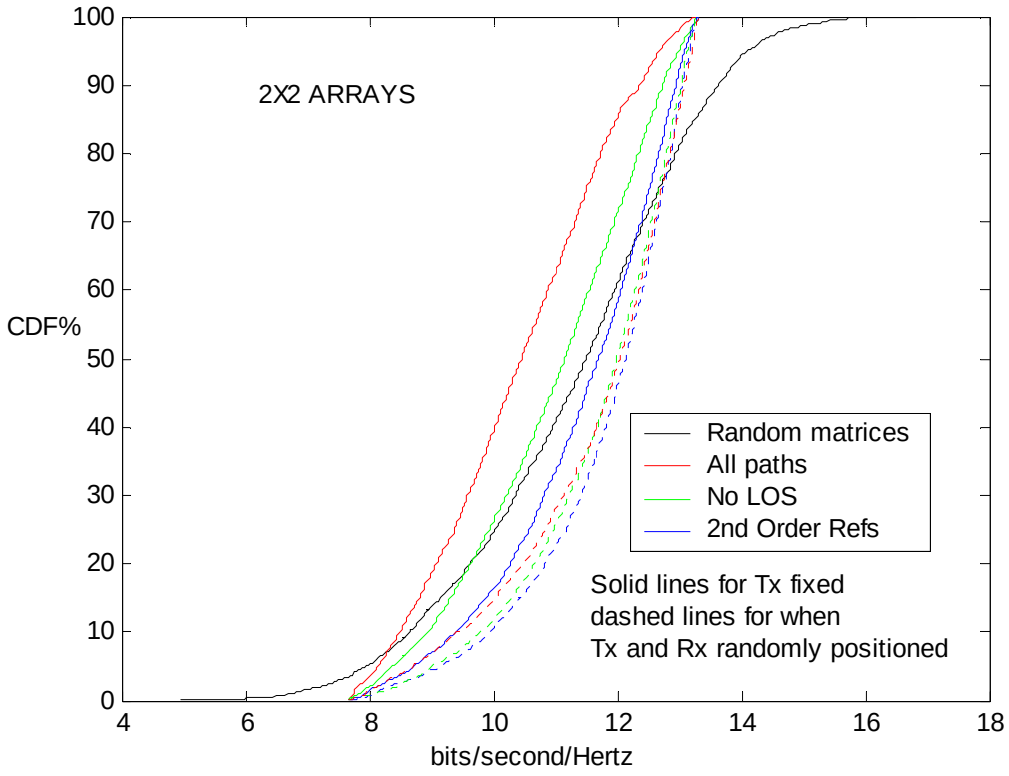

Figure 6.10 CDFs for 2x2 arrays under various conditions.

Thus, the precise location of the Tx-Rx pair must be considered as significant given the possibility of a relatively good performance for much of the potential Tx–Rx locations. Figure D.2 appendix D shows the maximum 30% locations under LOS conditions

normalised at 20 dB SNR at the Rx. At location A the initial capacity when all paths were present was at the low end of the range at 7.9 b/s/Hz. There was a similar rate of improvement and final capacity value achieved for multiple trials for any of the particular reconfiguration scenarios done with the Metropolis search. Figure 6.11 shows the average curves for five trials for the first 70 iterations after which no further significant improvement occurred. The relative smoothness of the increasing capacity was partly due to the averaging and the fact that the improvements are over a relatively small number of iterations compared to the 4x4 cases. As before, the Z dimension only case increased capacity in a gradual manner.

There was no significant difference in the final capacity improvement for most trials, with the exception of the Z-dimension only adjustment, when restricted to the receiver side. When all three dimensions were adjusted simultaneously the magnitude of the adjustments was broadly the same, mostly between $\lambda/4$ and $\lambda/2$ wavelength in any given dimension, for adjustment either at the Rx only or also at the Tx. Also the rate of improvement per iteration was the best on average, usually getting close to the maximum in less than 20 iterations. Thus, there was some advantage to flexible 3-D adjustments which were done at one side of the channel, the Rx.

In the case of single dimension adjustments there was no major difference between the X and Y cases compared to all dimensions when both the Tx and the Rx were adjusted. The element displacements were mainly in the range $\lambda/4$ and $\lambda/2$. When only the Rx was adjusted there were some cases of larger displacements, particularly for the Y-dimension case, with one element moved in the range of $1\ \lambda - 1.5\ \lambda$, thus requiring more

iterations. The Y-dimension element displacements increased the angular spread of the LOS components thus improving capacity. In effect the degrees of freedom when repositioning an array element in a 2x2 system is greater in so far as each element has only one other element near. Also, the total set of transmission paths that are present is significantly reduced with one element transmitting to two elements at the far end of the channel, instead of four. Thus finding locations that improve capacity requires fewer steps regardless of the dimensions being adjusted.

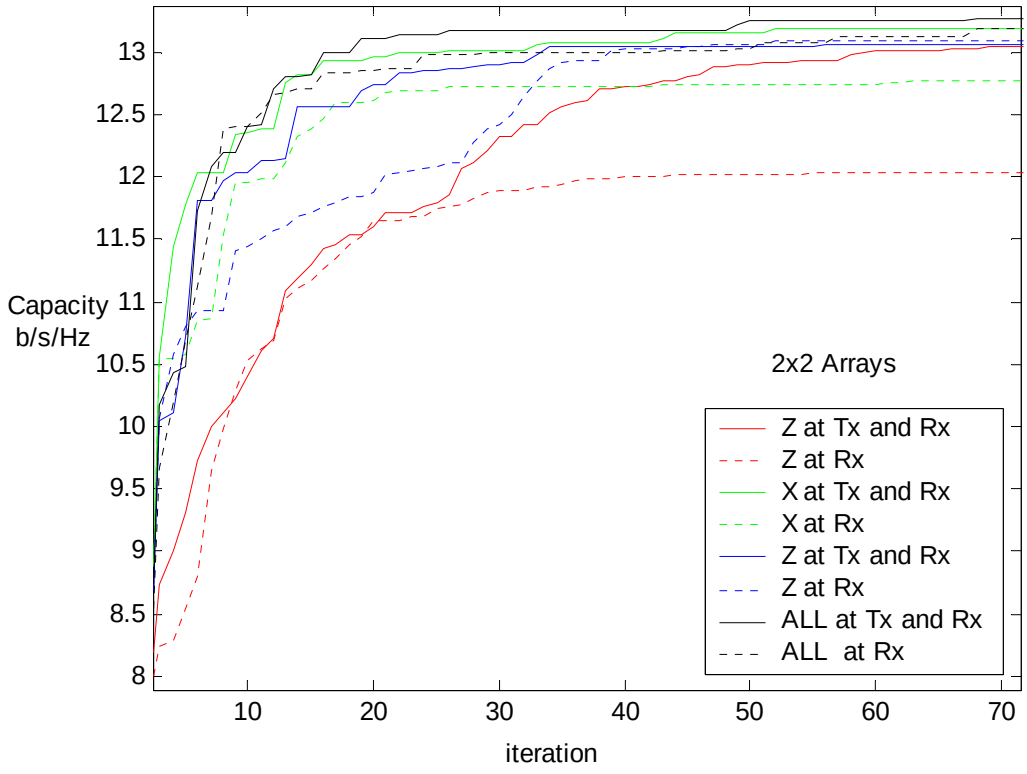

Figure 6.11 Capacity improvements for 2x2 array system.

As before the characteristic of the Z-plane adjustments was more gradual and the displacements larger, mostly ranging from 1 λ to 2 λ for each element in opposite directions. If one element was displaced by a significantly smaller distance then the other was by displaced by approximately twice the amount in the opposite direction.

The Z case was the only one in which a discernible repeatable pattern was noted. The Z adjustments were notably larger and the capacity was weaker when only adjusted at the Rx.

6.4.2 Validation tests for reconfigured 2x2 arrays

For each set of results obtained (the various adjustments performed either at both ends of the channel or just one) a simulation using the best element configuration was tested in order to determine if any of them provided a general improvement compared to the non-adjusted case. Similar to the 4x4 case there was only one instance that provided this, the Z adjustment at both ends of the channel. (The CDF of Figure D.3 appendix D shows the results for a number of configurations). Since the Z adjustments were notably better, these were further investigated using a number of estimated averages. There was no difference between the averages tested, all performed approximately the same. The following is the estimated average displacements in the Z-dimension used for some of the results in Figure 6.12 for the two elements at the Tx and the Rx.

$$\mathbf{Tx(1)=+2\lambda} \qquad \mathbf{Tx(2)= -4\lambda}$$

$$\mathbf{Rx(1)=-2\lambda} \qquad \mathbf{Rx(2)= +\lambda}$$

When both sides were scaled by 2, a maximum result was achieved regardless of varying any other parameters. The mean capacity was 13.7 b/s/Hz compared to 11.4 b/s/Hz for the random matrices. Further scaling of the dimensions did not improve performance. However, reducing them (by 10% of the average dimension, e.g. $+\lambda/10$ - $2\lambda/10$ at Tx, then 20% and 40%) did reduce the capacity to close to the non-adjusted case. As with the 4x4 case a number of other scenarios were tested such as reduced Y axis spacing, NLOS condition, perfect reflector surfaces and other locations for the Tx.

Selections of these are shown in Fig. 6.12. They confirm the general improvement using the Z-dimension adjustments.

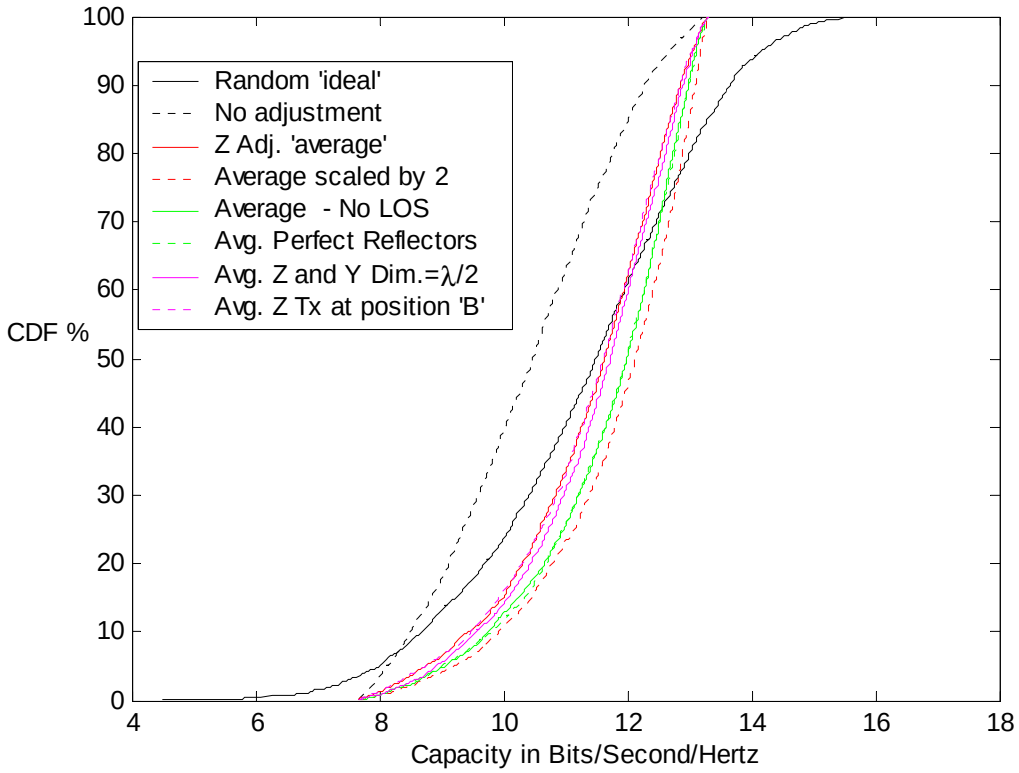

Figure 6.12 CDFs of capacity for 2x2 arrays with Z-dimension adjustments for 2 λ element spacing (Y-dimension).

6.4.3 Other locations

A number of trials were done at other locations in the room to verify that the improvements achieved by the Metropolis search were not associated with a single location pair. For example at location B for λ/2 element (initial) spacing under LOS conditions when the capacity was 16.2 b/s/Hz (4x4 arrays), applying the Metropolis search yielded a large improvement of over 50% to 24.5 b/s/Hz. This required shifts in 3 dimensions but was achieved in only 135 trials. The shifts averaged approximately λ/3 with a maximum of less than λ. When only the Z-dimension was adjusted, the performance level achieved was slightly higher and required shifts averaging

approximately 1.5 λ. As before the Z-only shift case was marked by small increasing steps. For the X or Y-dimension adjustment only, the results were generally lower.

In general the 24 b/s/Hz threshold was always achieved for various initial element spacings when the elements were adjusted in 3-dimensions. Simulations were done for when the initial element spacing was λ/2, λ, 2 λ and 4 λ for the LOS and NLOS conditions. A selection of these results for both propagation scenarios are provided in Figure D.4 appendix D and shows, for example, an improvement for the 1 λ initial spacing was 61% in the LOS case and 63% in the NLOS case. These required average displacements in any given direction of approximately λ/3 with maxima significantly below λ (less overall for the NLOS case).

The λ/2 and λ cases, after adjustment, arrived at similar levels in both LOS and NLOS cases at between 24 and 25 b/s/Hz. As noted in chapter 4 when power delivery from the transmitter to receiver is considered, the presence of the LOS components may allow for greater real efficiency in many instances. Thus, achieving the same level of performance in both cases after adjustment is noteworthy. Simulations (based on optimal element displacements with LOS) under NLOS conditions using the normalisation factor when LOS was present [6.15] confirmed this. On average the removal of the LOS component reduced capacity by between 10% and 15%. However, overall the result of doing this is complex and depends on location and initial conditions before optimising with the Metropolis search method. For instance, if the initial spacing is small (λ/2) then the LOS components contribute less to the achieved capacity thus optimising the array mostly affects the reflections. Consequently removal of the LOS component reduces overall

capacity minimally. When the spacing increases, the LOS components contribute more initially and their removal after adjustments has a greater impact in some cases.

The 2x2 array systems at the same location (B) had a capacity of just under the Rayleigh average at 11.2 b/s/Hz. It quickly increased to 13.2 b/s/Hz in 30 iterations, close to the maximum achievable. This required limited repositioning and as an example Figure 6.13 shows the top view of the room (X–Y displacements) and the side view (Z-X displacements). To deploy such a system would be realistic with only two elements and small adjustments. It is likely that smaller adjustments combined with limited repositioning of the arrays would achieve similar levels of capacity. As before, the problem with 3-D adjustments is the lack of general application to other Rx locations with the Tx fixed.

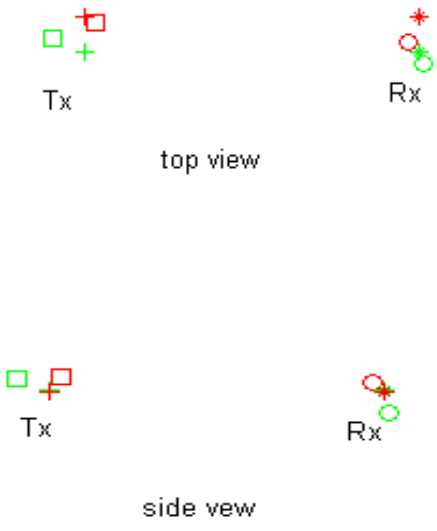

Figure 6.13 Examples of 2x2 arrays showing displacements. The crosses and stars indicate original positions while the box and circle shape show displaced positions. Top view shows X and Y-dimension changes while side view shows Z-dimension changes.

The Z only adjustments resulted in configurations that, as before, showed general improvement regardless of the position of the Tx or Rx. This was the case for all instances of Z-adjustments only, with some small variation in results. However, they did not exceed the average configurations determined for location A, but were similar and virtually identical for the 2x2 arrays. Figure D.5 appendix D shows the 4x4 and 2x2 cases at λ/2 spacing for this location (B) and also the earlier averages determined at A. The area of the room near the Tx was still the weakest capacity level region for this scenario (narrow element spacing and LOS dominating). The overall average capacity throughout the room was increased and not just the regions where the capacity was previously weaker. The single dimension that improves capacity most under these conditions must improve the angular spread of the dominant LOS paths. This depends on the relative positioning of the Tx and Rx, (as demonstrated by the improvements in the region near the Tx as shown by the results in chapter 4). Figure D.6 appendix D shows the situation regarding two relatively short range Tx-Rx pairs, at C and D, with regard to X and Z shifts (Tx(1) position). Due to the position of the array at C, the X-dimension shifts had a more significant effect on capacity. However, the Z-dimension shifts were noted to improve capacity more at most other locations as the Rx moved to a position directly opposite the Tx(1), as shown by the results from location D, and consequently the X-dimension shifts were not significant. Using three dimensional shifts at either location achieved a similar level with less iterations, more rapidly and with smaller displacements.

To assume a straight forward broadside arrangement at a specific location, even though it may generally be the best option in many cases as previously suggested, may not

always be correct. Rotating the axis of the array can achieve improvement due to the relative orientation of the Tx and Rx. However, at location C if the Rx is rotated ninety degrees (so that it is parallel to the nearest wall, perpendicular orientation) there was little difference in the initial capacity. Also, the improvements achieved were not that different from the original orientation for the X and Z-dimension displacements as shown on Figure D.6 appendix D. Both cases were weaker but again the X-dimension shifts, which are now along the axis of the array (Y), provided better improvement at this location due to the effect on the angular spread of the LOS components.

6.4.4 Other orientations of arrays

In chapter 4 various 4x4 array configurations were compared, as shown in Figure 4.4(a) and 4.7, and location E was used to determine the capacity improvements for these using the Metropolis search. The initial capacity for the three array structures was relatively low under LOS conditions for λ/2 element spacing at 10.7, 15.3 and 13.6 (b/s/Hz) for the perpendicular, square and cross arrays respectively.

The general trends for improvement were similar to the broadside arrays. Thus for example, when all dimensions were adjusted simultaneously there was nearly always a significant improvement to at least 24 b/s/Hz. The average element displacements varied but typically were in the range of λ/4 to λ/2. At wider initial element spacing, 2 λ for instance, this tended towards the lower end of that range. As before, single dimension adjustments resulted in good improvements but with larger displacements, particularly for the Z-dimension only, which ranged from 2 λ to 2.5 λ. As with the broadside case, the Z-dimension only adjustment yielded the best improvement when tested in other locations. Overall there was no case which generated better results

compared to the earlier average Z-dimension only case determined for the broadside arrays. The CDFs shown in Figure D.7 appendix D represent the results for λ/2 element spacing for both the three dimensional and Z-dimensions only adjustment cases and for comparison the broadside case is included. As before the 3-dimensional adjustments, which achieved a high level of capacity at location E, did not achieve any significantly better result than the non-adjusted broadside case (shown), which is better than any of the non-adjusted cases, perpendicular, square or cross arrays.

As there was a notable variation between short range e.g., less than 10 m from the Tx, and beyond 10 m for small element spacing in the broadside case, the mean was determined for the two regions. The range of 10 m was chosen to avoid excessive influence of increased element spacing due to angular spread of LOS components. Table 6.3 lists the means for the 3-D and Z-dimension only cases for the different configurations at λ/2 element spacing. At 2 λ element spacing there was little difference as noted in chapter 4, and for these modified configurations it was the same, particularly beyond a 10 m range as examined here. In this region the mean capacity for the broadside average Z-dimension adjusted case was approximately equal to the ideal random case at 22 b/s/Hz and all configurations with Z-dimension adjustments exceeded 20 b/s/Hz. Adjusting in the Z-dimension under NLOS conditions also provided good results.

6.5 Sparse Conditions

6.5.1 LOS only with Rx varied broadside array

For LOS components only at location A the capacity was 8.65 b/s/Hz at λ/2 element spacing. When varying the elements at the Rx the initial element spacing was significant for the fixed Tx side of the channel since the other side was rearranged. It was apparent from initial trials that large scale spacing of the Rx elements could achieve high levels of capacity. However, this gave rise to large displacements of the elements, due almost entirely to displacements in the Y-plane, i.e. the angular spreading described in chapter 4. In effect such arrangements are a form of distributed antenna [6.11][6.16] and the results suggest that for one end of the channel a wide separation of elements is worth considering, particularly if the LOS components are present. Apart from power delivery efficiency (and the possibility of reducing the transmission power) the wide distribution increases the likelihood of some paths arriving in an environment where objects may block some of the rays.

ALL PATHS	Mean Rx <10m	Mean Rx>10m	Overall Mean (b/s/Hz)
Non adjusted –broad λ/2	15.1	17.8	16.9
Non adjusted –broad 2λ	17.2	17.6	17.5
Broad 3D adjusted λ/2	18.6	20.3	19.7
Broad 3D adjusted 2 λ	17.1	18.8	18.2
Broad Z adjusted λ/2	19.3	22	21.1
Broad Z adjusted 2λ	19.8	21.2	20.8
Perp 3D adjusted λ/2	15.4	18.8	17.6
Perp 3D adjusted 2 λ	16.1	18.1	17.4
Perp Z adjusted λ/2	18.9	20.3	19.9
Perp Z adjusted 2λ	18.9	20.8	20.2
Square 3D adjusted λ/2	15.7	17.8	17.1
Square 3D adjusted 2λ	16.1	17.9	17.3
Square Z adjusted λ/2	18.3	20.6	19.8
Square Z adjusted 2λ	18.4	21.0	20.1
Cross 3D adjusted λ/2	15.8	19.2	18.1
Cross 3D adjusted 2λ	16.0	18.1	17.4
Cross Z adjusted λ/2	18.7	20.5	19.9
Cross Z adjusted 2λ	19.6	21.3	20.7

(a) Tables 6.3 continued on next page

NLOS (Std.)	Mean Rx <10m	Mean Rx>10m	Overall Mean (b/s/Hz)
Non adjusted –broad λ/2	16.9	19.7	18.7
Non adjusted –broad 2λ	18.9	18.8	18.8
Broad 3D adjusted λ/2	18.7	19.3	19.1
Broad 3D adjusted 2λ	19.4	19.3	19.3
Broad Z adj. λ/2	21	22.5	22
Broad Z adj. 2λ	21.3	22.0	21.8
Perp 3D adj λ/2	20.0	20.3	20.2
Perp 3D adj 2λ	18.9	20.0	19.6
Perp Z adj λ/2	20.0	21.2	20.8
Perp Z adj 2λ	20.6	21.5	21.2
Square 3D adj λ/2	19.9	21.0	20.6
Square 3D adj 2λ	19.0	19.4	19.2
Square Z adj λ/2	20.4	22.2	21.6
Square Z adj 2λ	20.3	21.8	21.3
Cross 3D adj λ/2	21	21.7	21.5
Cross 3D adj 2λ	19.4	20.0	19.8
Cross Z adj λ/2	21.1	21.8	21.5
Cross Z adj 2λ	20.8	21.6	21.3

(b)

Table 6.3 Comparison of capacity performance (spectral efficiency in bits/second/Hertz) of different array types at different Tx-Rx separation distance with Tx at Tx(1) position under both LOS conditions in table (a) and NLOS conditions in table (b).

With the limited number of closely spaced transmission paths the individual step adjustments were directly affected by the step size used in the Metropolis search. A larger algorithm step size usually resulted in faster convergence to the peak capacity achievable. Figure D.8 in appendix D shows an example using a step of 0.5 indicating the gradual improvement in capacity as the displacements increased for various fixed Tx array sizes. Although the displacements were relatively large (for the 4 λ case the maximum displacement was approximately 42 wavelengths in the Y-dimension) in the context of a distributed system such as that described in [6.11] they are reasonable. Also, the same dimensions provided good capacity at a number of other locations compared to the non-adjusted cases. The mean capacity was approximately the same as for random matrices (22.3 b/s/Hz) for an area covering most of the room for ranges greater than 3 m along the central axis. Figure D.9 in appendix D shows the adjusted Rx examples for both the 4 λ and λ/2 cases. In general, the wider the Tx element spacing the smaller the displacement at the other side of the channel. However, at 8 λ there was no improvement compared to the 4 λ case.

The mean of the channel correlation matrix, for successive iterations of the 4 λ case is shown in Figure D.10 appendix D. Overall this was strongly related to the channel capacity (a correlation of greater than 0.9 between the corresponding curves); as it decreased the channel capacity increased. However, there was a reverse of this trend after approximately the first 20 iterations which continued for about another 60. After that point the correlation between increasing capacity and decreasing mean correlation was close to unity. Thus, it was not simply the increasing spatial separation of the Rx elements that caused the capacity to increase. As noted in chapter 5, the signal

dispersion may also affect the capacity. In this case the rms delay spread was calculated across all 16 LOS components relative to zero, rather than the first arriving path. This resulted in a gradual increase in the rms delay spread as shown in Figure D.11 appendix D. Clearly increasing the separation of elements is likely to increase the delay spread. However, in a richer reflection environment, a significant variation occurs in those characteristics. In the simplified LOS only case there was much less variation particularly over the period when the mean of the channel correlation was varying significantly. This limited condition confirms that the increasing time spread of paths can result in higher capacity, including some instances when the mean of the channel correlation matrix is not low. Determining the capacity changes due to adjustments in a single plane confirmed the Y dimension shifts as being primarily responsible for the improvement in capacity.

6.5.2 LOS only with Tx and Rx varied

When both the Tx and Rx elements were varied, peak levels of capacity were achieved more readily in less iterations and required smaller element displacements. In the limited LOS only scenario the initial element spacing was not significant as both sides of the channel rearranged by similar displacements regardless. The larger step size (0.5) for the Metropolis search was preferable as it required less iterations to find a peak.

The element displacements were not dominated by any single dimension and the maximum displacements were in the range of 10-15 λ. The overall means were less than 8 λ when varying in three dimensions. For single dimension adjustments there was no significant improvement for the X-dimension however the Y-dimension did achieve a peak but with average displacements of 15-20 λ and similar for the Z-dimension but at a

slower rate of convergence to the peak. Thus the Y-dimension displacements dominated the process but not as dominantly as in the previous case. Figure D.12 appendix D shows a selection of results. Also included in appendix D.13 is a plot of the standard deviation of the eigenvalues which demonstrate how the search process moves the channel from being one in which a single dominant value exists, effectively a SISO channel, to one in which four approximately equal eigenvalues/channels are present. The example shown in Figure D.12 is for the 2 λ element spacing with XYZ dimensions varied. A clear correlation between the gradual increase in capacity and reduction in the deviation is observed. Included in appendix D (Figure D.14) are matrix examples of the correlation coefficients of the associated channel matrix **H** pre and post adaptation and a plot of the mean (of correlation matrix values) for each iteration (Figure D.15). Also in [6.17] and [6.18] it was shown that for maximal capacity (channel matrix is orthogonal) the determinant $\mathbf{HH}^*$ has real valued diagonal components and the off-diagonal ones will be zero; Figure D.16 in appendix D shows pre- and post-adaptive determinant examples. As with the single-sided adjustment, the rms delay spread was also increased by the element separation and correlated strongly with the increasing capacity, approximately a value of 0.95. This is shown in Figure D.17 in appendix D.

6.5.3 LOS and limited reflections – sparse conditions

An analysis of some combinations of paths was carried out. For example, the LOS and first order reflections or second order reflections only; at location F, with capacity level of approximately 11 b/s/Hz, an initial element spacing of 2 λ and adjustment in three dimensions. These examples demonstrate aspects of how the Metropolis adaptations perform in the presence of varying numbers of paths with different strengths. Initially the LOS and reflections from 1 or 2 walls were simulated (W1 and W2 on Figure 6.1)

and the results are shown on Figure 6.14 with the LOS only case for comparison. The pre-adaptation capacity levels were similar but the initial iterations resulted in a more rapid rise in capacity with increased total number of paths, although the final achieved capacities were much reduced compared to the LOS only case, when a Metropolis step size of 0.1 was used. This figure shows the actual capacity per simulation iteration and not just at the improved steps. The capacity variations at each step became larger as more paths were introduced. However, the element displacements required to achieve the peak capacity level was much less with the increased number of reflections. They were in the region of a 1 λ or 2 λ maximum for the LOS and one set of reflections and generally less than 1 λ when the second set of reflections was present. Notwithstanding this, the latter case achieved a marginally better final capacity with the more diverse set of transmission paths.

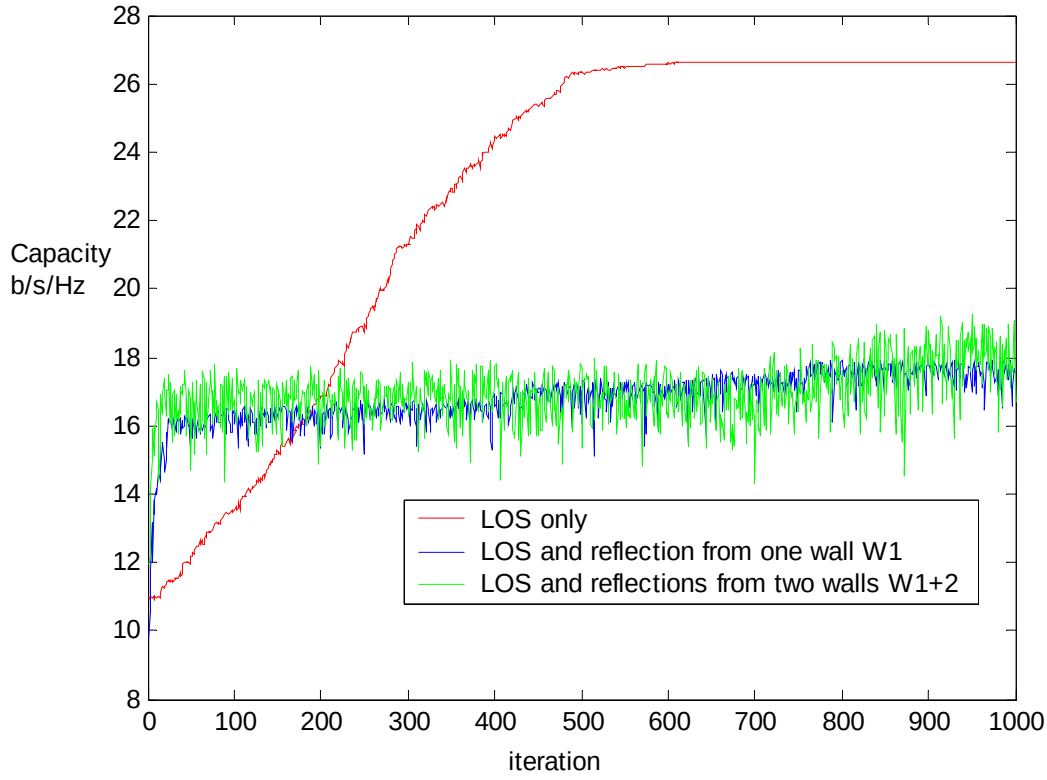

Figure 6.14 Limited path conditions examined at location F with broadside arrays of initial element spacing 2 λ with three dimensional adjustments.

Enhancing the reflections ($\Gamma = 1$ and normalised SNR of 20 dB at the Rx) demonstrated that the increased strength of the reflection transmission paths provided a more difficult environment for the Metropolis search to find capacity improvements. Thus much greater fluctuations in capacity occurred and an example is included in appendix D Figure D.18. This shows the case for the LOS and a single first order reflection with and without enhancement of the reflections. However, when the total transferred power in the reflections was increased; the improvements were more rapid and slightly better final values were achieved. Also the element displacements became slightly smaller for the peak values. For clarity Figure 6.15 shows the level of the successive peaks achieved for a number of scenarios which include the enhanced reflections (solid lines) and without enhancement (dashed lines). Overall when the

reflections were enhanced it led to higher capacity and lower element displacements. However, the scenario with either first or second order only reflections did not perform as well as cases with the LOS component. This is because the element displacements, although small, were still affecting the contribution to capacity from the LOS components more than the more diverse set of reflections. At the same time the increasing number of reflections provided a more diverse set of transmission paths and an improved channel correlation matrix, generating higher capacity. This is clear when considering the average correlation value for a number of cases as shown in Figure D.19 appendix D.

Another limited grouping of reflections considered was from the ceiling and floor. These were the most similar to the LOS in terms of length and thus relatively large array element shifts were likely to be present. When combined with the LOS components the results showed this to be the case; however the element displacements were approximately half the size of those for the LOS only and did not exceed a maximum of 5 λ. The final capacity achieved was slightly less than for the LOS alone; albeit still a high level and a more rapid rise as shown in Figure 6.16. When the floor and ceiling were set as perfect reflectors, the results were similar; although the final capacity level achieved was slightly lower and the element shifts were slightly less. When only the ceiling and floor reflections were considered the same final result was achieved with displacements not exceeding 5 λ.

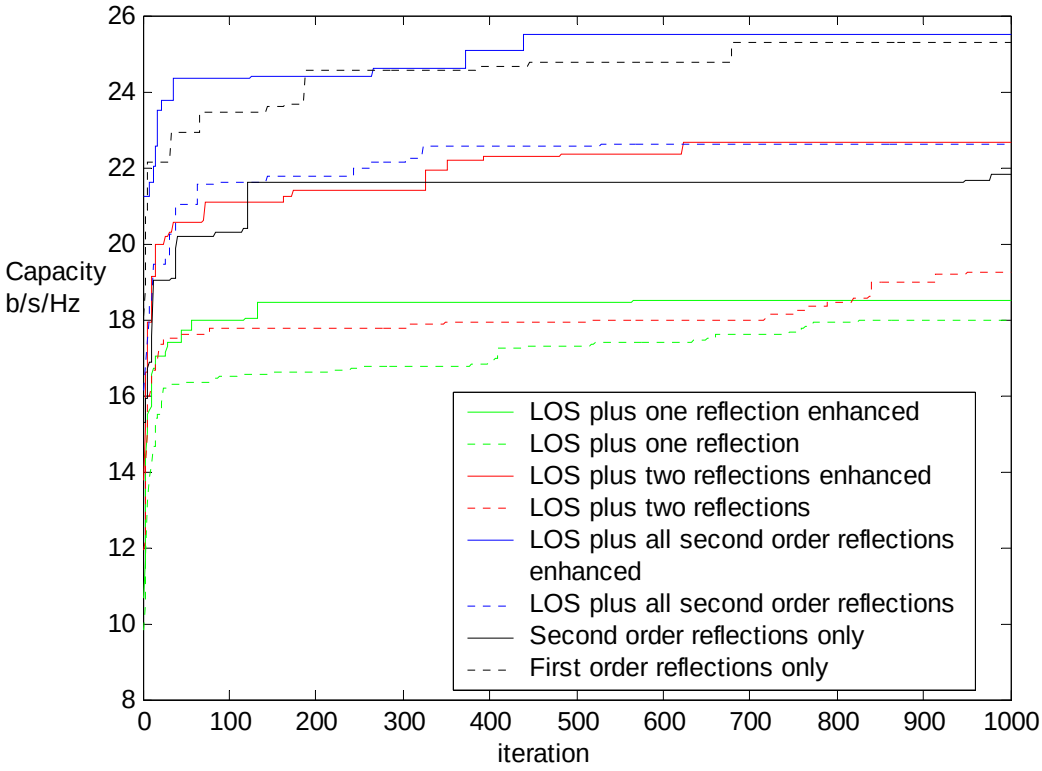

Figure 6.15 Various limited path conditions examined at location F with broadside arrays of initial element spacing 2 λ with three dimensional adjustments and examples of enhanced reflections.

These results suggest that in the absence (i.e. due to an obstruction) of LOS components the use of reflective material on the ceiling and floor may be a realistic deployment strategy to achieve good power transfer while taking advantage of adjusted arrays. To simulate such a scenario the first order reflections from ceiling and floor were combined with the second order reflections (no LOS or first order reflections present). A high level of capacity was achieved quickly but with much smaller element displacements in the region of 0.5 λ maximum but mostly less than 0.25 λ. Although the fluctuations were much larger than the more limited case, they were smaller than the more general case with all reflections present as shown in Figure D.20 in appendix D. A notable difference was the larger displacements in the vertical Z-dimension compared to other

cases in which the Y-dimension was nearly always the biggest. This result explains why the average Z-dimension shifts, which achieved more general improvement as they affected the reflections from the ceiling and floor. The key point in this regard is that (unlike the reflections from the four walls) there were less transmission paths being affected by the adjustments but sufficient to avoid large element displacements, such as those in the LOS only case. Similarly if reflections from two walls were omitted then it was possible to obtain larger element shifts in the X or Y-dimension. The array pattern that resulted was also capable of providing better results when the array was relocated throughout the room, compared to the arrays derived from the more general case.

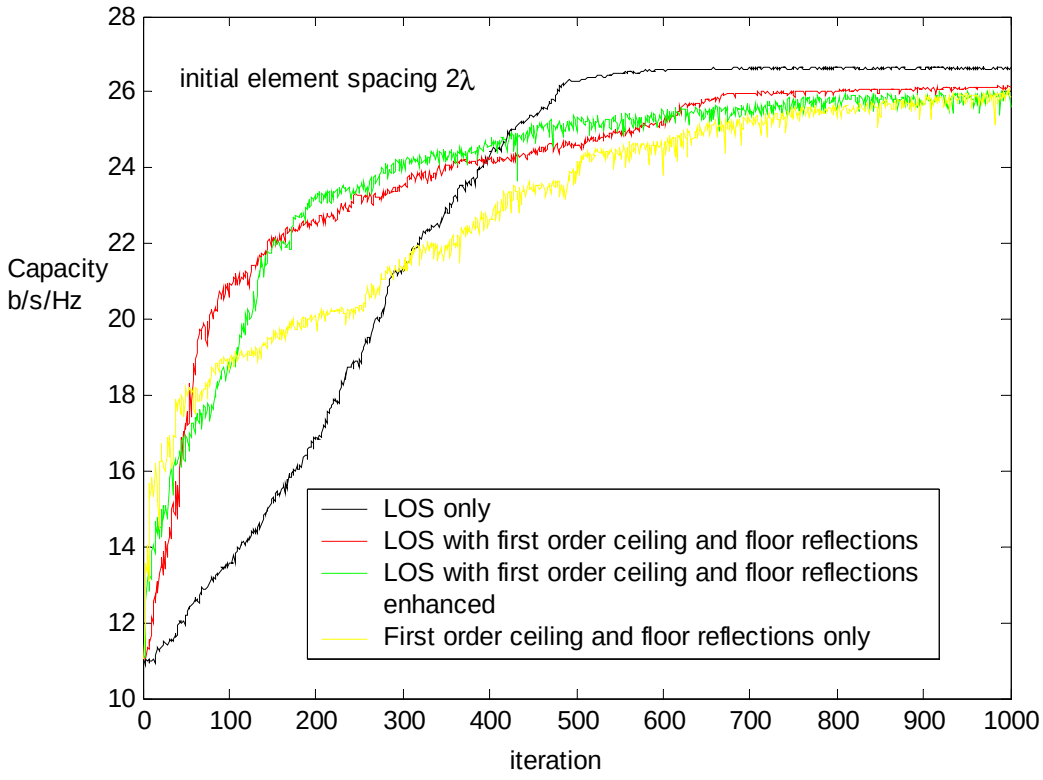

Figure 6.16 Limited path conditions considering reflections from floor and ceiling only.

Figure D.20 in appendix D also shows the case of second order reflections on their own. Note that this set of reflections tends to provide the most Rayleigh like results when considered for ULAs randomly repositioned throughout the room. However, the relative complexity makes it difficult for the Metropolis search to find significant improvement. When the first order ceiling and floor were introduced, with adjustments only in the Z-dimension, there was a reasonably fast rise to near peak value. This required a slightly larger displacement with a maximum of 2 λ; which was similar to the average Z-dimension only described earlier. The array arrangement did not achieve results as good as the previous structure when tested throughout the room, but did perform better than other arrangements (3-dimensional).

6.6 Conclusions

The Metropolis search method was capable of optimising arrays in a highly correlated environment for any given pair of Tx-Rx locations. The solutions found were specific to that particular scenario, i.e. the Tx and Rx location pairs. This may still be useful since the technique was capable of providing improved spectral efficiency with a minimum step adjustment of 5 mm. Thus it may be a feasible approach at one side of the channel while fixed wide spacing could be used at the other side such as an access point for instance.

The technique has also yielded results which show that some array structures using vertical (Z-dimension) displacements have a more general application. This appears to be the most likely complex array structure for combating the correlated channels present in indoor environments. Although such adjustments appear to reduce the correlation associated with LOS components in particular, they work equally well under NLOS

conditions. Furthermore, when the array axis is reduced (the Y-dimension), they maintain the same level of spectral efficiency on average. The less complex 2x2 arrays were particularly good insofar as the mean capacities achieved compared favourably to the ideal Rayleigh channels modelled by random matrices. Although the element displacements were several wavelengths the structures proposed are feasible.

If adjustment in the Z-dimension can be applied there is some scope for using square or cross array structures. However, adjusting ULAs with small spacing ($\lambda/2$) along the axis of the array, in a single dimension (Z) is more realistic; particularly if wide spacing could be applied at one side of the channel. Although the objective of this chapter was to focus on array element adjustments, the enhancement of reflections relative to the LOS would also be beneficial. The combination of these two adjustments would result in close to optimal spectral efficiency.

For limited propagation scenarios the results demonstrated the significance of the LOS component using this approach. The Metropolis search was capable of adjusting array element positions, albeit widely, for a limited number of paths. This emphasises that the cases where the wider element spacing has the greatest impact is where the LOS or a limited number of paths dominate and, as such, is important for some indoor or PAN scenarios. Conversely in the more general multipath case it is more difficult for the Metropolis algorithm to adjust at a rate of every iteration (or second iteration) since too many paths are simultaneously changing; and a more limited number of improvement steps occur. This also confirms the limitations of wider or diverse element spacing in

not achieving an improved performance in more reflection rich propagation environments particularly if no LOS components or strong reflections are present.

Under sparse conditions if the LOS is present, adjustment of arrays can result in significant improvements. Compared to the best results achieved with ULAs (see Table 5.3) the final capacity achievable is 80-90% of the mean achievable in ideal Rayleigh channels for cases of LOS components and one or two sets of reflections (Figure 6.14). Even in the case of enhanced reflections, ULAs struggle to achieve near optimum performance unless wide spacing of many wavelengths is used. This emphasises the fact that when fewer paths are adjusted for, it is easier to find solutions using the technique. Thus, for these particular conditions, the enhancement of reflections and adjustment of the arrays at a specific location should be considered.

6.7 References

[6.1] G. J. Foschini and M. J. Gans, "On limits of wireless communications in a fading environment when using multiple antennas", *Wireless Personal Communications,* Vol. 6, March, 1998, pp. 311–335.

[6.2] A. Grennan, C. Downing, B. Foley, "MIMO Capacity Enhancement by adjusting Element Positions using the Metropolis Algorithm in a Deterministic Model", *IEE Irish Signals and Systems Conference*, 2006, pp. 265-270.

[6.3] A. Grennan, C, Downing, B. Foley, "Application and analysis of MIMO systems using Metropolis algorithm", *Loughborough Antennas and Propagation Conference (LAPC*, Nov. 201*),* pp. 357-360.

[6.4] A. Grennan, M. Davis, C. Downing, “Near optimum array geometries for MIMO systems in a highly correlated environment”, *Loughborough Antennas and Propagation Conference (LAPC)*, Nov. 2013, pp. 357-360.

[6.5] J-S. Jiang, M.A. Ingram, “Enhancing Measured MIMO Capacity by Adapting the Locations of the Antenna Elements*”, IEEE Personal, Indoor, and Mobile Radio Communications,* Vol.3, 2002, pp. 1027-1031.

[6.6] O. Fernandez, M. Domingo, R.P. Torres, “Simple adaptive system to improve channel capacity”, *29th U.R.S.I. General Assembly*, Oct. 2005.

[6.7] A.M. Sayeed, V. Raghavan, “Maximising MIMO Capacity in Sparse Multipath with Reconfigurable Antenna Arrays”, *IEEE Journal of Selected Topics in Signal Processing*, Vol. 1 Issue 1, 2007, pp. 156-166.

[6.8] R. Mehmood, J.W. Wallace, “MIMO Capacity Enhancement Using Parasitic Reconfigurable Aperture Antennas (RECAPS)”, *IEEE Transactions on Antennas and Propagation*, Vol. 60, Issue 2, Pt.1, 2012, pp. 665-673.

[6.9] A.A.M, Saleh, R.A. Valenzuela, “A statistical model for indoor multipath propagation”, *IEEE Journal on Selected Areas in Communications,* Vol. 5, issue 2, 1997, pp. 128-137.

[6.10] R. Iernon-Fernandez, J. Molina-Garcia-Pardo, L. Juan-llacer, “Comparison between measurements and simulations of conventional and distributed MIMO system”, *IEEE Antennas and Wireless Propagation Letters*, Vol. 7, 2008, pp. 546-549.

[6.11] Z. Li, F. Luan; Y. Zhang, L. Xiao, L. Huang, S. Zhou, hidong; X. Xu; J Wang, “Capacity and spatial correlation measurements for wideband distributed MIMO channel in aircraft cabin environment”, *IEEE Wireless Communications and Networking Conference (WCNC)*, 2012, pp. 1175-1179.

[6.12] N. Metropolis, A. W Rosenbluth,. M.N. Rosenbluth, A. H Teller, E. Teller, "Equation of State Calculations by Fast Computing Machines", *J. Chem. Phys.* 21, 1953, pp. 1087-1092.

[6.13] I. Beichl, F. Sullivan, "The Metropolis Algorithm", *Computing in Science and Engineering*, Vol. 2, Issue 1, 2000, pp. 65-69.

[6.14] J.S. Jiang, M.A. Ingram, "Distributed source model for short-range MIMO", *IEEE 58th Vehicular Technology Conference 2003*,Vol.1, Autumn 2003, pp. 357-362.

[6.15] A. Z. Tang, A.S. Mohan, "Experimental Investigation of Indoor MIMO Ricean Channel", *IEEE Antennas and Wireless Propagation Letter*, Vol.4, 2005 pp. 55-58.

[6.16] R. Iernon-Fernandez, J. Molina-Garcia-Pardo, L. Juan-llacer, "Comparison between measurements and simulations of conventional and distributed MIMO system", *IEEE Antennas and Wireless Propagation Letters*, Vol. 7, 2008, pp. 546-549.

[6.17] D. Neirynck, C. Williams, A. Nix, M. Beach, "Personal area networks with line-of-sight MIMO operation", *IEEE Vehicular Technology Conference(63rd)*, Spring, 2006 pp. 2859-2862.

[6.18] D. Gesbert, H. Bolcskei, D.A. Gore, A.J. Paulraj, "Outdoor MIMO wireless channels: models and performance predictions", *IEEE Transactions on Wireless Communications*, Vol. 50, issue 12, December, 2002, pp. 1926-1934.

Chapter 7 Summary and Suggestions for Future Work

7.1 Overview of Thesis

There is no doubt that multi-antenna MIMO systems are capable of delivering large gains in spectral efficiency compared to their equivalent SISO systems. The problem that this thesis addresses is whether typical uniform array structures are capable of delivering the theoretical gains in a short-range indoor environment if an arbitrary approach is taken to their deployment. Also, the thesis proposes how the problem may be resolved or at least ameliorated through adjusting the array element spacing.

In practice many systems described as MIMO wireless (e.g. early 802.11n WLAN equipment) do not achieve improvements in spectral efficiency. This is because they are not employing true spatial multiplexing and decoding and are described as MIMO because they have more than one antenna connected. For instance, some systems are simply transmitting multiple copies of the same data stream (i.e. employing transmit diversity) to ensure some strong signal paths arrive at the Rx, typically a network access point. The Rx does not require multiple antennas to operate in this scenario. Similarly there are wireless network adapters for personal computers with multiple antennas which are attempting to detect a strong signal on at least one element (i.e. receive diversity). Tests on one such system found that removing two out of three antennas or widely separating them, did not affect the system performance. Such systems may meet the user requirements and in fact most standard SISO systems will, unless some extreme propagation condition arises. In such an event, the diversity due to multiple antennas may solve the problem. For a SISO system increasing the SNR by increasing the

transmitter power is the most likely solution, although some wireless systems (e.g.Wi-Fi) operate at their maximum power by default.

However, as data quantities, speeds and end-user points increase, there is ample motivation to seek more efficient systems such as MIMO techniques that fully exploit spatial multiplexing by transmitting multiple data streams in the same propagation channel and achieve high levels of spectral efficiency. Also, it may not be acceptable from a running cost or regulatory perspective to simply increase the transmission power to achieve better coverage in an indoor environment, particularly if battery powered mobile systems are considered. The higher spectral efficiency levels that may be achieved by MIMO systems is a potential means of avoiding this.

The results from the simulation tests conducted for this thesis suggest that many instances of system realisations for MIMO systems will result in spectral efficiency improvements compared to a SISO system, but not close to the optimal. It is possible to envisage system deployments that do utilise spatial multiplexing and easily achieve improvements of 50%-100% compared to a SISO, but theoretically they could be capable of much more. Sub-optimal performance may be difficult to detect in real systems particularly since they may employ complex protocols that include adaptive power transmission and clients that have large data storage capability for streaming applications. In fact the physical propagation environment is not explicitly monitored or managed by the majority of wireless data access points. During the actual deployment there is no information that could lead to conclusions about optimal performance, or otherwise, regarding the propagation medium. Thus there is a need to have deployment

strategies that do not require an excessive amount of manpower to implement, which is a significant cost factor, and are practical. These techniques may not always lead to an optimal system but could ensure that, on average, systems operate closer to the optimal theoretical capacity achievable.

In this thesis a ray-tracing simulation model, as described in chapter 3, was used to accurately determine the precise path lengths of the multiple rays between each element of a single pair of Tx and Rx arrays. Thus an accurate analysis of the geometric characteristics of the MIMO channel was performed, as described in chapter 4, for the two most common propagation scenarios researched, namely, multipath components including the line-of-sight (LOS) conditions and without the LOS (NLOS). The results provide a clear explanation of the likely performance of MIMO systems under these conditions and different array geometries. The conclusion for the chapter provided a number of recommendations for positioning the array elements and these are included below in a more general summary.

More limited propagation, or sparse conditions, were considered in chapter 5. It is clear that for limited propagation conditions, for example LOS only, that the geometry of the array can ensure good performance over short ranges if the element spacing is wide. ULAs are the best option but a wide spacing is unlikely to be feasible at both sides of the channel. A limited form of distributed antenna system with wide spacing of the elements at one side of the channel is probably realistic, but would require long antenna feeds to run from a typical access point. If smaller arrays are present at both ends then under LOS only conditions limited capacity is possible. However, if some limited extra

reflections can be introduced then under such sparse conditions a notable improvement is possible, achieving 60-70% the capacity of a Rayleigh channel. The dispersion characteristic analysis showed that smaller element spacing, approximating a SISO system in that regard, improves performance in regions of the room where the dispersion is a maximum. This does not apply to wider element spacing and explains the relatively good performance of narrow element spacing, even when the LOS components are present, since the channel correlation is often reduced in these regions as a result.

Chapter 6 demonstrated that it is possible to adjust the array geometry in order to decorrelate the channel matrix for optimal spectral efficiency. In effect the modified geometry of the array reduces the correlation of the multipath components and hence maximises the channel capacity. In general, the more degrees of freedom available to adjust the arrays the more likely that optimal capacity could be achieved, with fewer iterations and smaller displacements of the array elements from their original position. A significant improvement could be achieved if the adjustments were done at one side of the channel only, typically at levels close to the mean of a Rayleigh channel. It was verified that limiting adjustments to a minimum of 5 mm was sufficient for the Metropolis algorithm to find the optimal array configuration and a feasible approach for implementation.

Modifications that were done at both sides of the channel, in three dimensions, resulted in capacity levels in excess of the mean for a Rayleigh channel. However, this was limited to a specific Tx-Rx location pair. However, there were some instances of arrays

found that resulted in a more general improvement throughout the room. These array geometries were for adjustments in the Z-dimension only and were effective for both 2x2 and 4x4 arrays while the original element spacing (Y-dimension) was maintained in the range of $\lambda/2$ -2 λ. The adjustments proposed were realistic for system deployment but would require a flexible array mounting structure. In the case of sparse conditions it is possible to significantly improve the spectral efficiency for a pair of Tx-Rx locations. This is because the limited number of paths involved makes it easier for the Metropolis search to find an improved array structure. Nonetheless, under such conditions it is difficult to reach high levels of capacity for uniform arrays unless a wide spacing of elements is used (typically more than 5 λ) and thus an adaptive system, in which the individual element positions is adjusted, is worth consideration.

7.2 Summary of Main Findings

1. The indoor environment is unlikely to permit optimal MIMO channel capacity to be achieved for linear array structures if they are arbitrarily located in a room. This has been demonstrated by the extensive results in chapters 4 and 5 and the related appendices.
2. The propagation conditions of the channel are the main determinant of system performance for the environment considered and the impact on spectral efficiency over short ranges can vary significantly. In particular, this was more observed for short Tx-Rx distance (less than 10 m in the room considered, but dependent on room geometry) than for longer ranges.
3. Uniform linear arrays (ULAs) are the most likely structure to provide optimal spectral efficiency in most scenarios and other structures such as cross or square arrays are not a good alternative. This is a clarification of what others have

found for circular and rectangular arrays and suggests that modifications of linear arrays is the most likely approach to finding optimal array geometries.

4. The relative orientation of the ULA arrays and the element spacing have a significant on impact capacity at short ranges (<10 m here) but much less so at longer ranges. This confirmed a variety of results elsewhere but in this case they were produced within the same modelling environment. This is primarily due to the angles of arrival and departure of propagation rays, particularly the LOS, and leads to various conclusions about positioning arrays as discussed in chapter 3.
5. The advantages of having LOS components present (or strong first order reflections) are significant even though they are likely to be highly correlated. This is because of the impact on the SNR at the Rx and consequently, over short ranges, wide element spacing in ULAs is effective, as observed by others, for free space conditions in particular.
6. The propagation conditions can be significantly improved (i.e. become more Rayleigh like) by enhancing the strength of the reflections relative to the LOS components by changing the reflection coefficient of the room surfaces. Furthermore, the enhancement of the reflections effectively increases the SNR at the Rx. At longer ranges covering about 70% of the room considered, with only one wall providing stronger reflections, capacity levels equivalent to the ideal Rayleigh case were achieved.
7. For free space (i.e. LOS components only) or limited sparse propagation paths, increasing the element spacing is the most effective means of achieving improved spectral efficiency, especially if the element spacing can be increased

to many multiple wavelengths at both sides of the channel, e.g. 8 λ, throughout most of the room considered.

8. For a smaller element spacing under sparse propagation conditions, enhancing reflections can achieve spectral efficiency levels of 60-70% of Rayleigh channels.
9. For small ULA element spacing, λ/2 for instance, the system approximates that of a SISO as far as the dispersion characteristics of the channel are concerned. In such cases when the dispersion is large (i.e. a high value of rms delay spread) the channel correlation tended to be low and higher capacity resulted. The region of the room where this occurred was approximately the central area and, as such, is a good position to locate the Rx, assuming the Tx was positioned near an end wall.
10. Significant improvement in capacity can be achieved for a Tx-Rx location pair of low capacity, if the elements can be adjusted at one side of the channel using the Metropolis algorithm. This can be done with a minimum step size, in any given direction, of 5 mm.
11. Any given pair of Tx and Rx locations can achieve optimal spectral efficiency if adjustments are performed in three dimensions at both sides of the channel, without excessive displacement of the array elements from their original positions.
12. Array structures that provided a general improvement in spectral efficiency throughout the room, compared to non-adjusted ones, were found based on adjustments in a single dimension using the Metropolis algorithm. This was the

Z-dimension and the overall dimensions of the arrays were realistic for system deployments.

13. Under limited sparse propagation conditions the Metropolis algorithm is particularly efficient at improving the channel capacity since there are less propagations paths influencing the spectral efficiency.

7.3 Summary of Guidelines and Suggestions for Deploying MIMO Arrays

In this summary the short range is defined as less than 10 m for the room considered or approximately 30% of the area near the Tx side of the room as discussed in chapter 3.

- For short ranges

1. Always consider ULAs rather than other array structures (i.e. square or cross).
2. Do not block strong components such as the LOS as the benefits to SNR should normally be more significant than the problem of strong signal correlation of any strong signal components. There is a trade off between the contribution to capacity due to SNR levels and channel correlation, particularly over short ranges, when the LOS components dominate the SNR but are highly correlated. In this scenario the variations in geometric factors such as the array spacing affect the channel correlation without changing the SNR.
3. Make the element spacing as wide as possible at both sides of the channel and at one side, e.g. at an access point, it should always be as wide as possible.
4. If a wide spacing is possible then a broadside orientation of arrays is always best.
5. A perpendicular arrangement is preferable for small element spacing at short ranges and in-line orientations should be avoided. Also, for both long and short ranges, avoid corner locations for both sides of the channel.

6. Enhance reflections, if possible, from at least one surface. For the perpendicular arrangement the surface parallel to the Rx is the best choice.

- For longer ranges

7. At longer ranges (i.e. greater than 10 m in the room considered) there is limited benefit to varying the span of the array so consideration should be given to enhancing the propagation medium by improving the strength of the reflections. One surface is sufficient for significant improvement but the more that are used the better. The position of a fixed Tx in the centre of a room could also ensure, on average, reduced path lengths and optimal SNR at the Rx, but in-line orientations would be more likely.
8. Positioning small element spaced systems near central room locations (the Rx) rather than close to a wall is beneficial since the dispersion is usually maximum in these regions and this reduces the channel correlation.

- General recommendations

9. It was found that smaller 2x2 arrays are on average likely to result in a spectral efficiency closer to that predicted for ideal Rayleigh conditions compared to 4x4 systems. Increasing array size, for example beyond 4x4, is more likely to result in suboptimal systems and has been commented on in the literature.
10. In theory, the configuration of the array can be adjusted for any given pair of Tx-Rx locations using the Metropolis search technique to yield configurations that improve spectral efficiency, compared to standard linear structures at the same locations. Some level of adjustment, even the orientation of arrays, can substantially vary the capacity. This could occur at one side of the channel and if

the other was fixed with wide spacing, e.g. a network access point, then simple adjustments could improve the spectral efficiency.

11. Configurations based on single dimension adjustments, (i.e. the Z-dimension as described in chapter 6) can be deployed that yield a general improvement in spectral efficiency compared to standard ULAs. This could be considered in conjunction with the above guidelines since the arrays are based on ULAs including those with small (λ/2) element spacing.

7.4 Summary of Main Contributions of this Thesis

1. A comprehensive framework that encompasses many varied results throughout the literature was developed that can consistently explain a wide range of seemingly anomalous results.
2. It provides guidelines and suggestions for the deployment of regular array MIMO antenna systems. This includes identification of the interaction of array spacing and environment to create regions in the room of varying correlation of the multipath components and thus spectral efficiency.
3. It provides a coherent insight into the performance of MIMO systems under sparse propagation conditions.
4. It provides an original explanation of the specific impact that dispersion characteristics have on spectral efficiency regarding the array size and location of the Rx in the room.
5. It suggests a unique method, employing the Metropolis algorithm, for adjusting the position of the individual array elements to improve system performance. This is based on the precise calculation of all multipath components in three

dimensions, thus ensuring accurate determination of the impact of the array adjustments in any dimension.

6. It indicates array configurations developed using the Metropolis algorithm that provide a general improvement in spectral efficiency compared to non-adjusted arrays.

7.5 Limitations of this Thesis

1. The results are primarily based on extensive simulations and not on experimental data; apart from the SISO model. Some experiments were conducted on commercial MIMO products but it transpired that they only used standard diversity with the multiple antennas and no variations in the system performance were observed for geometric changes in the arrays; they were not employing true spatial multiplexing.
2. Simulation does not attempt to replicate a real communications system or environment as discussed in chapter 3; rather, it is intended as a study of the impact of geometrical and propagation factors in MIMO channels. However, the approach is consistent with the approach taken by others who have examined geometric and propagation factors for indoor MIMO channels.
3. Although most wireless networks consist of single access points and multiple clients, only a point-to-point communications link was considered in order to simplify the analysis. Thus, some of the results may not be readily applied to systems involving multiple clients and hence multiple MIMO communication channels.
4. Variation in antenna element types was not considered. Omni-directional is normally a popular option in MIMO channels due to the wide reception of

varying reflections and an ideal half wave dipole was modelled, which may not be realisable in practice. This may sometimes produce better results by detecting a richer set of reflections than a real antenna which may exhibit irregularities in its radiation pattern.

7.6 Suggestions for Future Work

1. As mentioned above, some measurements were attempted on systems described as MIMO but these appeared to only use traditional diversity techniques, a conclusion arrived at after various experiments. Thus, the identification and testing of commercial MIMO systems that do actually employ spatial multiplexing, and attempt to transmit multiple different data streams in the same propagation channel, is required by means of laboratory testing. Baseline performances for such systems must be established in order determine the actual level of spectral efficiency achievable if arbitrarily deployed. Subsequently, an investigation into the impact of geometric variations in the environment and arrays can be considered. In particular, the consideration of a wide spacing of the of array elements at one side of the network, e.g. the access point, could initially be performed to confirm such effects on spectral efficiency. Other basic adjustments such as those described in chapter 4 could also be tested, e.g. the relative orientation of arrays.

   Further experimentation on commercially available systems using a long term statistical measurement approach to investigate positioning of linear arrays using the guidelines in this thesis, could then be considered. Although extensive repositioning which was done in simulation is not feasible, it should be possible

to establish a baseline performance for arbitrarily positioned systems. Subsequently, a comparison could be done with systems applying some of the guidelines described, in particular, the use of enhanced reflections. In this regard, wall, ceiling and floor covering materials could be investigated for performance and the practicality of deployment. Other geometric variations such as the orientation of arrays and element spacing and structure could be examined in this manner. The performance of modified array structures that were found using the Metropolis algorithm, with displacements in the Z-dimension, could also be investigated.

2. The construction of a reconfigurable array platform that permits small scale adjustments of the individual array elements as described in chapter 6. This should be feasible since a minimum step size of 5 mm was confirmed in simulation as being sufficient for the Metropolis algorithm to find positions for the elements that significantly improve the spectral efficiency. This could be investigated initially at one side of the channel only with wide element spacing at the other. Parallel to this, further examination of the adaptive method could be investigated. In particular, investigation of a technique to achieve the same outcomes but with as few iterations as possible, since the practicality of such an approach would depend on it being implemented in a reasonable time. This is not an issue for simulation, but manual adjustments followed by measurements in actual systems could become time consuming.

A possible approach would be to develop a technique that stores steps (configurations of arrays) that generally improve capacity and use these, or similar, rather than test hundreds of random configurations. Conversely, the storage of bad configurations could help identify time wasting iterations and similar steps could be avoided. Some of the Z-dimensions structures that provided a general improvement in spectral efficiency, compared to non-adjusted arrays, could also be the basis for this approach.

3. Other optimisation algorithms could also be investigated. For instance, genetic algorithms are often considered for solving complex problems and the MIMO channel and array structures are a potential candidate for this application. In this regard a population of different array structures, such as those generated from the Metropolis algorithm could be the basis for the genetic algorithm search with the 'fitness' criteria being the capacity. Adjustments in orientations or small repositioning of the entire array could be performed and only structures that yield significant improvement in capacity could be retained for further iterations, such as repositioning to completely different Tx-Rx locations.

Using an adaptive technique, rather than the more general guidelines for linear arrays as discussed, would only be worthwhile for conditions in which the spectral efficiency is likely to be poor for a given system. In this regard consideration could be given to outdoor environments where the multipath components may not be as diverse (or possible to affect). A street canyon is a possible candidate and is broadly similar to an indoor corridor structure. In this

case the LOS components and a limited number of strong reflections are likely to dominate the SNR for many instances of Tx-Rx pair locations in the street and as such may be a good candidate for adaptive or reconfigurable array systems.

4. Combine the deterministic MIMO simulation model with a network simulation tool. The results could be compared with real MIMO systems as suggested in 1 and 2 above. The aim of doing this would be to develop a figure of merit for any given MIMO system deployment, on the basis that optimal performance is unlikely, taking into account the overall geometry of the environment, the arrays and the propagation conditions. This could be extended to outdoor environments, where the majority of public Wi-Fi hot spots are presently located. It could provide system planners with a realistic evaluation of the likely performance of systems employing MIMO technology. Parallel with this the impact of different antenna types and radiation patterns could be considered with the aim of providing a comprehensive tool for estimating the likely spectral efficiency of MIMO systems encompassing all layers and elements of the wireless communications link.

5. In most Wi-Fi network deployments there is a fixed single access point (AP) and multiple client terminals linked to it, some of which may be mobile. This gives rise to the question of optimal location for the AP with regard to the multiple client terminals, for a given environment. To some degree this has been addressed in chapter 6 when array configurations with Z-dimension

displacements were demonstrated to be capable of providing improved performance, on average, compared to non-adjusted arrays, for various locations for the Tx and Rx. Also, it was stated that a central room location may provide the best overall performance since it ensures that path lengths are minimised and consequently the SNR is maximised at the Rx; notwithstanding a high correlation for small element spaced arrays over short ranges.

However, if it is assumed that the client terminals are fixed, then it is possible that specific locations exist for positioning the AP (within the particular room geometry), which would ensure optimal spectral efficiency for the network. This would be a complex optimisation problem requiring the parallel calculation of spectral efficiency for every client device connected to the AP for each trial location. The Metropolis search approach could be used to seek the optimal location; possibly searching specific regions of the environment rather than attempting to test every possible location. This could also involve adjustment of the orientation and structure of the AP array.

Since the propagation conditions are the most likely factor to influence the spectral efficiency then this would most realistically be attempted in the context of some structures or surfaces being present to enhance the strength of the reflections. This could involve extending the modelling environment to consider irregular indoor structures that could be beneficial to generating improved propagation conditions for MIMO systems and the inclusion of objects that may do the same. It may be more practical to introduce stronger reflections using metallic objects rather than large areas of walls.

The issue of the data terminal being mobile significantly increases the complexity of this optimisation problem. It is possible that using more than one AP and switching between them may be a solution; but at the expense of extra hardware. An alternative approach, which was referred to earlier in this thesis, is the concept of a distributed MIMO system (D-MIMO). Such systems are potential candidates for one side of the channel and inherently provide some simple advantages. For instance they will usually have wide element spacing between each element at the AP, thus providing a significant advantage for LOS conditions over short ranges, regardless of the location of the data terminal. Also, the wide distribution of elements means that it is always likely that some strong signal components will arrive at the terminal, even if some are obstructed; ensuring that the SNR at the other side of the channel does not degrade. Thus, if a D-MIMO system is considered feasible, then the optimisation of the element locations with regard to a given environment is something that could be investigated, particularly with regard to the problem of optimal placement for scenarios involving mobile data terminals.

APPENDIX A

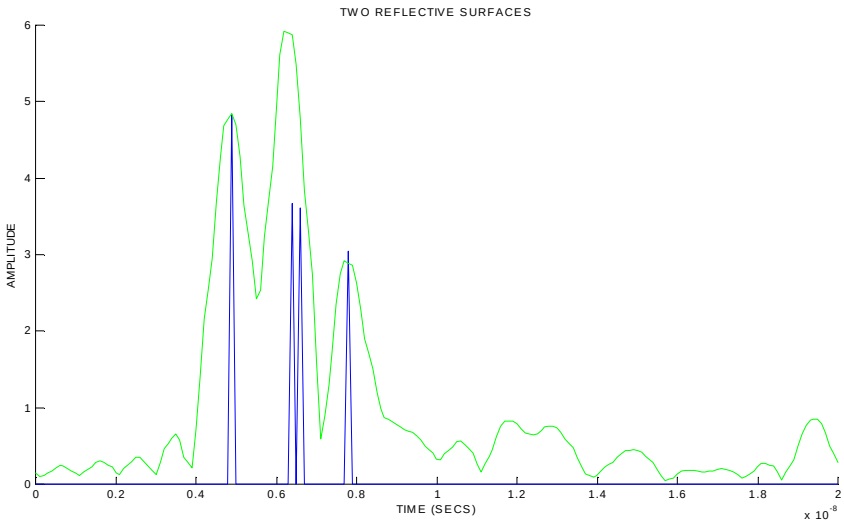

Figure A.1 Simplified measured and simulation outputs for comparison, showing LOS and two single first order reflections and a single second order reflection.

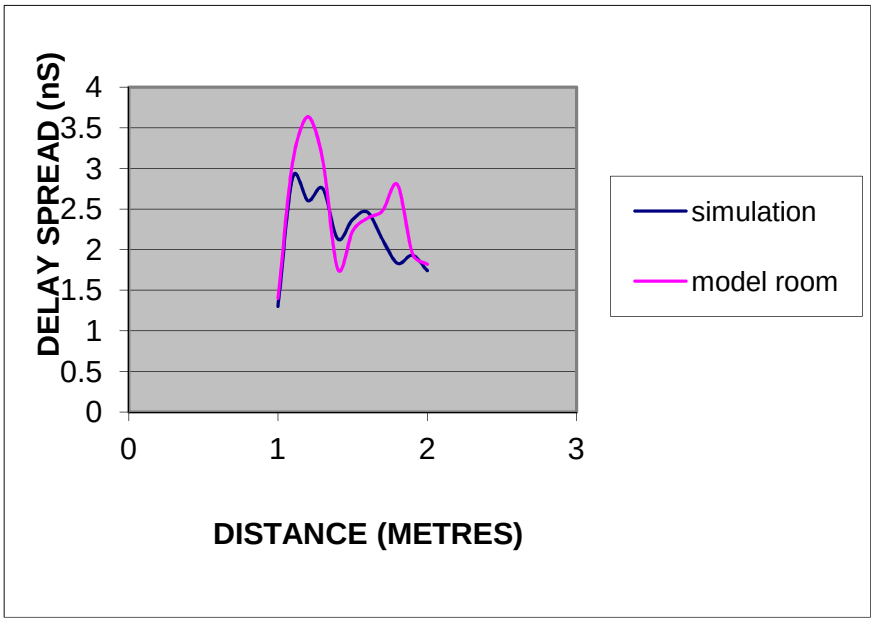

Figure A.2 Variation in rms delay spread (smoothed data points) with regard to distance for both the simulated and analyzer results. The line of sight distance was changed for each measurement by approximately 100 mm, from 1 metre to 2 metres.

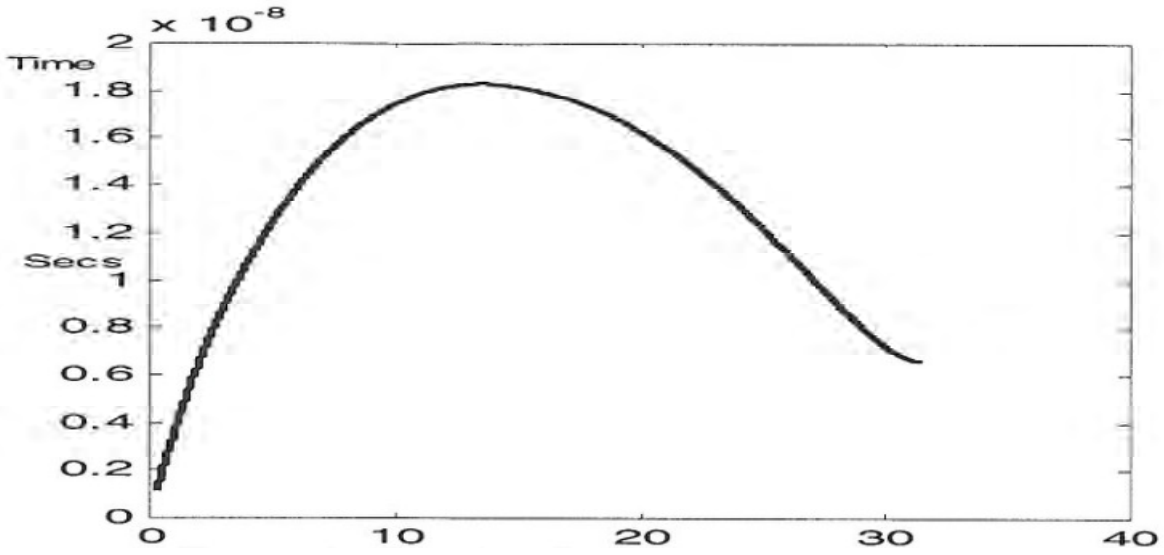

(a) ← Distance in metres →

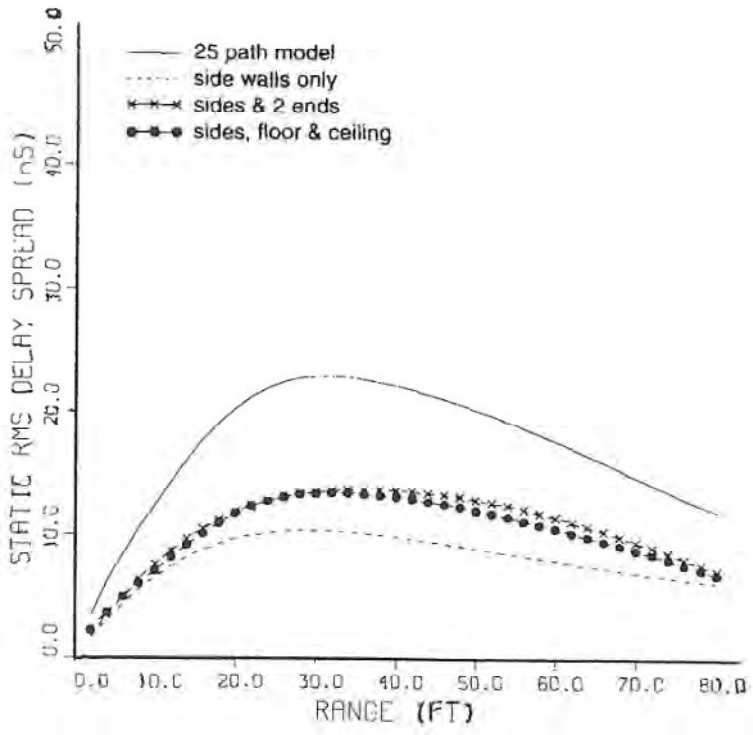

(b) The time is in nanoseconds and distance in feet in reference [26]

Figure A.3 Simulation generated rms delay spread in (a) and similar in (b) from reference paper [26] in chapter 3.

APPENDIX B

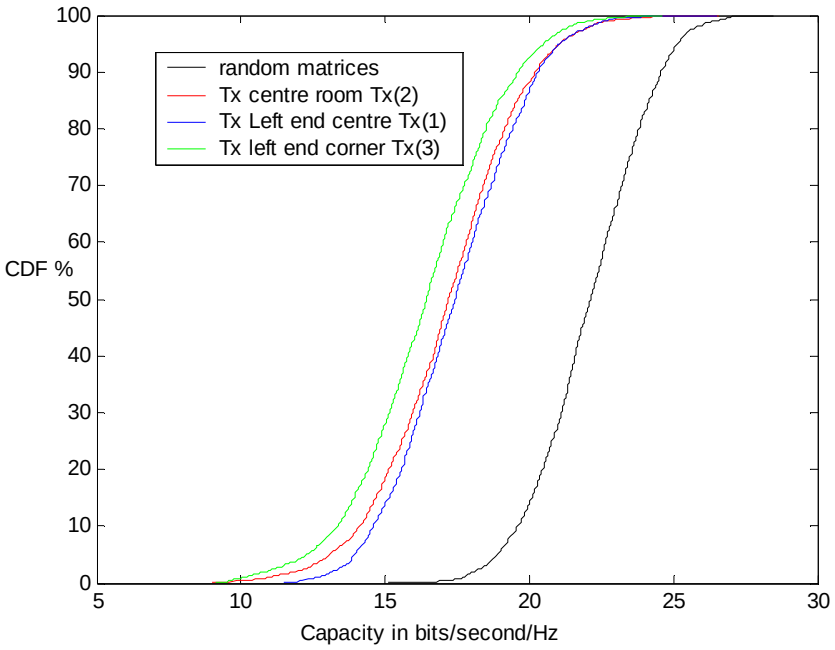

Figure B.1 CDFs for different fixed Tx locations for broadside 4x4 arrays with 2λ element spacing.

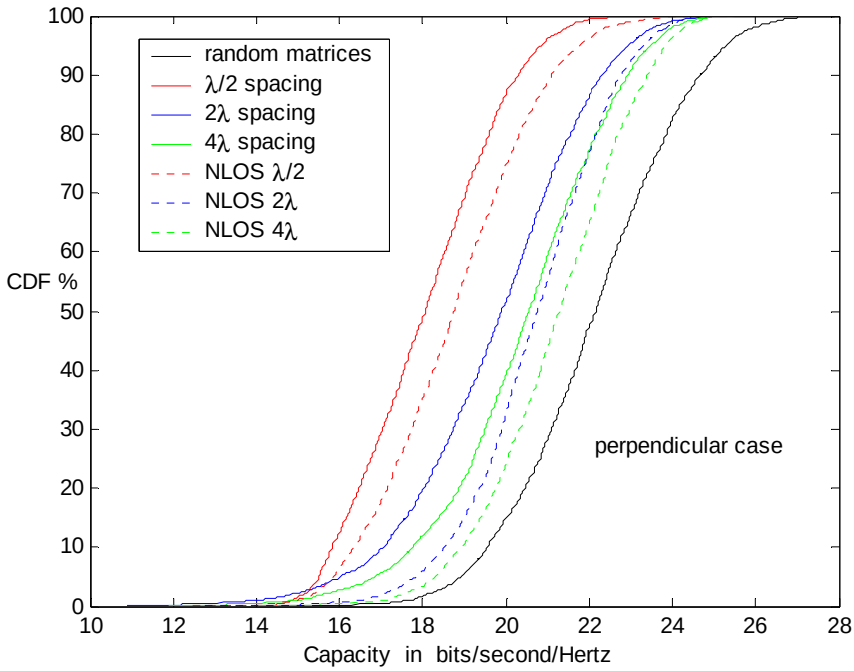

Figure B.2 CDFs for perpendicular 4x4 array orientations for all paths and NLOS conditions with Tx at Tx(1).

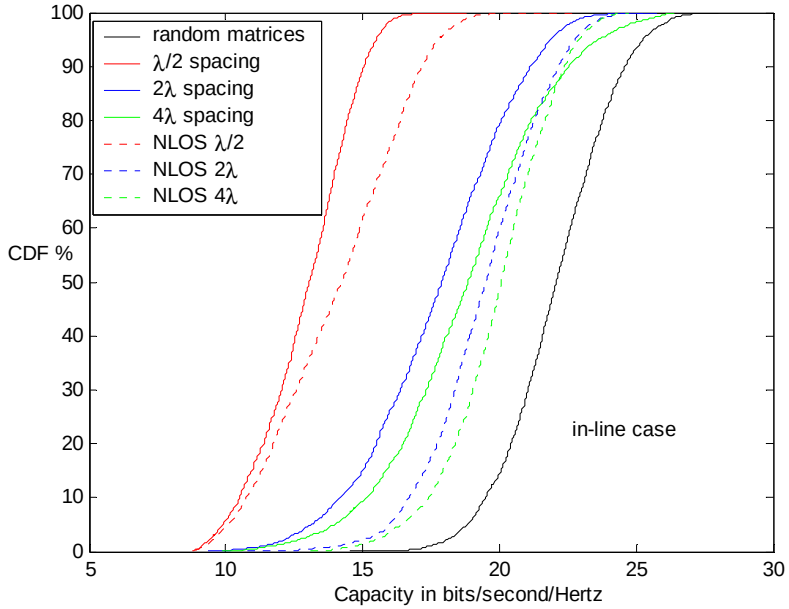

Figure B.3 CDFs for in-line 4x4 array orientations for all paths and NLOS conditions with Tx at Tx(1).

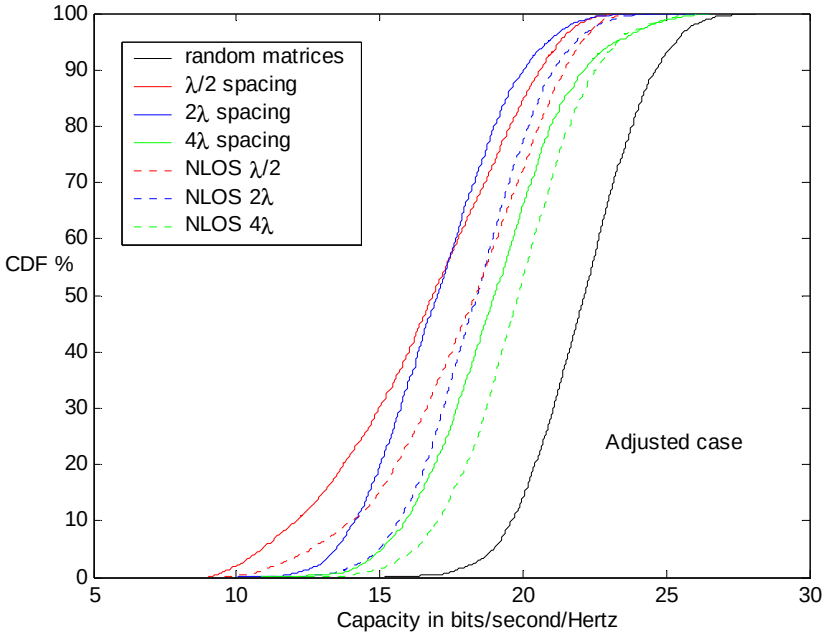

Figure B.4 CDFs for adjusted 4x4 array orientations for all paths and NLOS conditions with Tx at Tx(1).

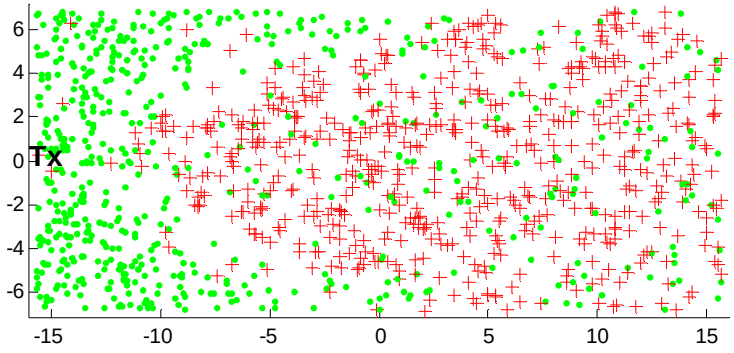

(a) Broadside orientation

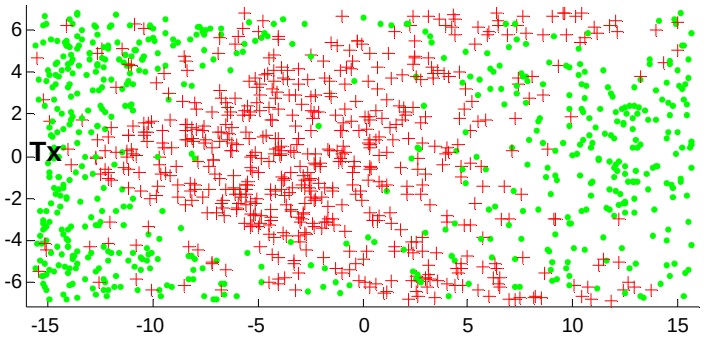

(b) Perpendicular orientation

Figure B.5 Maximum 20% (red crosses) and minimum 20% (green dots) regions for 2x2 arrays with Tx at Tx(1) (Figure 3.1) under LOS conditions; a) is broadside orientation and b) perpendicular orientation with λ/2 elements spacing and LOS conditions in both cases.

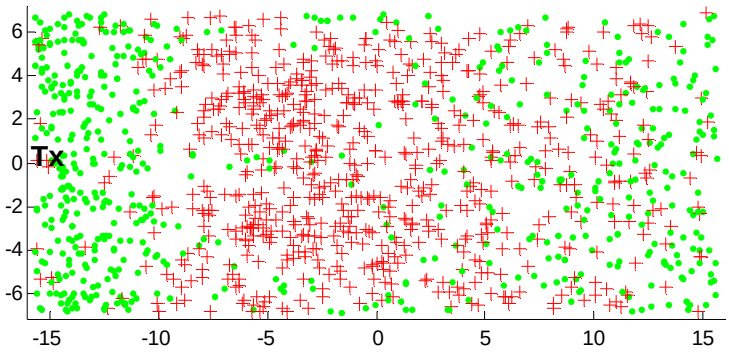

(a) Square arrays λ/2 LOS conditions.

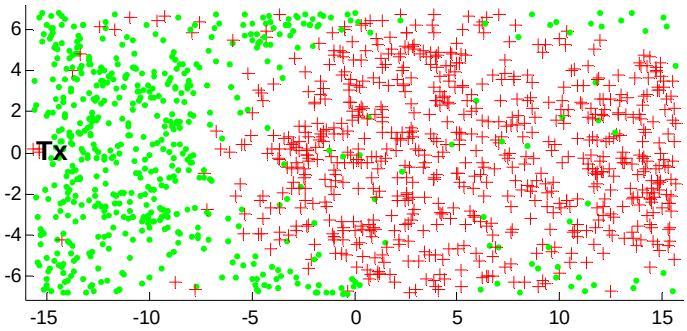

(b) Cross arrays 2λ LOS conditions.

Figure B.6 Maximum 20% (red crosses) and minimum 20% (green dots) regions for 4x4 square configuration array in (a) and 4x4 cross array configuration in (b) with Tx at Tx(1) under LOS conditions.

	Mean λ/2 LOS	Mean λ/2 NLOS	Mean λ/2 NLOS (Acc.)	Mean λ/2 LOS	Mean λ/2 NLOS	Mean λ/2 NLOS (Acc.)
Cross Tx&Rx	15.0	17.4	15.0	16.8	18.4	15.0
Cross Rx	15.9	17.5	14.6	17.1	17.1	15.4
Square Tx&Rx	13.9	15.1	12.6	17.0	18.4	15.0
Square Rx	14.9	16.0	13.4	17.1	18.2	15.1

Table B.1 Mean capacities for cross and square arrays at Tx and Rx compared with case when Tx is a ULA and Rx is a cross or square (the second and fourth row).

Figure B.7 The figures below are a selection of location plots for different LOS and NLOS arrangements of 4x4 arrays. The 'r' in brackets indicates that the reflection coefficient of the reflecting surfaces has been modified to Γ=1. The (Acc.) means that the removal of the LOS components has been accounted for. The listing below (a) to (r) describes the various configurations and indicates the overall mean and the means in the maximum regions (red) and the minimum regions (green).

Broadside ULAs

a. LOS (r) λ/2 mean= 19.3 Max. Mn.= 22.6 Min. Mn.= 14.5
b. LOS (r) 2λ mean= 19.7 Max. Mn.= 23.0 Min. Mn.= 16.2
c. LOS 4λ mean= 19.9 Max. Mn.= 23.3 Min. Mn.= 16.6
d. NLOS (Acc.) 4λ mean= 16.6 Max. Mn.= 22.3 Min. Mn.= 12.3

Perpendicular arrangement (ULAs)

e. LOS λ/2 mean= 13.5 Max. Mn.= 16.1 Min. Mn.= 10.9
f. LOS 4λ mean= 18.2 Max. Mn.= 22.0 Min. Mn.= 14.1
g. NLOS (Acc.) 4λ mean= 20.7 Max. Mn.= 15.6 Min. Mn.= 11.0

In Line arrangement (ULAs)

h. LOS λ/2 mean= 13.1 Max. Mn.= 15.7 Min. Mn.= 10.3
i. NLOS (Acc.) λ/2 mean= 11.6 Max. Mn.= 15.6 Min. Mn.= 8.5

Cross array at Tx and Rx

j. LOS λ/2 mean= 15.1 Max. Mn.= 18.2 Min. Mn.= 11.8
k. LOS 4λ mean= 17.1 Max. Mn.= 20.1 Min. Mn.= 14.2

Square array at Tx and Rx

l. LOS 2λ mean= 16.9 Max. Mn.= 20.6 Min. Mn.= 13.5
m. LOS 4λ mean= 18.1 Max. Mn.= 21.1 Min. Mn.= 14.9
n. NLOS (Acc.) 4λ mean= 15.6 Max. Mn.= 20.2 Min. Mn.= 11.4

ULA at Tx and Cross at Rx

o.	LOS λ/2	mean= 15.9	Max. Mn.= 19.4	Min. Mn.= 11.7
p.	NLOS (Acc.) λ/2	mean= 14.6	Max. Mn.= 19.5	Min. Mn.= 9.6

ULA at Tx and Square at Rx

q.	LOS 2λ	mean= 17.1	Max. Mn.= 20.6	Min. Mn.= 13.6
r.	LOS (r) 4λ	mean= 20.2	Max. Mn.= 23.1	Min. Mn.= 17.3

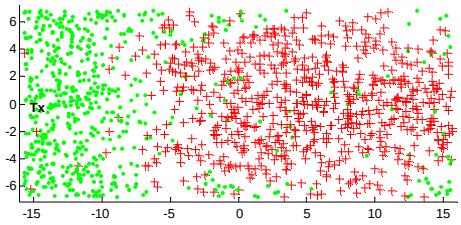

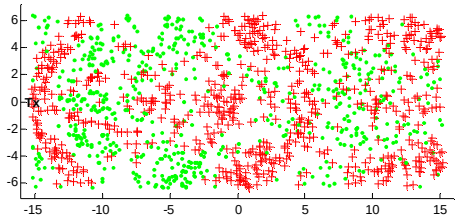

a. mean=19.3, Max.mean=22.6, Min. mean=14.5 b.mean=19.7, Max.mean=23.0, Min. mean=16.2

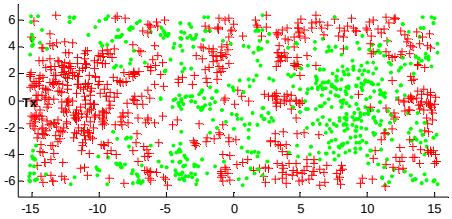

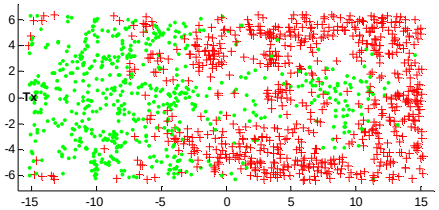

c. mean=19.9, Max.mean=23.3, Min. mean=16.6 d. mean=16.6 Max.mean=22.3 Min. mean=12.3

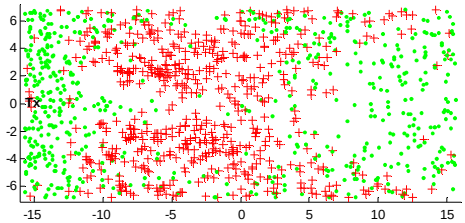

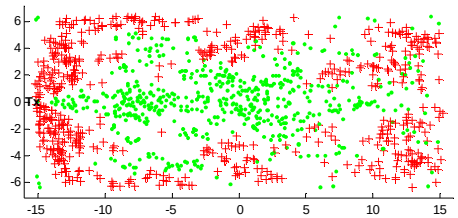

e. mean=13.5, Max.mean=16.1, Min. mean=10.9 f. mean=18.2 Max.mean=22.0 Min. mean=14.1

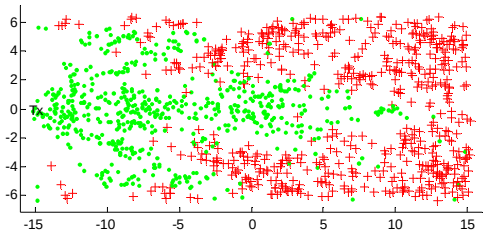

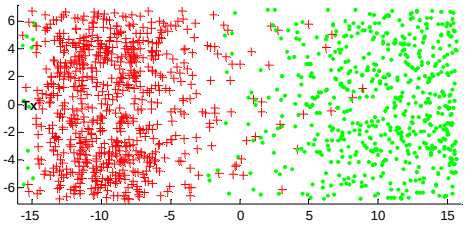

g. mean=15.6, Max.mean=20.7, Min. mean=11.0 h. mean=13.11 Max.mean=15.7 Min. mean=10.3

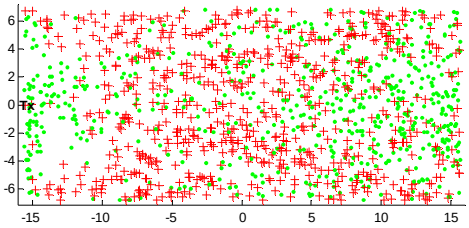

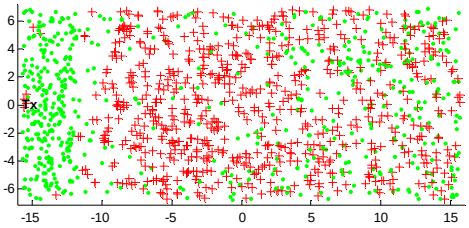

i. mean=11.6, Max.mean=15.6, Min. mean=11.0 j. mean=15.03 Max.mean=18.2 Min. mean=11.8

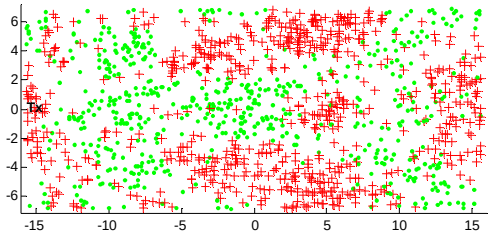

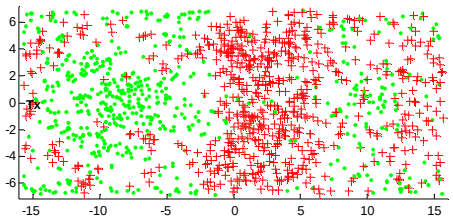

k. mean=17.1, Max.mean=20.1, Min. mean=14.2 l. mean=16.9 Max.mean=20.6 Min. mean=13.5

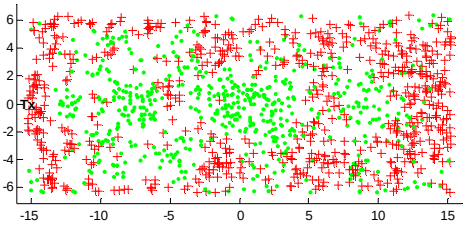

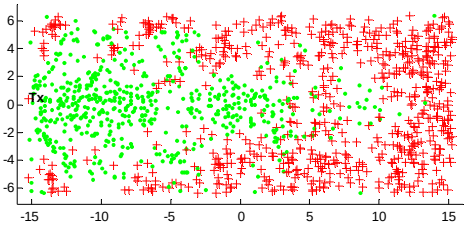

m. mean=18.1, Max.mean=21.1, Min. mean=14.9 n. mean=15.6 Max.mean=20.2 Min. mean=11.4

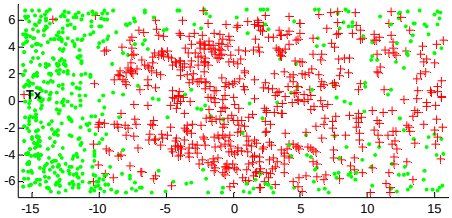

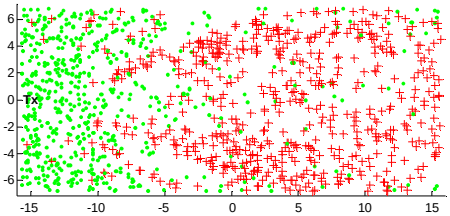

o. mean=15.9, Max.mean=19.4, Min. mean=11.7 p. mean=14.6 Max.mean=19.5 Min. mean=9.6

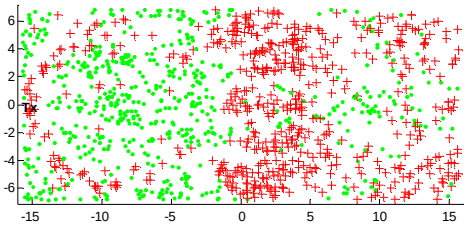

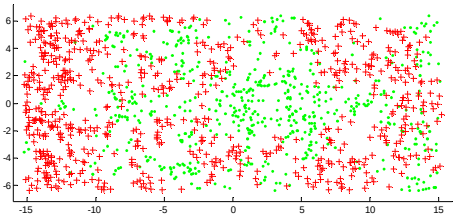

q. mean=17.1, Max.mean=20.6, Min. mean=13.6 r. mean=20.2 Max.mean=23.1 Min. mean=17.3

APPENDIX C

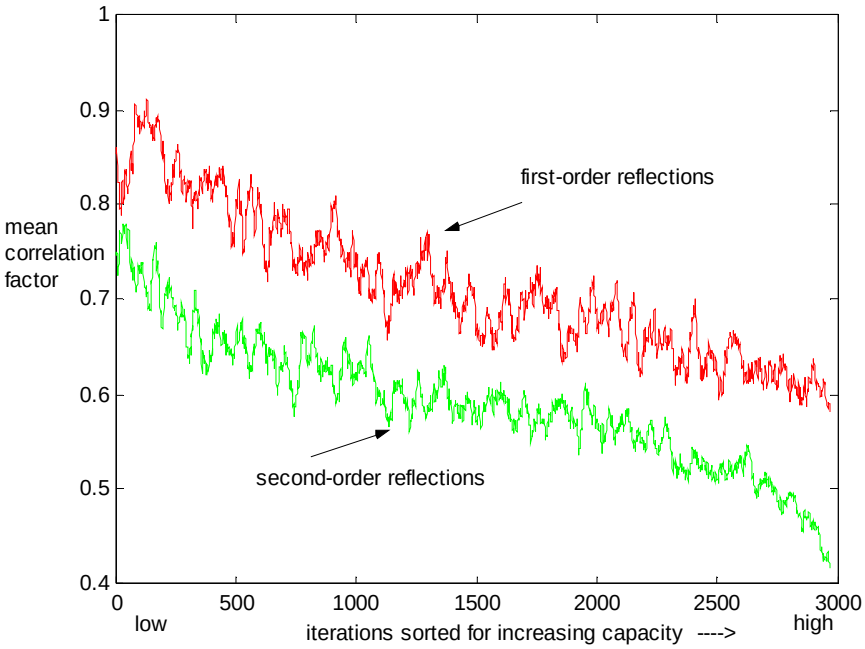

Figure C.1 Trend of mean values of channel correlation matrices versus increasing capacity for first-order reflections only and second-order reflections only. A 25 point moving average was employed to simplify the plot.

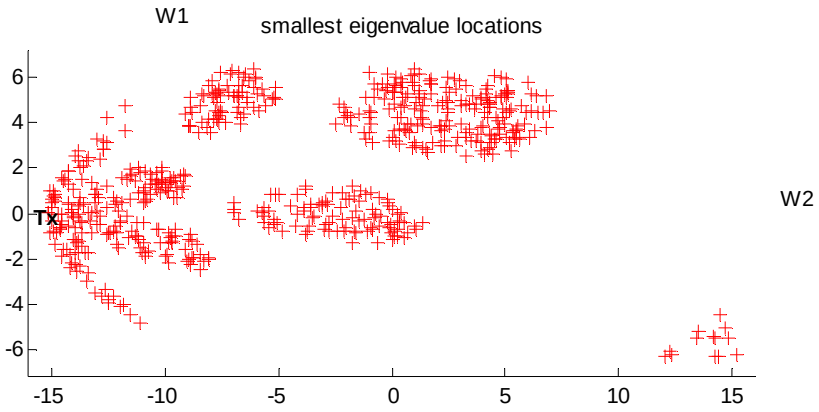

Figure C.2 Plot of maximum (20%) values of the smallest eigenvalue Eig 4 (corresponding to figure 5.8 in chapter 5 and table C.1 below). Note figure 5.8 is maximum (20%) capacity locations with LOS and reflections from one wall (W1).

Region Marked on figure 5.8	Eig1	Eig2	Eig3	Eig4
U	12.91	1.92	0.69	0.49
M	14.18	1.76	0.04	0.013
L	13.29	1.89	0.25	0.57

Table C.1 Typical eigenvalues (Eig 1/2/3/4) associated with regions marked on Figure 5.8. Note figure 5.8 is maximum (20%) capacity locations with LOS and reflections from one wall (W1).

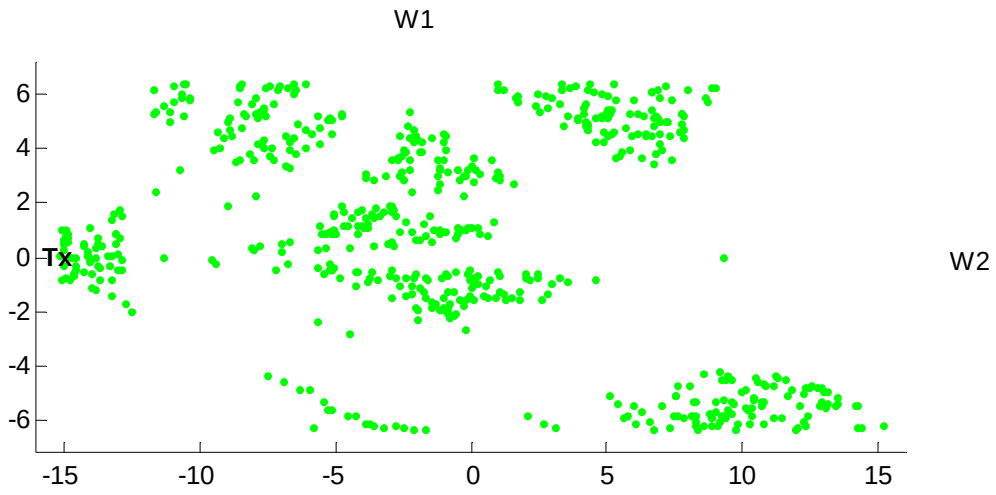

Figure C.3 Plot of locations where channel correlation is lowest (corresponding to figure 5.8 in chapter 5). This is done by plotting the mean value determined from the channel correlation matrix (20% of lowest values shown). Note Figure 5.8 is maximum (20%) capacity locations with LOS and reflections from 1 wall (W1).

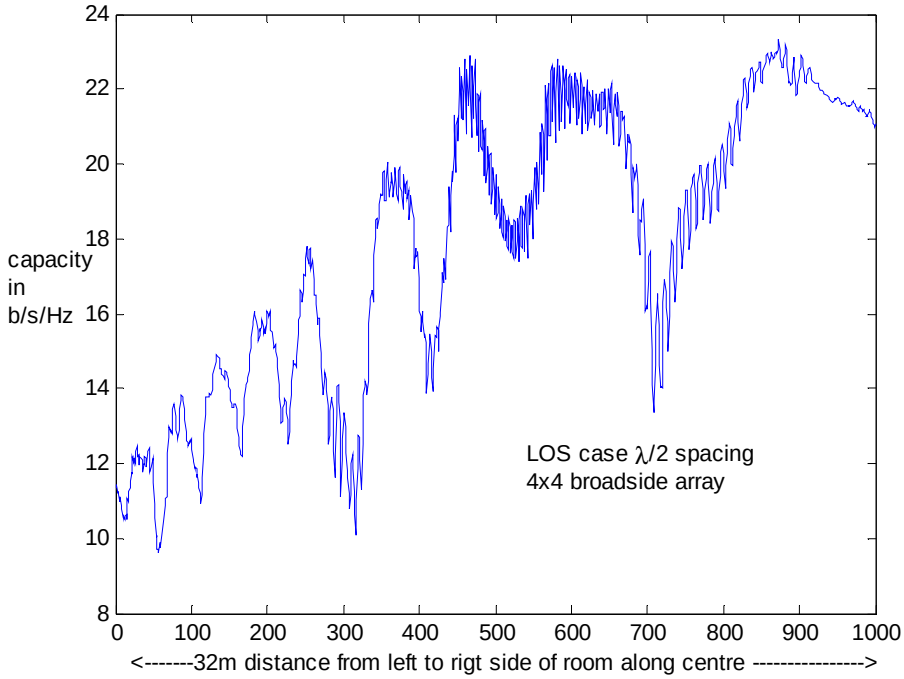

Figure C.4 The capacity in the LOS case for a 4x4 broadside MIMO system (λ/2 element spacing) Rx moving along centre axis of room from left to right.

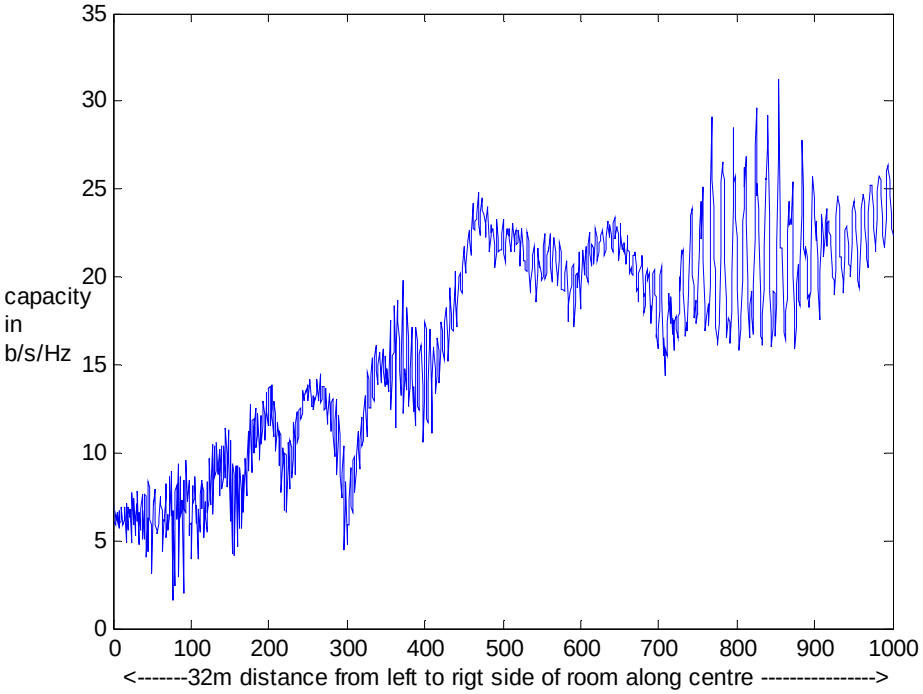

Figure C.5 Capacity of 4x4 broadside MIMO system NLOS case (λ spacing) Rx moving along centre axis of room, from left to right.

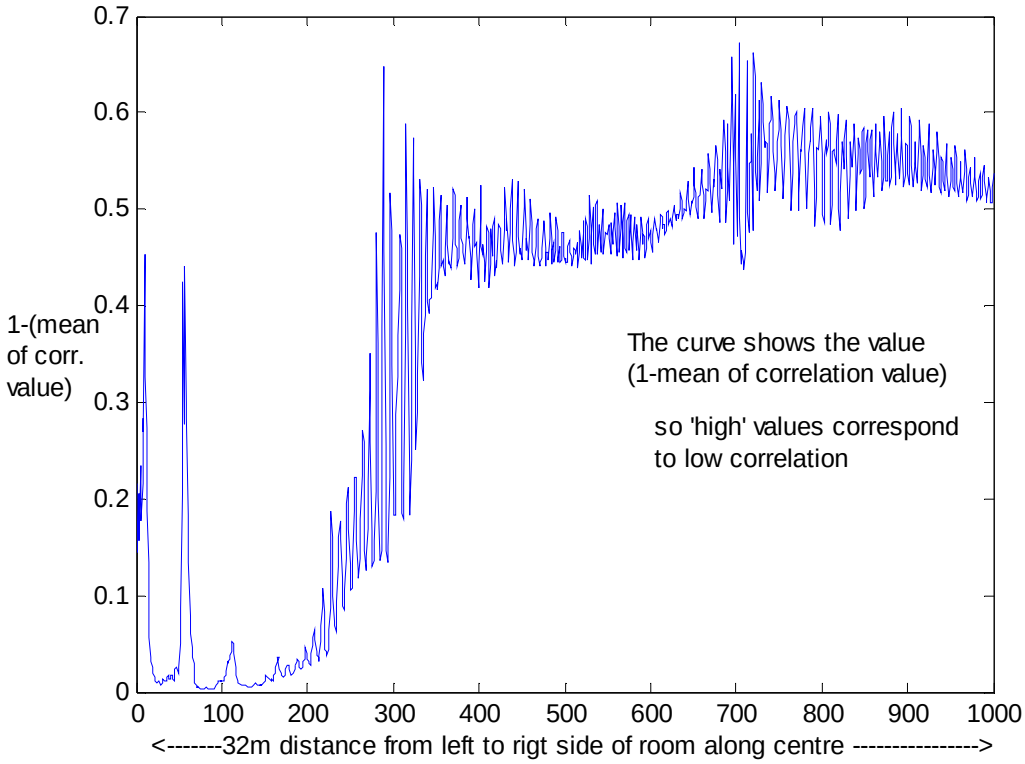

Figure C.6 Representation of mean channel correlation 4x4 MIMO system all paths present (λ/2 spacing) Rx moving along centre axis of room from left to right. Since low values of the mean tend to correspond to high values of capacity the plot shows the inverse value of the mean by subtracting the value from 1 (1 being the maximum correlation value). Thus larger values on the graph are those of lower correlation.

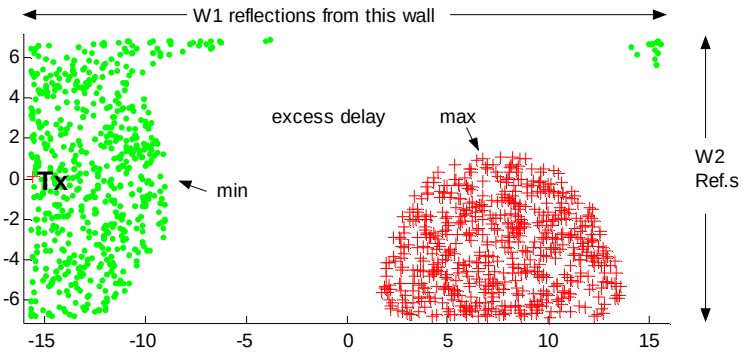

(a) P.T.O.for details

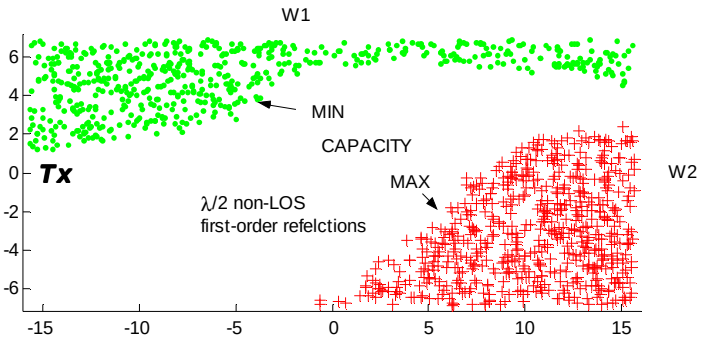

(b)

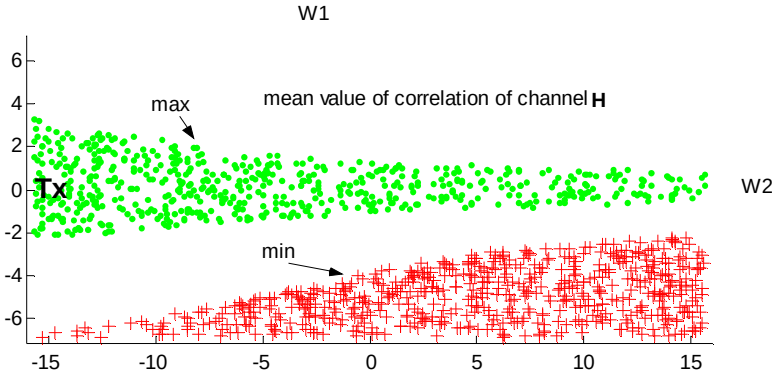

(c)

Figure C.7 Comparison of (maximum) 20% excess delay region (a) with maximum capacity (red) (b) and minimum 20% correlation mean value of channel **H** (red) in (c). Corresponding 'weak' 20% regions (green). First order reflections from W1 and W2 as indicated.

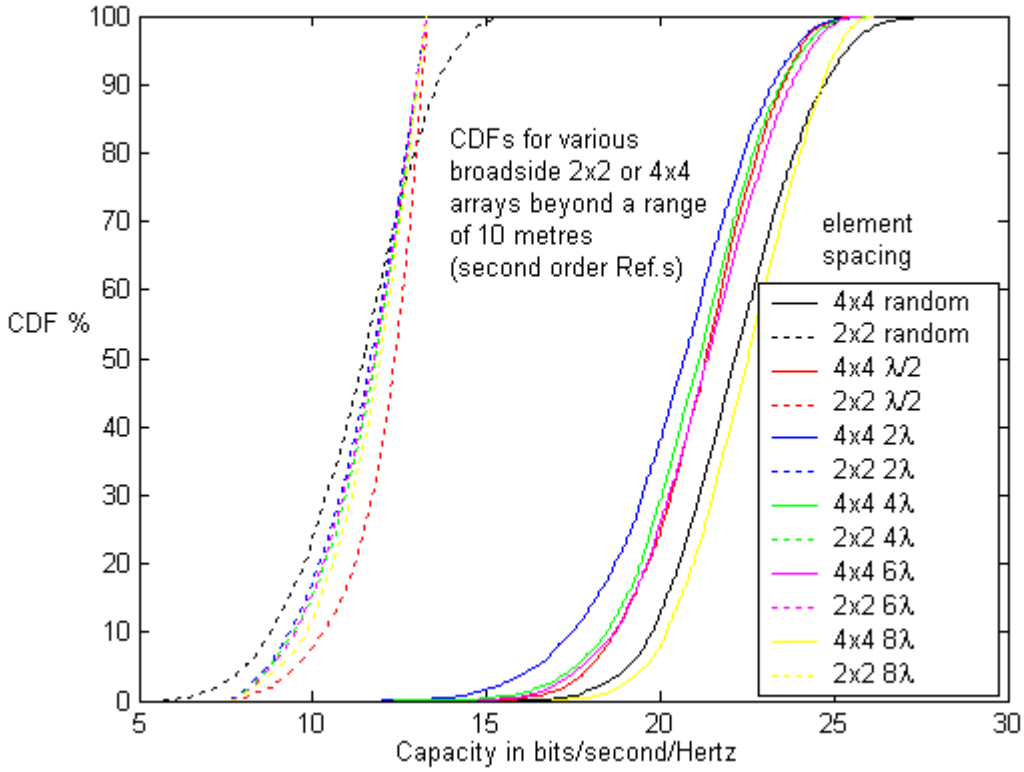

Figure C.8 CDFs or 2x2 and 4x4 broadside arrays at Tx –Rx separation distance greater than 10 m when only second order reflections considered and SNR normalised to 20 dB.

APPENDIX D

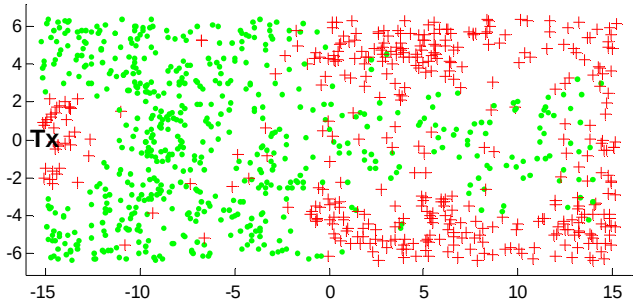

Figure D.1 The distribution of strongest (20%) and weakest (20%) locations throughout the room based on Z average adjustments at Tx and Rx all paths present. Tx at Tx(1) location.

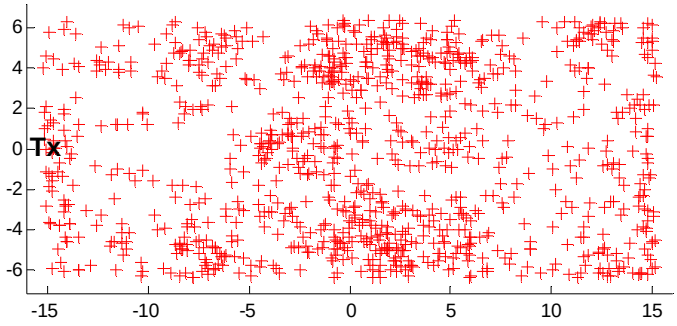

Figure D.2 The strongest 30% of capacity locations for 2x2 arrays under LOS conditions (values all greater than 11.16). Tx at Tx(1) location.

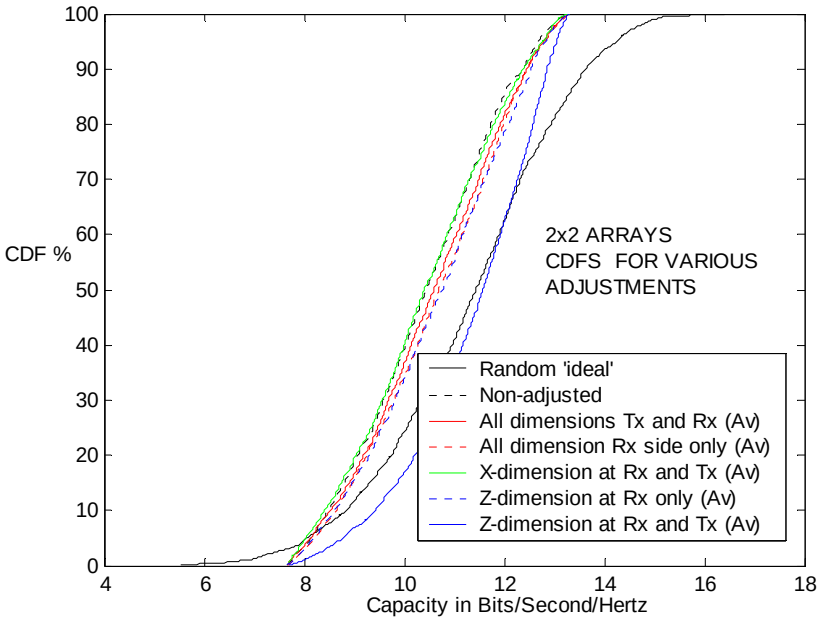

Figure D.3 CDFs for various scenarios for 2x2 arrays. The bracketed term (Av) means an average estimated configuration was used for the curve. (There were no significant differences in most cases so not all are shown).

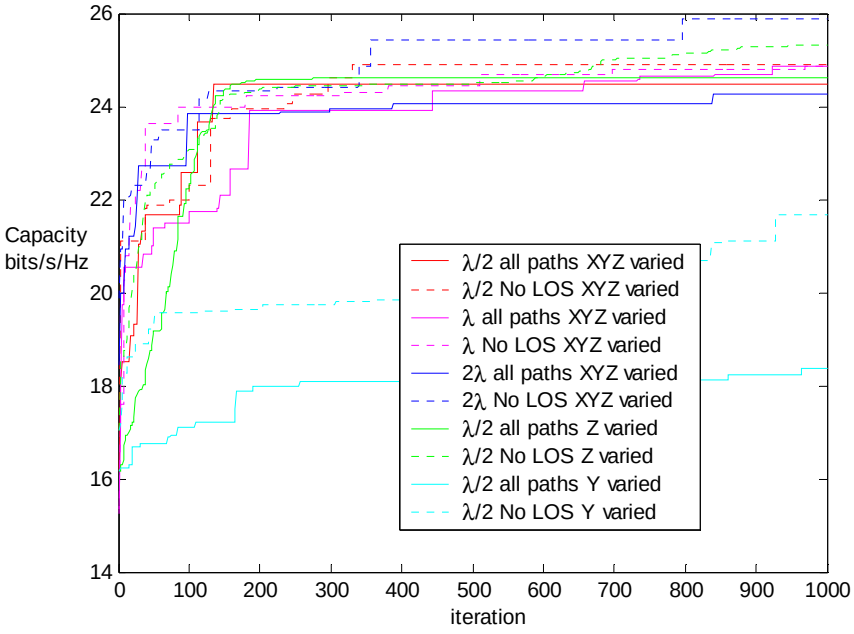

Figure D.4 Adjustments at location B for various initial element spacing under LOS conditions (all paths) and No LOS.

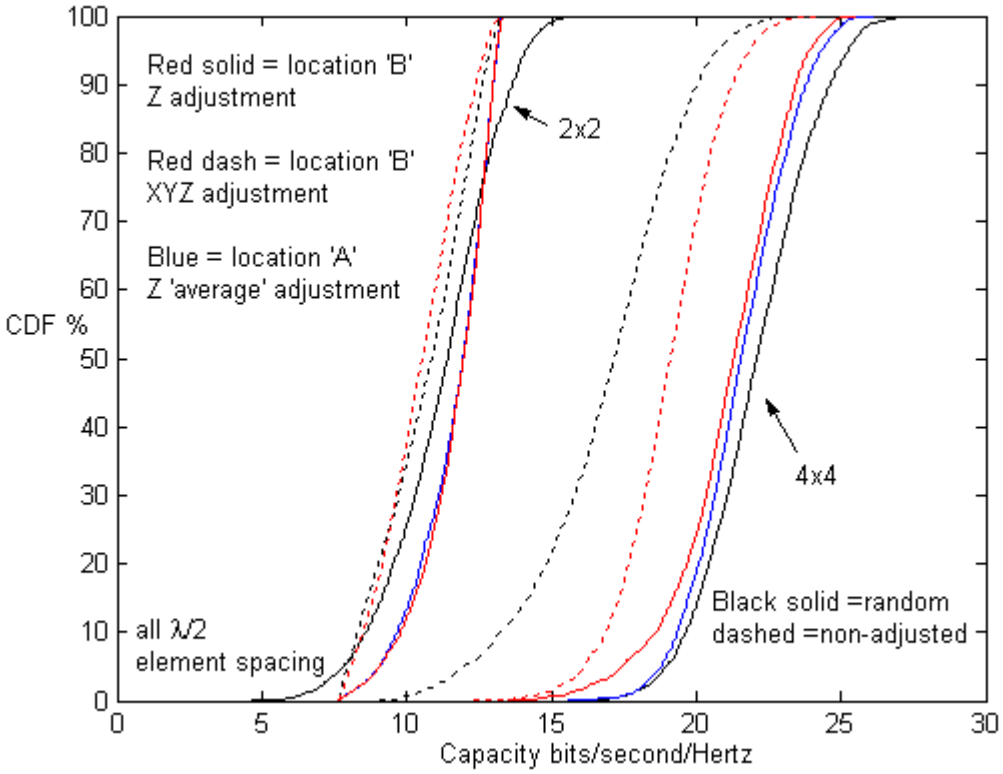

Figure D.5 CDFs at location A and B for 2x2 and 4x4 arrays for various adjusted arrays

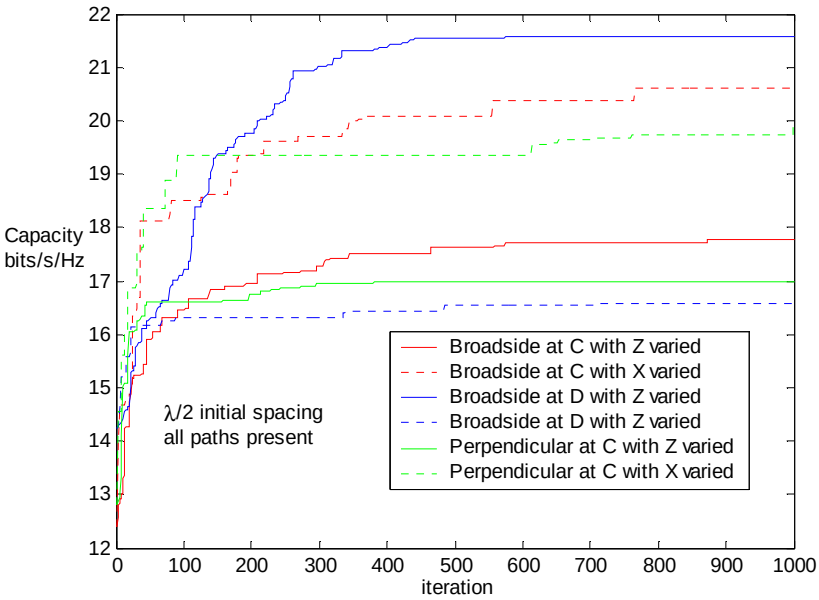

Figure D.6 Z and X dimension improvements at locations 'C' and 'D' for λ/2 initial spacing all paths present.

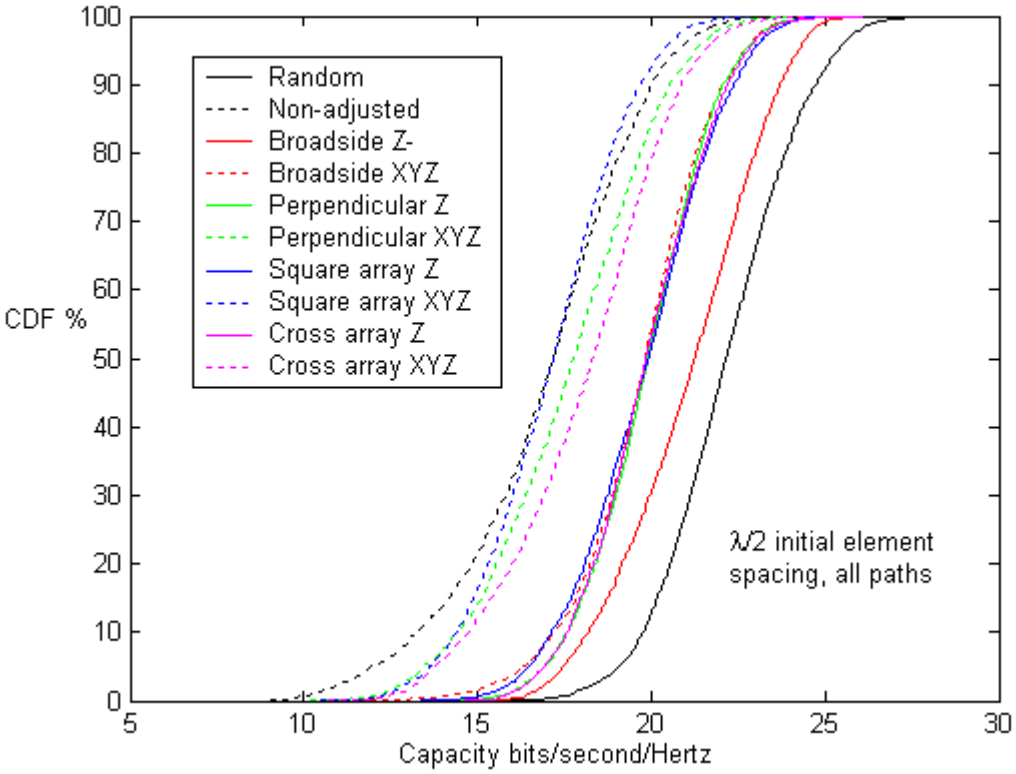

Figure D.7 Comparison of different array configurations with final/best adjustment of element for XYZ dimensions or Z dimensions only.

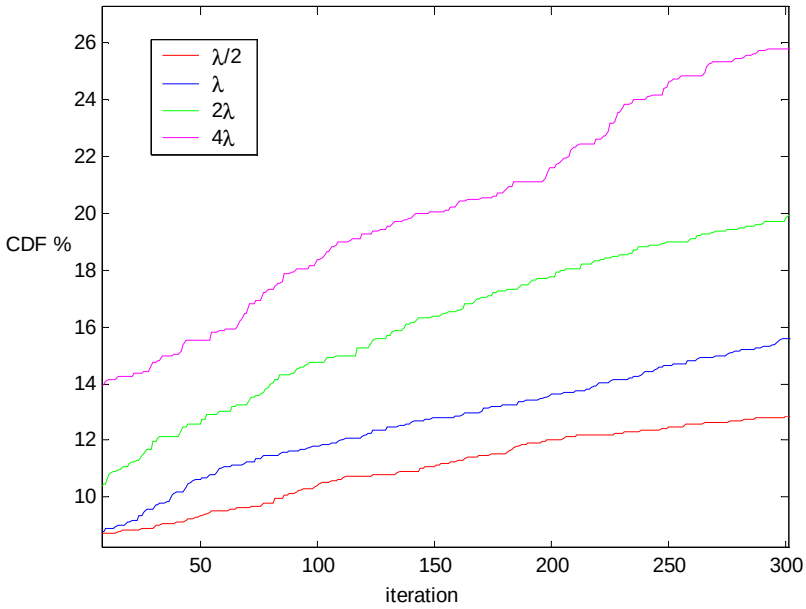

Figure D.8 Improvements achieved at location A for various initial element spacing when only LOS components present (free space) and adjustments at Rx only for broadside arrangements.

Figure D.9 Final adjustments at Rx for figure D.8 for two cases. On the left is 4 λ spacing initially (and at Tx) and the right is λ/2 initially (and Tx).

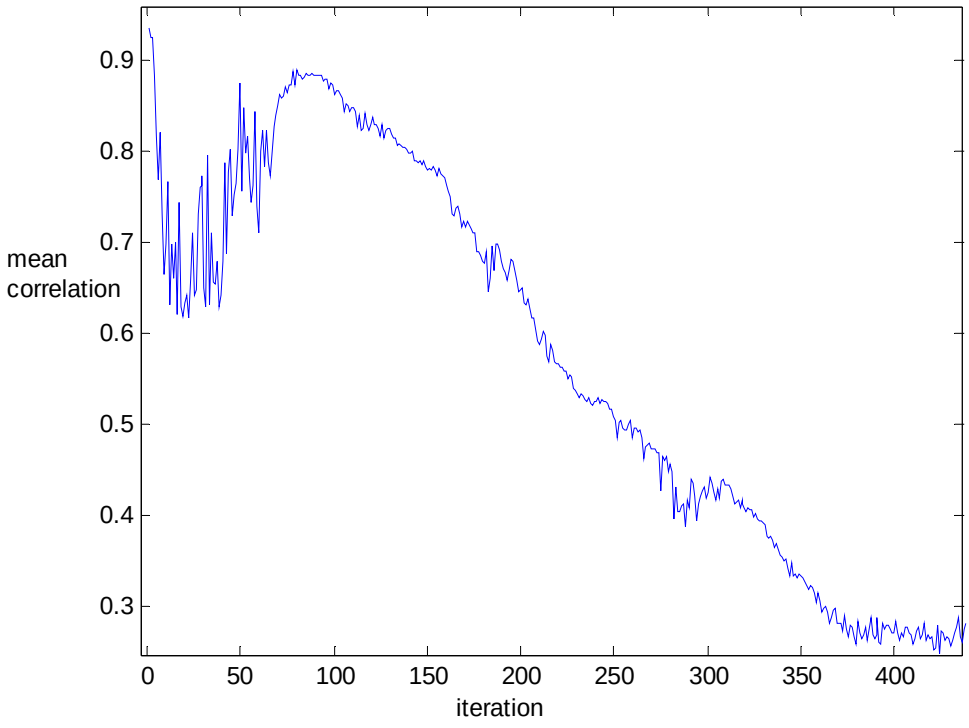

Figure D.10 The mean of the channel correlation matrix for the 4 λ curve in figure D.8

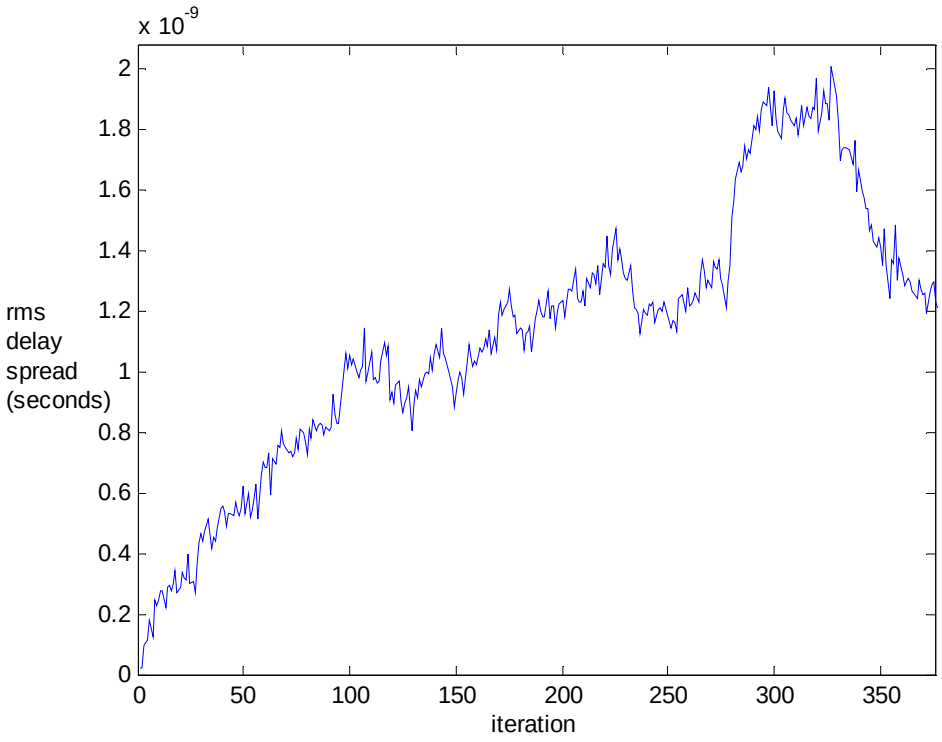

Figure D.11 The rms delay spread calculated across all 16 LOS components relative to zero for the 4 λ case in figure D.8 and D.10.

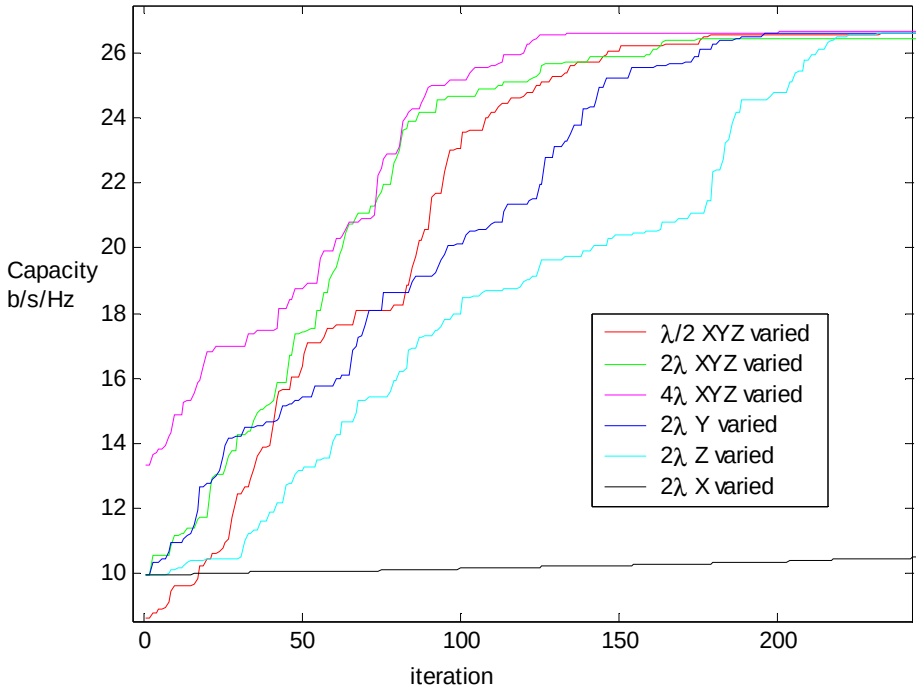

Figure D.12 LOS only case at location A when both the Tx and Rx were varied. Selection of results shown for XYZ dimensions varied and different initial element spacing; also for single dimensions varied with initial spacing of 2 λ.

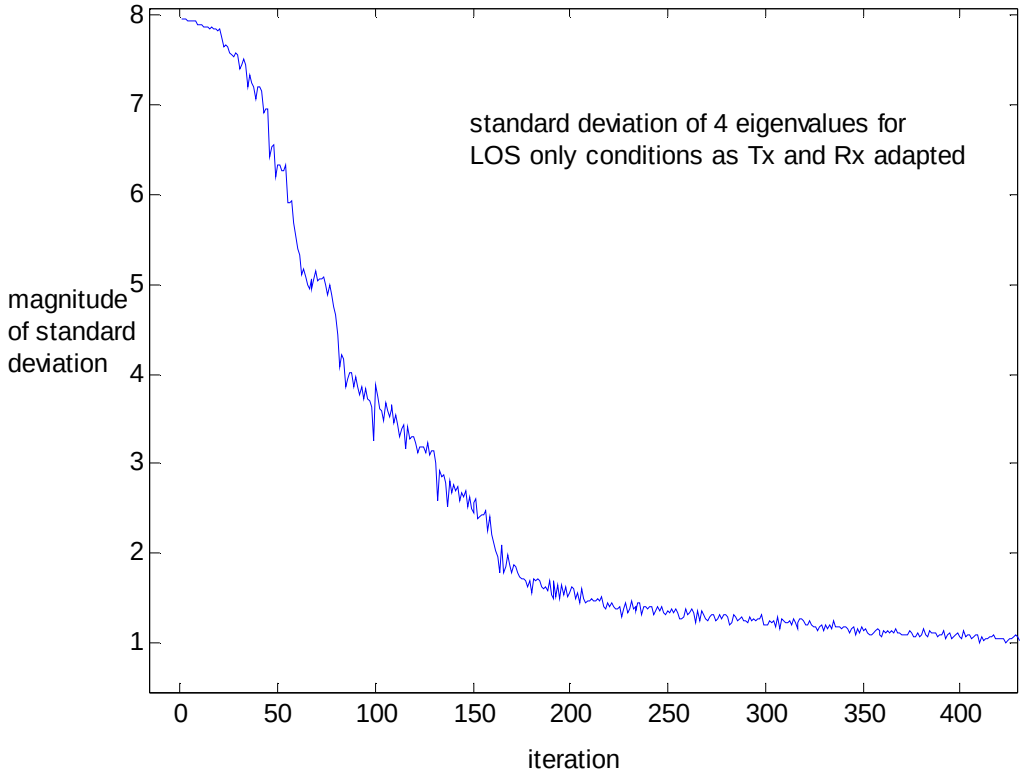

Figure D.13 Variation in the standard deviation of the 4 eigenvalues corresponding to the 2λ XYZ dimensions of example plotted in figure D.12. Note the deviation reduces as 4 approximately equal eigenvalues develop.

Pre-adaptation matrix

1.0000	0.9683	0.8968	0.8137
0.9683	1.0000	0.9789	0.9326
0.8968	0.9789	1.0000	0.9865
0.8137	0.9326	0.9865	1.0000

Post-adaptation matrix

1.0000	0.0003	0.0005	0.4392
0.0003	1.0000	0.0561	0.1572
0.0005	0.0561	1.0000	0.0577
0.4392	0.1572	0.0577	1.0000

Figure D.14 The channel correlation matrix before and after adaptation of array elements for the example in figure D.13. These correspond to the first and last iteration points in figure D.13.

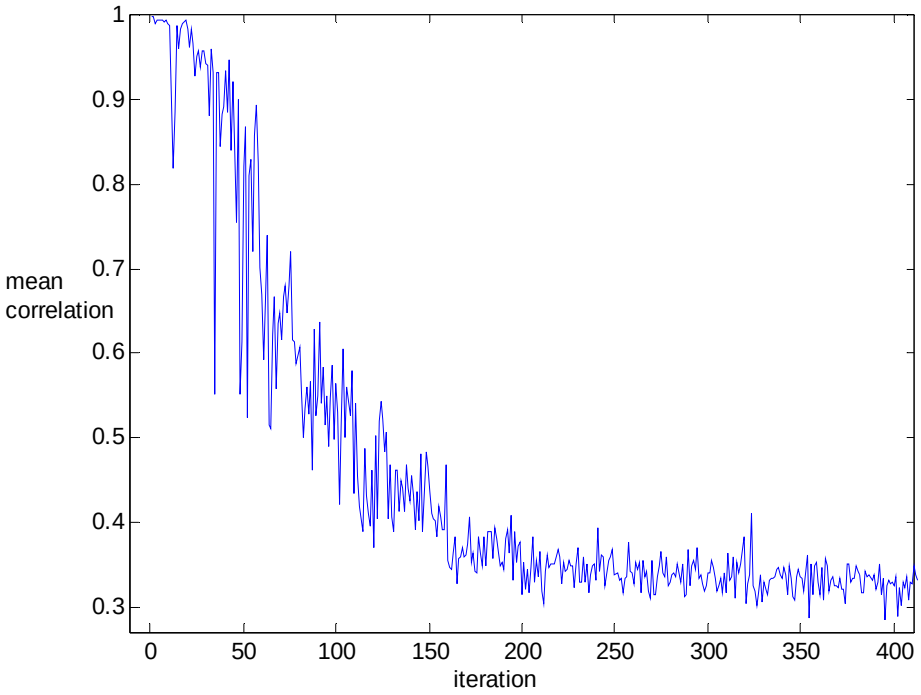

Figure D.15 A plot of the mean of the channel correlation matrix values (two matrix examples of which are shown in figure D.14) for figure D.13.

Pre-adaptation determinant				Post-adaptation determinant			
0.0046	**0.0045**	**0.0043**	**0.0037**	**0.0044**	**0.0002**	**0.0002**	**0.0001**
0.0045	**0.0046**	**0.0045**	**0.0041**	**0.0002**	**0.0045**	**0.0003**	**0.0001**
0.0043	**0.0045**	**0.0046**	**0.0044**	**0.0002**	**0.0003**	**0.0048**	**0.0000**
0.0037	**0.0041**	**0.0044**	**0.0046**	**0.0001**	**0.0001**	**0.0000**	**0.0046**

Figure D.16 The determinant $\mathbf{HH}^*$ for pre and post adaptation conditions for the example of figure D.12 (2λ XYZ instance and similar to figure D.14). Note that for maximal capacity the determinant $\mathbf{HH}^*$, has real valued diagonal components and the off-diagonal ones will be zero, which is approximately the case for the post-adaptation case shown on right. (* denotes complex conjugate).

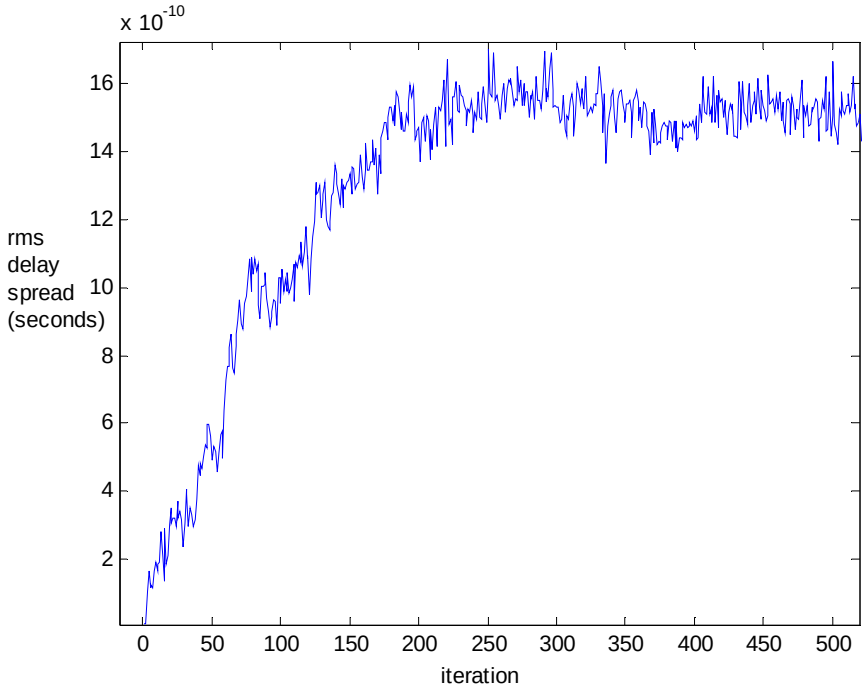

Figure D.17 The rms delay spread calculated across all 16 LOS components relative to zero for the 2 λ XYZ dimensions varied case of figure D.12, and corresponds to figures D.12 to D.16 above.

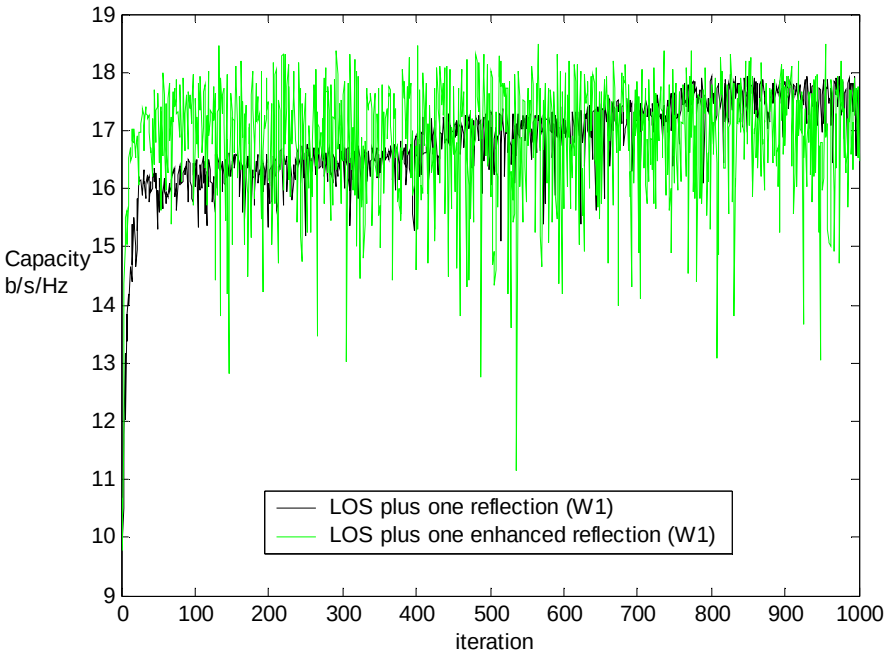

Figure D.18 Capacity fluctuations during Metropolis search for the case of the LOS and a single first order reflection, with and without enhancement of the reflections.

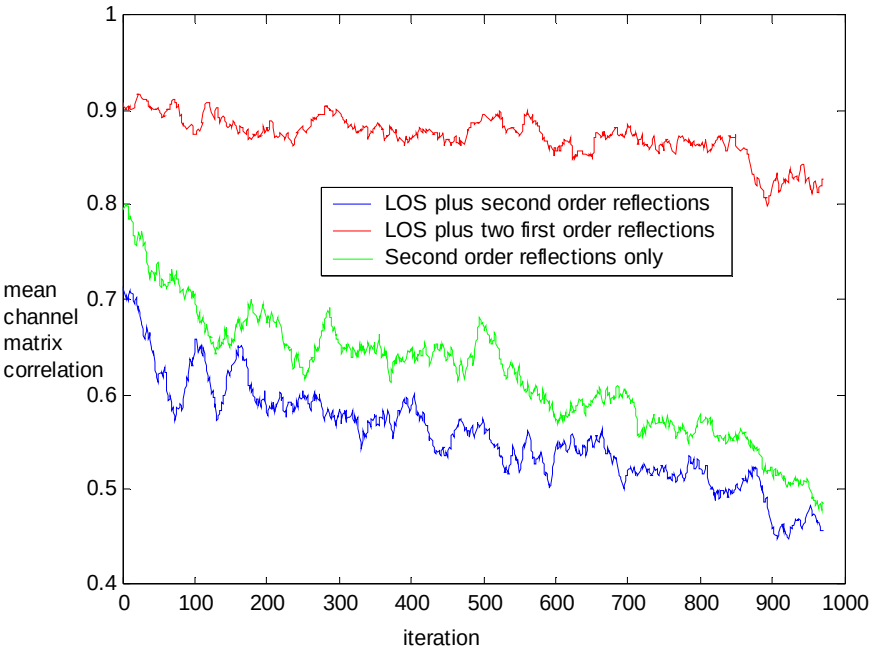

Figure D.19 The mean of the channel correlation as Metropolis search improves capacity under different limited sparse conditions. To observe the trend a 20 point moving average was used for this since the large fluctuations that occurred with reflections (for unsuccessful iterations of the Metropolis search) would make the graph difficult to read.

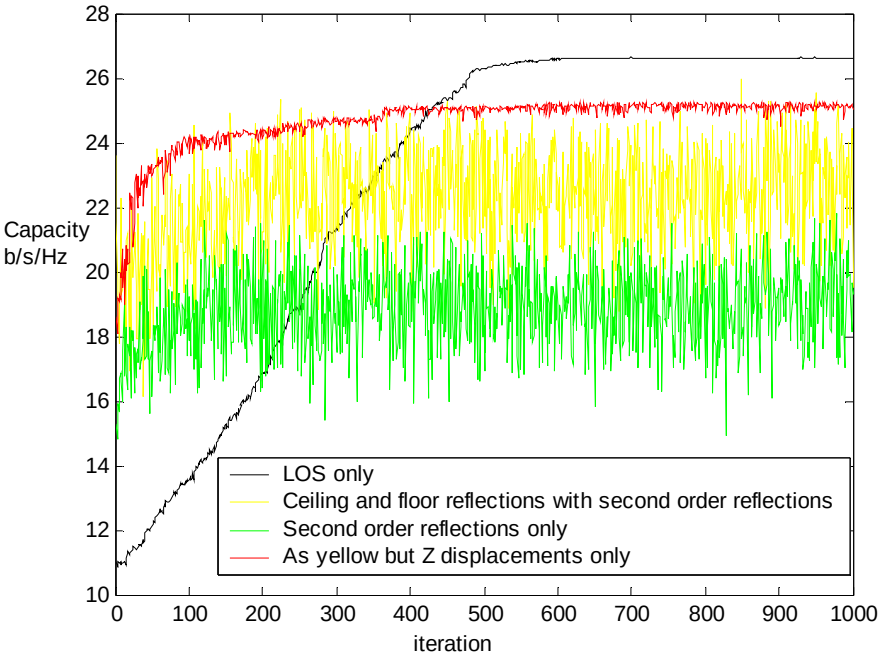

Figure D.20 Capacity fluctuations during Metropolis search under various limited propagation conditions

APPENDIX E

LIST OF EQUATIONS AND CORRESPONDING PAGE NUMBER.

Page 17

$$\mathbf{H} = \begin{bmatrix} h_{1,1} & h_{1,2} & \dots & h_{1,N} \\ h_{2,1} & \dots & \dots & h_{2.N} \\ \dots & & & \\ h_{M,1} & \dots & & h_{M,N} \end{bmatrix} \qquad (2.1)$$

$$C = log_2(1 + \rho|h|^2) \qquad b/s/Hz \qquad (2.2)$$

$$C = log_2\left(1 + \rho \sum_{i=1}^{M} |h_i|^2\right) \qquad b/s/Hz \qquad (2.3)$$

Page 18

$$C = log_2\left(1 + \frac{\rho}{N} \sum_{i=1}^{N} |h_i|^2\right) \qquad b/s/Hz \qquad (2.4)$$

$$C = log_2\left[det\left(I_M + \frac{\rho}{N}\, \boldsymbol{H}\boldsymbol{H}^*\right)\right] \qquad b/s/Hz \qquad (2.5)$$

$$C = \sum_{I=1}^{m} log_2\ \left(1 + \frac{\rho}{N}\lambda_i\right) \qquad b/s/Hz \qquad (2.6)$$

$$\Lambda = \begin{bmatrix} \lambda_1 & 0 & \dots & 0 \\ 0 & \lambda_2 & \dots & 0 \\ \dots & & & \\ 0 & \dots & & \lambda_N \end{bmatrix} \qquad (2.7)$$

Page 20

$$EDOF = \frac{1}{\lambda_{max}} \sum_{i=1}^{m} \lambda_i \qquad (2.8)$$

$$\left(\sqrt{N}-\sqrt{M}\right)^2 < \lambda_i < \left(\sqrt{N}+\sqrt{M}\right)^2 \qquad (2.9)$$

Page 47

$$\frac{P_r}{P_t} = G_t G_r \left(\frac{\lambda}{4\pi R}\right)^2 \qquad (3.1)$$

Page 53

$$H_{ij} = Normal\left(0, 1/\sqrt{2}\right) + \sqrt{-1}\cdot Normal\left(0, 1/\sqrt{2}\right) \qquad (3.2)$$

Page 63

$$\Gamma_{||} = \frac{-\varepsilon_r\, sin\theta + \sqrt{(\varepsilon_r - cos^2\theta)}}{\varepsilon_r\, sin\theta + \sqrt{(\varepsilon_r - cos^2\theta)}} \qquad (3.3)$$

$$\Gamma_{\perp} = \frac{sin\theta - \sqrt{(\varepsilon_r - cos^2\theta)}}{sin\theta + \sqrt{(\varepsilon_r - cos^2\theta)}} \qquad (3.4)$$

Page 64

$$Magnitude\ of\ Signal \propto \frac{cos(\frac{\pi}{2}cos\theta_{tx})}{sin\theta_{tx}} \times \frac{cos(\frac{\pi}{2}cos\theta_{rx})}{sin\theta_{rx}} \qquad (3.5)$$

Page 68

$$\bar{\tau} = \frac{\sum_k p(\tau_k)\tau_k}{\sum_k p(\tau_k)} \qquad (3.6)$$

$$\sigma_\tau = \sqrt{\overline{\tau^2} - (\bar{\tau})^2} \qquad (3.7)$$

$$\overline{\tau^2} = \frac{\sum_k p(\tau_k){\tau_k}^2}{\sum_k p(\tau_k)} \qquad (3.8)$$

Page 69

(3.9) same as (2.1) above and on page 17

Page 70

$$H_{ij} = \sum_k a_k e^{j(2\pi d_k)/\lambda} \qquad (3.10)$$

$$\mathbf{H} = \mathrm{A}\mathbf{H}' \qquad (3.11)$$

$$A = \left(\frac{1}{MN}\sum_{m=1}^{M}\sum_{n=1}^{N}|H_{mn}|^2\right) \qquad (3.12)$$

(3.13) same as (2.7) above and on page 18

$$C = \sum_{i=1}^{m} \log_2 \left(1 + \frac{\rho}{N}\lambda_i\right) \quad \text{b/s/Hz} \qquad (3.14)$$

Page 74

$$\mathbf{H} = A_{LOS}\, \mathbf{H'}_{NLOS} \qquad (3.15)$$

Page 132

$$C \propto \cos\theta \times \frac{d}{R} \qquad (5.1)$$

$$\frac{d_t d_r}{R} \geq \frac{\lambda}{M} \qquad (5.2)$$

Page 161

$$Element\ displacement = \pm n \times step \times \lambda \quad (6.1)$$

DESCRIPTION OF SIMULATION PROGRAM

This section describes the simulation program(s) in detail. It is based on the flowcharts in chapter 3 (Figure 3.7) and references the various equations used as listed in the previous pages in this appendix and in the thesis. The programs referred to are Matlab M-files and are referred to as MIMO MAIN, MIMO SUB, MAIN SISO (or just SISO) and Ray-tracer as per Figure 3.7.

1. MIMO MAIN Program

This purpose of this program is to estimate the spectral efficiency (i.e. the capacity) of the MIMO channel based on the channel matrix generated in the subprogram MIMO SUB. The matrix is normalised and then the eigenvalues of the normalised matrix are determined. These represent the gain of the individual parallel data channels and are used to estimate the total spectral efficiency for that particular

channel realisation. The program stores the various data elements, e.g. channel matrices, spectral efficiency, normalisation constants, eigenvalues and so forth for separate data analysis and plotting purposes as presented throughout the thesis. In addition, if adjustment of the array elements using the Metropolis algorithm is required then the initial determination of the random perturbations ('moves') and the decision to keep or discard them based on the cost factor (spectral efficiency) is performed in this program. Note the initial section of code is mainly the declaration of variables many of which are arrays for storing data elements which are saved when the simulation is finished in a MAT-file. Also the definitions of the size of the array and element spacing, room size etc. are defined in this section. For example, a 4x4 array is determined by defining an array size variable value N=16 which is used in the later SISO sub program when the precise location of the Tx and Rx elements are determined (SISO is called 16 times for a 4x4 array). Variations of the SISO program which effectively positions the array elements are used for different orientations of arrays or structures, e.g. linear or square arrays. The total number of realisations of the channel is also defined, e.g. 3000. For example, if the Tx is fixed and the Rx is randomly repositioned 3000 times (the random location is determined in the MIMO SUB program). The following are the key steps in the main loop of the MIMO MAIN program which typically would be repeated hundreds or thousands of times depending on the scenario being investigated.

a. Call the sub program MIMO SUB (see below) which returns a channel matrix **H.**
b. Normalisation of the channel matrix **H** using equations 3.11 and 3.12.
c. Determination of the eigenvalues of the normalised matrix (equation 3.13) which use the Matlab function eig(X).

d. Determination of spectral efficiency using equation 3.14.

e. If the array elements are to be repositioned then random displacements are calculated for each individual element at the Tx and Rx (equation 6.1) and it is the case that the location of both the Tx and Rx are now fixed, i.e. no random repositioning in MIMO SUB progarm. For each element three random 'moves' in each dimension X,Y and Z are determined. In the SISO subprogram, which positions the individual array elements, the three dimensional adjustments are used to position the elements at the Rx (and Tx if required). If only one dimension is adjusted, e.g. Z, then only that value is used. In the first iteration of the main loop the 'moves' are stored and used for the next iteration when a new capacity calculation is made. The new position is retained if the capacity is higher than the previous iteration and future 'moves' are relative to that position until the next improvement occurs (higher capacity). This is done in the MIMO MAIN program since that is where the capacity is calculated and is summarised as follows:

If (new capacity > previous capacity)

Accept new array element locations

Else

Reject and repeat using previous array element locations

2. MIMO SUB Program.

The main functions of this subprogram are to generate new random positions for the Rx (and possibly Tx) or to pass the specific new individual array location

and adjustment ‘moves’ if the Metropolis search is being used. This is done for each individual array element position required for the SISO program which is called 16 times for a 4x4 array. The values returned by the SISO program are used to populate the channel matrix **H** (used by the MAIN MIMO program). The program also determines and stores the rms delay spread and the mean excess delay calculated for a single pair of elements at the Tx and Rx.

A new random position is determined for the Rx (and possibly the Tx) before the main loop unless the Metropolis algorithm (MA) is being used and the following are the key steps in the main loop typically repeated 16 times for a 4x4 system.

a. If Metropolis algorithm is being used then the array element ‘offset position’ is determined for a particular iteration and the SISO program is called. The SISO program then determines the absolute position for a single Tx and Rx array element for a particular orientation or structure of array.
b. Using values determined by the SISO program and equation 3.10 an entry for the channel matrix (equation 3.9) is determined and the matrix is populated.
c. For a single iteration of the loop, the mean excess delay spread is calculated using equation 3.6 and the rms delay spread is determined using equations 3.7 and 3.8. The values are stored in arrays for later analysis and plotting.

3. SISO MAIN Program.

This program is called repeatedly depending on the size of the array and the main tasks in the sequence are as follows:

a. Using the randomly generated values for the Rx (and possibly Tx), or the offset adjustment values determined by the Metropolis algorithm, the precise location of a pair of elements at both the Tx and Rx is determined. These are determined in three dimensions relative to the centre point of the room (0, 0, 0) and also use the previously defined array element spacing, which may be different at the Tx and Rx. Note that for different array orientations or array structures, different versions of the same routine were used.

b. The ray-tracer program was called. This determines the LOS and all first and second order paths as described below.

c. The propagation conditions are defined and any components determined by the ray-tracer that are not required are set to zero. For instance for NLOS conditions the LOS component is set to zero magnitude. (Any combinations of sparse conditions are determined at this stage and thus the signal magnitudes and path lengths used in equation 3.10 in MIMO SUB).

4. Ray-tracer

This routine uses the method of images technique to trace reflection waves between two points in a room and the direct paths between the points, which represent an element at the Tx and Rx arrays. This is done in three dimensions and the path length (L) is used to determine the magnitude of the received signal (1/L). The magnitude is scaled according to equation 3.5 to represent the

radiation pattern for a half wave dipole antenna, thus requiring the calculation of the angle $\theta_{Tx/Rx}$ of the path of the ray relative to the vertical axis of the antenna at both the Tx and the Rx.

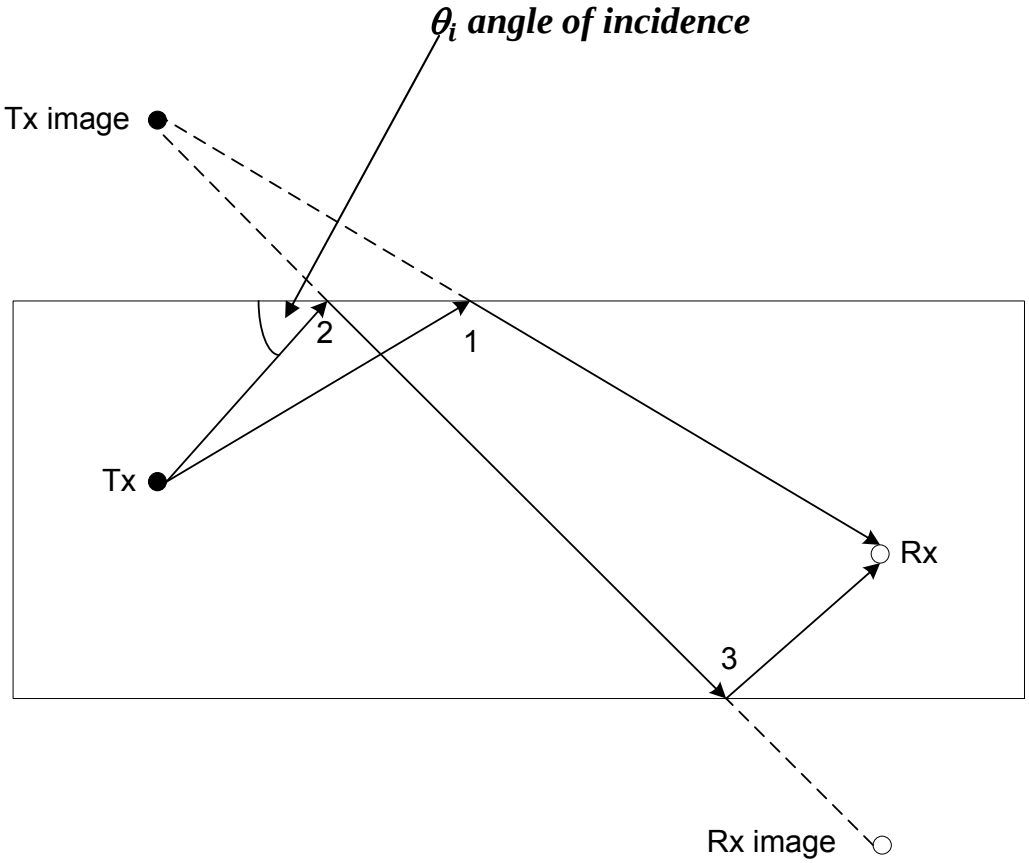

Figure E.1 Diagram showing first order and second order reflections as determined using images of the Tx and the Rx. The number '1' indicates the reflection point for a first order reflection and '2' and '3' are for a second order reflection The angle θ_i is an angle of incidence of a reflection, as used in equations (3.3) and (3.4).

For the case of reflected waves the reflection coefficients are also calculated according to equations (3.3) or (3.4) and the magnitude of the received signal is scaled accordingly. This requires the determination of the reflection point(s) and the angle(s) of incident (θ_i) of the reflected wave relative to the reflecting surface. An example of the angle incident is identified in figure E.1, (see section

3.4.3 and reference [3.1]). This is done using the method of images and in this program the location of the image of the Tx and the Rx is determined. An example is shown in two dimensions in figure E.1. A first-order reflection is determined by the path from the Tx image shown to the Rx and the reflection point is the intersection with the wall marked '1' on the diagram. A second order reflection is determined by the path from the Tx image to the Rx image and the intersections on the walls are the reflection points marked '2' and '3' on the diagram. In the simulation this is done in three dimesions. On completion both the magnitude and paths distance of the LOS and reflections are returned to the calling routine SISO.

FREQUENCY DOMAIN CHANNEL SOUNDING MEASUREMENT AND CALIBRATION PROCEDURE

The impulse response of the room was determined using a vector network analyser (VNA) with swept frequency oscillator and an S-parameter test set (the Hewlett Packard HP 8753b and the 85047A respectively) The diagram in Figure E.2 describes the overall test set up. The S-parameter test set measures the transmissivity (S_{21}) of the channel over the measured frequency range. (This is a frequency domain representation of the impulse response). The swept frequency oscillator generates a sequence of discrete frequencies centred on a particular carrier frequency. The time domain impulse response is derived from the frequency response by using the inverse discrete Fourier transform. A number of examples of the impulse response derived are provided in chapter 3 and appendix A. Further details about measurements and calibration procedures can be found in the user manual found at the following website.

http://exodus.poly.edu/~kurt/manuals/manuals/HP%20Agilent/HP%208753B%20Operating%20&%20Programming.pdf

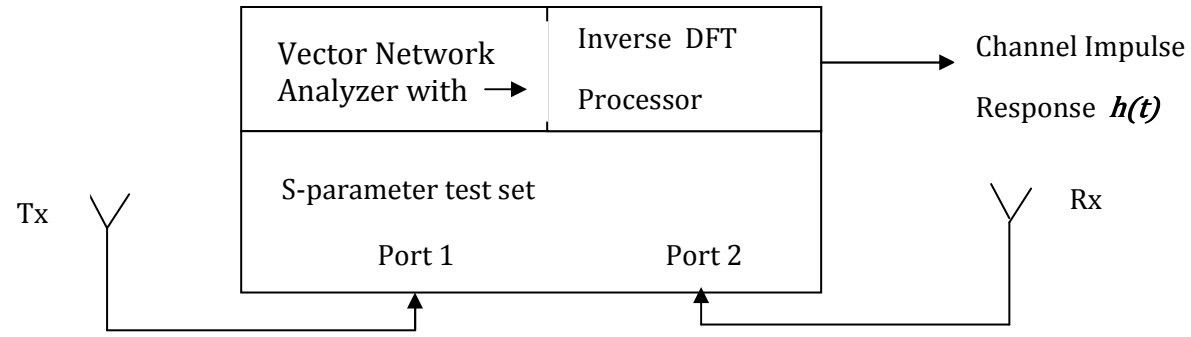

Figure E.2 Frequency domain channel impulse response measurement system

The test system requires calibration before measurements are made and the VNA has a number of calibration options which are selected from a menu invoked by the cal button. This requires a calibration kit which comprises of open circuits, short circuits and standard loads which are connected at various stages of the calibration process. A response calibration was performed to calibrate out the effects of the antenna leads when making measurements of S_{21} on two-ports as follows:

Calibration Procedure

1. Reset the network analyser by pressing the button on the front panel. Choose the frequency range by pressing the start frequency button on the front panel and entering a value, e.g. 1.9 GHz. Then press the stop button and enter a second value, e.g. 3 GHz.
2. Use the front panel button measure and choose S_{21} from the menu on the screen. Connect the lead to be calibrated between port 1 and port 2. Then press the format button and choose log magnitude to measure the magnitude of S_{21} in dB with respect to frequency. With the lead connected you will see the swept

frequency response, S_{21}, of the lead plotted over the frequency range. To make measurements which are not affected by the frequency response of the lead a response calibration is required.

3. Enter the calibration procedure by pressing the cal button and choose the calibration menu on the screen. From the calibration menu choose response.
4. The calibrate menu will invite you to connect standard loads of open (open circuit), short (short circuit) and thru (lead to port 2). Connect the open and short N-type male standards from the calibration kit in turn, taking great care with the connectors. Finally, connect the lead between port 1 and port 2 to establish the "thru" connection; this calibrates out the effects of the lead when making measurements. After connecting each standard load press the corresponding button. The VNA will confirm its measurement of the standard by beeping and underlining the icon on the button.
5. When you have completed connecting the last standard load press the done button. The VNA will now automatically calculate the calibration coefficients.

Publications List

1. A. Grennan, C. Downing, B. Foley, “Capacity variation of indoor radio MIMO systems using a deterministic Model”, *Irish Signals and Systems Conference,* 2003, pp. 548-553.
2. A. Grennan, C. Downing, B. Foley, “MIMO Capacity Enhancement by adjusting Element Positions using the Metropolis Algorithm in a Deterministic Model”, *IEE Irish Signals and Systems Conference,* 2006, pp. 265-276.
3. A. Grennan, C. Downing, B. Foley, “A Geometric Interpretation of Indoor MIMO Systems using a Deterministic Model”, *European Conference on Antennas and Propagation,* Edinburgh Nov. 2007, pp. 88-93.
4. A. Grennan, C. Downing, B. Foley, “Application and analysis of MIMO systems using Metropolis algorithm”, *Loughborough Antennas and Propagation Conference (LAPC)*”, Nov. 2010, pp. 357-360.
5. A. Grennan, M. Davis, C. Downing, “Analysis of array geometries for indoor MIMO systems using a deterministic model”, *Loughborough Antennas and Propagation Conference*” Nov. 2012, pp. 337-341.
6. A. Grennan, M. Davis, C. Downing, “Near optimum array geometries for MIMO systems in a highly correlated environment”, *Loughborough Antennas and Propagation Conference (LAPC)*”, Nov. 2013, pp. 357-360.